10-18-2018 10:00 AM

Ecology and Evolution of Dispersal in Metapopulations

Jingjing Xu
The University of Western Ontario

Supervisor
Wild, Geoff
The University of Western Ontario

Graduate Program in Applied Mathematics
A thesis submitted in partial fulfillment of the requirements for the degree in Doctor of Philosophy

Abstract

Dispersal plays a key role in the persistence of metapopulations, as the balance between local extinction and colonization is affected by dispersal. Dispersal is also the primary means by which a species' range changes, as well as an important mechanism for reducing competition and breeding among relatives. In this thesis, I present three pieces of work related to dispersal. The first two are devoted to the ecological aspect of delayed dispersal in metapopulations. The first one focuses on how dispersal may disrupt the social structure on patches from which dispersers depart. Examinations of bifurcation diagrams of the dynamical system show that a metapopulation will, in general, be either in the state of global extinction or persistence. The key finding is that dispersal, and the state changes associated with dispersal, have significant qualitative and quantitative effects on long-term dynamics only in a narrow range of parameter space, so life-history features other than dispersal (e.g., mortality rate) have a greater influence over metapopulation persistence. The second one asks whether the effort intending to enrich the metapopulation could always promote the persistence of metapopulations, incorporating time delays into the ODE models by Levins and Hanski. Investigations of critical delays and the absolute stability of equilibrium in DDE models show that: 1) delays associated with dispersal only cannot destabilize the population; 2) reducing local extinction in metapopulations with delays associated with available territories or establishment may lead to oscillations; 3) metapopulations with a structure based on the quality of occupied patches suffer less from the problem described in 2) caused by establishment delays. The third work studies the evolution of conditional/unconditional dispersal in environments with temporal global-scale fluctuations. Methods from theoretical evolutionary biology are applied, and perturbation methods, numerical procedures and individual-based simulations show that difference between conditional dispersal probabilities for poor and good environment states increases as fluctuation frequency and disparity of dispersal cost increase. At last, conclusions and discussion of the implication of the above studies to cooperative breeding are presented, as well as a future direction to construct a kin selection model and investigate the evolution of helping.

Keywords: Population Dynamics, Differential Equation, Inclusive-Fitness Theory, Reaction Norm, Ecological Constraint, Fragmented Habitat

Co-Authorship Statement

The dissertation herein is written by Jingjing Xu under the supervision of Dr. Geoff Wild. Chapter 2 is based on a paper published in Journal of Biological Dynamics co-authored with G. Wild. Chapter 3 is based on a paper in preparation for publication co-authored with G. Wild. Chapter 4 is based on a paper under review for publication in The American Naturalist co-authored with G. Wild. Chapter 5 is based on an on-going work co-authored with G. Wild. All authors contributed to the writing of the respective manuscripts.

Since Chapters 2, 3, and 4 are – or will be – papers co-authored by J. Xu and G. Wild, first-person plural pronouns are used therein. Chapters 1 and 5, by contrast, will not be submitted as co-authored papers, and so first-person singular pronouns are used there.

Acknowlegements

First and foremost, I would like to express my sincere gratitude to my supervisor Geoff Wild for the continuous support of my PhD, and for his knowledge, time commitment, infinite patience and encouragement. His insightful perspective in both mathematics and biology inspired me in our countless discussions. His guidance leaded me through my research and writing of the thesis. None of this would be possible without his advice.

Second, I am grateful to the Department of Applied Mathematics, in the University of Western Ontario, for offering me such an incredible opportunity to work with numerous knowledgeable professionals and intelligent fellow students for five years. I would also like to thank all the professors in the department, especially my supervisory committee, Lindi Wahl and Rob Corless, and professors in the mathematical biology group, Xingfu Zou and Pei Yu, for their valuable suggestions and enlightenment. In addition, I would like to express my gratitude to the administrative staff, especially Audrey Kager and Cinthia MacLean, as they have been always kind and helped me promptly ever since the beginning of my application of PhD program.

Third, I would like to thank fellow students in the department and my friends, in particular, Ao Li and Yang Wang, for their patience, feedback, discussions, and for all the fun we have had in the last few years.

Last but not least, I would like to thank my family for supporting and encouraging me throughout my study. In addition to all the help I received from the professionals when navigating through the ocean of doctoral research, it is the priceless company with my family and friends that made my days delightful at Western, so that I am strong enough to overcome all the obstacles and accomplish this dissertation eventually.

Contents

List of Figures

List of Tables

List of Appendices

Chapter 1

Introduction

1.0 Summary

In this chapter, I first provide background information and significance for the study of metapopulations, and its relation with the study of conservation biology in **section 1.1**. Then, I explain the core idea to model metapopulation dynamics, and visit basic previous models in **section 1.2**. Next, in **section 1.3**, I switch from the ecology, where dispersal probability is treated as a constant parameter, to the evolution of dispersal, where dispersal probability evolves, in metapopulations, and briefly describe the mechanisms and methodology for the evolution of dispersal. At last, I list my motivation, methodology and main results for Chapters 2-5 in **section 1.4**. To start with, let us have a look at the concept of *metapopulation* in the following section.

1.1 Metapopulation

The term *metapopulation* describes a population of populations that together form a patchwork of habitats between which species disperse (see Figure1.1) [30, 34, 88]. The emergence of the idea for metapopulation is related to the study of island biogeography by MacArthur and Wilson [49]. A lot of species live as a part of a metapopulation, that is, they live in patchy

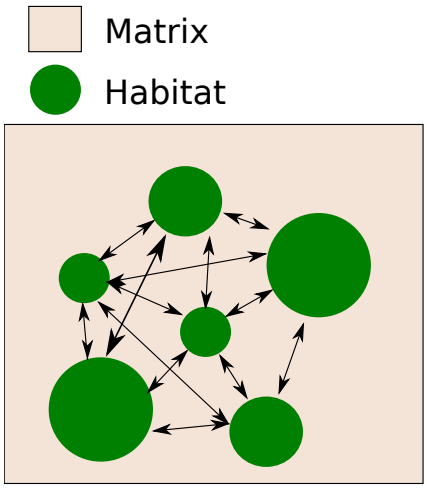

Figure 1.1: A cartoon of metapopulation: a mathematically simplified version

local populations separated in space by a matrix through which dispersal is possible, but in which breeding is impossible. Examples of natural metapopulations include the birds living in islands, fishes living in coral reefs [70], migratory species [78] and butterflies in fragmented landscapes [37].

Notably, local-population-level interactions are more frequent than metapopulation-level interactions. Given an area of habitat, if individuals live on breeding territories held by family units, but leave these units after some period of time, then they could also be said to exist as a metapopulation. For example, the Florida scrub jay lives in territories of island-like distributed short scrubs, and their basic breeding units are monogamy pairs, some of which are assisted by up to six helpers, but mostly zero to two [89].

1.1.1 Metapopulations, Human Activities and Conservation Biology

Human beings, ourselves, can be seen as forming a metapopulation. Moreover, human beings have a long history of fighting against some other metapopulations, such as, insect pests that move from one location to another. Indeed, in agriculture, the control of pests is one of the major concerns. By considering the insect populations as metapopulations, biologists are able to determine the most effective ways to control the population size of pests, and protect the yield

of crops [48, 76]. Furthermore, human migration, travel and trade have resulted in a massive scale of human-mediated movement of various species, including animals, plants, bacteria and viruses [5, 8], as human beings' ability of long-distance dispersal is without rival in nature.

Recently, human activities, including expanding of cities and roads, and exploring natural resources like forest, lead to fragmented forests and disconnected water systems. Such fragmented habitats, then, lead to more and more species living in communities of metapopulations, and eventually affect the ecology of those species greatly [3, 4, 14, 71, 83, 84]. Even worse, humans have begun to threaten the survival of other species as they develop more and more of the preferred living habitats of those species. On one hand, as the whole ecosystem is connected, the loss of some key species might gradually impact the whole trophic dynamics, and can finally influence the whole agriculture system that humans depend on. On the other hand, habitat fragmentation may lead to extinction of some species, and an irreversible loss of part of the gene pool in nature. Therefore, studying the persistence of such metapopulation species contributes to conservation of species [2].

The metapopulation structure of many communities has economic implications for conservation efforts. For example, to re-mediate or maintain metapopulations it may be necessary to establish and/or preserve dispersal corridors. Because those conservation efforts usually cost a large amount of money [50, 72], making sure it is put into where necessary and effective is of great significance. Understanding the dynamics, especially the effect of dispersal, is important. In addition, using metapopulation models to provide insight into conservation efforts and validate the effect of corridors is cost-efficient.

Human activities have altered many global scale conditions, including the global climate [22, 43, 53, 63, 85, 86]. For example, human activities have added a considerable amount to greenhouse gases that wrap the earth with a thermal blanket, reducing heat radiated to space, so lead to changes on global temperature and precipitation [43]. Those climate changes could result in changes of migration and regional distribution of plants [57], and also lead to changes of regional distribution of other species.

1.2 Metapopulation Dynamics

In the history of metapopulation study, the term itself was first used by Levins [48] to study pest control strategy, and the next year he used his metapopulation framework to study group selection as a potential route to the emergence of altruism. Traditional models of population dynamics reflect changes due to birth, death, and migration (dispersal). Similar demographic processes are captured by models of metapopulations, but their consequences for local populations is usually emphasized. In a metapopulation model, when a suitable unoccupied habitat is colonized by propagules produced elsewhere, the colonization is analogous to the birth of a new local population. Local populations can also suffer extinction, which parallels the death of an individual. Finally, the colonization of suitable habitats by propagules is mediated by migration (dispersal). The balance between local extinction events and colonization events, and how this balance contributes to the long-term dynamics of the system are the main concerns for the study of metapopulation dynamics.

Metapopulation models could be applied to study interactions between two species or more. For example, there is an elegant two-species metapopulation model showing how an inferior competitor can co-exist with a superior competitor owing to the inferior competitor's higher colonization rate or low extinction rate [see 47, 55]. But, my focus of metapopulation models is on the single-species, which I talk about in the following.

1.2.1 Mathematical Models of Metapopulation Dynamics

MacArthur and Wilson [49] studied extinction and colonization processes in their later tremendously well-cited book on island biogeography. They investigated the mainland-islands model, with dispersers from a mainland colonizing empty islands. Denoting the fraction of occupied islands by $p(t)$, a single-species version of their mainland-islands model is

$$dp(t)/dt = c\,(1 - p(t)) - e\,p(t), \tag{1.1}$$

where c and e are the colonization rate and extinction rate of islands. Note that the colonization per empty island is determined only by the mainland, not affected by the density of occupied islands.

MacArthur and Wilson's work [49] probably set the stage for Levins' metapopulation model [48]. Among all the work on metapopulations, Levins' model is recognized as seminal. What distinguishes Levins' model from other ones is that Levins simplified what happens inside each local population and the spatial relation among local populations, and emphasized the balance of local extinction and colonization processes. Despite the simplification, Levins' model did bring some valuable original ideas into the area of study. His model uses $p(t)$ to denote the fraction of local habitats occupied by local populations, so $1 - p(t)$ is the fraction of empty local habitats. By using c to represent the colonization rate of empty local habitats by dispersers from currently occupied local habitats, and e to represent the local extinction rate of currently occupied local habitats, Levins constructed a model taking the following simple form

$$dp(t)/dt = c\, p(t)\,(1 - p(t)) - e\, p(t). \tag{1.2}$$

The novelty of Levins' model (1.2) lies in the fact that MacArthur and Wilson [49] treat the mainland as the input to other islands, assuming the mainland is not susceptible to extinction, but Levins' model does not include such a hierarchy-like structure among the local habitats, allowing turnovers to occur on each local habitat. Consequently, model (1.1) and model (1.2) have distinct sources of colonization and therefore distinct positive equilibria: communities in model (1.1) represent a balance between extinction and colonization from extrinsic forces only, with the positive equilibrium, $1 - e/(c + e)$; meanwhile, model (1.2) emphasizes the balance between extinction and colonization from within the metapopulation, i.e., intrinsic, rather than extrinsic, with the positive equilibrium, $1 - e/c$, which is smaller than that in model (1.1).

To capture various features of single-species metapopulations, researchers have modified assumptions of Levins' model (1.2) by including infinite local population size and ignoring details associated with space. One modification is to consider a finite local population size, where

researchers can assess the effect of varying local population sizes and locations, or dispersers' interactions [24, 29]. Based on Levins' model, two types of approaches to achieve the goals are developed, including state transition models and incidence function models [28, 29, 74]. In this case, local extinction rate and colonization rate can be heterogeneous, depending on local population sizes [26, 27, 39]. Based on Levins' two compartment model (1.2), Hanski [27] developed a three compartment model by separating local populations into small ones and large ones, by which he shows that metapopulation can have two alternative stable states, corresponding to persistence and global extinction, respectively. Hanski presents his model to explore how dispersal can change the dynamics of metapopulation, and the model includes the observation that local population size is correlated with occupancy rate due to dispersal. Hastings [39] further discusses Hanski's model as an example after he constructs a model to argue that stochasticity and demographic features in local population level can be consistent with stability of metapopulation level.

Another modification of Levins' model is to consider spatially explicit local populations. Such models are developed to stress the importance of localized interactions [7, 13, 38, 42]. Those explicit-spatial-structure models arrange local habitats in a network of lattices and allow interactions only among nearby local habitats, so they can examine the effect of limited connection due to limited dispersal in metapopulation. Those spatially realistic models have been applied to study the metapopulation of the spotted owl in California [23, 46, 58] and the Glanville fritillary butterfly (*Melitaea cinxia*) in Finland [33, 35, 36]. Besides modified models to study single-species, Levin's model has also inspired some multi-species models to study the metacommunity dynamics of species with different relations, such as, competition, predation, and mutualism [26, 51, 54–56].

What I explore in **Chapter 2** is a single-species metapopulation model with spatially implicit finite local populations, following the route of the hierarchical structured metapopulation model studied by Hanski [27]. We are extending this branch of study on metapopulation dynamics by asking the question: how could dispersal contribute to the link between local

extinction and colonization? There is a consensus that the effect of dispersal plays a key role in the metapopulation dynamics [20, 30, 32, 64, 77, 87], and the effect of dispersal on local extinction rate has been referred to as a "rescue effect" in island biogeography [12]. While there has been work that explores how relatively healthy local populations can rescue ones of poorer quality, no consideration has been given to the negative impact such rescue events have on the healthy source populations. I remedy this in **Chapter 2**.

What I investigate in **Chapter 3** is based on Levins' model (1.2) and Hanski's model [27], and I explore how metapopulation dynamics change as local extinction is reduced when delays in establishment and dispersal are involved. Delays are expected to be an intrinsic part of metapopulation dynamics, as it takes time for individuals to move from one local population to another. Moreover, newly colonized habitats may not be able to send out propagules until founders manage to encounter one another and reproduce. Delays are often disregarded in models because they are difficult to measure [31]. However, delays may have otherwise unexpected dynamical consequences, and I explore this here.

1.3 Evolution of Dispersal in Metapopulations

I have so far left the term *dispersal* undefined, and have treated it as a colloquialism. Moving forward, however, will require a clearer definition of this term. Here, I will define dispersal as the act of attempting to reproduce away from one's place of birth. This definition is inspired by the one provided by Duputié and Massol [16], but it is not identical to theirs.

Dispersal of individuals from their natal habitat is an essential demographic process for many species, including animals and plants. Individuals' dispersal usually occurs in three stages: emigration from natal habitats, vagrancy before settling down, and immigration into a new habitat where they can reproduce [67]. Therefore, dispersal probability is relevant to the colonization rate that appears in models of metapopulation dynamics, such as those presented in the previous section. There, the colonization rate is treated as a constant demographic pa-

rameter. However, as dispersal is usually known to be heritable [66], therefore the dispersal probability itself can be influenced by natural selection, in principle, and evolve over time [see 60–62]. I turn my attention to this fact here.

Studying the evolution of dispersal is important. Dispersal of individuals facilitates the spread of genes, provided that individuals who dispersed survive during dispersal and manage to have offspring in new habitats [41]. In other words, dispersal can lead to the re-distribution of genes over space, in addition to the re-distribution of individuals. Therefore, not only is the evolution of dispersal driven by natural selection, but dispersal can also affect the force of natural selection on other traits.

Dispersal itself is a life-history trait that is of broad interest. Dispersal is the principal means by which species expand their ranges, for example as the climate warms [11, 15]. In addition, dispersal ensures genetic variation spreads throughout a population [1, 73]. Consequently, dispersal can work against forces that foster the emergence of new species [82]. Dispersal (or rather lack thereof) can also ensure relatives remain in close proximity to one another, and so set the stage for the evolution of more complex social behaviour [17, 75].

1.3.1 Mechanisms for the Evolution of Dispersal

Dispersal might be costly for individuals [9, 10, 40, 44, 59, 65]. During dispersal and afterwards, dispersing individuals might be exposed to an increased mortality risk [40], or face fierce competition at a new location and get a reduced number of offspring as a result [65]. These ideas raise intriguing questions: why disperse at all? What advantage does costly dispersal confer upon individuals? Several answers to these question have been explored. Answers, themselves, invoke mechanisms that may be broadly classified as either “interior” or “exterior” in nature. I refer to mechanisms coming from interactions with patchmates as “interior”, and refer to all other mechanisms as “exterior”, such as those due to environment and predation.

Interior mechanisms for the evolution of dispersal involve the need of individuals to reduce kin competition, and to avoid inbreeding [6, 10]. Staying at an individual’s own natal

habitat results in the individual's competition with its relatives for survival or breeding resources, while dispersing can reduce the intensity of natal kin competition. Inbreeding depression is caused by the recombination of deleterious recessive genes carried by relatives [21]. Lower dispersal probability can also lead to a larger probability of suffering from inbreeding depression, but more dispersal allows the species to escape from the risk of inbreeding.

Besides the above interior causes, the evolution of dispersal can also be driven by the exterior environment, so dispersal can be thought of as an adaptive response to environmental change and uncertainty [61, 67]. Experiments imply that dispersal might be a strategy for species to deal with ephemeral habitats [19]. In addition, changing environments might select for conditional dispersal [69], one explanation of which is bet hedging, which is a strategy using dispersal to reduce the variance of reproductive value caused by environmental uncertainty. Among those mechanisms driving the evolution of dispersal, my focus in **Chapter 4** is on the effect of global-scale environmental fluctuations, with a consideration of kin competition.

1.3.2 Kin Selection: a Methodology for Modelling the Evolution of Dispersal

A kin selection argument can be used as a powerful tool to track the force of natural selection on a genotype of dispersal [see 18, 21, 68, 79]. The kin selection argument is intimately linked to inclusive-fitness theory [25], which argues that whether or not an individual's behavior is favored by natural selection depends not only on the individual's direct fitness, which is gained from personal survival and production of descendant kin, but also on the individual's indirect fitness gained from survival and production of non-descendant kin. Kin selection arguments formulate a weighted sum of the fitness effects the individual confers upon its relatives and itself, where weights are, in general, products of measures of genetic relatedness and projected long-term contributions to the gene pool (i.e. reproductive value).

Let us revisit a model proposed by Taylor [79] to clarify the method and the steps. Consider an infinite, sexually-reproducing diploid population, with non-overlapping generations.

Suppose that individuals in the population are *monoecious*, meaning that they have both male and female reproductive parts. Suppose at the beginning of a given year/generation, individuals occur in local groups (i.e., *patches*) that consist of N individuals. Suppose further that the rest of the year/generation proceeds as follows:

- Each of the N individuals (parents) gives birth to a large number of offspring, then each parent dies.
- The offspring disperse to a new (uniform random) patch, independently, with probability d. Each disperser dies during its journey, independently, with probability c, where c is the *cost of dispersal*. Those individuals who do not disperse remain on their natal patch.
- Mating takes place uniformly at random among individuals on the same patch.
- Individuals compete uniformly at random (with replacement) for each of the N positions on a patch. Unsuccessful competitors die, and the entire process repeats.

Based on this sequence of events, I model the selective pressure acting on dispersal by asking how a small change to the probability with which an individual disperses, in turn, changes its inclusive fitness.

To answer the question posed, consider a mutant individual with a dispersal probability $d + \delta\,(\delta > 0)$. Obviously, this mutant individual is more likely than its non-mutant counterpart to pay the dispersal cost. To first-order in δ, then, the mutant's direct fitness is changed by $-\delta c$. The mutant's increased tendency to disperse has the "knock on" effect of reducing competition on its natal patch. This generates a benefit equal to δ (again, I am estimating to first-order in δ) that is given to the average competitor. It can be shown, to zeroth order in δ, that the average competitor is related to the mutant by a factor of hR. Here, $h = (1-d)/(1-cd)$ is the probability that the beneficiary was born on the same patch as the mutant, and R is the relatedness between two individuals, given that they were born on the same patch. Overall, then

$$\Delta W = (-c + hR)\delta$$

expresses the net change in the mutant's inclusive fitness. When the sign of ΔW is positive (resp. negative), selection favours (resp. disfavours) an increase in d, population wide. When $\Delta W = 0$, the evolution of d is at equilibrium with respect to selection.

To do anything meaningful with ΔW, the relatedness coefficient needs to be calculated. Taylor formulates relatedness as follows [see 52]:

$$R = \frac{\mathrm{cov}(G_y, H_x)}{\mathrm{cov}(G_x, H_x)}, \tag{1.3}$$

where H_x is the phenotype of individual x, and G_i is the phenotype of individual i ($i = x, y$). This formula captures the meaning of the relatedness coefficient, i.e., the strength of the correlation between the genotype of an individual y and the genotype of x (indicated by the covariance), compared with the strength of the correlation between the genotype of the individual x itself and its genotype. The closer the relatedness coefficient is to 1, the more genetically close those individuals x and y are. To zeroth order in δ, Hamilton and Michod [52] show that

$$R = \frac{\mathrm{cov}(G_y, G_x)}{\mathrm{cov}(G_x, G_x)} = \frac{f_{yx}}{f_{xx}}, \tag{1.4}$$

where f_{ij} is the coefficient of consanguinity between i and j, i.e., the probability that uniform random alleles from i and j have descended from a common ancestor without mutation. The previous expression simplifies to

$$R = \frac{f_{yx}}{(1 + f)/2}, \tag{1.5}$$

where f is the inbreeding coefficient of x, defined as the probability that homologous alleles in x have descended from a common ancestor without mutation.

Clearly, to calculate R need the help of two coefficients: f and f_{xy} (= g for the author's

convenience). Using a recursive conditioning argument, I get

$$f' = h^2 g, \tag{1.6}$$

$$g' = \frac{1}{N}\left[\frac{1+f+2h^2 g}{4}\right] + \frac{N-1}{N}[h^2 g], \tag{1.7}$$

where f' and g' are the coefficients in the next generation. Solving for equilibrium values of f and g, respectively, and using the formula above, I find

$$R = \frac{2g}{1+f} = \frac{1}{2N-(2N-1)h^2}. \tag{1.8}$$

By substituting R in my expression for ΔW, setting $\Delta W = 0$, and solving for $d = d^*$ I find that selection on dispersal is at equilibrium when

$$d^* = \frac{H+1-4Nc}{H+1-4Nc^2}, \tag{1.9}$$

where

$$H = \sqrt{1+8N(2N-1)c^2}. \tag{1.10}$$

Taylor and Frank [80] have a "neighbour modulated fitness" method that derives the inclusive fitness effect by considering the ways in which an individual's direct fitness is affected by its relatives, rather than the other way around, as I did above. The results generated by the Taylor-and-Frank approach [80] are equivalent to those generated in the more standard way [81].

1.4 Thesis Motivation and Outline

In **Chapter 2**, I ask: to what extent is the persistence of a metapopulation impacted when the dispersal associated with colonization events results in a diminished quality of source popula-

tion? Such diminished quality can disrupt the social structure of a source population, e.g., when a disperser functions as a helper in a cooperatively breeding group, the cooperative breeding structure may collapse after the helper disperses. To answer the question, I propose a simple model of a metapopulation in which local populations are made up of small numbers of individuals, with distinct social roles. I use my model to identify the conditions under which global extinction of the metapopulation can occur or be avoided. My analysis is focused on (but not solely dedicated to) the effect of dispersal rate, as dispersal events fuel colonization in a metapopulation, and have the potential to reduce the quality of those source populations which colonists leave behind. Surprisingly, I find that the impact of dispersal, as I have modelled it, is limited. This, in turn, suggests that the standard approach is likely useful when modelling metapopulations consisting of small concentrations of social species. I discuss the implication of my findings for natural populations, and their broader significance in light of model limitations.

In **Chapter 3**, I ask if delays can alter the effect of reducing local extinction rate on the stability and persistence of metapopulations, and if a "Paradox of Enrichment" can occur, i.e., if reducing local extinction can disrupt the stability of metapopulation and lead to global extinction. We first introduce a gallery of delay differential equation (DDE) models based on Levins' model and Hanski's model, by considering delays associated with availability of empty islands, delays associated with dispersal, and delays associated with establishment, and then I investigate the possibility for oscillations by checking the absolute stability of the positive stable equilibrium, and by determining critical transition delays. Next, we continue with the occurrence of the Paradox of Enrichment in models, in which the enrichment can lead to oscillations, I compare the timing of the occurrence of the Paradox of Enrichment in different models, and I argue that introducing a structure to metapopulations with establishment delay might be a way to resolve the Paradox of Enrichment, and that recording the increased recovery time can be used as a warning sign when the metapopulation approaches its bifurcation points. At last, I end with discussion of the impact of including delays in metapopulation modelling,

the occurrence of the Paradox of Enrichment and future directions.

In **Chapter 4**, I shift my focus to dispersal evolution. I ask if temporal global-scale environmental fluctuations can influence the evolution of dispersal, and if so, how the dispersal probability responds to the disparity between dispersal cost over the fluctuation and the frequency of fluctuation. I use mathematical models of a population that is divided into habitat patches of fixed finite size. The state of the environment in which the population exists fluctuates randomly between "good" and "poor" over time, and affects the cost of dispersal only. When dispersal cannot be adjusted based on the environment (unconditional dispersal), I find that environmental fluctuation exerts only a weak influence. Indeed, the approximations inherent to my mathematical analysis show that unconditional dispersal is affected by the environment through time-averaged costs alone. Results change when dispersal can be adjusted based on environmental conditions (conditional dispersal): dispersal occurs at a higher rate in good years when its cost is low. Furthermore, the disparity between dispersal in good versus poor years becomes more pronounced as either variance in dispersal cost increases, or environmental fluctuations become more frequent. I discuss findings in terms of the inclusive-fitness effects of dispersal. I also outline testable predictions arising from my findings. My interest in cooperatively breeding species resurfaces in this chapter, and the implications of my model predictions for cooperative-breeding species is discussed.

In **Chapter 5**, I summarize key points from previous chapters, and propose a future direction toward completing a theoretical picture of the evolution of cooperation by turning my attention to one of its important drivers, group augmentation. Inspired by work of Kokko et al. [45], I raise a question, that is, how can ecological constraints and group augmentation together impact the route of evolution of cooperative breeding. I provide some background information there and set up a model to guide further study.

Bibliography

[1] J. Aars and R. A. Ims. Population dynamic and genetic consequences of spatial density-dependent dispersal in patchy populations. *The American Naturalist*, 155(2):252–265, 2000.

[2] H. R. Akçakaya, G. Mills, and C. P. Doncaster. The role of metapopulations in conservation. *Key Topics in Conservation Biology*, pages 64–84, 2007.

[3] H. Andren. Effects of habitat fragmentation on birds and mammals in landscapes with different proportions of suitable habitat: a review. *Oikos*, pages 355–366, 1994.

[4] A. Andrews. Fragmentation of habitat by roads and utility corridors: a review. *Australian Zoologist*, 26(3-4):130–141, 1990.

[5] A. G. Auffret and S. A. Cousins. Humans as long-distance dispersers of rural plant communities. *PLoS One*, 8(5):e62763, 2013.

[6] B. Bengtsson. Avoiding inbreeding: at what cost? *Journal of Theoretical Biology*, 73(3): 439–444, 1978.

[7] M. Bevers and C. H. Flather. Numerically exploring habitat fragmentation effects on populations using cell-based coupled map lattices. *Theoretical Population Biology*, 55 (1):61–76, 1999.

[8] N. Boivin, R. Crassard, and M. Petraglia. *Human dispersal and species movement: from prehistory to the present*. Cambridge University Press, 2017.

[9] D. Bonte, H. Van Dyck, J. M. Bullock, A. Coulon, M. Delgado, M. Gibbs, V. Lehouck, E. Matthysen, K. Mustin, M. Saastamoinen, et al. Costs of dispersal. *Biological Reviews*, 87(2):290–312, 2012.

[10] D. E. Bowler and T. G. Benton. Causes and consequences of animal dispersal strategies: relating individual behaviour to spatial dynamics. *Biological Reviews*, 80(2):205–225, 2005.

[11] R. W. Brooker, J. M. Travis, E. J. Clark, and C. Dytham. Modelling species range shifts in a changing climate: the impacts of biotic interactions, dispersal distance and the rate of climate change. *Journal of Theoretical Biology*, 245(1):59–65, 2007.

[12] J. H. Brown and A. Kodric-Brown. Turnover rates in insular biogeography: effect of immigration on extinction. *Ecology*, 58(2):445–449, 1977.

[13] H. Comins, M. Hassell, and R. May. The spatial dynamics of host–parasitoid systems. *Journal of Animal Ecology*, pages 735–748, 1992.

[14] S. A. Cushman. Effects of habitat loss and fragmentation on amphibians: a review and prospectus. *Biological Conservation*, 128(2):231–240, 2006.

[15] M. B. Davis and R. G. Shaw. Range shifts and adaptive responses to quaternary climate change. *Science*, 292(5517):673–679, 2001.

[16] A. Duputié and F. Massol. An empiricist's guide to theoretical predictions on the evolution of dispersal. *Interface Focus*, 3(6):20130028, 2013.

[17] S. T. Emlen. The evolution of helping. i. an ecological constraints model. *The American Naturalist*, 119(1):29–39, 1982.

[18] S. A. Frank. Dispersal polymorphisms in subdivided populations. *Journal of Theoretical Biology*, 122:303–309, 1986. doi: 10.1016/S0022-5193(86)80122-9.

[19] N. A. Friedenberg. Experimental evolution of dispersal in spatiotemporally variable microcosms. *Ecology Letters*, 6(10):953–959, 2003.

[20] M. Gadgil. Dispersal: population consequences and evolution. *Ecology*, 52(2):253–261, 1971.

[21] S. Gandon. Kin competition, the cost of inbreeding and the evolution of dispersal. *Journal of Theoretical Biology*, 200:345–364, 1999. doi: 10.1006/jtbi.1999.0994.

[22] H. Gitay, S. Brown, W. Easterling, B. Jallow, J. Antle, M. Apps, R. Beamish, T. Chapin, W. Cramer, J. Frangi, et al. Ecosystems and their goods and services. In J. J. McCarthy, O. F. Canziani, N. A. Leary, D. J. Dokken, and K. S. White, editors, *Climate change 2001: impacts, adaptation, and vulnerability: contribution of Working Group II to the third assessment report of the Intergovernmental Panel on Climate Change*, volume 2, pages 235–342. Cambridge University Press, 2001.

[23] R. Gutiérrez and S. Harrison. Applying metapopulation theory to spotted owl management: a history and critique. *Metapopulations and wildlife conservation. Island Press, Washington, DC*, pages 167–185, 1996.

[24] M. Gyllenberg and D. S. Silvestrov. Quasi-stationary distributions of a stochastic metapopulation model. *Journal of Mathematical Biology*, 33(1):35–70, 1994.

[25] W. D. Hamilton. The genetical evolution of social behaviour. I and II. *Journal of Theoretical Biology*, pages 1–52, 1964. doi: 10.1016/0022-5193(64)90038-4.

[26] I. Hanski. Coexistence of competitors in patchy environment. *Ecology*, 64(3):493–500, 1983.

[27] I. Hanski. Single-species spatial dynamics may contribute to long-term rarity and commonness. *Ecology*, 66(2):335–343, 1985.

[28] I. Hanski. Patch-occupancy dynamics in fragmented landscapes. *Trends in Ecology & Evolution*, 9(4):131–135, 1994.

[29] I. Hanski. A practical model of metapopulation dynamics. *Journal of Animal Ecology*, pages 151–162, 1994.

[30] I. Hanski. Metapopulation dynamics. *Nature*, 396(6706):41–49, 1998.

[31] I. Hanski. Spatially realistic theory of metapopulation ecology. *Naturwissenschaften*, 88 (9):372–381, 2001.

[32] I. Hanski and T. Mononen. Eco-evolutionary dynamics of dispersal in spatially heterogeneous environments. *Ecology Letters*, 14(10):1025–1034, 2011.

[33] I. Hanski and I. Saccheri. Molecular-level variation affects population growth in a butterfly metapopulation. *PLoS Biology*, 4(5):e129, 2006.

[34] I. Hanski and D. Simberloff. The metapopulation approach, its history, conceptual domain, and application to conservation. In *Metapopulation biology*, pages 5–26. Elsevier, 1997.

[35] I. Hanski and C. D. Thomas. Metapopulation dynamics and conservation: a spatially explicit model applied to butterflies. *Biological Conservation*, 68(2):167–180, 1994.

[36] I. Hanski, T. Pakkala, M. Kuussaari, and G. Lei. Metapopulation persistence of an endangered butterfly in a fragmented landscape. *Oikos*, pages 21–28, 1995.

[37] I. Hanski, T. Schulz, S. C. Wong, V. Ahola, A. Ruokolainen, and S. P. Ojanen. Ecological and genetic basis of metapopulation persistence of the Glanville fritillary butterfly in fragmented landscapes. *Nature Communications*, 8:14504, 2017.

[38] M. P. Hassell, H. N. Comins, and R. M. May. Spatial structure and chaos in insect population dynamics. *Nature*, 353(6341):255–258, 1991.

[39] A. Hastings. Structured models of metapopulation dynamics. *Biological Journal of the Linnean Society*, 42(1-2):57–71, 1991.

[40] C. A. Johnson, J. M. Fryxell, I. D. Thompson, and J. A. Baker. Mortality risk increases with natal dispersal distance in American martens. *Proceedings of the Royal Society of London B: Biological Sciences*, pages 3361–3367, 2009.

[41] M. L. Johnson and M. S. Gaines. Evolution of dispersal: theoretical models and empirical tests using birds and mammals. *Annual Review of Ecology and Systematics*, 21(1):449–480, 1990.

[42] P. Kareiva and U. Wennergren. Connecting landscape patterns to ecosystem and population processes. *Nature*, 373(6512):299–302, 1995.

[43] T. R. Karl and K. E. Trenberth. Modern global climate change. *Science*, 302(5651): 1719–1723, 2003.

[44] H. Kokko and A. López-Sepulcre. From individual dispersal to species ranges: perspectives for a changing world. *Science*, 313(5788):789–791, 2006.

[45] H. Kokko, R. A. Johnstone, and T. H. Clutton-Brock. The evolution of cooperative breeding through group augmentation. *Proceedings of the Royal Society of London B: Biological Sciences*, 268(1463):187–196, 2001.

[46] W. S. LaHaye, R. Gutiérrez, and H. R. Akcakaya. Spotted owl metapopulation dynamics in southern california. *Journal of Animal Ecology*, pages 775–785, 1994.

[47] S. A. Levin. Dispersion and population interactions. *The American Naturalist*, 108(960): 207–228, 1974.

[48] R. Levins. Some demographic and genetic consequences of environmental heterogeneity for biological control. *Bulletin of the Entomological Society of America*, 15(3):237–240, 1969.

[49] R. H. MacArthur and E. O. Wilson. The theory of island biogeography. Technical report, 1967.

[50] M. B. Main, F. M. Roka, and R. F. Noss. Evaluating costs of conservation. *Conservation Biology*, 13(6):1262–1272, 1999.

[51] R. M. May. The effects of spatial scale on ecological questions and answers. *Large-scale Ecology and Conservation Biology*, pages 1–17, 1994.

[52] R. E. Michod and W. D. Hamilton. Coefficients of relatedness in sociobiology. *Nature*, 288(5792):694, 1980.

[53] S. A. Montzka, E. J. Dlugokencky, and J. H. Butler. Non-CO2 greenhouse gases and climate change. *Nature*, 476(7358):43, 2011.

[54] S. Nee. Mutualism, parasitism and competition in the evolution of coviruses. *Philosophical Transactions of the Royal Society of London B: Biological Sciences*, 355(1403): 1607–1613, 2000.

[55] S. Nee and R. M. May. Dynamics of metapopulations: habitat destruction and competitive coexistence. *Journal of Animal Ecology*, pages 37–40, 1992.

[56] S. Nee, M. P. Hassell, and R. M. May. *Two-species metapopulation models*, chapter 6, pages 123–147. Elsevier Inc., 1997.

[57] R. P. Neilson, L. F. Pitelka, A. M. Solomon, R. Nathan, G. F. Midgley, J. M. Fragoso, H. Lischke, and K. Thompson. Forecasting regional to global plant migration in response to climate change. *AIBS Bulletin*, 55(9):749–759, 2005.

[58] B. R. Noon and K. S. McKelvey. Stability properties of the spotted owl metapopulation in southern california. In J. Verner, K. S. McKelvey, B. R. Noon, R. Gutierrez, G. I. J. Gould, and T. W. Beck, editors, *The California spotted owl: a technical assessment of its current status. Gen. Tech. Rep. PSW-GTR-133.*, chapter 9, pages 187–206. Pacific Southwest Research Station, Forest Service, US Department of Agriculture, Albany, CA, 1992.

[59] V.-M. Pakanen, K. Koivula, M. Orell, S. Rytkönen, and K. Lahti. Sex-specific mortality

costs of dispersal during the post-settlement stage promote male philopatry in a resident passerine. *Behavioral Ecology and Sociobiology*, 70(10):1727–1733, 2016.

[60] K. Parvinen. Evolution of migration in a metapopulation. *Bulletin of Mathematical Biology*, 61(3):531–550, 1999.

[61] K. Parvinen. Evolution of dispersal in a structured metapopulation model in discrete time. *Bulletin of Mathematical Biology*, 68(3):655–678, 2006.

[62] K. Parvinen, U. Dieckmann, M. Gyllenberg, and J. A. Metz. Evolution of dispersal in metapopulations with local density dependence and demographic stochasticity. *Journal of Evolutionary Biology*, 16(1):143–153, 2003.

[63] H. Rodhe. A comparison of the contribution of various gases to the greenhouse effect. *Science*, 248(4960):1217–1219, 1990.

[64] D. Roff. The analysis of a population model demonstrating the importance of dispersal in a heterogeneous environment. *Oecologia*, 15(3):259–275, 1974.

[65] D. Roff. Dispersal in Dipterans: its costs and consequences. *Journal of Animal Ecology*, pages 443–456, 1977.

[66] D. A. Roff. Why is there so much variation for wing dimorphism? *Researches on Population Ecology*, 36:145–150, 1994. doi: 10.1007/BF02514929.

[67] O. Ronce. How does it feel to be like a rolling stone? ten questions about dispersal evolution. *Annual Review of Ecology, Evolution, and Systematics*, 38:231–253, 2007.

[68] O. Ronce, S. Gandon, and F. Rousset. Kin selection and natal dispersal in an age-structured population. *Theoretical Population Biology*, 58:143–159, 2000. doi: 10.1006/tpbi.2000.1476.

[69] O. Ronce, S. Brachet, I. Olivieri, P.-H. Gouyon, and J. Clobert. Plastic changes in seed dispersal along ecological succession: theoretical predictions from an evolutionary model. *Journal of Ecology*, 93(2):431–440, 2005.

[70] P. Saenz-Agudelo, G. P. Jones, S. R. Thorrold, and S. Planes. Connectivity dominates larval replenishment in a coastal reef fish metapopulation. *Proceedings of the Royal Society of London B: Biological Sciences*, 278(1720):2954–2961, 2011.

[71] D. A. Saunders, R. J. Hobbs, and C. R. Margules. Biological consequences of ecosystem fragmentation: a review. *Conservation Biology*, 5(1):18–32, 1991.

[72] D. Simberloff, J. A. Farr, J. Cox, and D. W. Mehlman. Movement corridors: conservation bargains or poor investments? *Conservation Biology*, 6(4):493–504, 1992.

[73] B. Sinervo and J. Clobert. Morphs, dispersal behavior, genetic similarity, and the evolution of cooperation. *Science*, 300(5627):1949–1951, 2003.

[74] P. Sjögren-Gulve and C. Ray. Using logistic regression to model metapopulation dynamics: large-scale forestry extirpates the pool frog. In D. R. McCullough, editor, *Metapopulations and wildlife conservation*, pages 111–138. Island Press, Washington, D.C., 1996.

[75] N. G. Solomon and J. A. French. *Cooperative breeding in mammals*. Cambridge University Press, 1997.

[76] N. C. Stenseth. How to control pest species: application of models from the theory of island biogeography in formulating pest control strategies. *Journal of Applied Ecology*, pages 773–794, 1981.

[77] A. D. Taylor. Metapopulations, dispersal, and predator-prey dynamics: an overview. *Ecology*, 71(2):429–433, 1990.

[78] C. M. Taylor and R. J. Hall. Metapopulation models for seasonally migratory animals. *Biology Letters*, page rsbl20110916, 2011.

[79] P. D. Taylor. An inclusive fitness model for dispersal of offspring. *Journal of Theoretical Biology*, 130:363–378, 1988. doi: 10.1016/S0022-5193(88)80035-3.

[80] P. D. Taylor and S. A. Frank. How to make a kin selection model. *Journal of Theoretical Biology*, 180(1):27–37, 1996.

[81] P. D. Taylor, G. Wild, and A. Gardner. Direct fitness or inclusive fitness: how shall we model kin selection? *Journal of Evolutionary Biology*, 20(1):301–309, 2007.

[82] X. Thibert-Plante and A. Hendry. Five questions on ecological speciation addressed with individual-based simulations. *Journal of Evolutionary Biology*, 22(1):109–123, 2009.

[83] S. C. Trombulak and C. A. Frissell. Review of ecological effects of roads on terrestrial and aquatic communities. *Conservation Biology*, 14(1):18–30, 2000.

[84] I. Turner. Species loss in fragments of tropical rain forest: a review of the evidence. *Journal of Applied Ecology*, pages 200–209, 1996.

[85] P. M. Vitousek, J. D. Aber, R. W. Howarth, G. E. Likens, P. A. Matson, D. W. Schindler, W. H. Schlesinger, and D. G. Tilman. Human alteration of the global nitrogen cycle: sources and consequences. *Ecological Applications*, 7(3):737–750, 1997.

[86] P. M. Vitousek, H. A. Mooney, J. Lubchenco, and J. M. Melillo. Human domination of earth's ecosystems. *Science*, 277(5325):494–499, 1997.

[87] S. Wang, B. Haegeman, and M. Loreau. Dispersal and metapopulation stability. *PeerJ*, 3:e1295, 2015.

[88] J. V. Wells and M. E. Richmond. Populations, metapopulations, and species populations: what are they and who should care? *Wildlife Society Bulletin (1973-2006)*, 23(3):458–462, 1995.

[89] G. E. Woolfenden and J. W. Fitzpatrick. *The Florida scrub jay: demography of a cooperative-breeding bird*, volume 20. Princeton University Press, 1984.

Chapter 2

Dispersal Altering Local States Has a Limited Effect on Persistence of a Metapopulation

2.1 Introduction

Many species occupy patchy habitats, existing as a collection of local populations separated from one another in space, but linked via dispersal [6]. Understanding the dynamics of these collections of local populations, or 'metapopulations', is especially important to conservation efforts, because landscapes have become increasingly fragmented due to human activities [28]. Indeed, a number of mathematical models have been used to predict the conditions under which global (cf. local) extinction of metapopulations can occur.

Levins [15] provided the seminal model of metapopulation dynamics. His is a two-compartment model that classifies local populations as either empty (extinct) or occupied. It predicts that a metapopulation will persist only when the rate of local extinction is outstripped by the rate of recolonizations by dispersers from occupied areas. If, instead, the local extinction rate happens to exceed the rate of recolonization, then Levins' model predicts extinction

on a global scale.

Since Levins' work [15], many more details have been incorporated into metapopulation models. Hanski [8], for example, recognized that small local populations are quite vulnerable to extinction, and that emigrants from larger local populations can be a particularly important source of colonists. To capture these ideas, Hanski [8] developed a three-compartment model that subdivides occupied local populations according to their sizes (small versus large). This more elaborate model, and others like it [e.g. 9], predict that the persistence of a metapopulation and its global extinction can be alternative steady states under a limited range of conditions. In other words, a stable metapopulation could be pushed to global extinction due to a sufficiently large reduction in the population size; this represents a significant departure from the original predictions made by Levins [15].

One assumption common to metapopulation models, like those proposed by Levins and Hanski, is that dispersal from a given source population, during the course of a colonization event, does not diminish the quality of the source itself [see 1, 18, 29]. In particular, dispersal of colonists from a source population does not render the source, itself, any more vulnerable to extinction. While this assumption is convenient, it may not be reasonable, especially if local population sizes are small, or if local population dynamics highly depends on the maintenance of certain social bonds (e.g. socializing between potential mates, or socializing between breeders and helpers in the nest) [14, 26].

In this paper we ask, to what extent is the persistence of a metapopulation impacted when the dispersal associated with colonization events results in a source population of diminished quality? To answer the question, we propose a simple model of a metapopulation in which local populations are made up of small numbers of individuals, with distinct social roles. We use our model to identify the conditions under which global extinction of the metapopulation can occur or be avoided. Our analysis is focused on (but not solely dedicated to) the effect of dispersal rate, as dispersal events fuel colonization in a metapopulation, and have the potential to reduce the quality of those source populations which colonists leave behind. Surprisingly,

we find that the impact of dispersal, as we have modelled it, is limited. This, in turn, suggests that the standard approach is likely useful when modelling metapopulations consisting of small concentrations of social species. We discuss the implication of our findings for natural populations, and their broader significance in light of model limitations.

2.2 Model

2.2.1 Preamble

In sections 2.2-2.4, we build a four-compartment model of metapopulation dynamics aimed at understanding the demographic and social mechanisms that drive local extinction and recolonizations in a metapopulation. Like previous authors [8, 9], we recognize that rates of extinction and recolonization depend on the different kinds of occupied areas found in a metapopulation. Unlike previous authors, though, the way in which we classify local populations will vary according to the social status of individuals. In particular, this means that certain social roles must be filled in order for key demographic events to occur, and we expect metapopulation dynamics to change to some degree as a result.

2.2.2 Main Assumptions

We consider a metapopulation made up of a very large number of territories. Each territory in the metapopulation can support at most two dominant individuals (as a breeding pair), with at most one non-breeding subordinate individual. In keeping with the conclusions of removal experiments with cooperatively breeding delayed dispersers [20], we assume if a subordinate happens to be found on a territory alongside only one dominant, the subordinate would immediately be recruited to the dominant class. It follows that any territory will be found in one of the four states: state 0, an empty territory; state 1, a territory with exactly one dominant and no subordinate; state 2, a territory with exactly two dominants and no subordinate; state 3, a

saturated territory with exactly two dominants and one subordinate.

At time t, the state of the entire metapopulation is $n(t) = (n_0(t), n_1(t), n_2(t), n_3(t))$, where $n_i(t)$ is the density (or number) of state-i territories. The metapopulation changes its state as a result of events associated with demographic processes, including mortality, birth, and dispersal. We discuss each demographic process, in turn, below.

2.2.3 Demographic Processes

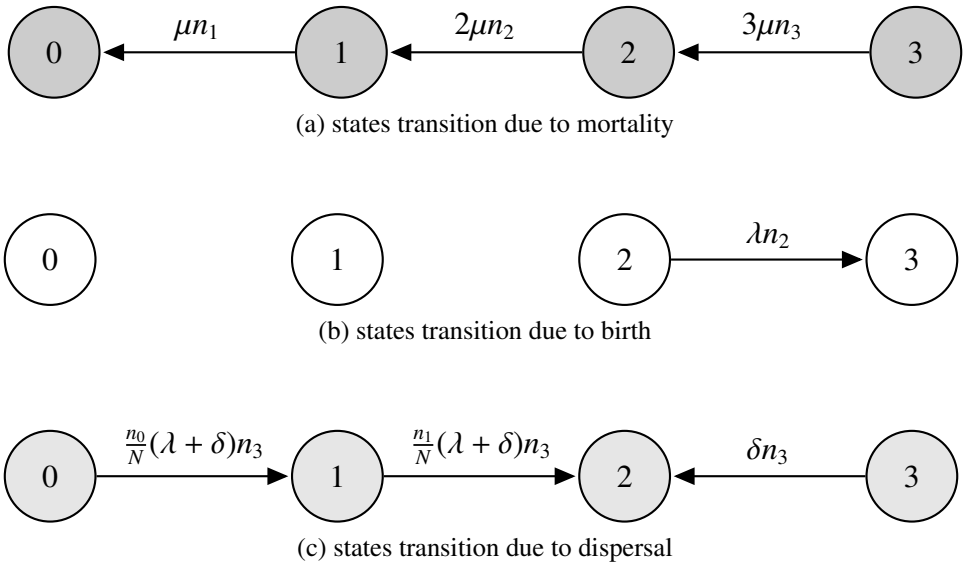

(a) states transition due to mortality

(b) states transition due to birth

(c) states transition due to dispersal

Figure 2.1: Transitions among territory states. The demographic processes lead to state transitions: (a) due to mortality, (b) due to birth, (c) due to dispersal. Note that arrows associated with mortality are all pointing to the left, arrows associated with birth are all pointing to the right, but arrows associated with dispersal are not of the same direction. Here, the total number of territories is $N = n_0 + n_1 + n_2 + n_3$.

Mortality

Each individual suffers mortality at rate of $\mu > 0$ per unit time. Mortality of individuals on a state-$i > 0$ territory implies a transition to state $i - 1$ (Figure 2.1a). As is clear from the figure 2.1a, the directions of arrows related to mortality rate are all pointing to left, which implies increasing mortality will promote global extinction.

Birth

A pair of dominant individuals gives birth at rate $\lambda > 0$ per unit time. If the dominant pair inhabits a state-2 territory, any newborn they produce immediately becomes a subordinate on the same territory. In this case, the state-2 territory transitions to state 3 (Figure 2.1b). While it is true that birth events occur on state-3 territories, newborns produced on those saturated territories are assumed to migrate; the associated state transitions are discussed below. In figure 2.1b and 2.1c, the directions of arrows due to birth are all pointing right, meaning that birth promotes persistence of metapopulation.

Dispersal

A subordinate individual emigrates from a state-3 territory at rate $\delta > 0$ per unit time. In addition, individuals born on a state-3 territory are assumed to emigrate at the moment of their birth (equivalently, the incumbent subordinate migrates the moment the birth event takes place and the newborn remains). Upon leaving a state-3 territory, an emigrant travels to a new territory, chosen uniformly at random, in an attempt to fill a dominant vacancy. If an emigrant chooses to travel to a territory with no dominant vacancy, that emigrant is assumed to die. In this way, dispersal is risky. In Figure 2.1c arrows associated with dispersal are not of the same direction, so the effect of dispersal on persistence of metapopulation is not obvious. This is indeed the basic motivation of this paper.

Our model of dispersal is consistent with the social behaviours of certain cooperatively breeding species who reject non-kin when these outsiders attempt to join their groups. Broadly speaking, the rejection of non-kin is predicted to occur whenever the group in question is in its most productive state (for example, groups that are in state 2) [22]. Our model of dispersal also leads to kin-based social groups which is consistent with a number of studies of avian cooperative breeding [see 10]. Of course, allowing only kin to join certain social groups does lead to inbreeding, but certain social species are known to tolerate inbreeding to some degree [19].

Overall, dispersal contributes to the transitions of territories from state 3 to state 2, from state 1 to state 2, and from state 0 to state 1 (Figure 2.1c). Importantly, transitions from state 3 to 2 at one locale can be linked to changes from state 1 to 2, or 0 to 1, at another locale. In this way, our model differs from earlier ones [8, 9] that treat the degradation in quality of local environments as independent events.

2.2.4 Dynamics

ODE System

Combining the processes given in Figures 2.1a-2.1c, we obtain the following ODEs for n_0 to n_3, respectively:

$$\begin{aligned}
\frac{dn_0}{dt} &= \mu n_1 - \frac{n_0}{N}(\lambda+\delta)n_3, \\
\frac{dn_1}{dt} &= -\mu n_1 + \frac{n_0}{N}(\lambda+\delta)n_3 + 2\mu n_2 - \frac{n_1}{N}(\lambda+\delta)n_3, \\
\frac{dn_2}{dt} &= (3\mu+\delta)n_3 - \lambda n_2 - 2\mu n_2 + \frac{n_1}{N}(\lambda+\delta)n_3, \\
\frac{dn_3}{dt} &= -(3\mu+\delta)n_3 + \lambda n_2,
\end{aligned} \tag{2.1}$$

where the total number of territories is $N = n_0 + n_1 + n_2 + n_3$. Note that $\frac{dN}{dt} = 0$, so the total density is a constant. We then nondimensionalize the system (2.1) using $w = \frac{n_0}{N}, x = \frac{n_1}{N}, y = \frac{n_2}{N}, z = \frac{n_3}{N}, \tau = t\lambda$, so it becomes

$$\begin{aligned}
\dot{w} &= mx - (1+d)wz, \\
\dot{x} &= -mx + (1+d)wz + 2my - (1+d)xz, \\
\dot{y} &= -y + (3m+d)z - 2my + (1+d)xz, \\
\dot{z} &= y - (3m+d)z,
\end{aligned}$$

where $m = \frac{\mu}{\lambda}$ is the nondimensionalized mortality rate of an individual, $d = \frac{\delta}{\lambda}$ is the nondimensionalized dispersal rate of a subordinate individual, and dots denote derivatives with respect to τ. Note that w, x, y, z are fractions of territories in a given state (state 0, state 1, state 2, state 3, respectively), and that τ marks time in terms of birth events ($\tau = 1$ when $t = \frac{1}{\lambda}$). Using $w + x + y + z = 1$ the previous system can be reduced to our final, three-dimensional system

$$\begin{aligned} \dot{x} &= -mx + (1+d)(1-x-y-z)z + 2my - (1+d)xz, \\ \dot{y} &= -y + (3m+d)z - 2my + (1+d)xz, \\ \dot{z} &= y - (3m+d)z. \end{aligned} \tag{2.2}$$

We present our analysis of the system (2.2) here, but numerical calculations are also outlined in the computer code included as supplemental files (see Appendix C.1).

Forward invariance of the system

Before exploring further properties of the system, we present a proposition that serves, for now, as a check on correctness of system (2.2). Of course, solutions that track fractions of some population ought to stay bounded within the simplex. Proposition 1 shows that this is true of solutions to the ODEs proposed above.

Proposition 1 *Solutions to* (2.2)*, paired with an initial condition, remain in the region*

$$C = \{(x, y, z) | x + y + z \leq 1,\ 0 \leq x, y, z \leq 1\},$$

as long as the initial condition is in the region C.

Proof We need only check that the dot product between the inward-pointing normal to C and the vector field $(\dot{x}, \dot{y}, \dot{z})$ is non-negative on boundaries of C.

Note that there are four sets that make up boundaries of C (its 'faces'). Those includes $x+y+z = 1$, $x = 0$, $y = 0$ and $z = 0$. On the face $x+y+z = 1$, the normal vector is $(-1, -1, -1)$,

which is pointing inward the region C. Then, we can get $(-1,-1,-1)\cdot(\dot{x},\dot{y},\dot{z}) = mx \geq 0$, which means the flow on the edge cannot cross the boundary. On the face $x = 0$, the normal vector is $(1,0,0)$ pointing inward, and $(1,0,0)\cdot(\dot{x},\dot{y},\dot{z})|_{x=0} = z(1-y-z)(d+1)+2my \geq 0$. Similar proof can be obtained on the other two faces $y = 0$ and $z = 0$.

2.3 Results

Focusing on system (2.2), it is obvious that there is an extinction equilibrium (when $(x,y,z) = (0,0,0)$), that always exists. As the reader will see, two additional (positive) equilibria may also exist, depending on the demographic parameters. We will investigate the stability of the extinction equilibrium in Section 2.3.1, and the existence and the stability of positive equilibria will be discussed in Section 2.3.2. We also study the effect of changing d and m on the persistence of metapopulation in Section 2.3.2.

2.3.1 Extinction Equilibrium

The vector $E_0 = (x,y,z) = (0,0,0)$ is an equilibrium solution to system (2.2). At this equilibrium, all of the territories are at state 0, so the species is absent from the metapopulation, and we call E_0 the 'extinction equilibrium'. To verify that the equilibrium is *locally asymptotically stable* (LAS), we consider the 3×3 Jacobian matrix, constructed by linearizing (2.2) about E_0:

$$J_{E_0} = \begin{bmatrix} -m & 2m & d+1 \\ 0 & -2m-1 & d+3m \\ 0 & 1 & -(d+3m) \end{bmatrix}.$$

We can see one of the eigenvalues of J_{E_0} is $-m < 0$. The sign of real part of the other two eigenvalues depends on the trace and determinant of a 2×2 matrix located in the lower right corner of J_{E_0}. The trace of that 2×2 submatrix is $-2m-1-(d+3m) < 0$, and its determinant is $2(d+3m)m > 0$, so the remaining two eigenvalues both have negative real part. It follows,

from the Routh-Hurwitz criteria [see, e.g. 4], that all of the eigenvalues of J_{E_0} have negative real parts, so the extinction equilibrium E_0 is LAS. Whether E_0 is globally asymptotically stable depends on the parameters, because there could be other equilibria. Hence, we have only the following proposition, in general.

Proposition 2 *For system* (2.2)*, there always exists a trivial extinction equilibrium, which is locally asymptotically stable.*

Proposition 2 distinguishes our model from earlier ones [8, 9] in that the extinction equilibrium in our model is stable for all parameters, not a subset of all parameters. We discuss this proposition in the final section.

2.3.2 Positive Equilibria

If $z = 0$, then the extinction equilibrium is the only steady-state solution to (2.2). Biologically speaking, $z = 0$ means there is no territory with a breeding pair and a subordinate, so there are not enough offspring being produced and subordinates to fill vacancies, which leads to the extinction of the population. When investigating the possibility of positive equilibria, then, we ought to consider $z \neq 0$ only.

If $z \neq 0$, then a positive equilibrium, if it exists, satisfies

$$\begin{aligned} -mx + (1+d)(1-x-y-z)z + 2my - (1+d)xz &= 0, \\ -y + (d+3m)z - 2my + (1+d)xz &= 0, \\ y - (d+3m)z &= 0, \end{aligned}$$

which is equivalent to

$$\begin{aligned} -mx + (1+d)(1-x-y-z)z &= 0, \\ -2my + (1+d)xz &= 0, \\ y - (d+3m)z &= 0. \end{aligned} \tag{2.3}$$

Using the last two equations in (2.3) we can express x and y in terms of z:

$$x = \frac{2(d+3m)m}{1+d}, y = (d+3m)z. \tag{2.4}$$

Substituting (2.4) into the first equation in (2.3), we obtain a quadratic equation for the equilibrium density of state-3 territories z. This can be solved to get,

$$z_{\pm} = \frac{d+1-2(d+3m)m \pm \sqrt{D}}{2(d+3m+1)(d+1)}, \tag{2.5}$$

where

$$D = (d+1-2(d+3m)m)^2 - 8m^2(d+3m)(d+3m+1) \tag{2.6}$$

is the discriminant. Of course, when $D > 0$, we have $0 < z_{\pm} < 1$ and the corresponding two positive equilibria using equations (2.4) and (2.5). We denote the two positive equilibria as $E_- = (x, y(z_-), z_-)$ and $E_+ = (x, y(z_+), z_+)$, respectively. When $D < 0$, there is no solution with real values. When $D = 0$, the two equilibria coincide, i.e. $z_+ = z_- = (d+1-2(d+3m)m)/(2(d+3m+1)(d+1))$, and we will not concern ourselves with stability. Indeed, it is the case $D > 0$ that concerns us in the proposition that follows.

Proposition 3 *System* (2.2) *has two positive equilibria if and only if* $D > 0$ *is satisfied. The equilibrium corresponding to a larger population size is locally asymptotically stable; the other is unstable.*

Proof The existence of two positive equilibria, when $D > 0$, has been shown above, so we only need to examine their stability. The claims about local stability can be proven by investigating the linearization of the system (2.2) about the corresponding positive equilibrium. The

characteristic polynomial associated with the operator from the aforementioned linearization is

$$f(\nu) = \begin{vmatrix} \nu + 2(d+1)z + m & (d+1)z - 2m & (d+1)(2x + y + 2z - 1) \\ -(d+1)z & \nu + 2m + 1 & -(d+1)x - (d+3m) \\ 0 & -1 & \nu + (d+3m) \end{vmatrix}.$$

Using equations (2.4), we simplify the polynomial and get

$$\begin{aligned} f(\nu) &= \nu^3 + \underbrace{\Big[2(d+1)z + (d+3m) + 3m + 1\Big]}_{=k_1}\nu^2 \\ &\quad + \underbrace{\Big[(d+1)^2z^2 + 2\,(d+1)(d+4m+1)z + m(d+5m+1)\Big]}_{=k_2}\nu \\ &\quad + \underbrace{\Big[2(d+1)z((d+1)(d+3m+1)z + (2(d+3m)m - (d+1)))\Big]}_{=k_3}. \end{aligned} \tag{2.7}$$

If the real parts of each of the roots of the polynomial are negative, then the equilibrium is locally asymptotically stable. The Routh-Hurwitz criteria for polynomials like (2.7) declares that all the roots of the equation have negative real parts if and only if each of $k_1 > 0, k_3 > 0$ and $k_1k_2 - k_3 > 0$ hold. For our polynomial, the three conditions are,

$$2(d+1)z + (d+3m) + 3m + 1 > 0, \tag{2.8a}$$

$$\Big[2(d+1)z + (d+3m) + 3m + 1\Big]\Big[(d+1)^2z^2 + 2\,(d+1)(d+4m+1)z + m(d+5m+1)\Big]$$

$$-\Big[2(d+1)z((d+1)(d+3m+1)z + (2(d+3m)m - (d+1)))\Big] > 0, \tag{2.8b}$$

$$2(d+1)z\Big[(d+1)(d+3m+1)z+(2(d+3m)m-(d+1))\Big]>0. \tag{2.8c}$$

It is obvious that the condition (2.8a) holds for all $z > 0$, because all parameters d, m are positive.To prove condition (2.8b) holds, we can partially expand the left-hand side of the expression to get,

$$\begin{aligned}
&2\ (d+1)^3 z^3+(3\,(d+3m)+7\,m+3)\,(d+1)^2 z^2\\
&+\Big(d+10\,m^2+2\ (4\,(d+3m)+5)\,m+2\,(d+3m)^2+4\,(d+3m)+3\Big)\,(d+1)\,z\\
&+m\,((d+3m)+3\,m+1)\,((d+3m)+2\,m+1)\,.
\end{aligned}$$

This is also positive for positive parameters d, m and nonnegative variable z. Since $z_\pm > 0$, it is true that both equilibria satisfy the condition (2.8a) and condition (2.8b).

As for the condition (2.8c), it is equivalent to $(d+1)(d+3m+1)z+(2(d+3m)m-(d+1)) > 0$, or

$$z > \frac{d+1-2(d+3m)m}{(d+1)(d+3m+1)}. \tag{2.9}$$

We then have

$$z_+ = \frac{d+1-2(d+3m)m+\sqrt{D}}{2(d+3m+1)(d+1)} > \frac{d+1-2(d+3m)m}{2(d+3m+1)(d+1)} > \frac{d+1-2(d+3m)m-\sqrt{D}}{2(d+3m+1)(d+1)} = z_-,$$

for $D > 0$. So, for $z = z_+$, the condition (2.8c) holds, and the equilibrium associated with $z = z_+$ is LAS. For $z = z_-$, the condition (2.8c) fails as the reverse inequality, so the equilibrium associated with z_- is unstable.

The consequences of propositions 2 and 3 for the bifurcation of solutions to system (2.2) are illustrated in Figure 2.2. In Figure 2.2, we use the discriminant D as a bifurcation parameter. If $D < 0$, we see that there is only one equilibrium, the extinction equilibrium, E_0, and it

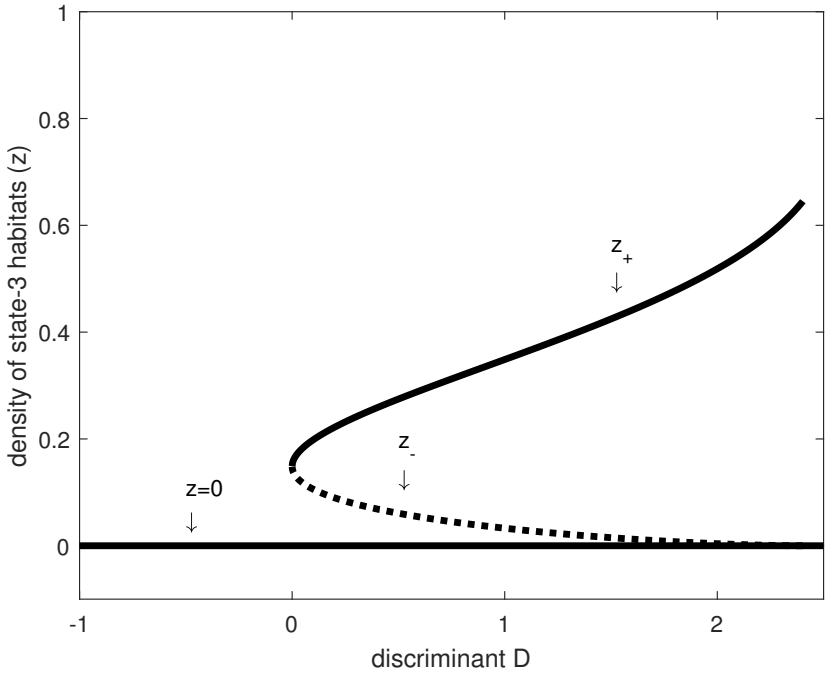

Figure 2.2: The bifurcation diagram of system (2.2). The equilibrium proportions of state-3 territories, generically denoted as z, change with increasing discriminant D, as does their respective stability properties. In the figure, $z = 0$ and z_+, correspond to locally stable equilibria E_0 and E_+, respectively, and are shown in solid lines. The value z_- corresponds to the locally unstable equilibrium, E_-, is shown as the dotted line. We obtain the corresponding values of the discriminant D and $z_\pm$, by fixing the dispersal rate d as a constant, and changing the mortality rate m.

is stable. At $D = 0$ a bifurcation occurs, and for $D > 0$ we see the appearance of a stable equilibrium (denoted E_+ in Figure 2.2) corresponding to z_+ and an unstable equilibrium (denoted E_- in Figure 2.2) corresponding to z_-. In biological terms, $D = 0$ can be viewed as a 'tipping point' [sensu 21] since any demographic or life-history changes that take D below zero also result in guaranteed extinction of the metapopulation.

At the tipping point $D = 0$, itself, the characteristic polynomial (2.7) has a zero root. By continuity, this means that near-equilibrium dynamics close to the tipping point will be dominated by small eigenvalues. Therefore we expect to see a critical slowing down for population density to get back to the stable positive equilibrium after perturbation [21]. In turn, that critical slowing down implies that, in a natural setting, perturbations of the stable equilibrium would

take longer to be corrected in those systems nearer to $D = 0$ (Figure 2.3), which might be an early sign that efforts to conserve the metapopulation need to be increased.

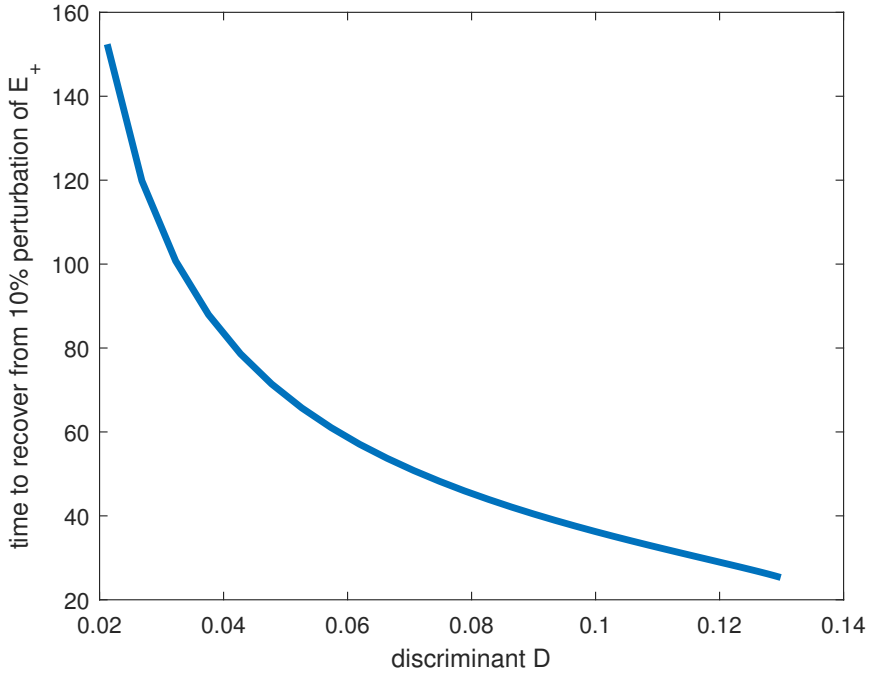

Figure 2.3: The relationship between the time required to recover from a 10% perturbation from E_+ and the discriminant D. We fix the mortality rate m as a constant, and change the dispersal rate d, to obtain corresponding values of correction time and the discriminant D. Other computational details included in supplementary files.

Close to this tipping point $D = 0$, we observe how the metapopulation can be affected by changing mortality rate and dispersal rate. For any given value of d, increasing mortality rate m will eventually lead the metapopulation to lose its stable positive equilibrium and go extinct, because $\frac{\partial D}{\partial m} < 0$ for all m and d (Figure 2.4 when d is a constant).

For given values of m, increasing dispersal rate d can have mixed effects on the metapopulation. Three cases are summarised as following (Figure 2.4). Firstly, if $m < m_1 = (\sqrt{2} - 1)/2$, then changing D does not change the sign of D, because $\frac{\partial D}{\partial d} > 0$ for all $d > 0$ with $D(m, 0) > 0$. So the metapopulation always has a stable positive equilibrium, and it always has a chance to persist. Secondly, if m is between m_1 and m_0, then increasing d will eventually push the metapopulation to extinction because $\frac{\partial D}{\partial d}\Big|_{D(d,m)=0} < 0$. Thirdly, if $m > m_0$, increasing d will not

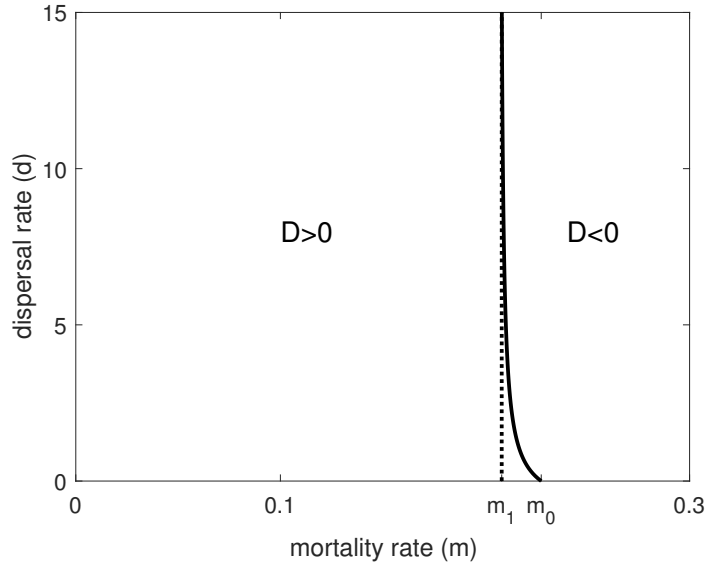

(a)

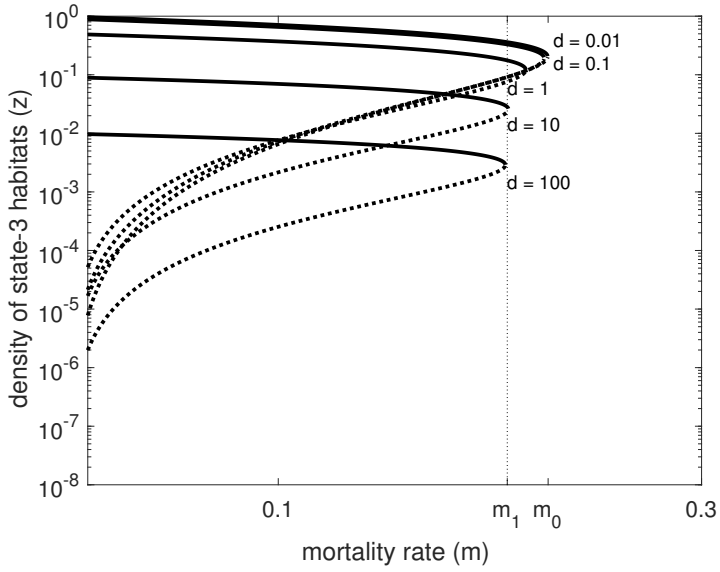

(b)

Figure 2.4: (a) The relationship between the sign of the discriminant D and parameters d and m. The solid curve is the contour of $D(d, m) = 0$. (b) The relationship between the equilibria (represented by equilibrium value of state-3 territories, $z_{\pm}$) and parameters and m, for various values of d.

change the sign of D, which stays negative. Overall, $m_0 - m_1$ gives the range of mortality rates over which we observe the negative effect of increasing d. Importantly, this range is small relative to the width of the region to the left of m_1, where increasing d does not affect the existence of E_+ (Figure 2.4). In sum, for the vast majority of parameter combinations, changing d does not bring populations closer to $D = 0$, and so does not bring them closer to extinction.

Figure 2.2 also suggests that there is a second kind of tipping point predicted by our model, when the metapopulation is to the right of the bifurcation ($D > 0$ in Figure 2.2). Specifically, the tipping point is a set (possibly a surface) that separates the basins of attraction for E_0 and E_+, respectively, on which we find E_- (Figure 2.5). This set is called the separatrix and usually consists of the stable manifold of the unstable equilibrium. This second kind of tipping

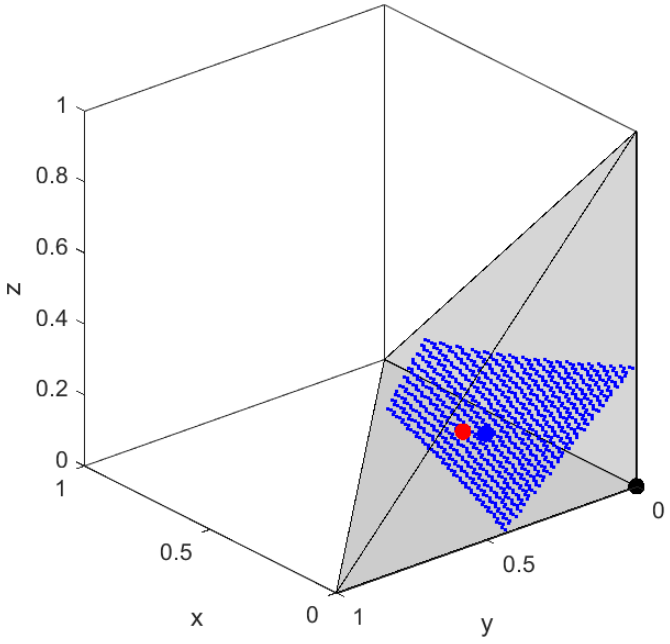

Figure 2.5: The boundary between the basin of attraction for E_0 and that for E_+. The boundary itself is shown as a dotted blue surface. Equilibria E_0 and E_+ are shown as the black dot and the red dot, respectively. The unstable equilibrium E_- is shown as the large blue dot on the boundary surface.

point has been identified in other metapopulation models, and is linked to an Allee effect, i.e. negative population growth below some density threshold [1, 18]. In our model, the tipping

point can be avoided in stable populations provided perturbations remain inside the basin of attraction for E_+ (region above the boundary surface in Figure 2.5).

Unfortunately, neither Figure 2.2 nor Figure 2.5 can clarify the effect of changing d on the volume of the basin of attraction for E_+. To take a more detailed look at the second kind of tipping point, we investigate the volume of the basin of attraction of E_+ and how it is affected by the change of demographic parameters d given m. Since obtaining an explicit expression of the boundary surface is not possible, we introduce a numerical way to measure the fraction of the volume of the basin of attraction of E_+ in the phase space C. First, we generate 10^5 random triples (x_0, y_0, z_0) in $[0, 1]^3$ and use those satisfying $x_0 + y_0 + z_0 \leq 1$ as initial conditions. From the initial conditions, we solve (2.2) using the Runge-Kutta-Fehlberg (RKF) method (see Appendix C.1.7). If the solution ends up in a small neighbourhood surrounding E_+ (resp. E_0), then the corresponding initial condition is assigned to the basin of attraction for E_+ (resp. E_0). We utilise Proposition 1 in numerical simulations: if solutions leave the region C, we attribute their departure to numerical errors and discard them. We divide the number of initial points ending up in the neighbourhood of E_+ (E_0, respectively) by the total number of valid initial points, and get the fraction of C that corresponds to the basin of attraction for each of E_+ and E_0. We are interested in the persistence of metapopulation, so we report the fraction of C that corresponds to the basin of attraction for E_+ in Figure 2.6. Numerical solution of (2.2) reveals a negative relationship between the value of $d > 0$ and the volume of the basin of attraction of E_+ (Figure 2.6b). Increasing dispersal rate only changes the volume of basin of attraction of E_+ dramatically in a narrow range where bifurcation occurs. It is obvious that for most of parameter space, change in dispersal rate does not significantly affect the metapopulation dynamics (the regions with constant mortality rate remain the same color when changing dispersal rate in most of Figure 2.6a).

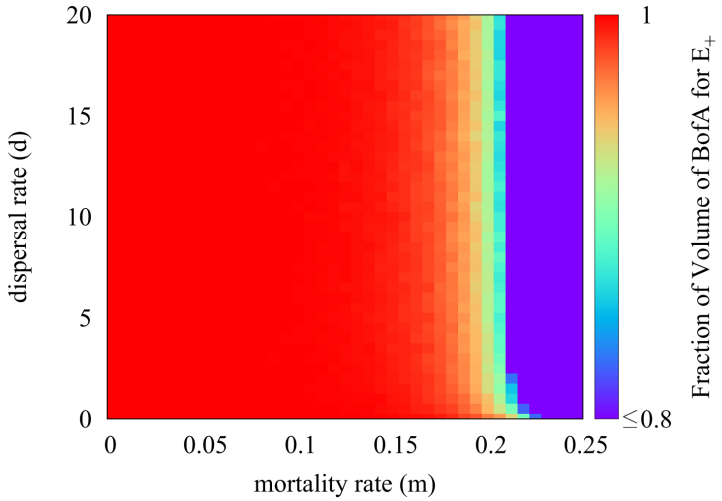

(a)

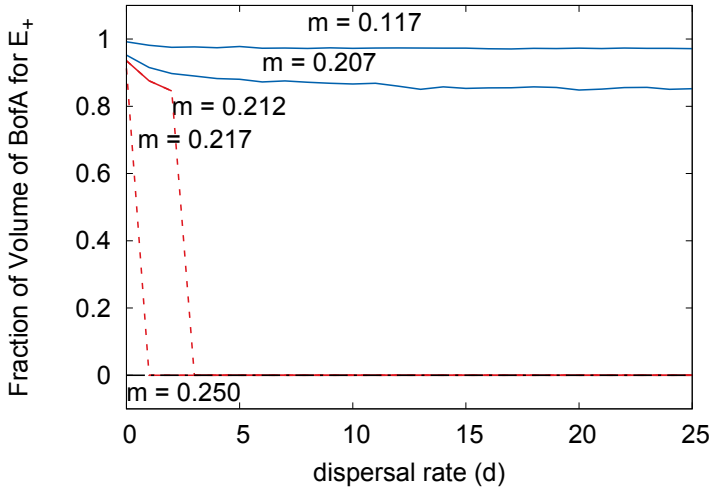

(b)

Figure 2.6: (a) Relationship between the volume of basin of attraction for the positive stable equilibrium E_+ and dispersal rate d and morality rate m (simulated results). (b) Five examples of the relationships in part (a) with specified values of m show the decreasing trend of the volume of basin of attraction, when increasing d.

2.4 Discussion

Metapopulation models describe how a balance between occupied and unoccupied habitat patches is, or is not, maintained by colonization and extinction events. Most of these models assume that would-be colonists do not alter the state of the patch they leave upon departure [see 1, 8, 9, 15, 18, 29]. When habitat patches are occupied by small numbers of individuals, however, dispersal by would-be colonists could leave a patch more susceptible to extinction associated with random events. If dispersal by individuals also disrupts social roles, then departure by colonists could have an even greater negative effect on the patches they leave behind.

In this paper we use a mathematical model to investigate how dispersal-associated state changes in a metapopulation might impact its dynamics. In particular, we are interested in extinction. In contrast to previous work [8, 9], our analysis shows that the extinction equilibrium is stable for all possible demographic conditions. The difference between our model and previous ones is due to the fact that successful colonization is a 'second-order' process. In our model, one colonist must be followed soon after by a second before reproduction can occur, and at low population densities this is very unlikely. Earlier models ignore the social complexities of the mating process, thereby allowing the extinction equilibrium to lose stability, under certain conditions.

Our model assumes local populations (patches) are occupied by small numbers of individuals, with distinct social roles. Admittedly, we make rigid assumptions about the way in which local populations are structured. However, our assumptions should emphasise, if not maximise, the influence of dispersal-related state changes on global dynamics. That said, our model predicts that dispersal from occupied patches, by socially subordinate individuals has limited impact on the global persistence of a metapopulation. While it is true that changing dispersal could, in some cases, tip the population toward (or away from) global extinction or make the population less robust in the face of perturbation, those cases represented only a very narrow range of parameter space. Our principal conclusion, then, is that dispersal-related state changes do not impact significantly on the long-term persistence of the metapopulation as a

whole. This does not mean that small local populations or social ties among neighbours play no role in metapopulation dynamics; rather, it means that the influence of dispersal is not as strong as the influence of other demographic processes like mortality.

The role played by dispersal in metapopulation dynamics is relevant to an on-going debate among conservation biologists about the use of dispersal corridors to prevent extinction [3, 5, 25]. On one hand, corridors are considered to be effective management tools because the movement they promote stems inbreeding depression, and is thought to reduce size variation among small local populations [23]. On the other hand, dispersal corridors may promote the spread of disease, introduce additional sources of mortality, and may otherwise be ineffective depending on the natural history of the species at risk [12, 24]. The resolution of the debate over the efficacy of dispersal corridors also has economic implications, as the construction of these corridors can cost several millions of dollars to establish and maintain [16, 25]. Insofar as conservation biologists are concerned with dispersal corridors impacting on the social lives of small local populations, our model's predictions can contribute to the resolution of the debate. In particular, we predict that any negative effects of dispersal would be observed in only a narrow range of background biological conditions. Provided corridors are used, our model indicates that concerns over the rate at which they are travelled are secondary to concerns about birth and mortality rates. Of course, movement corridors may benefit the metapopulation in some cases, and the demographic parameters should be monitored to assess the effectiveness of corridors. In that way, it is possible to reduce the cost-benefit ratio of investment for conservation.

Our conclusions should be tempered by the fact that our model, like all models, makes certain key assumptions. Perhaps the most important assumption we make is that demographic rates are fixed. Although this assumption is common in models of population dynamics, generally speaking, longevity and birth rates are understood as being shaped by selection [2]. Moreover, dispersal rate is expected to evolve [17], especially in response to social-evolutionary pressure imposed by small local-population [7, 13]. We have already identified a role for dis-

persal in a narrow range of parameter space. It is important to note that, if demographic rates were allowed to evolve, what seems to be a narrow range of parameter space could turn out to be exactly where selection on demographic traits pushes the metapopulation. Future work investigating the so-called 'eco-evolutionary dynamics' in metapopulations will resolve this issue.

One criticism that could be levied against our model has to do with the rather simplistic nature of the social interactions it incorporates. We have suggested, above, that our model captures certain elements of the biology of cooperative (i.e. communal) breeders. Certain other elements, though, are missing.

Before we launch into the missing elements, let us remind the reader that we have focused on relationships between mates, as well as on dominant-subordinate interactions among immediate neighbours. Most notably, subordinates can inherit dominant positions from their reproductively-active parents. This fits well with the goals of the paper: given the uncertainty associated with dispersal, departures by would-be colonists could definitely disrupt the productivity of patches they leave behind. The feature also fits with certain hypothesised incentives for cooperative breeding [27].

Despite the various positives, what makes our model a poor one for understanding cooperative breeding is that *cooperation* itself is missing, which could be investigated in future work. Subordinates in our model do nothing to change the birth or mortality rates of dominants, whereas these rates are observed to change in natural cooperatively-breeding populations [11]. Had our model incorporated richer social structure our conclusions may have changed—especially since cooperative interactions would be yet another thing for dispersal to disrupt. Importantly, incorporation of richer social structure would have (will) complicate the model, and so future work that seeks to resolve this issue must also find a way to cope with the perenial trade-off between realism and tractability.

Bibliography

[1] P. Amarasekare. Allee effects in metapopulation dynamics. *The American Naturalist*, 152(2):298–302, 1998.

[2] M. Begon, J. L. Harper, C. R. Townsend, et al. *Ecology. Individuals, populations and communities.* Blackwell scientific publications, 1986.

[3] P. Beier and R. F. Noss. Do habitat corridors provide connectivity? *Conservation Biology*, 12(6):1241–1252, 1998.

[4] N. Britton. *Essential mathematical biology*. Springer Science & Business Media, 2012.

[5] L. Gilbert-Norton, R. Wilson, J. R. Stevens, and K. H. Beard. A meta-analytic review of corridor effectiveness. *Conservation Biology*, 24(3):660–668, 2010.

[6] M. Gilpin. *Metapopulation dynamics: empirical and theoretical investigations*. Academic Press, 2012.

[7] W. D. Hamilton and R. M. May. Dispersal in stable habitats. *Nature*, 269(5629):578–581, 1977.

[8] I. Hanski. Single-species spatial dynamics may contribute to long-term rarity and commonness. *Ecology*, 66(2):335–343, 1985.

[9] A. Hastings. Structured models of metapopulation dynamics. *Biological Journal of the Linnean Society*, 42(1-2):57–71, 1991.

[10] B. J. Hatchwell. The evolution of cooperative breeding in birds: kinship, dispersal and life history. *Philosophical Transactions of the Royal Society of London B: Biological Sciences*, 364(1533):3217–3227, 2009.

[11] B. J. Hatchwell, P. R. Gullett, and M. J. Adams. Helping in cooperatively breeding long-tailed tits: a test of hamilton's rule. *Philosophical Transactions of the Royal Society of London B: Biological Sciences*, 369(1642):20130565, 2014.

[12] B. R. Hudgens and N. M. Haddad. Predicting which species will benefit from corridors in fragmented landscapes from population growth models. *The American Naturalist*, 161 (5):808–820, 2003.

[13] A. J. Irwin and P. D. Taylor. Evolution of dispersal in a stepping-stone population with overlapping generations. *Theoretical Population Biology*, 58(4):321–328, 2000.

[14] W. D. Koenig and J. L. Dickinson. *Ecology and evolution of cooperative breeding in birds*. Cambridge University Press, 2004.

[15] R. Levins. Some demographic and genetic consequences of environmental heterogeneity for biological control. *Bulletin of the Entomological Society of America*, 15(3):237–240, 1969.

[16] M. B. Main, F. M. Roka, and R. F. Noss. Evaluating costs of conservation. *Conservation Biology*, 13(6):1262–1272, 1999.

[17] M. A. McPeek and R. D. Holt. The evolution of dispersal in spatially and temporally varying environments. *The American Naturalist*, 140(6):1010–1027, 1992.

[18] R. McVinish and P. Pollett. Interaction between habitat quality and an Allee-like effect in metapopulations. *Ecological Modelling*, 249:84–89, 2013.

[19] H. Nichols. The causes and consequences of inbreeding avoidance and tolerance in co-operatively breeding vertebrates. *Journal of Zoology*, 2017.

[20] S. Pruett-Jones and M. Lewis. Sex ratio and habitat limitation promote delayed dispersal in superb fairy-wrens. *Nature*, 348(6301):541–542, 1990.

[21] M. Scheffer, J. Bascompte, W. A. Brock, V. Brovkin, S. R. Carpenter, V. Dakos, H. Held, E. H. Van Nes, M. Rietkerk, and G. Sugihara. Early-warning signals for critical transitions. *Nature*, 461(7260):53–59, 2009.

[22] S.-F. Shen, S. T. Emlen, W. D. Koenig, and D. R. Rubenstein. The ecology of cooperative breeding behaviour. *Ecology Letters*, 20(6):708–720, 2017.

[23] D. Simberloff. The contribution of population and community biology to conservation science. *Annual Review of Ecology and Systematics*, 19(1):473–511, 1988.

[24] D. Simberloff and J. Cox. Consequences and costs of conservation corridors. *Conservation Biology*, 1(1):63–71, 1987.

[25] D. Simberloff, J. A. Farr, J. Cox, and D. W. Mehlman. Movement corridors: conservation bargains or poor investments? *Conservation Biology*, 6(4):493–504, 1992.

[26] N. G. Solomon and J. A. French. *Cooperative breeding in mammals*. Cambridge University Press, 1997.

[27] P. B. Stacey and J. D. Ligon. The benefits-of-philopatry hypothesis for the evolution of cooperative breeding: variation in territory quality and group size effects. *The American Naturalist*, 137(6):831–846, 1991.

[28] W. L. Thomas et al. *Man's role in changing the face of the Earth*. The University of Chicago Press, London, 1956.

[29] S.-R. Zhou and G. Wang. Allee-like effects in metapopulation dynamics. *Mathematical Biosciences*, 189(1):103–113, 2004.

Chapter 3

"Paradox of Enrichment" in Metapopulations with Delays

3.1 Introduction

Many species experience their environment as a patchwork collection of suitable habitats interspersed throughout an unsuitable matrix, and connected to one another by dispersal. Such species are said to exist as *metapopulations*. As human-mediated fragmentation of the environment has increased, understanding the dynamics of metapopulations has become of critical importance to both conservation and ecological restoration [16, 18, 28, 36].

The seminal mathematical model of metapopulation dynamics was proposed by Levins (1969). That model considered a constant number of 'islands' of suitable habitats that were subject to local colonization events and local extinction events. Levins tracked the fraction of occupied islands, denoted $p(t)$, using

$$p'(t) = c\,(1 - p(t))\,p(t) - e\,p(t) \tag{3.1}$$

where c gives the rate at which colonists leave occupied islands, and e gives the rate at which islands suffer extinction.

It can be shown that, when the colonization rate c exceeds the extinction rate e, solutions to Eq. (3.1) tend to a steady-state value $\bar{p} = 1 - e/c$ over time. Otherwise, solutions to Eq. (3.1) tend to zero over time, and the metapopulation suffers global extinction. In mathematical terms, solutions to Eq. (3.1) exhibit a transcritical bifurcation as the bifurcation parameter $1 - e/c$ passes through zero.

Levins' model can be (and has been) modified in many ways. One extension, originally proposed by Hanski (1985) and later modified by Hastings (1991), divides occupied islands into two categories based on quality. Low-quality islands occur with frequency $p_\ell(t)$, and high-quality islands occur with frequency $p_h(t)$. Assuming (i) only low-quality islands are subject to extinction, (ii) only high-quality islands send out colonists, (iii) low-quality islands can become high-quality only through colonization, and (iv) high-quality islands can become low-quality due to degradation of the local population, we arrive at the following:

$$\begin{aligned} p'_\ell(t) &= c\,(1 - p_\ell(t) - p_h(t))\,p_h(t) - e\,p_\ell(t) + d\,p_h(t) - c\,p_\ell(t)\,p_h(t), \\ p'_h(t) &= c\,p_\ell(t)\,p_h(t) - d\,p_h(t), \end{aligned} \tag{3.2}$$

where d is the rate at which high-quality islands become low-quality because of degradation.

It can be shown that global extinction of the metapopulation is always a possibility for the model suggested by equation (3.2). In fact, when the colonization rate $c < d + 2\sqrt{d\,e}$, the long-term fate of the metapopulation can only be global extinction. When $c > d + 2\sqrt{d\,e}$ the metapopulation might persist over time, with the frequency of low-quality and high-quality islands tending to $\bar{p}_\ell = d/c$ and $\bar{p}_h = [(c-d) + \sqrt{(c-d)^2 - 4d\,e}]/(2c)$ over time (see Appendix A.1 for analysis). Persistence, however, requires that the the frequency of high-quality islands remain above some tipping point [sensu 34]. When high-quality islands are too infrequent, rescue of low-quality islands cannot counterbalance local extinctions and global extinction is the result. In mathematical terms, solutions to (3.2) exhibit a fold bifurcation, or saddle-node bifurcation, as the bifurcation parameter $c - (d + 2\sqrt{d\,e})$, or $e - (c-d)^2/(4d)$, passes through zero. For both models (3.1) and (3.2), reducing extinction rate e when other parameters (c

and d) are set to constant can save the metapopulation from global extinction, and increase the density of occupied islands.

Though the metapopulation models proposed by Levins and Hanski make slightly different predictions, they agree on the basic notion that increasing colonization and reducing extinction promotes metapopulation persistence. In this way, these models appeal to the same expectations about metapopulation dynamics that are likely to motivate conservation efforts. For example, it is often expected that facilitation of movement among patches will work to maintain the health of metapopulations at risk [2]. It is also expected that reduced local extinctions in a metapopulation will work to keep the metapopulation viable by minimizing threats to local populations [2].

While efforts to conserve metapopulations are reasonable, it may not be reasonable to expect that the positive effects those efforts have always resulted in stable, equilibrium dynamics. Indeed, a hint to this effect comes from consumer-resource theory. That theory predicts that increases to the carrying capacity of a population can, in fact, destabilize communities at equilibrium, and lead population densities to oscillate in a sustained manner over time [11, 27, 31]. This result is known as the "Paradox of Enrichment" and it has garnered empirical support [10, 32, 40].

The extent to which a "Paradox of Enrichment" might be found for metapopulations is unclear. Certainly, the predictions made by the ordinary differential equation (ODE) models of Levins and Hanski suggest that such a paradox is unlikely to crop up. The full range of possible metapopulation models, however, has yet to be explored. A Paradox of Enrichment might arise, for example, in a model based on delay differential equations (DDEs), as these are known to produce oscillatory dynamics in certain circumstances. In this paper, then, we turn our attention to DDE models of metapopulations, with the aim of investigating how the balance between colonization and extinction rates influences the stability of equilibrium solutions to DDE versions of Levins' and Hanski's works, respectively.

In this paper, we first introduce a gallery of DDE models based on Levins' model and

Hanski's model in section 3.2, by considering delays associated with availability of empty islands, delays associated with dispersal, and delays associated with establishment, and then we investigate the possibility for oscillations by checking the absolute stability of the positive stable equilibrium, and by determining critical transition delays. In section 3.3, we continue with the occurrence of the Paradox of Enrichment in models, in which the enrichment can lead to oscillations. We compare the timing of the occurrence of the Paradox of Enrichment in different models, and we argue that introducing a structure to metapopulations with establishment delay might be a way to resolve the Paradox of Enrichment, and that recording the increased recovery time can be used as a warning sign when the metapopulation approaches its bifurcation points. In section 3.4, we end with discussion of the impact of including delays in metapopulation modelling, the occurrence of the Paradox of Enrichment and future directions.

3.2 A Gallery of Models

In metapopulation dynamics, time delay can be associated with various factors, e.g. the density of available islands, dispersal of colonists, and establishment of (high-quality) habitable islands. We incorporate such delays in Levins' model (3.1) in section 3.2.1, and Hanski's model (3.2) in section 3.2.2. We investigate the possibility for oscillations by looking for regions of absolute stability (formally defined below) in the parameter space, and determine critical transition delays. We also examine the impact of reducing the extinction rate on the dynamics of metapopulations.

3.2.1 Three DDE versions of Levins' Model

Delay Associated with Available Islands: an equivalent to the logistic model with delay

We first consider a simple case where, for example, colonists need to collect resources from unoccupied islands before becoming established on unoccupied islands. If it takes τ time units for colonists to finish their work, or colonists need to get prepared τ time units before successful

colonization takes effect, then

$$p'(t) = c\,(1 - p(t-\tau))\,p(t) - e\,p(t). \tag{3.3}$$

For later use, define $F(p(t), p(t-\tau))$ as the right-hand side of the DDE. Note that when $c > e$, $\bar{p} = 1 - e/c$ solves the DDE. To address the stability of $\bar{p}$, we first perturb the solution for τ time units. Specifically, we add $\varepsilon(t) \leq \bar{\varepsilon}$, for some small $\bar{\varepsilon}$, to $\bar{p}$ beginning at time $t_0 - \tau$ until time t_0 (Figure 3.1). We then determine whether the perturbation grows or not.

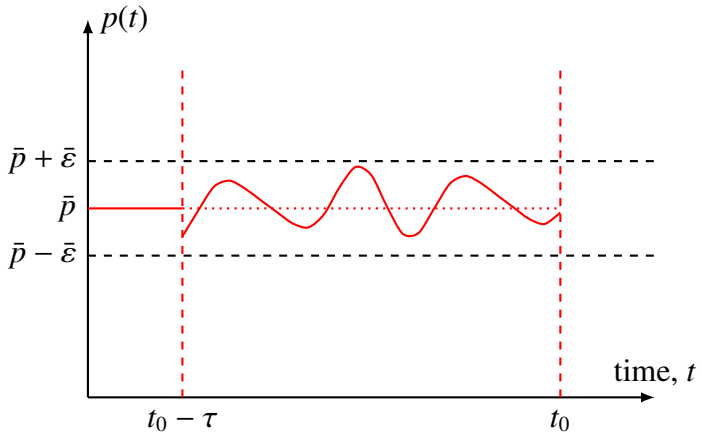

Figure 3.1: Perturbed equilibrium solution $\bar{p}$.

Given that $\varepsilon(t)$ is small, $\varepsilon'(t) \approx F(\bar{p},\bar{p}) + F_1(\bar{p},\bar{p})\,\varepsilon(t) + F_2(\bar{p},\bar{p})\,\varepsilon(t-\tau)$ which simplifies to $\varepsilon'(t) = -(c-e)\,\varepsilon(t-\tau)$. By substituting solutions of the form $\varepsilon(t) = \exp\{s\,t\}$ into the expression for ε', we arrive at the characteristic equation $s = -(c-e)\exp\{-s\,\tau\}$. For a general method to get the characteristic equation for single DDEs and DDE systems, see Appendix A.2. At this point it is clear that the analysis is identical to that for the well-known Hutchinson equation (the DDE version of logistic growth [3, 22, 33]). We can conclude, therefore, that $\bar{p}$ becomes unstable whenever

$$\tau > \frac{1}{(c-e)}\frac{\pi}{2} = \tau_0. \tag{3.4}$$

Numerical examples illustrate the result (Figure 3.2), where we choose parameters so that the critical delay is $\tau_0 = \pi$, and oscillation occurs when $\tau > \tau_0$. Inequality (3.4) predicts that when

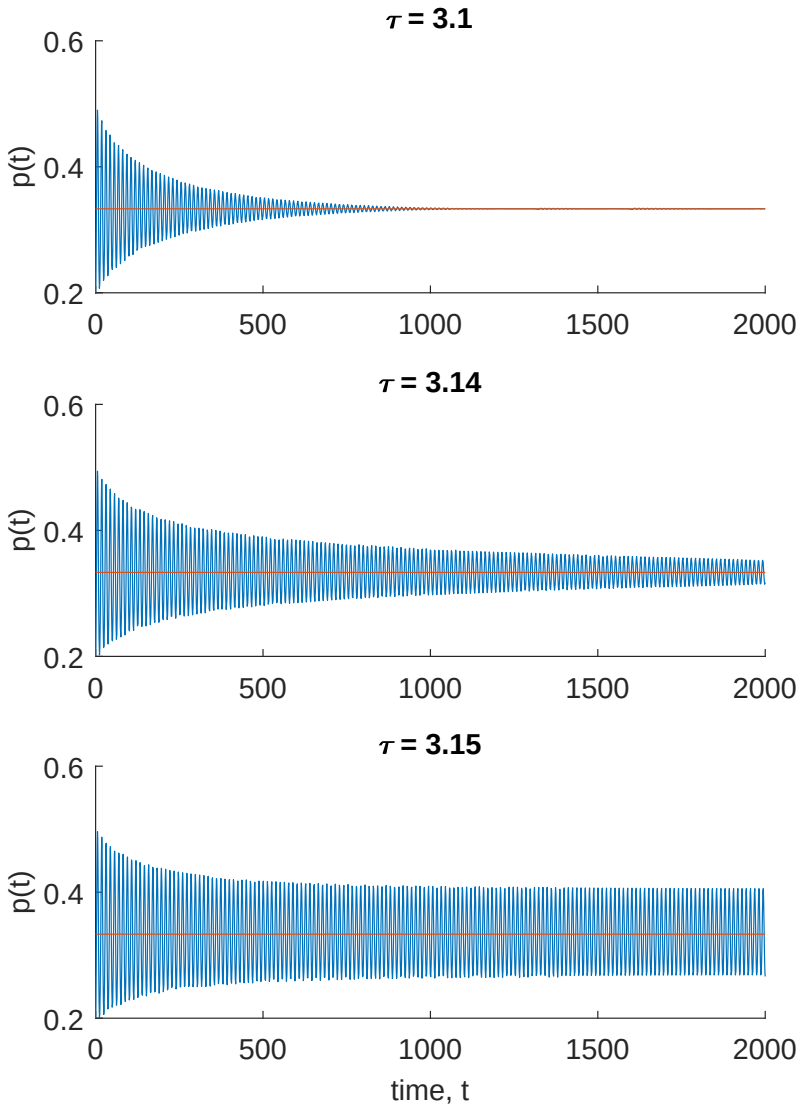

Figure 3.2: Numerical solutions to DDE version (3.3) of Levins' model for various delays, τ. Parameter values were $c = 3/2$ and $e = 1$, and so the critical delay is $\tau_0 = \pi$. Solutions in this paper are generated by Matlab's `dde23` routine [35] with simple modifications of function `odefinalize` to keep the densities in $[0, 1]$.

colonization rate is much greater than extinction rate, the critical delay is small, and we expect

instabilities to occur only when delays associated with available islands are long. By contrast, when colonization rates exceed extinction rates by only a small amount, instabilities require very long delays. We summarize the above analysis in the following proposition:

Proposition 4 *For Eq.* (3.3)*, whenever the colonization rate c is larger than the extinction rate e, i.e., $c > e$, there exists a critical delay τ_0, where $\tau_0 = \frac{1}{(c-e)}\frac{\pi}{2}$, so that once the delay exceeds the critical value, the positive equilibrium is de-stabilized.*

Delay Associated with Dispersal

Now suppose the delay is associated with dispersal time, e.g. it takes τ units of time for a colonist to reach a new island. In this case, we have

$$p'(t) = c\,(1 - p(t))\,p(t-\tau) - e\,p(t). \tag{3.5}$$

Using a similar method for Eq. (3.3), we can get the linearized differential equation of Eq. (3.5) about $\bar{p} = 1 - e/c$ if $c > e$, $\varepsilon'(t) = -c\,\varepsilon + e\,\varepsilon(t-\tau)$. By substituting solutions of the form $\varepsilon(t) = \exp\{s\,t\}$, we again arrive at the characteristic equation $s = -c + e\exp\{-s\,\tau\}$.

Now we check if there is a region in the parameter space where the positive equilibrium exists but cannot be destabilized. If such a region exists, the positive equilibrium, which is stable in the corresponding ODE without any delay, is defined as having *absolute stability* in this region, meaning that the positive equilibrium is stable for any delay [sensu 37, page 56], i.e., the positive equilibrium is *absolutely stable*. In the following sections, we use the 'absolute stability' in the DDE analysis to refer to the absolute stability of the positive equilibrium that is stable in the corresponding ODE model. Using the techniques in Appendix A.5, we can prove that the positive equilibrium has absolute stability as long as it exists, i.e., $c > e$. Note that even though there is a delay associated with dispersal in Eq. (3.5), there will not be any oscillation around the positive equilibrium. So, we have the following proposition:

Proposition 5 *For Eq.* (3.5)*, there does not exist any critical delay for any pair of c and e whenever colonization rate c is larger than the extinction rate e, i.e., the positive equilibrium is stable for all* (c, e) *satisfying* $c > e$.

This model (3.5) and the previous model (3.3) both consider delays affecting the colonization term, but they make different predictions about the possibility of oscillatory metapopulation dynamics. In model (3.3), the delay associated with available islands, hence available resources, can lead to oscillations. However, in model (3.5), the delay is associated with the dispersing time of colonists, and there cannot be any oscillation for however long delay of dispersal.

Delay Associated with Establishment

If establishment takes time, then we might track occupied islands using the following DDE:

$$p'(t) = c\,(1 - p(t-\tau))p(t-\tau) - e\,p(t). \tag{3.6}$$

Note that because an establishment event needs both a colonist and an unoccupied island, those two items should both be τ time units before the successful colonization takes effect if the establishment itself needs τ time units. Now, the perturbation satisfies $\varepsilon'(t) = -e\,\varepsilon(t) + (2\,e - c)\,\varepsilon(t-\tau)$. If we again use the ansatz $\varepsilon(t) = \exp\{s\,t\}$, then the characteristic equation is

$$s + e = -(c - 2e)\,\exp\{-s\,\tau\}. \tag{3.7}$$

We can analyze the roots of the characteristic equation (3.7), obtain the critical delay, and prove the absolute stability of Eq. (3.6) (see Appendix A.3), and we obtain the following proposition:

Proposition 6 *For Eq.* (3.6)*,*

(i) if colonization rate c is larger than the extinction rate e but not too large $(e < c < 3\,e)$*, then the positive equilibrium is stable for any delay, i.e., it cannot be de-stabilized;*

(ii) if colonization rate c is much larger than the extinction rate e $(c > 3\,e)$*, then there exists a*

critical delay τ_0 *, where* $\tau_0 = \frac{1}{v}\arctan\left(-\frac{v}{e}\right) + \frac{\pi}{v}$*, with* $v = \sqrt{(c-e)(c-3e)}$*, so that once the delay exceeds the critical value, the positive equilibrium is de-stabilized.*

3.2.2 Two DDE versions of Hanski's Model

Delay Associated with Dispersal

In our next model, we assume only high-quality islands are able to send out colonists, e.g. high-quality islands can support taller plants so that the wind can carry the seeds further and we might expect that high-quality islands are more likely to produce more seeds and more high-quality fruits to attract animals to consume and then carry the seeds in their guts. Suppose that time associated with the dispersal of a colonist from a high-quality island to an empty island or a low-quality island requires τ time units. Then our model is:

$$\begin{aligned} p_\ell'(t) &= c\,(1 - p_\ell(t) - p_h(t))\,p_h(t-\tau) - e\,p_\ell(t) + d\,p_h(t) - c\,p_\ell(t)\,p_h(t-\tau), \\ p_h'(t) &= c\,p_\ell(t)\,p_h(t-\tau) - d\,p_h(t). \end{aligned} \tag{3.8}$$

The DDE system (3.8) has the same equilibria as the ODE system (3.2). We can get the following proposition by investigating the absolute stability (see Appendix A.4):

Proposition 7 *For model* (3.8)*, the positive equilibrium exists if and only if* $c > d + 2\sqrt{d\,e}$*, and the same condition ensures the absolute stability of the positive equilibrium.*

Therefore, the region of absolute stability coincides with the region of existence of the positive equilibrium in both of the model (3.5) and the model (3.8).

Delay Associated with Establishment of High-Quality Islands from Low-Quality Islands

In metapopulations, it might take a long time to establishment a high-quality island from a low-quality island. For example, seeds of most plants have a delay before germination [5]. Suppose that time associated with the transition of an island from low-quality to high-quality

requires τ time units. Then,

$$\begin{aligned} p'_\ell(t) &= c\,(1 - p_\ell(t) - p_h(t))\,p_h(t) - e\,p_\ell(t) + d\,p_h(t) - c\,p_\ell(t-\tau)\,p_h(t-\tau), \\ p'_h(t) &= c\,p_\ell(t-\tau)\,p_h(t-\tau) - d\,p_h(t). \end{aligned} \tag{3.9}$$

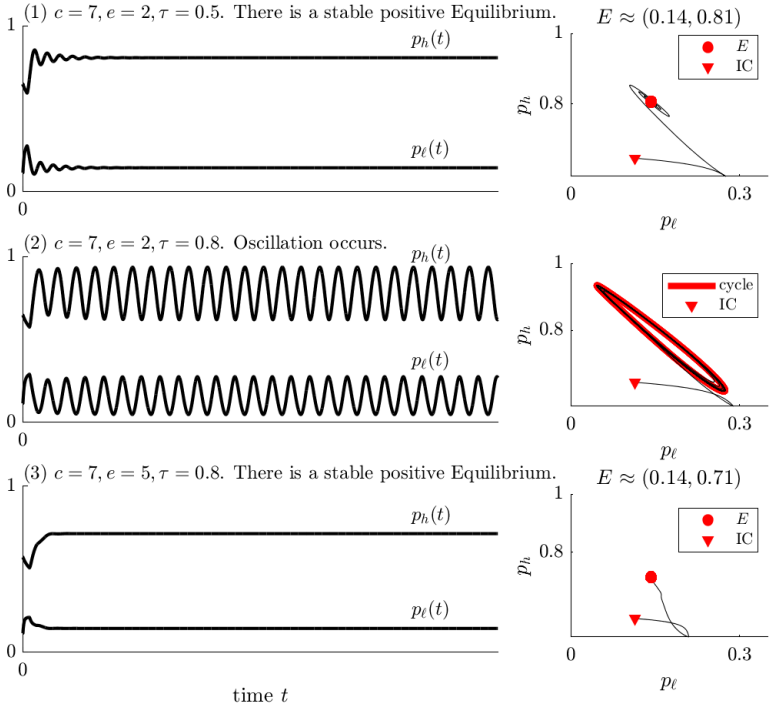

Figure 3.3: Three numerical solutions of system (3.9) with a constant colonization rate $c = 7$ and a constant degradation rate $d = 1$. For each case, $p_\ell(t)$ and $p_h(t)$ are shown on the left panel, and the corresponding trajectory is shown on the right panel. The value of extinction rate e is the same in the cases on top in the middle. The value of delay τ is the same in the cases in the middle and on bottom. The middle case shows an oscillation, and the other two show the system goes to a positive equilibrium.

The DDE system (3.9) has the same equilibria as the ODE system (3.2), including a stable extinction equilibrium, $(0, 0)$, and two possible positive equilibria $\left(\frac{d}{c}, \frac{(c-d) \pm \sqrt{(c-1)^2 - 4\,d\,e}}{2\,c}\right)$, of which $E = \left(\frac{d}{c}, \frac{(c-d) + \sqrt{(c-d)^2 - 4\,d\,e}}{2\,c}\right)$ is stable in system (3.2), and the other is unstable. The existence of the positive equilibria requires $e < \frac{(c-d)^2}{4\,d} = e_u$ and $c > d$.

Solving the system (3.9) numerically gives some interesting cases, in which positive equi-

libria become de-stabilized when changing either the delay τ or the extinction rate e. Numerical simulations with different delays but the same value of the extinction rate show that oscillation might occur when the delay increases, which is not a surprising outcome for a DDE system. However, numerical simulations with the same delay but different values of the extinction rate also show that reducing the extinction rate can de-stabilize the stable equilibrium. The latter case inspires us to re-consider our intuitive expectation that reducing extinction rate e can always lead populations to a stable steady state. Figure 3.3 shows numerical solutions of system (3.9) with different pairs of values of the extinction rate e and delays τ when fixing values for the colonization rate c and the degradation rate d.

Analyzing the absolute stability and calculating the critical delay, we can obtain the following proposition (see Appendix A.5 and Appendix A.6 for calculations):

Proposition 8 *For system* (3.9)*,*

(i) on condition that the colonization rate is intermediate ($d < c < 3\,d$), the positive equilibrium cannot be de-stabilized as long as it exists ($e < e_u$, where $e_u = \frac{(c-d)^2}{4\,d}$);

(ii) when the colonization rate is large $c > 3\,d$, the positive equilibrium cannot be de-stabilized if the extinction rate satisfies $e_l < e < e_u$, where $e_l = \frac{(3\,c-d)\,(c-3\,d)}{16\,d}$;

(iii) when the colonization rate is large $c > 3\,d$, there exists a critical delay $0 < \tau_0 \in \mathcal{R}$, so that oscillation occurs for any delay larger than τ_0, on condition that the extinction rate e is small enough, $e < e_l$.

See Appendix A.6 for the expression of τ_0.

The statement (i) in Proposition 8 points out the oscillation-free region in the parameter space for system (3.9). Figure 3.4 shows the region where the positive equilibrium E is absolutely stable and oscillation does not occur regardless of the magnitude of delay τ, given $d = 1$. From Figure 3.4, we can observe that when colonization rate $c > d = 1$, where the existence of E is possible, if the colonization rate is relatively small, i.e., $c < 3$, smaller extinction rate ($e < e_u$) always ensures existence and stability of E at the same time; however, if the colonization rate is relatively large, i.e., $c > 3$, medium extinction rate ($e_l < e < e_u$) always ensures

existence and stability of E, but smaller extinction rate ($e < e_l$) may lead to oscillations.

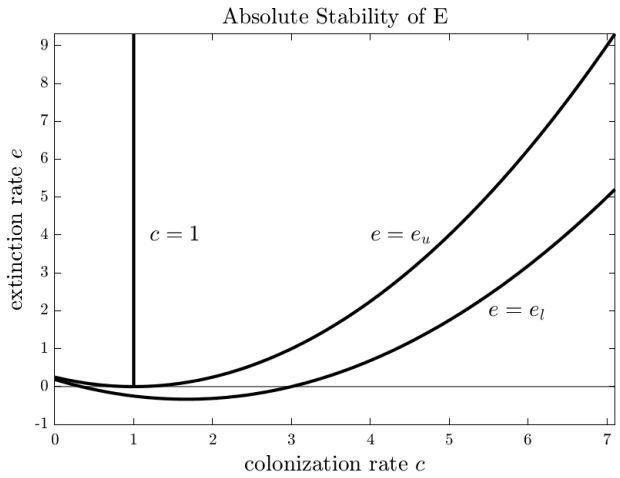

Figure 3.4: Absolute stability region for system (3.9) is shown in the first quadrant between the curves $e = e_l$ and $e = e_u$ ($d = 1$).

3.3 The Paradox of Enrichment

3.3.1 The Paradox of Enrichment in DDE versions of Levins' model

Solutions to model (3.5) do not develop oscillatory behaviour when we reduce the extinction rate, so no analogue to the Paradox of Enrichment occurs. In models (3.3) and (3.6), oscillations might occur when either reducing extinction rate or increasing delays. Therefore, the Paradox of Enrichment can occur for both models (see Figure 3.5). If we fix both the delay and the colonization rate to constants in models (3.3) and (3.6), reducing the extinction rate below the colonization rate can protect the metapopulation against global extinction to a possible positive equilibrium that is stable, and reducing the extinction further can de-stabilize the positive equilibrium. The difference is that model (3.6) with delays associated with establishment provides a longer 'safe' range of the extinction rate for the positive equilibrium to remain stable, compared with model (3.3) with delays associated with available islands. In addition, when reducing the extinction rate e from $e = c$, the positive equilibrium $1 - e/c$ of density of occu-

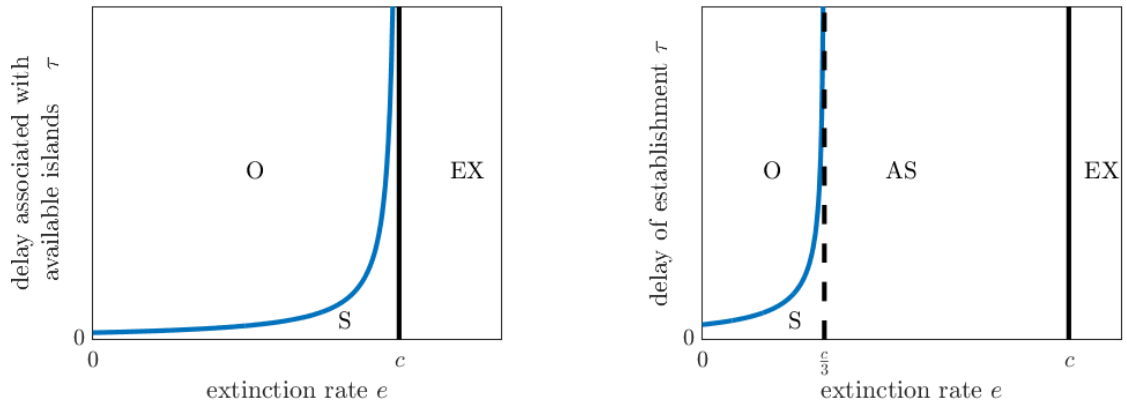

Figure 3.5: The Paradox of Enrichment: (a) for Eq. (3.3) and (b) for Eq. (3.6). Four types of regions are: (O): oscillation occurs around the positive equilibrium if $\tau > \tau_0$; (S): the positive equilibrium is stable for $\tau < \tau_0$; (EX): extinction only, the positive equilibrium does not exist; (AS): the positive equilibrium is stable for all τ.

pied islands grows from 0, and the density of occupied islands keeps increasing to more than $1 - (c/3)/c = 2/3$ for model (3.6) before oscillations occur, but for model (3.3), the density of occupied islands cannot grow to such a relatively high level, $2/3$, before oscillation occurs. So, compared with model (3.3), which considers delays associated with available islands, model (3.6) with delays associated with establishment has the following two properties as the the extinction rate reduces: first, oscillations are observed later if the extinction rate is reduced at the same speed, and second, the maximum oscillation-free positive equilibrium is larger.

Figure 3.6 shows how enrichment can lead to extinction of a metapopulation in model (3.6). If we start from large extinction rate, where the metapopulation is doomed to a global extinction, then reducing extinction rate (i.e., enriching the metapopulation) can result in very interesting dynamics. As we reduce the extinction rate from an initially large value, a stable positive equilibrium appears. Further reductions in extinction lead to oscillations that destabilize the equilibrium; further reductions still, cause the amplitude of oscillations to grow. Finally, the metapopulation tends to extinction when the extinction rate is even smaller.

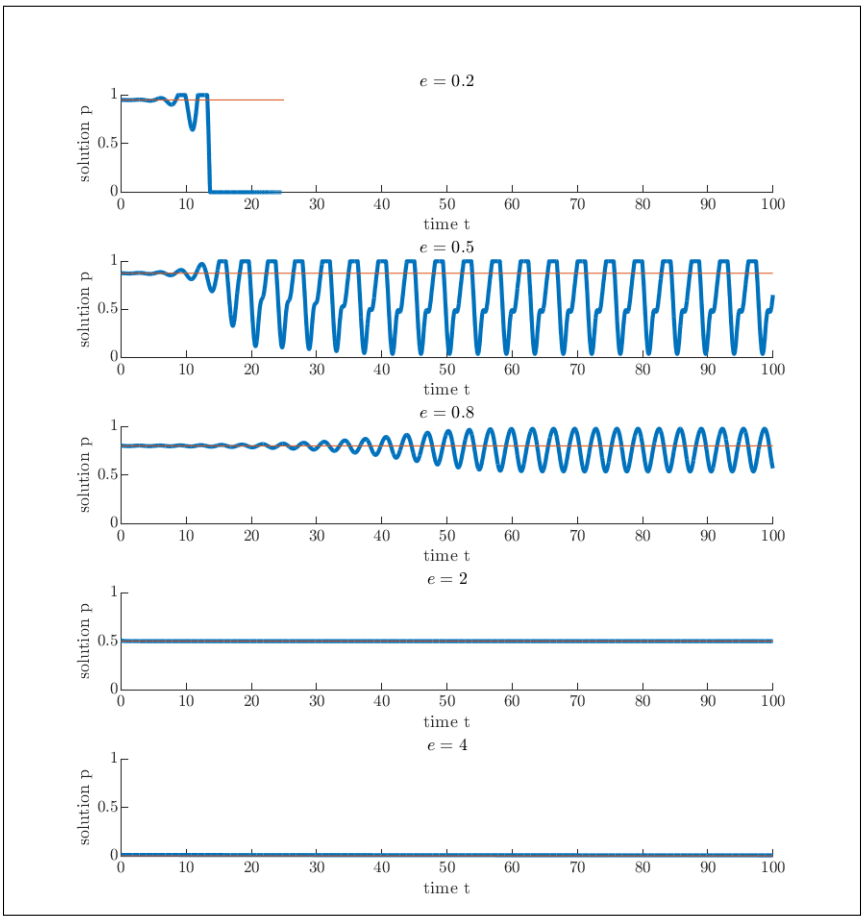

(a)

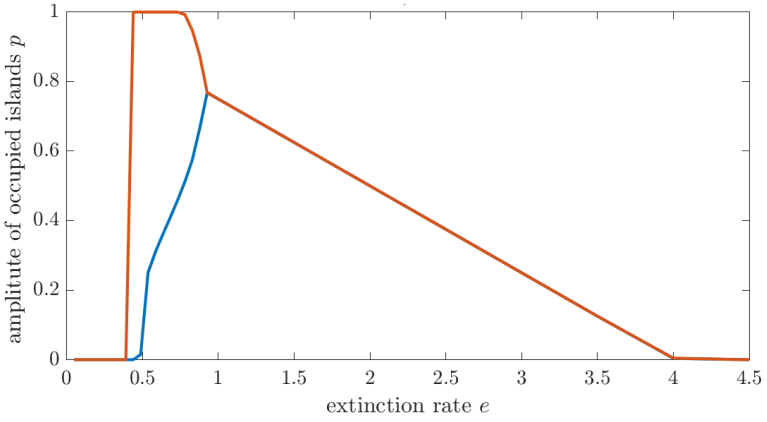

(b)

Figure 3.6: The Paradox of Enrichment: for Eq. (3.6). As extinction rate reduces, the oscillation leads to extinction. (a): examples when fixing $c = 4$ and $\tau = 1$ and changing e. (b): the amplitude of solutions around the positive equilibrium where it exists, and connected with the global extinction equilibrium where the positive equilibrium does not exist (also with $c = 4$ and $\tau = 1$).

3.3.2 The Paradox of Enrichment in DDE versions of Hanski's model

Solutions to model (3.8) do not develop an oscillatory behaviour when we reduce the extinction rate, so the Paradox of Enrichment does not occur. For model (3.9), from Proposition 8 and Figure 3.4, we can see that reducing the extinction rate when the colonization rate is relatively small, i.e., $d < c < 3\,d$, helps to possibly save the metapopulation from global extinction, by facilitating a stable positive equilibrium. However, reducing the extinction rate when the colonization rate is relatively large in model (3.9), i.e., $c > 3\,d$, might lead to oscillations, i.e., the Paradox of Enrichment in DDE version of Hanski's model (3.9) might occur when $c > 3\,d$.

Figure 3.7 presents where the Paradox of Enrichment might occur in the parameter space in system (3.9) when $c > 3\,d$, and shows four numerical solutions to system (3.9). It provides an answer to the question arising from Figure 3.3: what can lead to the de-stabilization of the positive stable equilibrium in system (3.9)? The answer is that two factors can result in the de-stabilization of E in system (3.9), i.e., increasing the delay τ and the reducing extinction rate e.

Introducing structure to islands might resolve the Paradox of Enrichment

Although model (3.6) and model (3.9) both consider the delay associated with establishment, model (3.9) includes a structure for occupied islands, classifying the occupied islands into those with a low quality and those with a high quality, and thus might limit the possibility for the Paradox of Enrichment to occur. On one hand, such structure in model (3.9) can provide an extra 'safe zone' for metapopulations: when the colonization rate c is not too large and not too small relative to the degradation rate d, i.e., $d < c < 3\,d$, the positive equilibrium is stable for any delay. On the other hand, when reducing extinction rate to a small value $e < e_l$, the global extinction due to oscillations, which occurs in model (3.6), does not show up in our simulations of solutions to model (3.9) .

Similar with Figure 3.6b, we can check the amplitude of the density of the total occupied

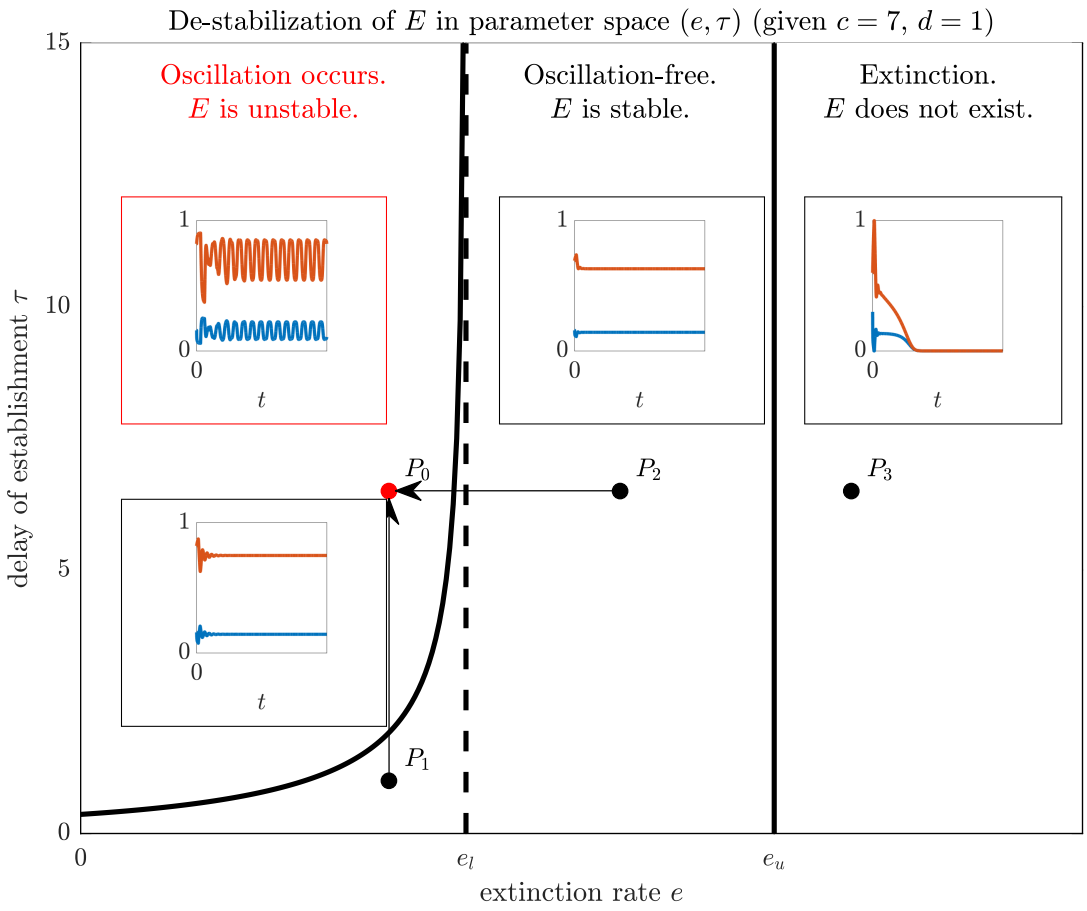

Figure 3.7: The Paradox of Enrichment for system (3.9). With constant colonization rate at $c = 7$ and constant degradation rate at $d = 1$, there are three cases in the parameter space (e, τ) for the existence and stability of the positive equilibrium E, separated by the solid curve $\tau = \tau_0(e)$ on the left and the solid line $e = e_u$ on the right. i) On the upper left of the solid curve, i.e., $\tau > \tau_0$, oscillations could occur. ii) In the oscillation-free middle region, where E is stable, one part is when $\tau < \tau_0$ and $e < e_l$, and the other part is the region between $e = e_l$ and $e = e_u$, i.e., the absolute stability region for E. iii) In the region on the right of the solid line $e = e_u$, the positive equilibria do not exist. Four numerical results are also illustrated here corresponding to the closest dots in the figure, with the (e, τ) chosen at P_1, P_2 and P_3 leading to stable equilibria, and (e, τ) chosen at P_0 leading to oscillation. The two arrows are the two possible ways to de-stabilize the stable positive equilibrium E.

islands in model (3.9) by numerical simulations and record the maximum and minimum densities for oscillatory metapopulations (see Figure 3.8). We find that the minimum itself achieves

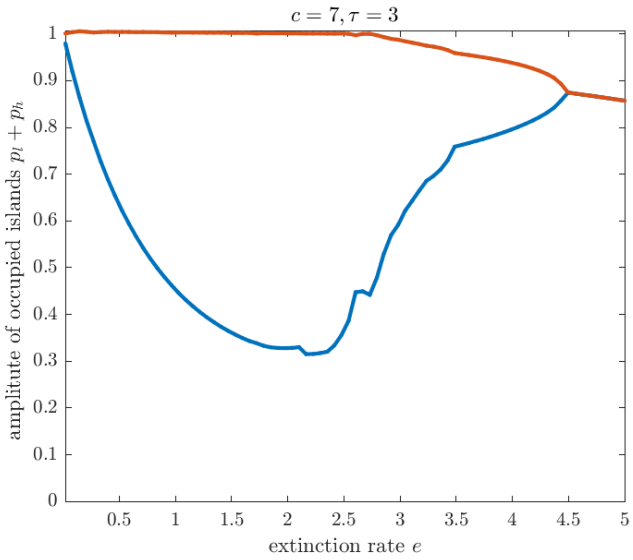

Figure 3.8: The amplitude of the total density of occupied islands $p_\ell + p_h$ by numerical simulations when changing the extinction rate e. Enrichment increases the amplitude of oscillations first, and then reduces the amplitude.

a minimum as e is changed. The non-monotonic relationship between the amplitude of oscillations and extinction rate implies that the Paradox of Enrichment still occurs in model (3.9), but with a smaller possibility compared with model (3.6). We explain those implications in the following.

First, oscillations occur when we reduce the extinction rate (i.e., enriching the metapopulation) in model (3.9), and the minimum value of the amplitude of oscillations continues to decline as the extinction rate gets smaller until the minimum reaches its own minimum. We expect that the same intensity of natural disasters or human interventions might not affect an oscillatory metapopulation with a relatively large minimum value of the amplitude of oscillation, as much as an oscillatory metapopulation with a relatively small minimum value of the amplitude of oscillation. Therefore, smaller minimum value of the amplitude of oscillation could lead to a larger global extinction risk. In this sense, the Paradox of Enrichment still occurs. Second, however, as the extinction rate reduces further, the amplitude starts to decline once

the minimum of the amplitude moves away from its own minimum (around $e = 2$ in Figure 3.8), which is a quite different behaviour compared with model (3.6) (see Figure 3.6b), where oscillation continues to grow until global extinction occurs eventually. Hence, continuing to enrich the metapopulation when the extinction rate is already small can reduce the possibility of global extinction.

Overall, metapopulations in model (3.9) do not go extinct as easily as in model (3.6) when extinction rate reduces, although de-stabilized positive equilibria are usually associated with increased global extinction risk [3] and reducing the extinction rate might increase global extinction risk in a range of intermediate extinction rate in model (3.9). So, quality-structured islands might be an alleviation to the Paradox of Enrichment when we consider the delay associated with establishment. The influence of reducing the extinction rate, which could lead to the Paradox of Enrichment, can be predicted by checking the recovery time from perturbations about the positive equilibrium, and we examine the critical slowing down in the following section.

Detecting bifurcations by checking for critical slowing down

When a system is approaching its bifurcation point, critical slowing down of recovery from a perturbation about the positive equilibrium is extensively observed and useful in many research areas [13, 34]. Numerical simulations of model (3.9) show that critical slowing down could occur both when a fold bifurcation occurs, where two positive equilibria emerge, and when a Hopf bifurcation occurs, where oscillations around a positive equilibrium occurs (see Figure 3.9). Figure 3.9 shows examples of such critical slowing down. The results are consistent with our analysis of the critical values of delays and extinction rate (see the dashed lines in Figure 3.9). Such critical slowing down is useful as an early warning sign when the metapopulation is about to go extinct or develop oscillatory behaviours.

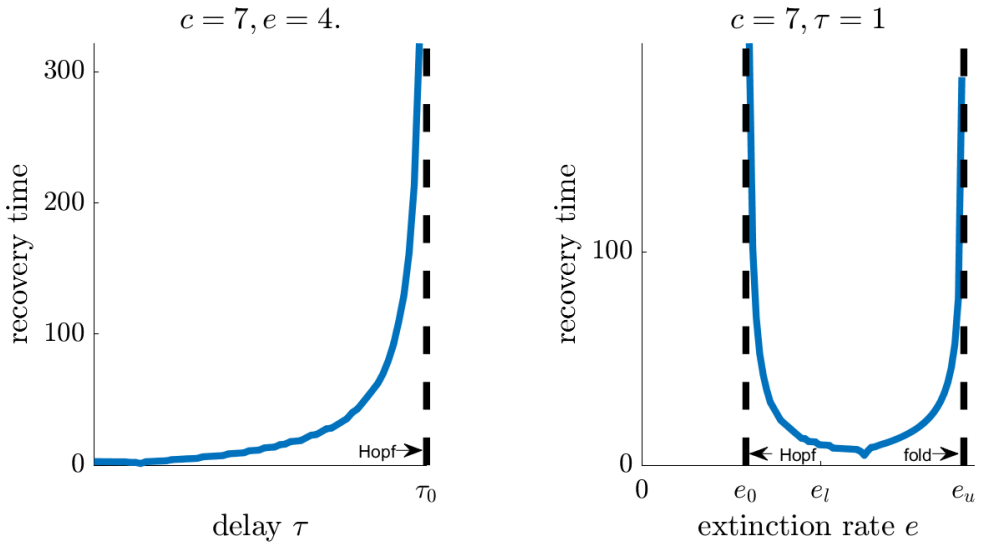

Figure 3.9: Critical slowing down of recovery time from a perturbation about the positive equilibrium occurs when a bifurcation is about to occur. (a) E is stable when $\tau < \tau_0$. A Hopf bifurcation occurs when delay τ passes $\tau = \tau_0$. (b) E is stable when $e_0 < e < e_u$, where e_0 is the solution of system (A.28) given c and τ. A critical transition occurs at both ends of this region (e_0, e_u) of e: a Hopf bifurcation occurs on the left when the extinction rate passes $e = e_0$, and a fold bifurcation occurs on the right when the extinction rate e passes $e = e_u$.

3.4 Discussion

The balance between extinction events and re-colonization events is essential in metapopulation models. Reducing the extinction rate or increasing the colonization rate can increase the stable density of occupied islands in both of the seminal metapopulation model by Levins [25] and the quality-structured model by Hanksi [17], based on Levins' model. However, whether the effort intending to enrich the metapopulation could always promote the persistence of metapopulations is questionable, in light of the existence of the 'Paradox of Enrichment' in consumer-resource dynamics.

In this paper, we incorporate delays into well-known ODE models [17, 25], and use DDE models to investigate if the Paradox of Enrichment occurs in metapopulations, as DDEs are known to lead to oscillations. We incorporate delays into the ODE models by Levins and Hanski, investigate the possibility for oscillations in the DDE model by checking the absolute stability of the positive equilibrium that is stable in the corresponding ODE model, and examine the critical transition delay if it exists.

We show that the Paradox of Enrichment does not occur in the DDE models we studied with delays associated with dispersal only, but may occur in models with delays associated with available islands or with establishment of (high-quality) islands. By comparing the two DDE models which incorporate establishment delays, we find that including a structure based on the quality of occupied islands may alleviate the Paradox of Enrichment in the metapopulation model by saving the metapopulation from global extinction when the extinction rate is small, although the oscillation amplitude is still increasing when the extinction rate reduces from the critical point where cycling occurs. In models where the Paradox of Enrichment is possible, metapopulations can develop oscillatory behaviours due to reduced local extinction rate, and metapopulations either go extinct globally (see Figure 3.6), or have a smaller lower bound for the oscillatory density of occupied islands (see Figure 3.8). Recording the recovery time from perturbations about the positive stable equilibrium can be used as a warning sign when the metapopulation is about to oscillate, as well as when the metapopulation approaches its

saddle-node bifurcation point.

We obtain the parameter region of absolute stability for each model, i.e., the conditions under which the positive equilibrium remains stable regardless of the magnitude of delay. In the region where the positive equilibrium exists, the region of absolute stability excludes the possibility of oscillations. With the delays included, we expect DDEs to have oscillatory behaviours, but we find that delays associated with dispersal only cannot de-stabilize the stable metapopulation in our models, as the region of absolute stability coincides with the region of existence for the positive equilibrium (see Propositions 5 and 7). We incorporate the delay associated with dispersal, because dispersal is known to play an important role for the metapopulation stability [8], which is controversial [1, 39, 42]: on one hand, dispersal makes re-colonization possible, reduces local extinction, and hence can rescue the metapopulation from global extinction [4, 41]; on the other hand, frequent dispersal might result in spatial synchrony, destroy the heterogeneity of metapopulations, and hence might make the metapopulation vulnerable to threats, such as disease [12, 15, 26]. However, although dispersal has already shown its importance in the persistence of metapopulation, we discover that delays associate with dispersal cannot affect the dynamics of the metapopulation, which is, I would say, a peculiar feature of metapopulations, but also a advantageous feature, indeed.

Delays associated with establishment can de-stabilize the metapopulation about the positive equilibrium, i.e., the Paradox of Enrichment may occur, based on the result that there are regions where the positive equilibrium is not absolutely stable in models (3.6) and (3.9) (see Propositions 6 and 8). Comparing Propositions 6 and 8, we can find the following similarity and differences of models (3.6) and (3.9). For the DDE version (3.6) of Levins' model with delayed establishment, an interesting result is that when the extinction rate e is intermediate, i.e., $(c/3 < e < c)$, the positive equilibrium cannot be de-stabilized, but when the extinction rate continues to decline $(e < c/3)$ oscillations can occur, leading to global extinction. For the DDE version (3.9) of Hanski's model with delayed establishment, we find some interesting properties when positive equilibria exist: i) at a intermediate degradation rate $(c/3 < d < c)$,

metapopulations cannot be de-stabilized; ii) for smaller degradation rates ($d < c/3$), metapopulations with intermediate extinction rate will not be de-stabilized about their positive equilibrium; iii) for smaller degradation rates ($d < c/3$), metapopulations with small extinction rate can be de-stabilized when establishment delay exceeds a critical transition threshold. The degradation rate d in model (3.9) and the extinction rate e in model (3.6) both reflect the loss of islands that are capable of sending out colonists, so it is reasonable that the regions of absolute stability in models (3.6) and (3.9) both highlight the critical values c and $c/3$. Moreover, the quality-structured model (3.9) require both of the degradation rate and the extinction rate to be small to generate oscillatory behaviours, which is in effect limiting the possibility of de-stabilization, and alleviates the Paradox of Enrichment.

The Paradox of Enrichment emerging in our DDE models (3.3), (3.6) and (3.9) results from the two-sided effect of increasing the extinction rate: metapopulations can be rescued from global extinction if the extinction rate falls below the colonization rate, but metapopulations could go extinct or have an increased amplitude of oscillations when the extinction rate is too small. Such a Paradox of Enrichment is not only a theoretical phenomenon. We can get a hint from the work by Molofsky et. al. [29]. In Molofsky et. al.'s simulations which is based on their experimental data, the most connected metapopulations do not have the minimum extinction risk [see Fig. 6. in 29]. Since the connectivity indicates how easy the colonization events can occur, it is reasonable to deem the most connected metapopulations to have the largest colonization rate. Although we have been talking about the effect of changing the extinction rate in our models, we can actually interpret the results in terms of changing the colonization rate alternatively because the effect of reducing the extinction rate is equivalent to the effect of increasing the colonization rate (see Figure 3.4). Therefore, intermediate colonization rate can ensure stability of the positive equilibrium, but large colonization rate can lead to de-stabilization and even global extinction. Hence, Molofsky et. al.'s simulations [29] can be seen as a support for our Paradox of Enrichment. If we accept that the migration rate is related to the colonization rate, there is another experiment [7] confirming the negative effect

of high migration rate on the stability of metapopulations, compared with low migration rate.

To the best of the authors' knowledge, there is no empirical evidence in nature reported for the Paradox of Enrichment in a metapopulation study. Also, it is, undoubtedly, difficult to empirically test the paradox, because it involves a careful examination of time lags [19]. The scarcity and the difficulty might be due to the following three reasons. First, many researchers have focused on the impact of factors associated with dispersal, as dispersal is an essential composition of metapopulations. Although delays associated with dispersal are expected in nature, our models have predicted that the Paradox of Enrichment cannot occur to metapopulations with dispersal delays alone. If this is the case in nature, research interests on delay might be discouraged. Second, some researchers argue that a strict metapopulation structure in nature is rare [9]. Moreover, the delay associated with establishment is usually not easy to observe and measure [3], since establishment events might not affect each breeding season, e.g. a lot of birds breed yearly, which might not be affected be establishment delays shorter than a year. Tropical birds can breed several times a year because of favourable environment [38], so it might be easier to use those birds to test the paradox. Although, tracking the oscillations might require a very long time in nature. Third, there might be natural mechanisms to resolve this paradox, just like what we find when including a structure based on islands' quality: the Paradox of Enrichment is alleviated. Despite the scarcity and the difficulties, experiments might be done using laboratory materials, as in [7, 14, 23].

Hanski and Ovaskainen show that, after metapopulations fall below a threshold for survival, the time lag to extinction could be great [20]. Our models include delays in the metapopulation dynamics, so that the metapopulation might have an 'inertia' to survive. For example, a one-time short term catastrophe will be carried on periodically depending on the delay, but will not destroy the metapopulation all at once. In this sense, our models with establishment delays provide another way of thinking about the Allee affect [6], which describes the situation when the growth of density is negative if the density of a metapopulation is below a threshold. Without delays, a metapopulation goes extinct whenever it is below a threshold (usually, an

unstable positive saddle node). But with delays involved, the metapopulation may be below the threshold for a while, but recover afterwards, because it has some 'savings' from earlier due to delays, i.e., some islands undergoing establishment that are able to send out colonists later. As long as the metapopulation does not stay below the threshold for too long, it might be able to recover.

Research on metapopulations is associated closely with conservation biology [21, 24]. Human-mediated habitat fragmentation and degradation have caught much attention in biodiversity [18, 30]. Strategies of metapopulation conservation usually include increasing connectivity, or reducing extinction rate. However, going too far is as bad as not going far enough when it comes to the conservation efforts. From our predictions, reducing extinction rate too much might lead to global extinction. Properly planned conservation effort can prevent a metapopulation from extinction, but too much might be harmful.

In this paper, we use the modified routine `dde23` in MATLAB (and bounded DDE function for model (3.9)) to simulate metapopulation densities numerically (see the caption of Figure 3.2). We need to modify it because our densities are bounded, but the routine in MATLAB does not offer constraints to solutions. An adaptive numerical scheme might be developed in the future to better handle bounded solutions as a complement to our work. The routine `ddesd` might be useful to solve our problem.

Our work considers the impact of spatially homogeneous enrichment, while spatially heterogeneous enrichment should be more common and worthy of investigation. Also, experimental studies of the Paradox of Enrichment in metapopulation might provide further insights. One possibly useful research area to apply our models is on the control of pest metapopulations. For example, if the life cycle of a pest species includes a delay that is not neglectable so that oscillations might be possible, experiments include the following steps to test our theory: allow the local extinction rate of the pest metapopulations to reduce first, observe whether the metapopulation oscillates; as the reducing of extinction rate, whether the oscillation amplitude gets larger; as the extinction rate declines further, whether global extinction might occur.

Bibliography

[1] K. C. Abbott. A dispersal-induced paradox: synchrony and stability in stochastic metapopulations. *Ecology Letters*, 14(11):1158–1169, 2011.

[2] H. R. Akçakaya, G. Mills, and C. P. Doncaster. The role of metapopulations in conservation. *Key Topics in Conservation Biology*, pages 64–84, 2007.

[3] J. Arino, L. Wang, and G. S. Wolkowicz. An alternative formulation for a delayed logistic equation. *Journal of Theoretical Biology*, 241(1):109–119, 2006.

[4] J. H. Brown and A. Kodric-Brown. Turnover rates in insular biogeography: effect of immigration on extinction. *Ecology*, 58(2):445–449, 1977.

[5] C. Burrows. Patterns of delayed germination in seeds. *New Zealand Natural Sciences*, 16:13–19, 1989.

[6] F. Courchamp, L. Berec, and J. Gascoigne. *Allee effects in ecology and conservation*. Oxford University Press, 2008.

[7] S. Dey and A. Joshi. Stability via asynchrony in Drosophila metapopulations with low migration rates. *Science*, 312(5772):434–436, 2006.

[8] U. Dieckmann, B. O'Hara, and W. Weisser. The evolutionary ecology of dispersal. *Trends in Ecology & Evolution*, 14(3):88–90, 1999.

[9] E. A. Fronhofer, A. Kubisch, F. M. Hilker, T. Hovestadt, and H. J. Poethke. Why are metapopulations so rare? *Ecology*, 93(8):1967–1978, 2012.

[10] G. F. Fussmann, S. P. Ellner, K. W. Shertzer, and N. G. Hairston Jr. Crossing the Hopf bifurcation in a live predator-prey system. *Science*, 290(5495):1358–1360, 2000.

[11] M. E. Gilpin and M. Rosenzweig. Enriched predator-prey systems: theoretical stability. *Science*, 177(4052):902–904, 1972.

[12] E. E. Goldwyn and A. Hastings. When can dispersal synchronize populations? *Theoretical Population Biology*, 73(3):395–402, 2008.

[13] E. Gopalakrishnan, Y. Sharma, T. John, P. S. Dutta, and R. Sujith. Early warning signals for critical transitions in a thermoacoustic system. *Scientific Reports*, 6:35310, 2016.

[14] B. D. Griffen and J. M. Drake. Environment, but not migration rate, influences extinction risk in experimental metapopulations. *Proceedings of the Royal Society of London B: Biological Sciences*, 276(1677):4363–4371, 2009.

[15] N. Haddad, B. Hudgens, E. Damschen, D. Levey, J. Orrock, J. Tewksbury, A. Weldon, J. Liu, V. Hill, and A. Morzillo. Assessing positive and negative ecological effects of corridors. *Sources, sinks, and sustainability. Cambridge University Press, Cambridge, UK*, pages 475–503, 2011.

[16] I. Hanksi and M. Gilpin. Metapopulation dynamics: brief history and conceptual domain. *Biological Journal of the Linnean Society*, 42:3–16, 1991.

[17] I. Hanski. Single-species spatial dynamics may contribute to long-term rarity and commonness. *Ecology*, 66(2):335–343, 1985.

[18] I. Hanski. Metapopulation dynamics. *Nature*, 396(6706):41–49, 1998.

[19] I. Hanski. Spatially realistic theory of metapopulation ecology. *Naturwissenschaften*, 88 (9):372–381, 2001.

[20] I. Hanski and O. Ovaskainen. Extinction debt at extinction threshold. *Conservation Biology*, 16(3):666–673, 2002.

[21] I. Hanski and D. Simberloff. The metapopulation approach, its history, conceptual domain, and application to conservation. In *Metapopulation biology*, pages 5–26. Elsevier, 1997.

[22] G. E. Hutchinson. Circular causal systems in ecology. *Annals of the New York Academy of Sciences*, 50(1):221–246, 1948.

[23] A. R. Ives, S. T. Woody, E. V. Nordheim, C. Nelson, and J. H. Andrews. The synergistic effects of stochasticity and dispersal on population densities. *The American Naturalist*, 163(3):375–387, 2004.

[24] W. F. Laurance. Theory meets reality: how habitat fragmentation research has transcended island biogeographic theory. *Biological Conservation*, 141(7):1731–1744, 2008.

[25] R. Levins. Some demographic and genetic consequences of environmental heterogeneity for biological control. *Bulletin of the Entomological Society of America*, 15(3):237–240, 1969.

[26] A. Liebhold, W. D. Koenig, and O. N. Bjørnstad. Spatial synchrony in population dynamics. *Annual Review of Ecology, Evolution, and Systematics*, 35:467–490, 2004.

[27] R. M. May. Limit cycles in predator-prey communities. *Science*, 177(4052):900–902, 1972.

[28] D. R. McCullough. *Metapopulations and wildlife conservation*. Island Press, 1996.

[29] J. Molofsky and J.-B. Ferdy. Extinction dynamics in experimental metapopulations. *Proceedings of the National Academy of Sciences of the United States of America*, 102(10): 3726–3731, 2005.

[30] S. P. Riley, R. M. Sauvajot, T. K. Fuller, E. C. York, D. A. Kamradt, C. Bromley, and R. K. Wayne. Effects of urbanization and habitat fragmentation on bobcats and coyotes in southern California. *Conservation Biology*, 17(2):566–576, 2003.

[31] M. L. Rosenzweig. Paradox of enrichment: destabilization of exploitation ecosystems in ecological time. *Science*, 171(3969):385–387, 1971.

[32] S. Roy and J. Chattopadhyay. The stability of ecosystems: a brief overview of the paradox of enrichment. *Journal of Biosciences*, 32(2):421–428, 2007.

[33] S. Ruan. Delay differential equations in single species dynamics. In *Delay differential equations and applications*, pages 477–517. Springer, 2006.

[34] M. Scheffer, J. Bascompte, W. A. Brock, V. Brovkin, S. R. Carpenter, V. Dakos, H. Held, E. H. Van Nes, M. Rietkerk, and G. Sugihara. Early-warning signals for critical transitions. *Nature*, 461(7260):53–59, 2009.

[35] L. F. Shampine and S. Thompson. Solving DDEs in MATLAB. *Applied Numerical Mathematics*, 37(4):441–458, 2001.

[36] D. Simberloff. The contribution of population and community biology to conservation science. *Annual Review of Ecology and Systematics*, 19(1):473–511, 1988.

[37] H. L. Smith. *An introduction to delay differential equations with applications to the life sciences*. Springer, 2011.

[38] P. C. Stouffer, E. I. Johnson, and R. O. Bierregaard Jr. Breeding seasonality in central amazonian rainforest birds. *The Auk*, 130(3):529–540, 2013.

[39] E. Tromeur, L. Rudolf, and T. Gross. Impact of dispersal on the stability of metapopulations. *Journal of Theoretical Biology*, 392:1–11, 2016.

[40] B. Veilleux. An analysis of the predatory interaction between paramecium and didinium. *Journal of Animal Ecology*, pages 787–803, 1979.

[41] T. Vogwill, A. Fenton, and M. A. Brockhurst. Dispersal and natural enemies interact to drive spatial synchrony and decrease stability in patchy populations. *Ecology Letters*, 12 (11):1194–1200, 2009.

[42] S. Wang, B. Haegeman, and M. Loreau. Dispersal and metapopulation stability. *PeerJ*, 3:e1295, 2015.

Chapter 4

Evolution of Dispersal with Temporal, Global-Scale Fluctuations in its Cost

4.1 Introduction

Dispersal of individuals from their birthplace can be an adaptive means of reducing competition among kin [16, 47], and avoiding inbreeding depression [18, 43]. Dispersal can also be an advantageous strategy for coping with, or otherwise exploiting, variable environmental conditions [10, 17], and on this point much has been written. Early theoretical work demonstrated that dispersal changes in response to environmental variability, possibly because such changes provide individuals with a way to average-out the fitness peaks and valleys encountered over space and time (van Valen, 1971; Gillespie, 1981; Levin et al., 1984; see also Cohen and Levin, 1991). More recently, models have shown that environmental variability can lead to disruptive selection, coexistence of distinct dispersal phenotypes, and possibly the emergence of new species [3, 35–37].

Despite the many studies devoted to the evolution of dispersal in variable environments, gaps in our understanding still exist. Previous work, for example, has focused exclusively on haploid asexual species [6, 35, 42], often with large local populations [4, 24, 36, 37]. More

importantly, previous work has neglected the effects of temporal environmental fluctuations when these show a strong positive correlation across local populations. Neglect in this regard likely stems from the expectation that, when local populations are large, costly dispersal from one location to another in a similar state will be selected against [e.g. 36]. Of course, one will not have the same expectations when local population sizes are small [16, 47]; but there are three, even better reasons for investigating these kinds of environmental fluctuations.

The first reason to focus on the effect of global-scale environmental variability is that the relevant factors, like seasonal temperature variation, act as dispersal cues for some species [1, 11, 54]. The use of environmental cues in this way raises questions about its adaptive significance. Second, it is predicted that species ranges will respond to large-scale environmental shifts associated with climate change [2]. Since dispersal is the primary mechanism by which range expansions occur, these predictions have led to calls for further investigations into the evolution of dispersal in the face of geographically widespread environmental change [49]. Third, dispersal in any kind of environment – including those that fluctuate over time – will determine genetic relatedness among neighbours, and so will indirectly exert influence on the evolution of a variety of social behaviours [5, 39, 53]. This is particularly relevant to the study of certain cooperative-breeding systems, where individuals delay dispersal and independent reproduction to help rear offspring produced by relatives [13]. Indeed, temporal environmental variability has been identified as a key driver of cooperative breeding [45], but remains poorly understood [46].

Here, we devise and analyse several models for the evolution of dispersal in an environment that changes over time in a random fashion. With an eye toward better understanding the origin of cooperative-breeding systems, we assume that during some years the global state of the environment is poor, and in other years is good [e.g. as described by 46]. We also focus on the impact this environmental variation has on dispersal cost, recognizing that dispersal cost is only one of the ecological constraints faced by cooperative breeders [13].

Although we are interested in commenting on cooperative-breeding systems, ours is a

model of dispersal evolution only. We present approximate expressions for the stable rate of dispersal, and the stable rates of dispersal expressed conditional upon environmental state. Our analysis shows that models without environmental variation provide a reasonably accurate picture of the evolution of unconditional dispersal, when variance in dispersal cost is not large. Our analysis also leads us to predict that more frequent environment fluctuation will favour the evolution of more divergent conditional dispersal phenotypes. We explain predictions in terms of the temporal autocorrelation in environmental state, and (as suggested above) we discuss their implications for the origin of cooperative breeding, in particular.

4.2 Models

4.2.1 Life Cycle

The overall structure of the model is standard. We consider an ideally infinite population of diploid sexual hermaphrodites. At the beginning of a given year, the infinite population is subdivided into groups of N adult individuals. Groups, themselves, persist on patches of habitat that are identical in quality.

We assume that the global state of the environment in which the population exists changes from one year to the next in a random fashion (Appendix B.1). Specifically, the environment varies according to a Markov process, and is either found in a "poor" state, or a "good" state in any particular year. For simplicity, we assume that the environment changes state from one year to the next with probability s. The symmetry, here, implies that environmental states appear equally often over time, on average (this assumption, in particular, is addressed in the Discussion). The variable s will be a single convenient measure of environmental fluctuation. If s is small then it is very likely that the environment will not change state from one year to the next; if s is large, then a year-to-year change in environmental state is likely. In addition, as s increases the correlation between successive environmental states decreases (Figure 4.1). Importantly, the kind of random variation between two states we propose here is in line with

the natural history of cooperative-breeding species [13, 46].

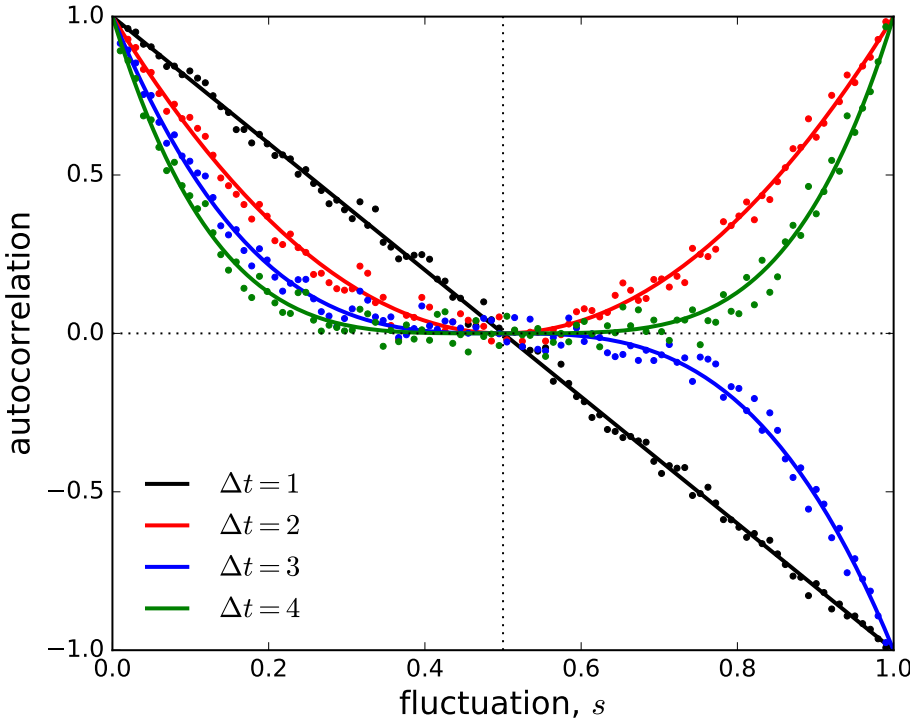

Figure 4.1: Relationship between the autocorrelation of environmental state and the degree of environmental fluctuation, s. Correlations between environmental states separated by $\Delta t = 1$ to 4 are shown. Points show calculated autocorrelations from a simulation of environmental change over 1 000 time periods. Solid lines provide theoretical correlations that follow $(1-2s)^{\Delta t}$ (see Appendix B.1).

At the beginning of a given year, each of the adults in a group is prepared to give birth. Indeed, each adult produces a very large number of offspring early in the year. Following the birth of their offspring, each adult dies. We also assume that each offspring matures following the death of adults. We continue to call these mature individuals "offspring," however, to avoid confusion.

Next, one of two things occurs. In one version of our model, offspring disperse in search of a new patch, then mating takes place at random among offspring that find themselves on the same patch. In an alternative version of our model, random within-patch mating occurs

prior to offspring dispersal. Following Taylor [47], the former version of the model is termed "Dispersal Before Mating" (DM) and the latter is termed "Dispersal After Mating" (MD). In the most general formulation of both versions of the model, we allow dispersal to be conditional upon the current state of the environment. We use d_e to denote the probability with which a given offspring disperses in search of a new patch, given that the environment during the year of its birth is in state e, where $e = p$ if poor and $e = g$ if good. This type of conditional tendency to disperse could be tied, for example, to thermal sensitivity [2].

In keeping with available evidence [40], we will treat offspring dispersal d_e as a phenotype that is determined, in an additive manner, by the alleles found at a single autosomal locus. That said, it is not always the genotype of the offspring itself that will determine d_e. In the "Parental Control" version of the model, in fact, it is the genotype of the parent that we assume determines d_e—specifically, the parent who gave birth to the offspring in question. Such a case might arise in plants when parental genotype affects offspring dispersal by determining seed size. In the "Offspring Control" version of the model, we make the more usual assumption that it is the offspring's own genotype that determines, d_e.

During dispersal, some of the dispersing offspring are assumed to die before finding a new patch. The probability that a dispersing offspring dies is denoted c_e, and depends on the environmental state. The probability c_e captures the cost of dispersal. Given the assumptions made above, $c = (c_p+c_g)/2$ represents the time-averaged cost of dispersal, and if $\sigma = (c_p-c_g)/2$ then σ^2 gives the variance in cost. Importantly, the time-averaged cost of dispersal and its variance are both independent of environmental fluctuation measured by s.

Once the dispersal phase is complete, competition to become one of the N adults found on a given patch in the next year occurs. We assume this competition occurs among all of the offspring found on the same patch. We model competition in the usual way: as a fair lottery, with winners for each of the N available spots chosen with replacement. It follows that the likelihood with which any of the N spots is won by an offspring native to the patch is given by $h_e = (1 - d_e)/(1 - c_e d_e)$. It also follows that the expected contribution made to the gene

pool in the very distant future by any given offspring competing on the patch is proportional to $v_e = 1/(1 - c_e d_e)$. In other words, v_e expresses a competitor's "reproductive value" [15].

When the competition phase is complete, those without a spot on a patch die. The environment for the coming year is then randomly determined, we relabel offspring as adults, the current year ends, and the entire process above repeats.

Different organisms time dispersal differently [12, 41]. We investigate DM and MD to reflect this diversity, and for completeness. Offspring control makes sense, because the individuals genotype often controls its phenotype (e.g., eye colour). Parental control of offspring dispersal may seem strange, but it could occur in many taxa. For example, a parent plant could allocate more/ less resources to each seed it produces to make it heavier/ lighter, or might invest in structures that promote dispersal via, say, wind. Animal parents, for their part, may simply evict offspring from territories [8, 31].

4.2.2 The Inclusive-Fitness Effect of Dispersal

The mathematical model we derive centres on "the inclusive-fitness effect of dispersal." The inclusive-fitness effect of dispersal describes how a small increase in an offspring's tendency to disperse (d_e), in turn, changes the inclusive fitness [25] of the individual who controls offspring dispersal. We derive mathematical expressions for the inclusive-fitness effect of dispersal using standard tools [48] in Appendix B.2. For the present discussion, though, a more biologically motivated development, modified from Taylor [47], will suffice.

Consider an offspring, in environment e, who was forced to disperse (for some unspecified reason that is of no consequence to us) when the typical action would have been to remain on its natal site. Now ask, how has this event changed the inclusive fitness of the individual whose genotype controls offspring dispersal?

The first change is that the offspring in question incurs the risk of dying during dispersal. In the DM model, the increased tendency to disperse means that the offspring is more likely to miss out on being fertilized (success through female function) and on fertilizing another

individual (success through male function) once the dispersal phase is complete. Hence

$$\text{DM:} \quad c_e \left(\frac{v_e}{2} + \frac{v_e}{2} \right) R_e = c_e v_e R_e \tag{4.1}$$

is the appropriate inclusive-fitness cost, where R_e is the relatedness between the dispersed offspring and the individual who controls its dispersal (the definition of genetic relatedness as well as calculation of all relatedness measures can be found in Appendix B.3). In the MD model, risk associated with increased probability of dispersing means that the offspring and the patchmate who fertilized the offspring both miss out on the opportunity to produce offspring. Therefore

$$\text{MD:} \quad c_e \left(\frac{v_e}{2} R_e + \frac{v_e}{2} \bar{R}_e \right) = c_e v_e \frac{R_e + \bar{R}_e}{2} \tag{4.2}$$

is the appropriate cost, where $\bar{R}_e$ is the relatedness between the offspring's average contemporary patchmate and the individual controlling offspring dispersal.

The second change is related to reduction in competition among relatives owing to (for want of a better term) the unscheduled departure of the offspring in question. For both the DM and MD models, the unscheduled departure removes competition, valued at $2(v_e/2) = v_e$, from the offspring's natal patch. This provides a benefit of equal value to the average competitor on the offspring's natal patch [22], and because this average competitor is native to the patch with probability h_e, we record

$$\text{DM and MD:} \quad v_e h_e \bar{R}_e \tag{4.3}$$

as the inclusive-fitness benefit.

By subtracting the inclusive-fitness costs (equations 4.1 and 4.2, respectively) from the benefit (equation 4.3), we arrive at the inclusive-fitness effect of dispersal in environment e, denoted ΔW_e:

$$\text{DM:} \quad \Delta W_e = (-R_e\, c_e + \bar{R}_e\, h_e)\, v_e, \quad e = p, g, \tag{4.4a}$$

$$\text{MD:} \quad \Delta W_e = \left(-\frac{R_e + \bar{R}_e}{2} c_e + \bar{R}_e h_e \right) v_e, \quad e = p, g. \tag{4.4b}$$

When ΔW_e is positive (resp. negative) selection favours an increase (resp. decrease) in d_e, so an equilibria pair (d_p, d_g) needs to satisfy $\Delta W_p = 0$ and $\Delta W_g = 0$. This motivates the computational model of evolution described in the next section.

When dispersal cannot be expressed conditional upon the environment, the model is restricted by $d_p = d_g = d$. In this case the inclusive-fitness effect is

$$\Delta W = \frac{1}{2}\Delta W_p + \frac{1}{2}\Delta W_g \Big]_{d_p = d_g = d} \tag{4.5}$$

where the one-half factors reflect the fraction of time the environment spends in one state or the other (formally, the factors reflect total reproductive values of individuals given their environment; see Taylor and Frank, 1996). As before, the sign of ΔW determines whether selection favours an increase or a decrease in d.

We will consider the evolution of a dispersal phenotype to be at equilibrium when the corresponding inclusive-fitness effect is zero. For the conditional-expression model in (4.4), an "equilibrium phenotype pair" can be found by solving the equations $\Delta W_p = 0$ and $\Delta W_g = 0$, simultaneously, for the pair of variables, d_p and d_g. This problem is more difficult than our notation suggests, since the inclusive-fitness effects are coupled through their constituent relatedness coefficients. For the case in which dispersal cannot be expressed conditional upon e (equation 4.5) a single "equilibrium phenotype" can be found by solving $\Delta W = 0$ for d. Of course, other kinds of evolutionary outcomes are possible—for example, dispersal phenotypes may take extreme values like zero or one. However, we will focus on cases where evolution due to selection is at equilibrium.

4.2.3 Mathematical Analysis

The analytical techniques we use involve treating our model like a perturbed version of one that has no environmental variation, namely that desribed by Taylor [47]. We treat σ as a perturbation parameter, and we expand key variables in the model as power-series in this parameter. Approximate results are then obtained by neglecting terms of order $O(\sigma^2)$. Mathematical details can be found in Appendix B.4.

4.2.4 Numerical Procedures, Simulations, and Model Validation

In Appendix B.5 we describe an iterative numerical procedure that estimates the equilibrium phenotype or phenotype pair. The procedure begins with several guesses at the equilibrium or equilibrium pair. Each guess is then updated, independently, by changing it a small amount in a direction that is consistent with the sign of the corresponding inclusive-fitness effect. This is continued until updated guesses differ from one another only by some small amount. By virtue of its construction, the procedure confirms that equilibria are evolutionary attractors. Code for the numerical procedure, provided in Appendix B.5, can be run on a desktop computer.

In Appendix B.5 we also describe an individual-based simulation of the model. In contrast to the discussion that led to the inclusive-fitness effect, our simulation assumes a finite number of patches, and explicitly allows for mutations. The simulation also treats selection as a multi-level version of a Wright-Fisher process [see e.g. 14], and does not rely on inclusive-fitness based arguments.

Because the simulation is more computationally intensive than the numerical procedure, we used it only as a means of validating the numerical predictions in a small number of test cases. Simulation results from the test cases we investigated agreed very closely with the predictions we generated numerically (see Appendix B.5). Close agreement was found for each version of the model we constructed (DM/MD, Parental/Offspring Control). Still, small discrepancies were observed when numerical predictions were close to either zero or one. We attributed these discrepancies to the inherent mutation bias in the simulated process near zero

or one: in the simulation, dispersal phenotypes that took values less than zero (resp. greater than one) following mutation were assigned values slightly greater than zero (resp. less than one).

4.3 Results

4.3.1 Unconditional Dispersal

Our results are more readily understood if we give first consideration to the models in which dispersal is not expressed conditional on the environment (i.e. models based on equation 4.5, where $d_p = d_g = d$). In these cases, we find that, to first order in σ, equilibrium dispersal phenotypes, denoted as d_0, correspond to predictions made by models that treat the environment as constant [16, 47]. To be clear, the correspondence is established by replacing a constant cost of dispersal in previous models with the time-averaged one we use here, c (table 4.1). Our predictions about unconditional dispersal rates certainly make intuitive sense given the interpretation of σ^2, and given that we neglect terms of order $O(\sigma^2)$. Still, agreement between approximate and numerical results are close, even for larger values of σ (e.g. Figure 4.2a,b).

Table 4.1: Predicted unconditional probability of dispersal d_0 from mathematical analysis.

	Model	d_0	H
DM	Parental Control	$\frac{H+1-2Nc}{H+1-2Nc^2}$	$\sqrt{1+4N(N-1)c^2}$
	Offspring Control	$\frac{H+1-4Nc}{H+1-4Nc^2}$	$\sqrt{1+8N(2N-1)c^2}$
MD	Parental Control[a]	$\frac{(N-1)c+1-H}{(N-H)c}$	$\sqrt{1+(N+1)(N-1)c^2}$
	Offspring	$\frac{H+1-2Nc}{H+1-2Nc^2}$	$\sqrt{1+4N(N-1)c^2}$

Cases with $N = 1$ can be resolved by treating N as a continuous variable and taking an appropriate limit.

[a] This model was not considered by Taylor [47].

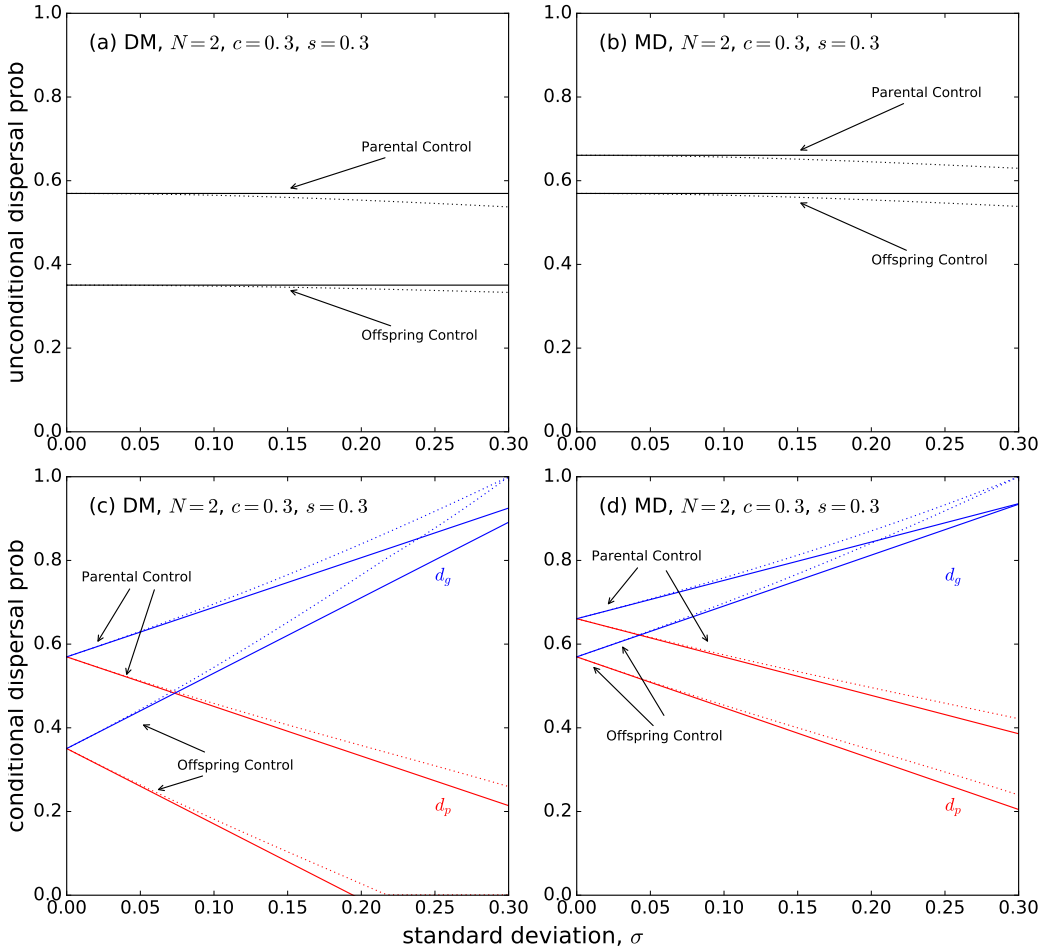

Figure 4.2: A comparison of predictions made by iterative numerical determination of equilibrium or equilibrium pairs (dotted lines), and those made by approximations based on small degree of environmental variation (solid lines). Results are presented for the DM and MD models, respectively, with either Parental or Offspring control of dispersal. We assume (a, b) unconditional expression of dispersal, or (c,d) conditional expression of dispersal (red = poor environmental state, blue = good environmental state). As expected, agreement begins to break down as environmental variation, measured by σ, increases. However, numerical predictions and approximations are still close. Approximations are not valid whenever at least one of d_p or d_g takes a boundary value of zero or one.

4.3.2 Dispersal Conditional on Environmental State

The effect of environmental variation is predicted to be seen when dispersal is conditional upon environmental state e. In this case, equilibrium phenotype pairs can be written as

$$d_p = d_0 + \left(\frac{d_0 h_0}{1 - c h_0} - \frac{1 - c}{(1 - c h_0)^2} \delta h \right) \sigma + O(\sigma^2) \tag{4.6a}$$

$$d_g = d_0 - \left(\frac{d_0 h_0}{1 - c h_0} - \frac{1 - c}{(1 - c h_0)^2} \delta h \right) \sigma + O(\sigma^2) \tag{4.6b}$$

where d_0 comes from table 4.1 and depends on the model considered, where $h_0 = (1 - d_0)/(1 - cd_0)$, and where δh captures how h_e changes with σ. Expressions for δh are presented in table 4.2, and these also depend on which version of the model is being considered. We find that approximate expressions for equilibrium pairs of dispersal phenotypes in (4.6) agree closely with corresponding numerical predictions, even as variance in cost is increased substantially (Figure 4.2c,d). In addition, by averaging equations in (4.6) over time, we see that overall dispersal rates approximately agree with predictions from models of constant environments, represented by d_0.

Table 4.2: Expressions for δh found in formulas for conditional probabilities of dispersal d_e.

	Model	δh
DM	Parental Control	$-\frac{H-1}{2(N-1)c^2} \; \frac{2H+8N^2c^2s-4Nc^2s^2-3Nc^2+2}{2(4N(N-1)c^2s-H^2)+H(4Nc^2s(s-2)+3Nc^2-2)}$
	Offspring Control	$-\frac{H-1}{2(2N-1)c^2} \; \frac{H+16N^2c^2s-8Nc^2s^2-2Nc^2+1}{4Nc^2s(4N-1-2s)+H(2Nc^2-1-4Nc^2s)-H^2}$
MD	Parental Control	$-\frac{H-1}{(N-1)c^2} \; \frac{(8Ns+4s^2-8N-1)-(8Ns-4s^2+16s-7)H}{2s(4N-4s^2+8s-3)-(1-2s)(4s^2-8s+7)H^2-H(8Ns+4s^2-8N-1)}$
	Offspring	$-\frac{H-1}{2(N-1)c^2} \; \frac{[8s(N+1)-(4s^2+3)](N-1)c^2+2(1-2s)(H-1)}{2[s-H^2(1-s)]-H(1-2s)[2((N-1)c^2s-1)-3(N-1)c^2]}$

The appropriate expression for H can be found in the corresponding entry of table 4.1.
Cases with $N = 1$ can be resolved by treating N as a continuous variable and taking an appropriate limit.

An equilibrium phenotype pair, d_p and d_g, responds to changes in the variance of dispersal cost in an unsurprising way—one that can be understood by considering personal fitness

interests only. As the variance in dispersal cost increases, the cost of dispersal, itself, in any given year will deviate from its time-average to a greater extent. As a result, dispersal in a poor (resp. good) environment becomes more (resp. less) costly, and d_p decreases (resp. d_g increases) (Figure 4.2c,d). While it is true that increased (resp. decreased) dispersal cost will also increase (resp. decrease) the likelihood that benefits of dispersal are more (resp. less) strongly felt by relatives, these indirect changes in inclusive fitness are not expected to match the direct implications of dying during dispersal.

Changes in the the degree of environmental fluctuation elicit consistent changes to equilibrium pairs d_p and d_g, independent of the time-averaged cost of dispersal and its variance. Remarkably, as the environment fluctuates more frequently our models predict a decrease in dispersal in poor environments, and a concomitant increase in dispersal in good environments (Figure 4.3). In contrast to the previous result, the effect here can be explained by making reference to the indirect benefit of dispersal provided to relatives. To see this clearly, consider a situation in which environmental fluctuations are frequent, so that the state of the environment in one year is strongly negatively correlated with that in the next (Figure 4.1, black line). In this case, a good year is very likely to have been preceded by a poor year. That is to say, a good year is very likely to have been preceded by a year in which dispersers were few (Figure 4.2c,d), successful dispersers were even fewer, and philopatry rates (measured as h_p) were high. We expect, therefore, relatedness among patchmates in a good year to be high; combine this with the low direct cost of dispersal in a good year, an resulting increased willingness to reduce local competition makes intuitive sense. The same argument can be used (mutatis mutandis) to explain why dispersal in poor environments is reduced as environmental fluctuation increases.

In addition to providing us with brand new lessons, our results confirm previous ways of thinking about the evolution of dispersal. Previous models, for example, have predicted evolutionarily stable dispersal rates are reduced when either patch size, or cost of dispersal increases [e.g. 47, 52]. Figure 4.3 shows clearly that adaptive dispersal rates decrease as N becomes larger, and as time-averaged cost of dispersal goes up.

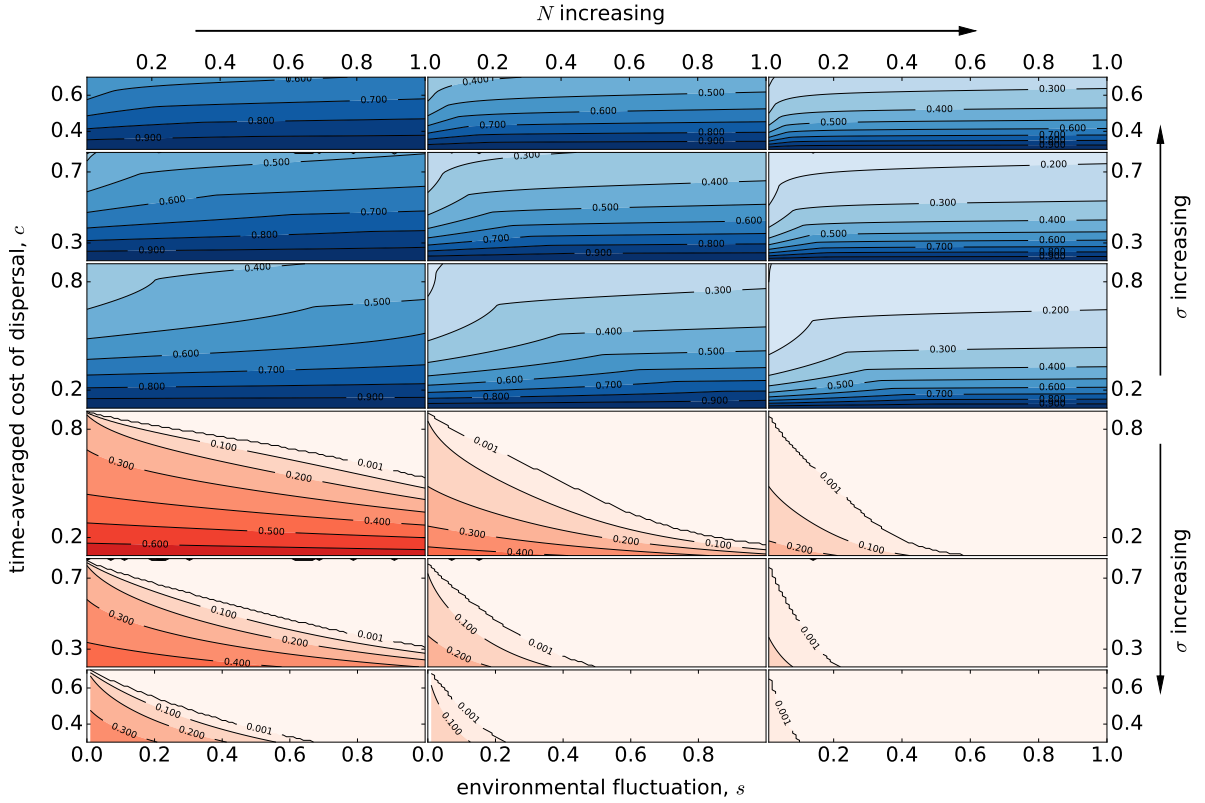

Figure 4.3: The relationship between environmental fluctuation, time-averaged cost of of dispersal, and the conditional probability of dispersing for the DM Model with Parental Control of dispersal. Numerical predictions for dispersal when environmental state is good are shown in blue (top three rows), while those for dispersal when environmental state is poor are shown in red (bottom three rows). Results for group size $N = 2, 4, 8$ and for standard deviation in cost $\sigma = 0.1, 0.2, 0.3$ are shown. All else being equal, increased environmental fluctuation is predicted to promote dispersal under good conditions, and philopatry when conditions are poor. Increased time-averaged cost is predicted to reduce conditional dispersal, as is increasing group size. The wavy nature of the contour of height 0.001 is an artefact of the numerical procedure.

Our results also add to our understanding of parent-offspring conflict [sensu 50]. It is well-established that offspring dispersal rates are greater when they are determined by a parent's genotype, relative to when they are determined by the genotype of the offspring itself [38, 47, see also Figure 4.2a,b]. Unsurprisingly, we find the parent-offspring conflict over dispersal persists when dispersal is expressed conditional upon environmental state (e.g. Figure 4.2c,d). However, the extent of the conflict, measured as the difference between the predictions of the Parental Control model minus those of the Offspring Control model, does not show a consistent response to environmental fluctuation (Figure 4.4).

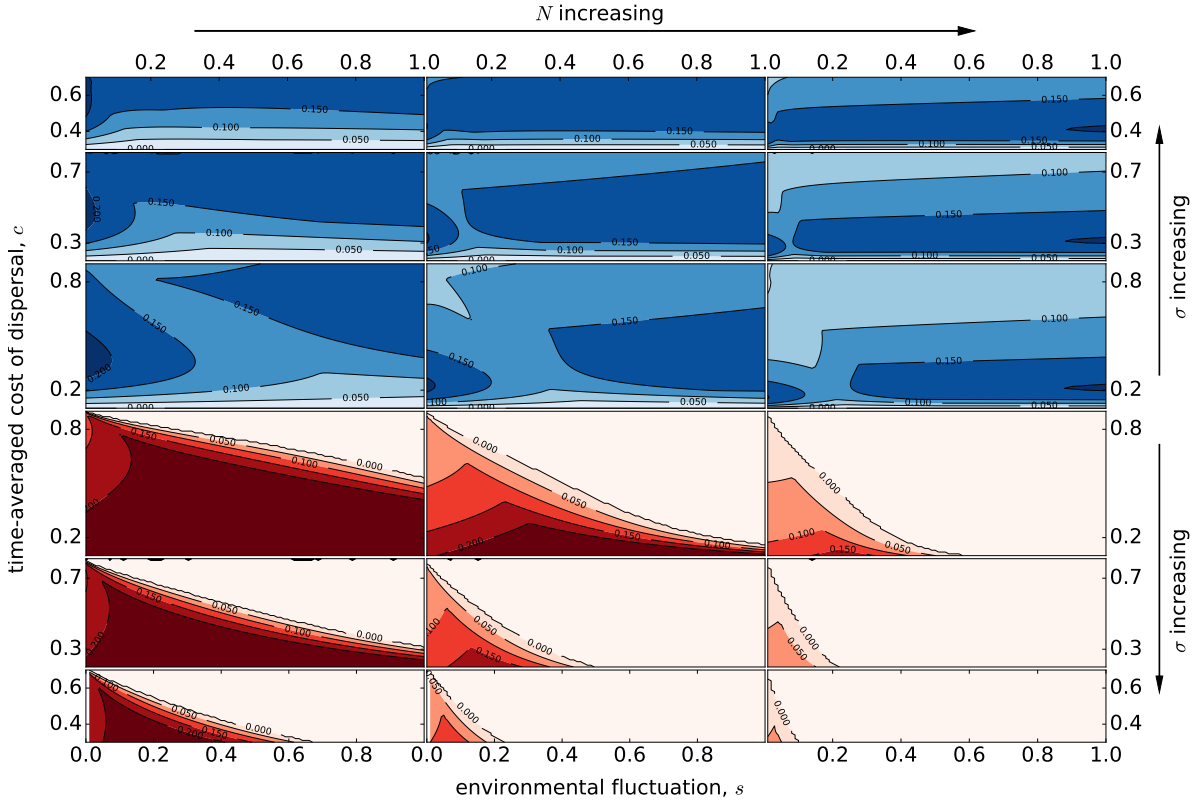

Figure 4.4: The relationship between environmental fluctuation, time-averaged cost of dispersal, and the extent of parent-offspring conflict over conditional tendency to disperse for the DM Model. Here, the extent of conflict is measured as d_e with Parental Control minus d_e with Offspring Control. Numerical predictions for dispersal when environmental state is good are shown in blue (top three rows), while those for dispersal when environmental state is poor are shown in red (bottom three rows). Results for group size $N = 2, 4, 8$ and for standard deviation in cost $\sigma = 0.1, 0.2, 0.3$ are shown. The wavy nature of the contour of height 0.000 is an artefact of the numerical procedure.

4.4 Discussion

4.4.1 General Issues

Dispersal is a trait whose evolution can be influenced by a wide variety of interacting factors, including the possibility for competition among kin [47], the degree of risk associated with inbreeding [18], the possibility of achieving adaptations to local conditions [3], amount of overlap among generations [28, 42], demographic stochasticity [6], and the extent and nature of environmental variation [37]. Here, we have devised models to examine the evolution of dispersal primarily in response to temporal environmental fluctuation. As mentioned in the Introduction, previous theoretical work along similar lines has relied on models with large local populations and/or haploid asexual genetics [4, 6, 24, 35–37, 42]. Our focus on small local populations allows us to emphasize the inclusive-fitness effects associated with dispersal in a fluctuating environment. Furthermore, the consideration we give to diploid sexual systems opens the door to questions about conflict over dispersal when the state of the environment is uncertain.

Given that we have taken a new look at dispersal, what new things have we found? In terms of unconditional dispersal rates, the simple answer is: very little. The symmetry inherent in our treatment of environmental variation, as well as the small-σ approximations we use mean that the rates of unconditional dispersal we predict are almost identical to those predicted by models that assume constant environments [16, 26, 47]. We do note, however, that when applying models of constant environments in scenarios where the environment fluctuates, the relevant costs to consider are the time-averaged ones.

Though our predictions about unconditional dispersal based on analytical approximations show no dependence on temporal environmental variation, numerical results suggest a slight dependence exists. Specifically, we find that evolutionarily stable levels of unconditional dispersal are altered slightly as the difference between cost of dispersal in poor and good environments goes up. Following Gillespie (1981), we could reasonably speculate that dispersal

is a reflection of genotypes "hedging their bets" by maximizing geometric-mean fitness. Alternatively, there may be a way to look at reduced dispersal rates predicted by our models as an individual-level adaptation meant to maximize inclusive fitness. Future work could confirm this alternative view by exploring a small-σ approximation to a higher degree of accuracy. Granted, the quantitative discrepancy that could potentially be explained is small, as evidenced in Figure 4.2a,b. Still, finding a qualitative interpretation for terms associated with more accurate approximations would not only provide further justification for the use of intentional language to describe evolution in stochastic environments [see 21], but also help recent efforts to outline a general design principle for understanding adaptation [19].

Turning our attention to conditional dispersal, we do find some new lessons emerging from our analyses. As might be expected, we predict that dispersal occurs more readily in good times when its cost is low. We also predict that the difference between individuals' tendency to disperse in good versus poor environmental states increases as the fluctuations between these states becomes more frequent. These predictions are certainly testable, and may, in fact, represent a valuable opportunity to connect theoretical models to empirical patterns. Historically, tests of theoretical predictions concerning the evolution of dispersal have been hampered by practical difficulties associated with differentiating between dispersers and non-dispersers, estimating dispersal costs, and generally meeting the idealized assumptions of most models [29]. However, there are a few reasons why previous obstacles might not hinder field biologists looking to test the predictions we make here. First, our predictions are not focused on precise dispersal rates, rather they are focused on *changes* in dispersal rates, and *changes to differences* in dispersal rates. This means that details concerning how one differentiates between a disperser and a non-disperser may be less important than ensuring that the definition of "disperser," whatever that may be, is applied in a consistent manner. Second, one of our predictions links the tendency to disperse with the degree of environmental fluctuation. Therefore, provided a reasonable connection can be made between environmental state and dispersal cost, precise estimation of the latter would not be required. What would be required, instead,

is an estimate of how frequently the relevant environmental state changes between dispersal events, and presumably such an estimate could be easily obtained. Third, none of the qualitative predictions we would suggest be tested is sensitive to model details. Indeed, we have investigated four different model variations (DM versus MD, Parent versus Offspring Control), and our simulation results (Appendix B.5) indicate that our predictions should be robust to deviations from the ideal assumptions made by our inclusive-fitness model.

In addition to the new lessons above, we find that the extent of parent-offspring conflict becomes more difficult to predict when the environment changes. Difficulties in this regard, are likely driven by the fact that the divergent perspectives of parents and offspring, respectively can only diverge so far: the probability of dispersal must remain between zero and one. So, while a small environmental change may exacerbate conflict, as the size or frequency of changes continues to grow perspectives will tend to align. We argue that challenges associated with predicting the extent of parent-offspring conflict are made up for, at least in part, by the fact that we are able to provide clear mathematical expressions for predicted dispersal rates when σ is small.

4.4.2 Implications for Cooperative Breeding

It is well understood that, in order for dispersal to be an effective means of escaping poor environmental conditions, the spatial scale on which it occurs must exceed that on which positive correlations in environmental conditions are observed [7, 27]. Some species, however, inhabit regions where the same environmental conditions are experienced over large geographic distances, and fluctuate from one year to the next [45]. Dispersal by individuals in these species, therefore, cannot be viewed as a means of improving personal circumstances. Instead, dispersal in these species can be viewed through the lens of the theory we present here, because the global-scale environmental fluctuations we introduce serve to model the regional-scale variation they experience.

Good examples of the kind of species to which our work may apply come from the

cooperative-breeding birds of Australia and Africa. The temporal variability in the environment faced by these birds has been found to be positively associated with their cooperative-breeding tendencies [13, 45]. To explain the positive association, authors typically emphasize the fecundity benefits of social aggregations [13, 44, 46], but evidence suggests that dispersal costs also incentivize the formation and maintenance of cooperative-breeding groups [32]. Indeed, Rubenstein [44] has argued that environmental variation might also lead to limited dispersal, increased relatedness among groups, and ultimately cooperative breeding. To support his perspective, Rubenstein [44] cited theoretical work that demonstrates, among other things, that increased variation in fecundity reduces the pool of ancestors available to present-day neighbours, and builds present-day relatedness as a result [33]. The models we propose make a more direct connection between environmental fluctuation and the scope for the emergence cooperative breeding. Specifically, our models show clearly that dispersal under adverse conditions is low and becomes lower as fluctuations become more frequent. Based on this, we can conclude that environmental fluctuations encourage closer associations among relatives which sets the stage for the emergence of cooperative breeding. We also stress that we allowed dispersal to be contingent on the state of the environment, and we have assumed that all groups experience the environment in the same way. Both of these features reflect issues relevant to the biology of cooperative breeders and are not dealt with elsewhere [see 33].

4.4.3 Limitations and Technical Considerations

Like all models, the ones we present here are limited by their assumptions. One possible limiting assumption might be that group size is not altered by a change in environmental state. By keeping group size constant we were able to approximate using earlier models that ignored environmental fluctuation [47], which in turn provided us with a way to achieve new analytical results. Future work could relax this assumption and consider groups whose size increases in good years and decreases in poor years. We can speculate that larger (resp. smaller) groups in good (resp. poor) years may reduce (resp. increase) the inclusive-fitness benefits of dispersal

in those years, but the overall effect on the evolution of dispersal will likely depend on how group size differs in good versus poor years. We expect the predictions we make here to hold for relatively small differences in group size, like those we might expect to observe, year-over-year, in cooperative-breeding groups.

We have also neglected reduction in fitness associated with inbreeding depression, in our models. Certainly, evidence of inbreeding depression can be found in natural populations [e.g. 23], including populations of cooperative breeders to which we think our models may be most relevant [30]. Incorporating the possibility of inbreeding depression into our models may be a fruitful next step. It is difficult to see how this model feature would interact with the aforementioned complication, namely fluctuating group size. We could once again speculate that in good (resp. poor) years the possibility for inbreeding depression would be reduced (resp. increased), as groups are large (resp. small) in size, and so there would be less (resp. more) incentive to disperse. Again, though, the extent to which our conclusions change will depend on how strong the depression is assumed to be.

Finally, temporal environmental change was not modelled in the most general way possible. We considered only two environmental states, but this is in keeping with views expressed by those studying cooperatively breeding species [e.g. 46], and with previous theoretical work on social evolution in temporally varying environments [39]. We have, in fact, taken a step beyond the modelling approach developed by Rodrigues and Gardner [39]. Those authors assume the probability of the population moving into a new state is independent of its current state (see their Appendix H), which implies that the autocorrelations that drive some of the results we present here could not be established using their framework. Of course, unlike Rodrigues and Gardner [39], we have a population that spends half of its time in one state, and half of its time in the other state. This feature of our model, however, was critical in permitting us to change the extent to which fluctuations occur without also changing the time-averaged cost of dispersal or its variance (see Appendix B.1). Any future work that relaxes our assumptions about temporal environmental change should be aware of the potential for fluctuation to confound

other economic aspects of dispersal.

Bibliography

[1] A. Battisti, M. Stastny, E. Buffo, and S. Larsson. A rapid altitudinal range expansion in the pin processionary moth produced by the 2003 climatic anomaly. *Global Change Biology*, 12:662–671, 2006. doi: 10.1111/j.1365-2486.2006.01124.x.

[2] M. P. Berg, E. T. Kiers, G. Driessen, M. van der Heijden, B. W. Kooi, F. Kuenen, M. Liefting, H. A. Verhoef, and J. Ellers. Adapt or disperse: understanding species persistence in a changing world. *Global Change Biology*, 16(2):587–598, 2010. doi: 10.1111/j.1365-2486.2009.02014.x.

[3] S. Billiard and T. Lenormand. Evolution of migration under kin selection and local adaptation. *Evolution*, 59:13–23, 2005. doi: 10.1111/j.0014-3820.2005.tb00890.x.

[4] F. Blanquart and S. Gandon. Evolution of migration in a periodically changing environment. *American Naturalist*, 177:188–201, 2011. doi: 10.1086/657953.

[5] M. G. Bulmer and P. D. Taylor. Dispersal and the sex ratio. *Nature*, 284:448–449, 1980. doi: 10.1038/284448a0.

[6] C. Cadet, R. Ferrire, J. A. J. Metz, and M. van Baalen. The evolution of dispersal under demographic stochasticity. *American Naturalist*, 162:427–441, 2003. doi: 10.1086/378213.

[7] J. Clobert, J. F. Le Galliard, J. Cote, S. Meylan, and M. Massot. Informed dispersal, hetergeneity in animal dispersal syndromes and the dynamics of spatially structured populations. *Ecology Letters*, 12:197–209, 2009. doi: 10.1111/j.1461-0248.2008.01267.x.

[8] T. Clutton-Brock, P. Brotherton, R. Smith, G. McIlrath, R. Kansky, D. Gaynor, M. O'riain,

and J. Skinner. Infanticide and expulsion of females in a cooperative mammal. *Proceedings of the Royal Society of London B: Biological Sciences*, 265(1412):2291–2295, 1998.

[9] D. Cohen and S. A. Levin. Dispersal in patchy environments: the effects of temporal and spatial structure. *Theoretical Population Biology*, 39:63–99, 1991. doi: 10.1016/0040-5809(91)90041-D.

[10] R. F. Denno. The evolution of dispersal polymorphisms in insects: The influence of habitats, host plants and mates. *Researches on Population Ecology*, 36:127–135, 1994. doi: 10.1007/BF02514927.

[11] O. DiIorio and R. E. Gürtler. Seasonality and temperature-dependent flight dispersal of *Triatoma infestans* (Hemiptera: Reduviidae) and other vectors of Chagas disease in western Argentina. *Journal of Medical Entomology*, 54:1285–1292, 2017. doi: 10.1093/jme/tjx109.

[12] A. Duputié and F. Massol. An empiricist's guide to theoretical predictions on the evolution of dispersal. *Interface Focus*, 3(6):20130028, 2013.

[13] S. T. Emlen. The evolution of helping. I. An ecological constraints model. *American Naturalist*, 119:29–39, 1982. doi: 10.1086/283888.

[14] W. J. Ewens. *Mathematical population genetics 1: Theoretical introduction*. Springer, New York, NY, 2004.

[15] R. A. Fisher. *The genetical theory of natural selection*. Clarendon Press, Oxford, UK, 1930.

[16] S. A. Frank. Dispersal polymorphisms in subdivided populations. *Journal of Theoretical Biology*, 122:303–309, 1986. doi: 10.1016/S0022-5193(86)80122-9.

[17] M. Gadgil. Dispersal: population consequences and evolution. *Ecology*, 52:253–261, 1971. doi: 10.2307/1934583.

[18] S. Gandon. Kin competition, the cost of inbreeding and the evolution of dispersal. *Journal of Theoretical Biology*, 200:345–364, 1999. doi: 10.1006/jtbi.1999.0994.

[19] A. Gardner. Adaptation as organism design. *Biology Letters*, 5:861–864, 2009. doi: 10.1098/rsbl.2009.0674.

[20] J. H. Gillespie. The role of migration in the genetic structure of populations in temporally and spatially varying environments. III. Migration modification. *American Naturalist*, 117:223–233, 1981. doi: 10.1086/283703.

[21] A. Grafen. Formal Darwinism, the individual-as-maximizing-agent analogy and bet-hedging. *Proceedings of the Royal Society, B*, 266:799–803, 1999. doi: 10.1098/rspb.1999.0708.

[22] A. Grafen and M. Archetti. Natural selection of altruism in inelastic viscous homogeneous populations. *Journal of Theoretical Biology*, 252:694–710, 2008. doi: 10.1016/j.jtbi.2008.01.021.

[23] P. J. Greenwood, P. H. Harvey, and C. M. Perrins. Inbreeding and dispersal in the great tit. *Nature*, 271:52–54, 1978. doi: 10.1038/271052a0.

[24] J. M. Greenwood-Lee and P. D. Taylor. The evolution of dispersal in spatially varying environments. *Evolutionary Ecology Research*, 3:649–665, 2001.

[25] W. D. Hamilton. The genetical evolution of social behaviour. I and II. *Journal of Theoretical Biology*, pages 1–52, 1964. doi: 10.1016/0022-5193(64)90038-4.

[26] W. D. Hamilton and R. M. May. Dispersal in stable habitats. *Nature*, 269:578–581, 1977. doi: 10.1038/269578a0.

[27] R. Ims and D. Ø. Hjermann. Condition-dependent dispersal. In J. Clobert, E. Danchin, A. A. Dhondt, and J. D. Nichols, editors, *Dispersal*, pages 203–216. Oxford University Press, Oxford, UK, 2001.

[28] A. J. Irwin and P. D. Taylor. Evolution of dispersal in a stepping-stone population with overlapping generations. *Theoretical Population Biology*, 58:321–328, 2000. doi: 10.1006/tpbi.2000.1490.

[29] M. L. Johnson and M. S. Gaines. Evolution of dispersal: theoretical models and empirical tests using birds and mammals. *Annual Review of Ecology and Systematics*, 21:449–480, 1990. doi: 10.1146/annurev.es.21.110190.002313.

[30] W. D. Koenig, M. T. Stanback, and J. Haydock. Demographic consequences of incest avoidance in the cooperatively breeding acorn woodpecker. *Animal Behaviour*, 57:1287–1293, 1999. doi: 10.1006/anbe.1999.1093.

[31] H. Kokko and P. Lundberg. Dispersal, migration, and offspring retention in saturated habitats. *The American Naturalist*, 157(2):188–202, 2001.

[32] J. Komdeur. Variation in individual investment strategies among social animals. *Ethology*, 112:729–747, 2006. doi: 10.1111/j.1439-0310.2006.01243.x.

[33] L. Lehmann and F. Balloux. Natural selection on fecundity variance in subdivided populatoins: kin selection meets bet hedging. *Genetics*, 176:361–377, 2007. doi: 10.1534/genetics.106.066910.

[34] S. A. Levin, D. Cohen, and A. Hastings. Dispersal strategies in patchy environments. *Theoretical Population Biology*, 26:165–191, 1984. doi: 10.1016/0040-5809(84)90028-5.

[35] F. Massol and F. Débarre. Evolution of dispersal in spatially and temporally variable environments: the importance of life cycles. *Evolution*, 69:1925–1937, 2015. doi: 10.1111/evo.12699.

[36] A. Mathias, É. Kisdi, and I. Olivieri. Divergent evolution of dispersal in a heterogeneous landscape. *Evolution*, 55:246–259, 2001. doi: 10.1111/j.0014-3820.2001.tb01290.x.

[37] M. A. McPeek and R. D. Holt. The evolution of dispersal in spatially and temporally varying environments. *American Naturalist*, 140:1010–1027, 1992. doi: 10.1086/285453.

[38] U. Motro. Optimal rates of dispersal. III. Parent-offspring conflict. *Theoretical Population Biology*, 23:159–168, 1983. doi: 10.1016/0040-5809(83)90011-4.

[39] A. M. M. Rodrigues and A. Gardner. Evolution of helping and harming in heterogeneous populations. *Evolution*, 66:2065–2079, 2012. doi: 10.1111/j.1558.5646.2012.01594.x.

[40] D. A. Roff. Why is there so much variation for wing dimorphism? *Researches on Population Ecology*, 36:145–150, 1994. doi: 10.1007/BF02514929.

[41] O. Ronce. How does it feel to be like a rolling stone? ten questions about dispersal evolution. *Annual Review of Ecology, Evolution, and Systematics*, 38:231–253, 2007.

[42] O. Ronce, S. Gandon, and F. Rousset. Kin selection and natal dispersal in an age-structured population. *Theoretical Population Biology*, 58:143–159, 2000. doi: 10.1006/tpbi.2000.1476.

[43] D. Roze and F. Rousset. Inbreeding depression and the evolution of dispersal rates: A multilocus model. *American Naturalist*, 166(6):708–721, 2005. doi: 10.1086/497543.

[44] D. R. Rubenstein. Spatiotemporal environmental variation, risk aversion, and the evolution of cooperative breeding as a bet-hedging strategy. *Proceedings of the National Academy of Sciences, USA*, 108:10816–10822, 2011. doi: 10.1073/pnas.1100303108.

[45] D. R. Rubenstein and I. J. Lovette. Temporal environmental variability drives the evolution of cooperative breeding in birds. *Current Biology*, 17:1414–1419, 2007. doi: 10.1016/j.cub.2007.07.032.

[46] S. F. Shen, S. T. Emlen, W. D. Koenig, and D. R. Rubenstein. The ecology of cooperative breeding behaviour. *Ecology Letters*, 20:708–720, 2017. doi: 10.1111/ele.12774.

[47] P. D. Taylor. An inclusive fitness model for dispersal of offspring. *Journal of Theoretical Biology*, 130:363–378, 1988. doi: 10.1016/S0022-5193(88)80035-3.

[48] P. D. Taylor and S. A. Frank. How to make a kin selection model. *Journal of Theoretical Biology*, 180:27–37, 1996. doi: 10.1006/jtbi.1996.0075.

[49] J. M. J. Travis, M. Delgado, G. Bocedi, M. Baguette, K. BartoÅ, D. Bonte, I. Boulangeat, J. A. Hodgson, A. Kubisch, V. Penteriani, M. Saastamoinen, V. M. Stevens, and J. M. Bullock. Dispersal and species responses to climate change. *Oikos*, 122:1532–1540, 2013. doi: 10.1111/j.1600-0706.2013.00399.x.

[50] R. L. Trivers. Parent-offspring conflict. *American Zoologist*, 14:249–264, 1974. doi: 10.1093/icb/14.1.249.

[51] L. van Valen. Group selection and the evolution of dispersal. *Evolution*, 25:591–598, 1971. doi: 10.1111/j.1558.1971.tb01919.x.

[52] G. Wild and P. D. Taylor. Kin selection models for the co-evolution of the sex ratio and sex-specific dispersal. *Evolutionary Ecology Research*, 6:481–502, 2004.

[53] G. Wild, T. Pizzari, and S. A. West. Sexual conflict in viscous populations: The effect of the timing of dispersal. *Theoretical Population Biology*, 80(4):298 – 316, 2011. ISSN 0040-5809. doi: 10.1016/j.tpb.2011.09.002.

[54] A. J. Zera and R. F. Denno. Physiology and ecology of dispersal polymorphism in insects. *Annual Review of Entomology*, 42:207–230, 1997. doi: 10.1146/annurev.ento.42.1.207.

Chapter 5

Conclusions, Discussion and a Future Direction

In this dissertation, I examined two aspects of dispersal in metapopulations – the aspect of ecology and the aspect of evolution. Dispersal can serve as a fixed ecological parameter over a short period of time, and it can evolve under the force of natural selection in the long run. To unveil the effect of dispersal on metapopulations from the ecological perspective, I devoted two pieces of work herein. In the first piece of work, I focused my attention on a rarely studied consequence of dispersal, i.e., a disrupted social structure at the dispersed individual's natal habitat and a reduced quality of that habitat thereafter. Most work does not consider this negative effect of dispersal on the habitats from which individuals depart [14, 15, 25, 32], but it is not clear that this effect of connecting degradation and colonization can be ignored in species with small local populations on patches, and/or rigid social structures. My key finding is that a metapopulation will, in general, be found either in the state of global extinction or in the state of persistence, but dispersal, and those state changes at the point of origin associated with dispersal, have significant qualitative and quantitative effects on long-term dynamics only in a narrow range of parameter space. I conclude that life-history features other than dispersal (e.g., mortality rate) have a greater influence over metapopulation persistence. That is what I did in

Chapter 2.

The second piece of work on the impact of dispersal on metapopulations is presented in **Chapter 3**. As dispersal plays a key role in the balance between extinction events and re-colonization events in metapopulation dynamics, I studied how delay relevant to dispersal can alter the stability and persistence of metapopulations. Without including delays, the seminal metapopulation model by Levins [25] and the quality-structured model by Hanksi [14] both predict an increase in the stable density of occupied islands when either the extinction rate is decreased or the colonization rate is increased. However, whether changes like these, possibly aimed at enriching a metapopulation, could always promote its persistence is questionable, especially in light of what I know from classical consumer-resource dynamics. Those classical dynamics show that enriched equilibrium populations may become destabilized, with population densities oscillating substantially. This "Paradox of Enrichment" motivates my work in Chapter 3. I explored that paradox by looking at a variety of DDE models based on ODEs presented by Levins [25] and Hanksi [14], as DDEs are known to lead to oscillations. I investigated the possibility for oscillations in the DDE model by checking the absolute stability of the positive equilibrium that is stable in the corresponding ODE model, and examined the critical transition delay if it exists. My major findings are: i) the Paradox of Enrichment does not occur at all in DDE models with delays associated with dispersal, ii) the Paradox of Enrichment is possible in models with delays associated with available islands or with establishment of (high-quality) islands, iii) including a structure based on the quality of occupied islands in the DDE model with establishment delays may alleviate the Paradox of Enrichment. I speculate there might be at least three reasons for the scarcity of the empirical evidence for the existence of a Paradox of Enrichment for metapopulations in nature. First, many researchers have focused on the impact of factors associated with dispersal, and therefore delays associated with dispersal might have been studied. Research interests on delay might have been discouraged, as models I examined here, which other researchers might also have studied, predicted that the Paradox of Enrichment cannot occur to metapopulations with dispersal delays alone. Second, the de-

lay associated with establishment is usually not easy to observe and measure [1], especially when strict metapopulation structures in nature are rare [11]. Third, there might be natural mechanisms to resolve this paradox, just like what we find when including a structure based on the quality of islands: the Paradox of Enrichment is alleviated. The discussion also includes suggestions on conservation biology based on the predictions.

Finally, I turned my attention to the evolution of dispersal in **Chapter 4**, where I studied how temporal global-scale fluctuations of environment impact the evolution of dispersal in an infinite diploid metapopulation with small local population on patches. I restricted the environment to fluctuate between a "good" global state and a "poor" global state, and I assumed that the fluctuation follows a Markov process, meaning that how likely the environment will remain in the same state depends on its current state. In addition to group size and average dispersal cost, I focused on two key factors of such fluctuation: the frequency of fluctuation, and the degree of distinction between "good" and "poor" states, i.e., the difference of dispersal cost in different states. I constructed models to study multiple cases: conditional dispersal v.s. unconditional dispersal, dispersal before mating (DM) v.s. mating before dispersal (MD), and parental control v.s. offspring control. Most interesting results come from the case for conditional dispersal: 1) dispersal probability is higher in years of good state; 2) the disparity between the probability of dispersal in good versus poor years becomes more pronounced as either of the two key factors I mentioned above increases. My work differs from that of others, as other researchers usually assume haploid asexual species, large local population sizes, and independence of local population states [2, 5, 12, 28, 29, 31, 37].

The lessons about dispersal arising from previous chapters have some implications for the study of cooperative breeding, as delayed dispersal is a defining life-history decision for many cooperative breeding species [20, 21]. In cooperatively breeding species, certain individuals may delay their dispersal and reproduction to serve as non-reproducing "helpers" who defend nests and territories, act as sentinels, and/or provide alloparental care to offspring produced by others. Cooperative breeding species provide researchers with a rich set of natural scenarios

in which to test ideas about the emergence and maintenance of helping, and social complexity. Examples of cooperative breeders include the Florida scrub jay, *Aphelocoma coerulescens* [10, 19, 44], the red-cockaded woodpecker, *Leuconotopicus borealis* [26, 42], the meerkat, *Suricata suricatta* [7, 8], and the Arctic fox, *Vulpes lagopus* [23, 39].

Here I present a few ideas about the emergence and maintenance of helping based on the conclusions drawn from previous chapters. First, I predict that delayed dispersal by auxiliary individuals can be tolerated under a broad range of conditions. Furthermore, I learn that the evolution of conditional dispersal in response to environmental fluctuations encourages individuals to stay at their natal patches in poor-state environment, and therefore the evolution of conditional dispersal may provide a bedrock for cooperative breeding to evolve. Interestingly, in my first piece of work, I have learned that dispersal only has a very limited effect in the persistence of metapopulations, even though the dispersal of individuals can disrupt the social structure of a source population, e.g., dispersal of helpers can lead to the collapse of the cooperative breeding groups, and therefore dispersal, or delayed dispersal, is driving the fluctuation of the social environment. One possible future direction is to investigate how the result from Chapter 2 will change when traits like dispersal or helping evolve. The environment I mention above is not a global factor, say, weather, but a *social environment*, e.g., a social structure within a local population. The social environment changes as auxiliaries disperse to breed independently, both for themselves and their natal patchmates, because they change the state of the territory they leave behind. One of the social structures in evolutionary biology involving a significant theoretical challenge is cooperation, one striking example of which in nature is cooperative breeding species. Decades of study have revealed that cooperation can, in fact, be advantageous for many reasons [13, 33, 34, 41].

Studies of cooperatively breeding species have traditionally focused on the fitness of interacting individuals. In particular, researchers have asked whether the fitness costs borne by helpers who delay reproduction are outweighed by the fitness benefits that they, or their relatives, receive [3, 6, 13]. Many explanations in this vein have divorced costs and benefits from

a clear ecological context [3, 4, 16, 18, 36, 38]. Although theory has repeatedly demonstrated the importance of understanding the evolution of cooperative breeding in a clear ecological framework [9, 24, 30, 35, 43], the full impact of ecological circumstances on the evolution of cooperative breeding is not yet known. Here, I rephrase the proposal of the future work as completing a theoretical picture of the evolution of cooperation by turning my attention to one of its important drivers, *group augmentation*.

The term *group augmentation* refers to those situations in which individuals survive or reproduce better in larger groups, and thus, members of a group may have a tendency to stay longer in the group, or even sacrifice a portion of their benefit to increase the group size [17, 22, 45]. In this case, group augmentation means that breeders on the territory from which a disperser originated are possibly more apt to die. How this affects the long-term evolution of cooperation among cooperative breeders is not clear. It might, however, be resolved with a class-structured kin-selection model . Briefly, I would propose that progress could be made by considering a wild-type population with overlapping generations, in which each individual must be found in one of the following four stages whenever we observe the population: stage 0): a floater, who has no territory, thus, not enough resource, to reproduce; stage 1): a potential helper, an offspring that stays with its parent; stage 2): a solitary breeder living alone in a territory and having enough resource to reproduce; stage 3): a potential cooperative breeder living with a potential helper in stage 1, and having enough resource to reproduce ("potential", in the sense that there is no actual helping behaviour). Individuals in this population would experience demographic events in some fixed order; e.g. breeders would give birth to one offspring with a stage-specific probability; previous-year potential helpers survive with a probability, and disperse as floaters; newborns disperse with a probability depending on their parents' stage, and those who stay become helpers this year; the breeders survive with a stage-specific probability, and the stage of breeders is determined by the presence of a helper, who can inherit the territory and become a breeder if the accompanying breeder dies; surviving floaters have a chance to become a breeder whenever there is a vacant territory. Based on such demographic processes,

it is easy to obtain the transition matrix among those individual stages, and determine an equilibrium density. After introducing a mutant population with real helpers, who are willing to boost breeders' survival and/or fecundity probability in a cost of their own survival rate, kin selection argument [40] can be used to generate a model. Although multiple parameters are involved, multivariate analysis methods [27] can help with the extraction of primary conditions for the evolution of helping. For example, simulations of evolution of probability of delaying dispersal and helping can be performed by fixing the parameters, such as, survival probability of individuals in each class, fecundity probability of breeders, efficiency coefficients of helping effort on fecundity and survival of cooperative breeders, and group augmentation factor. Such simulations have multiple input variables, and one output variable to indicate if helping evolves in each simulation, so multivariate analysis methods, like principle component analysis, can provide a clue for ranges of the main factors that predict the occurrence of helping in terms of statistics. The model will get more interesting when we take the group augmentation factor into consideration.

Bibliography

[1] J. Arino, L. Wang, and G. S. Wolkowicz. An alternative formulation for a delayed logistic equation. *Journal of Theoretical Biology*, 241(1):109–119, 2006.

[2] F. Blanquart and S. Gandon. Evolution of migration in a periodically changing environment. *American Naturalist*, 177:188–201, 2011. doi: 10.1086/657953.

[3] A. F. Bourke. *Principles of social evolution*. Oxford University Press, 2011.

[4] J. L. Brown. *Helping and communal breeding in birds: ecology and evolution.* Princeton University Press, 1987.

[5] C. Cadet, R. Ferrire, J. A. J. Metz, and M. van Baalen. The evolution of disper-

sal under demographic stochasticity. *American Naturalist*, 162:427–441, 2003. doi: 10.1086/378213.

[6] T. Clutton-Brock. Breeding together: kin selection and mutualism in cooperative vertebrates. *Science*, 296(5565):69–72, 2002.

[7] T. Clutton-Brock and M. Manser. Meerkats: cooperative breeding in the Kalahari. In W. D. Koenig and J. L. Dickinson, editors, *Cooperative breeding in vertebrates: studies of ecology, evolution, and behavior.*, chapter 17, pages 294–317. Cambridge University Press, Cambridge, 2016.

[8] T. H. Clutton-Brock, P. N. Brotherton, A. Russell, M. O'riain, D. Gaynor, R. Kansky, A. Griffin, M. Manser, L. Sharpe, G. M. McIlrath, et al. Cooperation, control, and concession in meerkat groups. *Science*, 291(5503):478–481, 2001.

[9] S. T. Emlen. The evolution of helping. i. an ecological constraints model. *The American Naturalist*, 119(1):29–39, 1982.

[10] J. W. Fitzpatrick and R. Bowman. Florida scrub-jay: Oversized territories and group defense in a fire-maintained habitat. In W. D. Koenig and J. L. Dickinson, editors, *Cooperative breeding in vertebrates: studies of ecology, evolution, and behavior.*, chapter 5, pages 77–96. Cambridge University Press, Cambridge, 2016.

[11] E. A. Fronhofer, A. Kubisch, F. M. Hilker, T. Hovestadt, and H. J. Poethke. Why are metapopulations so rare? *Ecology*, 93(8):1967–1978, 2012.

[12] J. M. Greenwood-Lee and P. D. Taylor. The evolution of dispersal in spatially varying environments. *Evolutionary Ecology Research*, 3:649–665, 2001.

[13] W. Hamilton. The genetical evolution of social behaviour. i. *Journal of Theoretical Biology*, 7(1):1–16, 1964.

[14] I. Hanski. Single-species spatial dynamics may contribute to long-term rarity and commonness. *Ecology*, 66(2):335–343, 1985.

[15] A. Hastings. Structured models of metapopulation dynamics. *Biological Journal of the Linnean Society*, 42(1-2):57–71, 1991.

[16] B. J. Hatchwell. The evolution of cooperative breeding in birds: kinship, dispersal and life history. *Philosophical Transactions of the Royal Society of London B: Biological Sciences*, 364(1533):3217–3227, 2009.

[17] S. A. Kingma, P. Santema, M. Taborsky, and J. Komdeur. Group augmentation and the evolution of cooperation. *Trends in Ecology & Evolution*, 29(8):476–484, 2014.

[18] S. A. Kingma, K. Bebbington, M. Hammers, D. S. Richardson, and J. Komdeur. Delayed dispersal and the costs and benefits of different routes to independent breeding in a cooperatively breeding bird. *Evolution*, 70(11):2595–2610, 2016.

[19] W. D. Koenig and J. L. Dickinson. *Ecology and evolution of cooperative breeding in birds*. Cambridge University Press, 2004.

[20] H. Kokko and J. Ekman. Delayed dispersal as a route to breeding: territorial inheritance, safe havens, and ecological constraints. *The American Naturalist*, 160(4):468–484, 2002.

[21] H. Kokko and P. Lundberg. Dispersal, migration, and offspring retention in saturated habitats. *The American Naturalist*, 157(2):188–202, 2001.

[22] H. Kokko, R. A. Johnstone, and T. H. Clutton-Brock. The evolution of cooperative breeding through group augmentation. *Proceedings of the Royal Society of London B: Biological Sciences*, 268(1463):187–196, 2001.

[23] C. Kullberg and A. Angerbjörn. Social behaviour and cooperative breeding in arctic foxes, Alopex lagopus (L.), in a semi-natural environment. *Ethology*, 90(4):321–335, 1992.

[24] H. C. Leggett, C. El Mouden, G. Wild, and S. West. Promiscuity and the evolution of cooperative breeding. *Proceedings of the Royal Society of London B: Biological Sciences*, 279(1732):1405–1411, 2012.

[25] R. Levins. Some demographic and genetic consequences of environmental heterogeneity for biological control. *Bulletin of the Entomological Society of America*, 15(3):237–240, 1969.

[26] J. D. Ligon. Behavior and breeding biology of the red-cockaded woodpecker. *The Auk*, 87(2):255–278, 1970.

[27] B. F. Manly and J. A. N. Alberto. *Multivariate statistical methods: a primer*. Chapman and Hall/CRC, 2016.

[28] F. Massol and F. Débarre. Evolution of dispersal in spatially and temporally variable environments: the importance of life cycles. *Evolution*, 69:1925–1937, 2015. doi: 10.1111/evo.12699.

[29] A. Mathias, É. Kisdi, and I. Olivieri. Divergent evolution of dispersal in a heterogeneous landscape. *Evolution*, 55:246–259, 2001. doi: 10.1111/j.0014-3820.2001.tb01290.x.

[30] D. V. McLeod and G. Wild. Ecological constraints influence the emergence of cooperative breeding when population dynamics determine the fitness of helpers. *Evolution*, 67(11): 3221–3232, 2013.

[31] M. A. McPeek and R. D. Holt. The evolution of dispersal in spatially and temporally varying environments. *American Naturalist*, 140:1010–1027, 1992. doi: 10.1086/285453.

[32] R. McVinish and P. Pollett. Interaction between habitat quality and an Allee-like effect in metapopulations. *Ecological Modelling*, 249:84–89, 2013.

[33] M. A. Nowak and K. Sigmund. Evolution of indirect reciprocity. *Nature*, 437(7063): 1291, 2005.

[34] H. Ohtsuki and Y. Iwasa. The leading eight: social norms that can maintain cooperation by indirect reciprocity. *Journal of Theoretical Biology*, 239(4):435–444, 2006.

[35] I. Pen and F. J. Weissing. Sex-ratio optimization with helpers at the nest. *Proceedings of the Royal Society of London B: Biological Sciences*, 267(1443):539–543, 2000.

[36] H.-U. Reyer. Breeder-helper-interactions in the pied kingfisher reflect the costs and benefits of cooperative breeding. *Behaviour*, 96(3):277–302, 1986.

[37] O. Ronce, S. Gandon, and F. Rousset. Kin selection and natal dispersal in an age-structured population. *Theoretical Population Biology*, 58:143–159, 2000. doi: 10.1006/tpbi.2000.1476.

[38] P. B. Stacey and J. D. Ligon. The benefits-of-philopatry hypothesis for the evolution of cooperative breeding: variation in territory quality and group size effects. *The American Naturalist*, 137(6):831–846, 1991.

[39] O. Strand, A. Landa, J. D. Linnell, B. Zimmermann, and T. Skogland. Social organization and parental behavior in the arctic fox. *Journal of Mammalogy*, 81(1):223–233, 2000.

[40] P. D. Taylor and S. A. Frank. How to make a kin selection model. *Journal of Theoretical Biology*, 180(1):27–37, 1996.

[41] R. L. Trivers. Parent-offspring conflict. *Integrative and Comparative Biology*, 14(1):249–264, 1974.

[42] J. R. Walters and V. Garcia. Red-cockaded woodpeckers: alternative pathways to breeding success. In W. D. Koenig and J. L. Dickinson, editors, *Cooperative breeding in vertebrates: studies of ecology, evolution, and behavior.*, chapter 4, pages 58–76. Cambridge University Press, Cambridge, 2016.

[43] G. Wild and C. Koykka. Inclusive-fitness logic of cooperative breeding with benefits of

natal philopatry. *Philosophical Transactions of the Royal Society of London B: Biological Sciences*, 369(1642):20130361, 2014.

[44] G. E. Woolfenden and J. W. Fitzpatrick. *The Florida scrub jay: demography of a cooperative-breeding bird*, volume 20. Princeton University Press, 1984.

[45] J. Wright. Helping-at-the-nest and group size in the arabian babbler turdoides squamiceps. *Journal of Avian Biology*, pages 105–112, 1998.

Appendix A

Appendix for Chapter 3

A.1 Analysis of Eq. (3.2)

Eq. 3.2 admits a trivial equilibrium solution (the *extinction equilibrium*) that is easily determined to be locally asymptotically stable for all parameter combinations. If $c > d + 2\sqrt{d\,e}$, then there exists a pair of non-trivial (and biologically meaningful) equilibrium solutions, denoted $E = (\bar{p}_\ell, \bar{p}_{h,+})$ and $T = (\bar{p}_\ell, \bar{p}_{h,-})$, respectively, where

$$\bar{p}_\ell = \frac{d}{c}$$

and

$$\bar{p}_{h,\pm} = \frac{(c-d) \pm \sqrt{(c-d)^2 - 4\,d\,e}}{2\,c}.$$

It is also easy to show by using Routh-Hurwitz stability criterion that, when it exists, E is locally asymptotically stable, while T, when it exists, is unstable.

A.2 Characteristic Equation

Analysis in this appendix and the following ones follows theory found in [2] [also see 1, 3]. To analyze the stability of a DDE system near its equilibrium, one first needs to obtain the characteristic equation. In this appendix, we present a standard method used to obtain it.

For the simplest case, we have the following non-linear DDE,

$$x(t)' = f(x(t), x(t-\tau)), \tag{A.1}$$

where $f(x, y)$ is a non-linear function of x and y. We need to linearize the equation near an equilibrium x_0. Letting $\varepsilon(t) = x(t) - x_0$, then, Eq. (A.1) is equivalent to

$$(x_0 + \varepsilon(t))' = f(x_0 + \varepsilon(t), x_0 + \varepsilon(t-\tau)).$$

For simplicity, let $x_\tau = x(t-\tau)$. Using a Taylor expansion, we have

$$\begin{aligned} f(x, x_\tau) &= f(x_0, x_0) + f_1'|_{(x_0,x_0)}(x - x_0) + f_2'|_{(x_0,x_0)}(x_\tau - x_0) \\ &\quad + O((x - x_0)^2) + O((x_\tau - x_0)^2) + O((x_\tau - x_0)(x - x_0)) \quad (\text{as } (x, x_\tau) \longrightarrow (x_0, x_0)) \\ &\approx f_1'|_{(x_0,x_0)}(x, x_\tau) \cdot (x - x_0) + f_2'|_{(x_0,x_0)}(x, x_\tau) \cdot (x_\tau - x_0), \end{aligned}$$

where $f(x_0, x_0) = 0$. So, Eq. (A.1) can be approximated after linearization in the following way:

$$\varepsilon'(t) = a\, \varepsilon(t) + b\, \varepsilon(t-\tau), \tag{A.2}$$

where constants $a = f_1'|_{(x_0,x_0)}(x, x_\tau)$ and $b = f_2'|_{(x_0,x_0)}(x, x_\tau)$.

Now we can obtain the characteristic equation by assuming solutions to Eq. (A.2) have the form $\varepsilon(t) = k\, e^{\lambda t}$, where $k \neq 0$, and $\lambda \in C$. Substituting the form of solution into Eq. (A.2), we have

$$\begin{aligned} & \varepsilon'(t) = a\, \varepsilon(t) + b\, \varepsilon(t-\tau), \\ \Longleftrightarrow \quad & \lambda\, k\, \exp(\lambda\, t) = a\, k\, \exp(\lambda\, t) + b\, k\, \exp(\lambda\, (t-\tau)) \\ \Longleftrightarrow \quad & \lambda = a\, + b\, \exp(-\lambda\, \tau) \end{aligned}$$

Therefore, the characteristic equation is

$$\lambda - a\, - b\, \exp(-\lambda\, \tau) = 0. \tag{A.3}$$

The characteristic equation (A.3) can be generalized into

$$\det(\lambda I - A \ - B \ \exp(-\lambda \tau)) = 0, \tag{A.4}$$

for DDE systems in the following form,

$$\mathbf{x}'(t) = A \ \mathbf{x}(t) + B \ \mathbf{x}(t - \tau), \tag{A.5}$$

where $\mathbf{x}(t) = (x_1(t), x_2(t), \cdots, x_n(t))$, and A and B are $n \times n$ matrices. Using the characteristic equation, we can obtain critical delays and regions of absolute stability, as is shown in the following sections.

A.3 For Proposition 6: Analysis of Critical Delay in Eq. (3.6)

We check the sign of real solutions to Eq. (3.7) first. Recall that $c > e$. If $c > 2e$ then no positive values of s satisfy the characteristic equation. If $c \leq 2e$, then there are real roots, but they are negative and no instabilities arise. If $c = 2e$, then $s = -e < 0$ is the only solution to the characteristic equation. If $c < 2e$, then there is a unique real root, but that root is negative, because $c > e$. (Note that when $s = 0$ the left-hand side of the characteristic equation simplifies to e, while the right-hand side simplifies to $2e - c$. Thus $c > e$ implies $e > 2e - c$, and so the root must be to the left of $s = 0$).

Next, we look for complex solutions to Eq. (3.7) of the form $s = u + i\,v$ (without losing generality, assume $v > 0$). The characteristic Eq. (3.7) becomes

$$u + i\,v + e = -(c - 2\,e) \ \exp\{-u\,\tau\} \, (\cos v\,\tau - i \ \sin v\,\tau),$$

which gives us

$$\begin{aligned} u + e &= -(c - 2\,e) \ \exp\{-u\,\tau\} \ \cos v\,\tau, \\ v &= \quad (c - 2\,e) \ \exp\{-u\,\tau\} \ \sin v\,\tau. \end{aligned}$$

If $c = 2e$, then the equations cannot be satisfied, and so we consider only cases where $c \neq 2e$.

Instability of $\bar{p}$ is imminent when $u = 0$ and so

$$-\frac{e}{c-2\,e} = \cos v\,\tau, \tag{A.6}$$

$$\frac{1}{c-2\,e}\,v = \sin v\,\tau. \tag{A.7}$$

Since $c > e$, we can be sure that $e > 2\,e-c$. It follows that whenever $c < 2\,e$, $e/(2\,e-c) > 1$ and so no solution to the previous system exists. If $c > 2\,e$, then $-e/(c-2\,e) < 0$; a solution to the previous system of equations, therefore, requires

$$\frac{e}{c-2\,e} \leq 1 \;\leftrightarrow\; c \geq 3\,e,$$

because we need $\cos v\,\tau \geq -1$. If $c = 3e$, then Eq. (A.6) and Eq. (A.7) become $-1 = \cos v\,\tau$ and $v/e = \sin v\,\tau$, from which we obtain contradicting results $v\,\tau = 2\pi n + \pi\,(n = 0, \pm1, \pm2, \ldots)$ and $v = 0$. Therefore, there is no solution when $c \leq 3e$.

When $c > 3e$, there are an infinite number of products $v\tau$ that satisfy Eq. (A.6) and Eq. (A.7). We obtain them in the following way. First, divide Eq. (A.7) by Eq. (A.6), and we have $v/(-e) = \tan v\,\tau$, from which we solve for $v\,\tau$:

$$v\,\tau = n\pi + \arctan\left(-\frac{v}{e}\right), \quad n = 0, \pm1, \pm2, \ldots$$

In addition to $v > 0$, $\tau > 0$, and $\cos v\,\tau < 0$, we know that $\sin v\,\tau$ must be positive because $v/(c-2e) > 0$. This allows us to refine the previous statement to

$$v\,\tau = 2n\pi + \left[\pi - \arctan\left(\frac{v}{e}\right)\right], \quad n = 0, 1, 2, \ldots$$

so

$$\tau = \frac{1}{v}\left[2n\pi + \left[\pi - \arctan\left(\frac{v}{e}\right)\right]\right], \quad n = 0, 1, 2, \ldots$$

Now,

$$\tau_0 = \frac{1}{v}\left[\pi - \arctan\left(\frac{v}{e}\right)\right], \quad n = 0, 1, 2, \ldots \tag{A.8}$$

and v can be obtained by taking squares of Eq. (A.6) and Eq. (A.7) and adding them up.

Then we can get $\frac{e^2+v^2}{(c-2e)^2} = \cos^2 v\tau + \sin^2 v\tau = 1$, so

$$v = \sqrt{(c-2e)^2 - e^2} = \sqrt{(c-e)(c-3e)}. \tag{A.9}$$

In summary, now we know that there are two cases when there exists a positive equilibrium ($c > e$). One case is there is no critical delay when $c \leq 3e$; the other case is there exist critical delays when $c > 3e$, with the smallest one shown in Eq. (A.8), where v is in Eq. (A.9).

A.4 For Proposition 7: Absolute Stability

To start with, we need to get the condition for the existence of two distinct positive equilibria. By denoting an equilibrium as $(\bar{p}_\ell, \bar{p}_h) = (X, Y)$, X and Y satisfy

$$\begin{aligned} c(1-X-Y)Y - eX + dY - cXY &= 0, \\ cXY - dY &= 0. \end{aligned}$$

Then, there is an extinction equilibrium $(0, 0)$, and two possible distinct positive equilibria:

$$\begin{aligned} X &= \frac{d}{c}, \\ Y_\pm &= \frac{(c-d) \pm \sqrt{(c-d)^2 - 4\,d\,e}}{2\,c}, \end{aligned}$$

if $c > d$ and $(c-d)^2 - 4\,d\,e > 0$ (we are not interested in the case when two positive equilibria merge into one equilibrium). And those two conditions can be combined to obtain $c > d + 2\sqrt{d\,e}$, which is the first part of the Proposition 7.

In general, it is difficult to obtain the global stability of a DDE system, especially if it is non-linear. However, we can investigate its behavior near its positive equilibrium E, as we are most interested in the stability about the equilibrium E. First, we need to obtain the characteristic equation for model (3.8) to look into the absolute stability of positive equilibrium

E:

$$X = \frac{d}{c}, \tag{A.10}$$

$$Y = Y_+ = \frac{(c-d) + \sqrt{(c-d)^2 - 4\,d\,e}}{2\,c}. \tag{A.11}$$

We linearize Eq. (3.8) about the equilibrium E by perturbing near E. Letting $p_\ell(t) = x(t) + \frac{d}{c}$ and $p_h(t) = y(t) + Y$, we obtain a linear DDE system

$$\begin{bmatrix} x'(t) \\ y'(t) \end{bmatrix} = A \begin{bmatrix} x(t) \\ y(t) \end{bmatrix} + B \begin{bmatrix} x(t-\tau) \\ y(t-\tau) \end{bmatrix},$$

where

$$A = \begin{bmatrix} -2\,Yc - e & -Yc + d \\ Yc & -d \end{bmatrix}, \quad B = \begin{bmatrix} 0 & (-Y+1)\,c - 2\,d \\ 0 & d \end{bmatrix}. \tag{A.12}$$

Recall that for linearized DDE systems, the characteristic equation can be calculated using

$$\det(\lambda I - A\ - B\ \exp(-\lambda\,\tau)) = 0. \tag{A.13}$$

Substituting Eq. (A.11) in the above equation, our characteristic equation can be written as

$$p(\lambda) + q(\lambda)\ \exp(-\lambda\,\tau) = 0, \tag{A.14}$$

where $$p(\lambda) = \lambda^2 + (2\,Yc + d + e)\,\lambda + Y^2c^2 + Ycd + de, \tag{A.15}$$

$$q(\lambda) = Y^2c^2 - Yc^2 - de - d\lambda. \tag{A.16}$$

The key idea of deciding the absolute stability [sensu 2, page 56] relies on the fact that stability is lost whenever a complex-valued root of the characteristic equation (see Appendix A.2) to cross the complex plane from left to right (the equilibrium loses its stability if and only if the sign of the real part of the root switches from negative to positive). Since we just need to deal with $p(\lambda)$ and $q(\lambda)$ in the form of polynomials, continuity holds here.

If we put Eq. (A.14) as $p(\lambda) = -q(\lambda)\ \exp(-\lambda\,\tau)$, we can check what occurs when λ

is on the imaginary axis, i.e., $\lambda = iv\,(0 < v \in \mathcal{R}$ without losing generality), that is, $p(iv) = -q(iv)\exp(-iv\tau)$. Applying Euler's formula, we have

$$\begin{aligned} p(iv) &= -(\mathrm{Re}(q(iv)) + i\ \mathrm{Im}(q(iv)))(\cos(v\tau) - i\sin(v\tau)) \\ &= (-\mathrm{Re}(q(iv))\cos(v\tau) - \mathrm{Im}(q(iv))\sin(v\tau)) - i(\mathrm{Im}(q(iv))\cos(v\tau) - \mathrm{Re}(q(iv))\sin(v\tau)). \end{aligned}$$

Taking the modulus of both sides, we have $|p(iv)| = |q(iv)|$. So $|p(iv)|$ should not be equal to $|q(iv)|$, when we do not want the root of characteristic equation to change the sign of its real part. In fact, if we need the equilibrium to be stable [sensu 2, Proposition 4.9], then we need to make sure $|p(iv)| > |q(iv)|$ holds for all positive values of v, or

$$|q(iv)|^2 - |p(iv)|^2 < 0. \tag{A.17}$$

Substituting Equations (A.15)-(A.16), and $\lambda = iv$ into the inequality (A.17), we collect the terms in the resulting polynomial on the left side according to the degree of v, and Eq. (A.17) becomes

$$-v^4 - \left(2\,Y^2c^2 + 2\,c\,(d+2\,e)\,Y + e^2\right)v^2 - Yc\,(2\,Yc - c + d)\left(Yc^2 + Ycd + 2\,de\right) < 0. \tag{A.18}$$

Recall that c, d,e, Y are all positive, so we can see the coefficients for v^4 and v^2 are negative. For v^0, we need to look at the sign of $2\,Yc - c + d$ by substituting Eq. (A.11) into it:

$$2\,Yc - c + d = \sqrt{(c-d)^2 - 4\,de} > 0,$$

whenever $(c-d)^2 - 4\,de > 0$. So, Eq. (A.17) is satisfied whenever there are two distinct positive equilibria, and the equilibrium is absolutely stable in the region $(c-d)^2 - 4\,de > 0$. That is the second part of the Proposition 7.

A.5 For Proposition 8, Part I: Absolute Stability

Here we use the similar method as in the previous section to show the proof for a simple case $d = 1$ of model (3.9), which we use to get Figure 3.4, but a general proof is easy to obtain. We

linearize Eq. (3.9) about the equilibrium E by perturbing near E. Letting $p_\ell(t) = x(t) + \frac{1}{c}$ and $p_h(t) = y(t) + Y$, where

$$Y = \frac{(c-1) + \sqrt{(c-1)^2 - 4\,e}}{2\,c}, \tag{A.19}$$

we have a linear DDE system

$$\begin{bmatrix} x'(t) \\ y'(t) \end{bmatrix} = A \begin{bmatrix} x(t) \\ y(t) \end{bmatrix} + B \begin{bmatrix} x(t-\tau) \\ y(t-\tau) \end{bmatrix},$$

where

$$A = \begin{bmatrix} -(c\,Y + e) & c\,(1-2Y) \\ 0 & -1 \end{bmatrix}, B = \begin{bmatrix} -c\,Y & -1 \\ c\,Y & 1 \end{bmatrix}. \tag{A.20}$$

For linearized DDE systems, the characteristic equation can be calculated using

$$\det(\lambda I - A\ - B\ \exp(-\lambda\,\tau)) = 0. \tag{A.21}$$

Substituting Eq. (A.20) in the above Eq. (A.21), our characteristic equation can be written as

$$p(\lambda) + q(\lambda)\ \exp(-\lambda\,\tau) = 0, \tag{A.22}$$

where
$$p(\lambda) = \lambda^2 + (c\,Y + e + 1)\,\lambda + c\,Y + e, \tag{A.23}$$

$$q(\lambda) = (c\,Y - 1)\,\lambda + Yc^2 - 2\,c\,Y - 3\,e. \tag{A.24}$$

Then we substitute Eqs. (A.23)-(A.24), and $\lambda = iv$ into the inequality (A.17), and we collect the terms in the resulting polynomial on the left side according to the degree of v. Then we obtain

$$-v^4 - \left(2\ (e+1)\,cY + e^2\right)v^2 + \left(Yc^2 - 3\,cY - 4\,e\right)\left(Yc^2 - cY - 2\,e\right) < 0. \tag{A.25}$$

In order to make sure the inequality (A.25) holds for all positive v, we need all the coefficients of the polynomial in v on the left to be negative. All the coefficients except the constant term are negative because e, c, Y are positive, so we just need $\left(Yc^2 - 3\,cY - 4\,e\right)\left(Yc^2 - cY - 2\,e\right) < 0$, that is, $Yc^2 - 3\,cY - 4\,e < 0 < Yc^2 - cY - 2\,e$. We can prove $0 < Yc^2 - cY - 2\,e$ holds as long as

$e < \frac{(c-1)^2}{4}$ and $c > 1$ (i.e., when positive equilibria exist). Solving $Yc^2 - 3\,cY - 4\,e < 0$, we have

$$e > \frac{(3\,c-1)\,(c-3)}{16} = e_l. \tag{A.26}$$

In conclusion, equilibrium E is stable for any delay, if

$$e \in \left(\frac{(3\,c-1)\,(c-3)}{16}, \frac{(c-1)^2}{4}\right),\ c > 1, \tag{A.27}$$

assuming $d = 1$.

A.6 For Proposition 8, Part II: Calculating Critical Delay τ_0

For $e < e_l$, a critical delay τ_0 can be calculated by solving the following implicit system when c and e are given:

$$\begin{aligned} \cos(\tau\, v) &= f(c, e, v), \\ \sin(\tau\, v) &= g(c, e, v), \end{aligned} \tag{A.28}$$

where v is the imaginary part of the characteristic value $\lambda = i\,v$. We just need to consider the characteristic value on the imaginary axis, because the critical transition occurs when real part of the characteristic value change its sign, i.e., when λ is on the imaginary axis of the complex plane. In fact, we rewrite Equations (A.22)-(A.24) as

$$\exp(-\lambda\,\tau) = -\frac{p(\lambda)}{q(\lambda)}, \tag{A.29}$$

$$p(\lambda) = \lambda^2 + (c\,Y + e + 1)\,\lambda + c\,Y + e, \tag{A.30}$$

$$q(\lambda) = (c\,Y - 1)\,\lambda + Yc^2 - 2\,c\,Y - 3\,e. \tag{A.31}$$

Now substitute Equations (A.30) and (A.31) into (A.29), and then substitute $\lambda = u + iv$ in the resulting equation. Without losing generality, we assume $v > 0$. Then we match real parts and imaginary parts of left side and right side of resulting equation, using Euler's formula. Letting

$u = 0$, we get

$$\cos(\tau v) = f(c, e, v), \tag{A.32}$$

$$\sin(\tau v) = g(c, e, v), \tag{A.33}$$

where $f(c, e, v) = \mathrm{Re}\left(-\frac{p(iv)}{q(iv)}\right)$ and $g(c, e, v) = -\mathrm{Im}\left(-\frac{p(iv)}{q(iv)}\right)$. Their expressions are given in the following:

$$\begin{aligned} f(c, e, v) &= -\frac{(cY + d + e)\, v^2 (cY - d) + \left(Ycd + de - v^2\right)\left(2\, Y^2c^2 - Yc^2 - de\right)}{(cY - d)^2 v^2 + \left(2\, Y^2c^2 - Yc^2 - de\right)^2}, \\ g(c, e, v) &= -\frac{(cY + d + e)\, v \left(2\, Y^2c^2 - Yc^2 - de\right) - \left(Ycd + de - v^2\right)(cY - d)\, v}{(cY - d)^2 v^2 + \left(2\, Y^2c^2 - Yc^2 - de\right)^2}, \end{aligned}$$

where $Y = \frac{c-d+\sqrt{(c-d)^2-4\,de}}{2c}$. We can solve for a positive real value of v from $(f(c, e, v))^2 + (g(c, e, v))^2 = 1$, and substitute it back into Eqs. (A.32) and (A.33) to solve for τ_0, making sure τ_0 is the smallest positive solution. We use Maple to calculate the expressions for v:

$$v = \frac{1}{2}\sqrt{2\sqrt{16\, Y^2\left(Y - \frac{1}{2}\right)^2 c^4 - 8\, Ye\left(-\frac{Ye}{2} + d\,(Y - 1)\right)c^2 - 8\, Ye\,(d - e)\left(d + \frac{e}{2}\right)c + e^4} - 4\,(d + e)\,cY - 2\,e^2}, \tag{A.34}$$

and critical delay τ_0:

$$\tau_0 = \begin{cases} \frac{1}{v}\arctan\left(\frac{g(c,e,v)}{f(c,e,v)}\right), & \text{if } f(c, e, v) > 0 \text{ and } g(c, e, v) > 0, \\ \frac{1}{v}\arctan\left(\frac{g(c,e,v)}{f(c,e,v)}\right) + \frac{\pi}{v}, & \text{if } f(c, e, v) < 0, \\ \frac{1}{v}\arctan\left(\frac{g(c,e,v)}{f(c,e,v)}\right) + \frac{2\pi}{v}, & \text{if } f(c, e, v) > 0 \text{ and } g(c, e, v) < 0. \end{cases} \tag{A.35}$$

Bibliography

[1] K. Gopalsamy. *Stability and oscillations in delay differential equations of population dynamics*, volume 74. Springer Science & Business Media, 2013.

[2] H. L. Smith. *An introduction to delay differential equations with applications to the life sciences*. Springer, 2011.

[3] Q. Zhou. Modelling Walleye population and its cannibalism effect. Master's thesis, Western University, London, Ontario, Canada, 2017.

Appendix B

Appendix for Chapter 4

B.1 Environmental Stochasticity

Suppose the global state of the environment is random, and let $T_{p|e}$ (resp. $T_{g|e}$) denote the probability that the population is next in a poor state (resp. good state) given that it is currently in state $e = p, g$. The stochastic transitions between states are, therefore, governed by a Markov Chain with transition matrix ,

$$T = \begin{bmatrix} T_{p|p} & T_{p|g} \\ T_{g|p} & T_{g|g} \end{bmatrix}.$$

Using the fact that $T_{g|p} = 1 - T_{p|p}$, and $T_{p|g} = 1 - T_{g|g}$, one can show that the environment spends a $\pi_p \times 100\%$ of the time in the poor state, and $\pi_g \times 100\%$ of the time in the good state, where $\pi_p = T_{p|g}/(T_{g|p} + T_{p|g})$, and $\pi_g = T_{g|p}/(T_{g|p} + T_{p|g})$. It is instructive to notice that the denominator of π_e is proportional to the total amount of probability mass transferred between states, while the numerator gives the probability mass transferred to e from the other state.

For later use, we also introduce the backward environmental transition matrix

$$S = \begin{bmatrix} S_{p|p} & S_{g|p} \\ S_{p|g} & S_{g|g} \end{bmatrix} = \begin{bmatrix} \frac{T_{p|p}}{T_{p|p}+T_{p|g}} & \frac{T_{p|g}}{T_{p|p}+T_{p|g}} \\ \frac{T_{g|p}}{T_{g|p}+T_{g|g}} & \frac{T_{g|g}}{T_{g|p}+T_{g|g}} \end{bmatrix}.$$

The matrix entries $S_{p|e}$ (resp. $S_{g|e}$) gives the probability that the environment was most recently in the poor (resp. good) state, given that it is currently in state e. If we assume $T_{p|g} = T_{g|p} = s$,

as we do in the main text, then

$$\begin{aligned} T_{p|p} + T_{p|g} &= 1 - T_{g|p} + T_{p|g} = 1 \\ T_{g|p} + T_{g|g} &= T_{g|p} + 1 - T_{p|g} = 1 \end{aligned}$$

and so

$$S = \begin{bmatrix} S_{p|p} & S_{g|p} \\ S_{p|g} & S_{g|g} \end{bmatrix} = \begin{bmatrix} T_{p|p} & T_{p|g} \\ T_{g|p} & T_{g|g} \end{bmatrix} = \begin{bmatrix} 1-s & s \\ s & 1-s \end{bmatrix}$$

with $\pi_p = \pi_g = 1/2$. By contrast, if we assume that $T_{p|p} = T_{p|g} = t$, as some authors have done [see 1, their Appendix H], then

$$T = \begin{bmatrix} t & t \\ 1-t & 1-t \end{bmatrix}$$

and

$$S = \begin{bmatrix} 1/2 & 1/2 \\ 1/2 & 1/2 \end{bmatrix}$$

with $\pi_p = t$ and $\pi_g = 1-t$. When $S_{e|p} = S_{e|g} = 1/2$, environmental states at two different points in time are not correlated with one another.

In the model described in the main text, we consider the cost of dispersal in environment e, denoted c_e. In general, the time-averaged cost of dispersal is $c = \pi_p c_p + \pi_g c_g$ and the associated variance is $\sigma^2 = \pi_p \pi_g (c_p - c_g)^2$. When $\pi_p = \pi_g = 1/2$ the aforementioned average and variance simplify to $(c_p + c_g)/2$ and $[(c_p - c_g)/2]^2$, respectively. By assuming $T_{p|g} = T_{g|p} = S_{g|p} = S_{p|g} = s$, as we do in the main text, we get $\pi_e = 1/2$ and are therefore able to adjust s without changing either c or σ^2. Any effect on dispersal evolution observed, in that case, can be attributed to changes in s alone.

It is also important to understand the temporal autocorrelation between environmental states, and the theoretical correlation formula associated with Figure 4.1. Let X_t denote the state of the environment at some time t. If the environment is poor at time t then $X_t = 0$, and if the environment is good at time t then $X_t = 1$. Based on the discussion above, and the

assumption that $T_{p|g} = T_{g|p} = s$, we get

$$E[X_t] = \Pr(X_t = 1) = \frac{1}{2} \quad \text{and} \quad \mathrm{Var}(X_t) = E[X_t^2] - E[X_t]^2 = \frac{1}{2} - \frac{1}{4} = \frac{1}{4}$$

for all t. Now, let $P_{\Delta t}$ denote the conditional probability $\Pr(X_{t+\Delta t} = 1 \,|\, X_t = 1)$ for some positive integer Δt. It is straightforward to show that $P_{\Delta t}$ satisfies

$$P_{\Delta t+1} = P_{\Delta t}(1 - s) + (1 - P_{\Delta t})s, \quad \text{subject to} \quad P_1 = 1 - s. \tag{B.1}$$

Solving the initial value problem in (B.1) gives $P_{\Delta t} = [(1 - 2s)^{\Delta t} + 1]/2$. It follows that

$$E[X_t\, X_{t+\Delta t}] = \Pr(X_{t+\Delta t} = 1 \,|\, X_t = 1)\ \Pr(X_t = 1) = \frac{(1 - 2s)^{\Delta t} + 1}{4}$$

and

$$\mathrm{Cov}(X_t, X_{t+\Delta t}) = E[X_t\, X_{t+\Delta t}] - E[X_t]\, E[X_{t+\Delta t}] = \frac{(1 - 2s)^{\Delta t}}{4}.$$

Using the definition of correlation, we find

$$\mathrm{Corr}(X_t, X_{t+\Delta t}) = \frac{\mathrm{Cov}(X_t, X_{t+\Delta t})}{\sqrt{\mathrm{Var}(X_t)}\,\sqrt{\mathrm{Var}(X_{t+\Delta t})}} = \frac{(1 - 2s)^{\Delta t}/4}{\sqrt{1/4}\,\sqrt{1/4}} = (1 - 2s)^{\Delta t}$$

which is the formula that appears in the caption to Figure 4.1.

B.2 Deriving the Inclusive-Fitness Effect

Fitness is, of course, a key component of inclusive fitness. Our fitness measure will focus on offspring prior to dispersal. We fix attention on such an offspring born into an environment in state e. The *fitness* of this focal offspring will be the expected number of offspring it produces in the next year, weighted by genetic contribution. The *fitness function*, w, is a mathematical description of fitness and takes two arguments: (i) $d_{\bullet,e}$, the probability with which the focal offspring disperses, and (ii) $\bar{d}_e$, the probability with which the average offspring born on the same patch, and in the same year as the focal individual disperses. The function w will also depend on the population-average probability of dispersal, d_e, but this will not be included as an argument.

To develop w for the DM model we note that with probability $1 - d_{e,\bullet}$, the focal individual competes on its natal patch, and with probability $(1 - c_e)d_{e,\bullet}$ the focal individual competes on a foreign patch. Provided it survives the dispersal phase of the life-cycle, the focal individual expects to be fertilized by one individual (success through female function), and it expects to fertilize one individual (success through male function). When it competes on its natal site the focal individual and the individual it fertilized both secure a spot on the patch, independently, with probability in proportion to $1/(1 - \bar{d}_e + (1 - c_e)d_e)$. When it competes on a foreign patch spots are secured with probability in proportion to $1/(1 - c_e d_e)$.

$$\text{DM:} \quad w(d_{\bullet,e}, \bar{d}_e) = \left(\frac{1 - d_{\bullet,e}}{1 - \bar{d}_e + (1 - c_e)d_e} + \frac{(1 - c_e)d_{\bullet,e}}{1 - c_e d_e} \right) \left(\frac{1}{2} + \frac{1}{2} \right)$$

where $1/2 + 1/2$ is included to emphasize the fact that the focal individual expects to contribute half of its genes to each of two offspring—one through female function, the other through male function.

The fitness function for the MD model is developed in a similar manner. However, in the MD model the fitness function must reflect the possibility that success through female and male function might be realized on different patches. We find that

$$\begin{aligned} \text{MD:} \quad w(d_{\bullet,e}, \bar{d}_e) = \frac{1}{2} \left(\frac{1 - d_{\bullet,e}}{1 - \bar{d}_e + (1 - c_e)d_e} + \frac{(1 - c_e)d_{\bullet,e}}{1 - c_e d_e} \right) \\ + \frac{1}{2} \left(\frac{1 - \bar{d}_e}{1 - \bar{d}_e + (1 - c_e)d_e} + \frac{(1 - c_e)\bar{d}_e}{1 - c_e d_e} \right). \end{aligned}$$

The first term on the right of the previous line describes fitness through female function, while the second describes fitness through male function.

Let $A_{p|e} = T_{p|e} w(d_{\bullet,e}, \bar{d}_e)$ denote the expected number of offspring in a poor environment, produced in the next year by the focal offspring. Similarly, let $A_{g|e} = T_{g|e} w(d_{\bullet,e}, \bar{d}_e)$ denote the expected number of offspring in a good environment, produced in the next year by the focal

offspring. Given those definitions, the matrix

$$A = \begin{bmatrix} T_{p|p}\, w(d_{\bullet,p}, \bar{d}_p) & T_{p|g}\, w(d_{\bullet,g}, \bar{d}_g) \\ T_{g|p}\, w(d_{\bullet,p}, \bar{d}_p) & T_{g|g}\, w(d_{\bullet,g}, \bar{d}_g) \end{bmatrix}$$

can be used to describe the (linear) dynamics of the focal offspring's genetic lineage. When the dominant eigenvalue of A, call it λ, is greater than 1, the focal individual's genetic lineage is increasing in frequency in the population.

When $d_{\bullet,e} = \bar{d}_e = d_e$, for $e = p, g$, it is easy to see that $A = T$. Consequently, $\lambda = 1$ and is associated with left and right eigenvectors,

$$v = \begin{bmatrix} 1 \\ 1 \end{bmatrix}, \quad u = \begin{bmatrix} \pi_p \\ \pi_g \end{bmatrix}$$

respectively. In addition, following Taylor and Frank [4], the marginal changes in fitness for the DM model are

$$\text{DM:} \quad \begin{cases} R_p \frac{\partial A}{\partial d_{\bullet,p}} + \bar{R}_p \frac{\partial A}{\partial \bar{d}_p}\Big]_{d_{\bullet,p}=\bar{d}_p=d_p} = \begin{bmatrix} T_{p|p}(-R_p\, c_p + \bar{R}_p\, h_p)v_p & 0 \\ T_{g|p}(-R_p\, c_p + \bar{R}_p\, h_p)v_p & 0 \end{bmatrix} \\ R_g \frac{\partial A}{\partial d_{\bullet,g}} + \bar{R}_g \frac{\partial A}{\partial \bar{d}_g}\Big]_{d_{\bullet,g}=\bar{d}_g=d_g} = \begin{bmatrix} 0 & T_{p|g}(-R_g\, c_g + \bar{R}_g\, h_g)v_g \\ 0 & T_{g|g}(-R_g\, c_g + \bar{R}_g\, h_g)v_g \end{bmatrix} \end{cases}$$

where R_p is the relatedness between the focal offspring and the individual controlling the focal offspring's dispersal, and $\bar{R}_p$ is the relatedness between the focal offspring and the individual controlling the dispersal of the average offspring born on the same patch (see Appendix B.3). As described in the main text $h_e = (1 - d_e)/(1 - c_e\, d_e)$ gives the probability that an individual native to a given patch is competitively displaced, when the environment is currently in state e. Also, $v_e = 1/(1 - c_e\, d_e)$ gives the reproductive value of an individual competing on a patch in a

year when the environment is in state e. For the MD model, the marginal changes in fitness are

$$\text{MD:} \quad \begin{cases} R_p \frac{\partial A}{\partial d_{\bullet,p}} + \bar{R}_p \frac{\partial A}{\partial \bar{d}_p}\Big]_{d_{\bullet,p}=\bar{d}_p=d_p} = \begin{bmatrix} T_{p|p}(-\frac{R_p+\bar{R}_p}{2} c_p + \bar{R}_p h_p)v_p & 0 \\ T_{g|p}(-\frac{R_p+\bar{R}_p}{2} c_p + \bar{R}_p h_p)v_p & 0 \end{bmatrix} \\ R_g \frac{\partial A}{\partial d_{\bullet,g}} + \bar{R}_g \frac{\partial A}{\partial \bar{d}_g}\Big]_{d_{\bullet,g}=\bar{d}_g=d_g} = \begin{bmatrix} 0 & T_{p|g}(-\frac{R_g+\bar{R}_g}{2} c_g + \bar{R}_g h_g)v_g \\ 0 & T_{p|g}(-\frac{R_g+\bar{R}_g}{2} c_g + \bar{R}_g h_g)v_g \end{bmatrix} \end{cases}$$

Continuing with the method of analysis laid out in Taylor and Frank [4] method, the inclusive-fitness effect of increased natal dispersal is

$$v \cdot \left(R_e \frac{\partial A}{\partial d_{\bullet,e}} + \bar{R}_e \frac{\partial A}{\partial \bar{d}_e}\Big]_{d_{\bullet,e}=\bar{d}_e=d_e} \right) u$$

which simplifies to

$$\Delta w_e(d_e) = \begin{cases} (-R_e c_e + \bar{R}_e h_e)\,\alpha_e & \text{for DM} \\ \left(-\frac{R_e+\bar{R}_e}{2} c_e + \bar{R}_e h_e\right)\alpha_e & \text{for MD} \end{cases}$$

where $\alpha_e = \pi_e v_e$ gives the total reproductive value of offspring born in a year where the environment is in state e. Notice that we study $\Delta W_e = \Delta w_e(d_e)/\pi_e$ in the main text (equation 4.4). This is justified because we restrict attention to $\pi_p = \pi_g = 1/2$, and because we are interested only in the sign of the inclusive-fitness effect. When dispersal occurs with probability d, irrespective of environmental state, the inclusive-fitness effect is simply

$$\Delta w(d) = \Delta w_p(d) + \Delta w_g(d)$$

which equivalent by ΔW in the main text (equation (4.5)), since $\pi_p = \pi_g = 1/2$.

The sign of the inclusive-fitness effect tells us how selection shapes dispersal. When the inclusive-fitness effect is positive, selection favours an increase in the corresponding probability of offspring dispersal, and when it is negative, selection favours a decrease. It follows that dispersal is at *intermediate evolutionary equilibrium* when the inclusive fitness effect is zero. Dispersal will be at a *boundary equilibrium*, when either $\Delta w_e(1) > 0$ or $\Delta w_e(0) < 0$ (alternatively, $\Delta w(1) > 0$ or $\Delta w(0) < 0$). The former case corresponds to complete dispersal, while the

latter corresponds to complete natal-patch philopatry.

B.3 Genetic Relatedness

Relatedness in our models is defined in terms of identity by descent. Two alleles are said to be *identical by descent* if we can trace their respective lines of descent back to a single, common ancestral allele. The ancestral history of alleles, therefore, will be of critical importance. We explore that history in the next subsection. We round out this section of the appendix with the actual calculation of relatedness between pairs of individuals in the model.

B.3.1 The Relationship Between Pairs of Alleles

To facilitate biological interpretation of relatedness, we investigate the history of pairs of alleles at the dispersal locus, backward in time, until they reach a common ancestor. Consider two alleles sampled with replacement from the population following the death of adults, but before either dispersal or mating of offspring occurs. These two alleles may be observed:

1. as physically distinct copies, carried on different chromosomes by the same individual, when $e = p$;

2. as physically distinct copies, carried on different chromosomes by the same individual, when $e = g$;

3. as physically distinct copies, carried by different individuals on the same patch, when $e = p$;

4. as physically distinct copies, carried by different individuals on the same patch, when $e = g$;

5. as the same physical copies, carried by one individual,

6. on different patches, carried by different individuals.

We will refer to state 5 as the *coalescent state* and state 6 as the *acoalescent state*. Importantly, because the model population is infinitely large, a pair of alleles in the acoalescent state will not have lines of descent that trace back to a common ancestor (rather, the probability that lines of descent trace back to a common ancestor is negligible). Overall, we treat the transition among the various states as a Markov process, and the coalescent and acoalescent states, respectively, as absorbing states. We present the Markov-process model below for both DM and MD models.

Dispersal Before Mating (DM)

Consider two alleles currently in state 1 or state 2. Because the alleles are found on different chromosomes (and because selfing almost surely does not occur), their ancestors must have been found in different individuals the year before. With probability $h_p^2 S_{p|e}$ the immediate ancestors were found in state 3, and with probability $h_g^2 S_{g|e}$ they were in state 4. With probability $1 - h_p^2 S_{p|e} - h_g^2 S_{g|e}$ the immediate ancestors were in the acoalescent state (state 6). If P_{ij} denotes the probability that a pair of alleles currently in state i originated from one that was most recently in state j, then

$$\begin{bmatrix} P_{11} & \dots & P_{16} \\ P_{21} & \dots & P_{26} \end{bmatrix} = \begin{bmatrix} 0 & 0 & h_p^2 S_{p|p} & h_g^2 S_{g|p} & 0 & 1 - (h_p^2 S_{p|p} + h_g^2 S_{g|p}) \\ 0 & 0 & h_p^2 S_{p|g} & h_g^2 S_{g|g} & 0 & 1 - (h_p^2 S_{p|g} + h_g^2 S_{g|g}) \end{bmatrix}.$$

Now consider two alleles currently in state 3 or 4. Regardless of the state of the environment, the alleles originated from the same individual in the previous generation with probability $1/(2N)$; they originated from different individuals with probability $1 - 1/(2N)$. Given that the alleles originated from same individual in the previous generation, they existed as physically distinct copies with probability $1/2$, and were not physically distinct with probability $1/2$. It follows that the probability with which the alleles were most recently in: (i) state 1 is $S_{p|e}/(4N)$, (ii) state 2 is $S_{g|e}/(4N)$, and (iii) state 5 is $1/(4N)$. Given that the alleles originated from different individuals in the previous year, they were most recently in: (i) state 3 with probability $(1 - 1/(2N))h_p^2 S_{p|e}$, (ii) state 4 with probability $(1 - 1/(2N))h_g^2 S_{g|e}$, and (iii) state 6

with probability $(1 - 1/(2N)) - (1 - 1/(2N))h_p^2 S_{p|e} - (1 - 1/(2N))h_g^2 S_{g|e}$. It follows that

$$\begin{bmatrix} P_{31} & \dots & P_{36} \\ P_{41} & \dots & P_{46} \end{bmatrix}$$
$$= \begin{bmatrix} \frac{1}{4N}S_{p|p} & \frac{1}{4N}S_{g|p} & \frac{2N-1}{2N}h_p^2 S_{p|p} & \frac{2N-1}{2N}h_g^2 S_{g|p} & \frac{1}{4N} & \frac{2N-1}{2N} - \frac{2N-1}{2N}(h_p^2 S_{p|p} + h_g^2 S_{g|p}) \\ \frac{1}{4N}S_{p|g} & \frac{1}{4N}S_{g|g} & \frac{2N-1}{2N}h_p^2 S_{p|g} & \frac{2N-1}{2N}h_g^2 S_{g|g} & \frac{1}{4N} & \frac{2N-1}{2N} - \frac{2N-1}{2N}(h_p^2 S_{p|g} + h_g^2 S_{g|g}) \end{bmatrix}.$$

For completeness,

$$\begin{bmatrix} P_{51} & \dots & P_{56} \\ P_{61} & \dots & P_{66} \end{bmatrix} = \begin{bmatrix} 0 & 0 & 0 & 0 & 1 & 0 \\ 0 & 0 & 0 & 0 & 0 & 1 \end{bmatrix}.$$

Overall, the matrix P describes the stochastic process associated with tracing the origins of alleles backward in time. Note that

$$P = \left[\begin{array}{cc|cc} & & 0 & 1 - (h_p^2 S_{p|p} + h_g^2 S_{g|p}) \\ & Q & 0 & 1 - (h_p^2 S_{p|g} + h_g^2 S_{g|g}) \\ & & \frac{1}{4N} & \frac{2N-1}{2N} - \frac{2N-1}{2N}(h_p^2 S_{p|p} + h_g^2 S_{g|p}) \\ & & \frac{1}{4N} & \frac{2N-1}{2N} - \frac{2N-1}{2N}(h_p^2 S_{p|g} + h_g^2 S_{g|g}) \\ \hline 0 & & 1 & 0 \\ & & 0 & 1 \end{array}\right]$$

where

$$Q = \begin{bmatrix} 0 & 0 & h_p^2 S_{p|p} & h_g^2 S_{g|p} \\ 0 & 0 & h_p^2 S_{p|g} & h_g^2 S_{g|g} \\ \frac{1}{4N}S_{p|p} & \frac{1}{4N}S_{g|p} & \frac{2N-1}{2N}h_p^2 S_{p|p} & \frac{2N-1}{2N}h_g^2 S_{g|p} \\ \frac{1}{4N}S_{p|g} & \frac{1}{4N}S_{g|g} & \frac{2N-1}{2N}h_p^2 S_{p|g} & \frac{2N-1}{2N}h_g^2 S_{g|g} \end{bmatrix}. \tag{B.2}$$

The matrix Q describes transitions among transient states $i = 1, \dots, 4$. If θ_{ij} denotes the expected number of years the process spent in transient state j, given that it is currently in transient state i, then the matrix of these expectations can be expressed as

$$\Theta = I + Q + Q^2 + \dots. \tag{B.3}$$

As is shown in elementary treatments of stochastic processes [see 2], we can treat (B.3) as a matrix version of a geometric series. Therefore,

$$\Theta = (I - Q)^{-1}. \tag{B.4}$$

Dispersal After Mating (MD)

For the MD model, the matrix P from the previous subsection changes. The changes that are most relevant to this work are those that appear in the matrix Q. This matrix is now written as

$$Q = \begin{bmatrix} 0 & 0 & S_{p|p} & S_{g|p} \\ 0 & 0 & S_{p|g} & S_{g|g} \\ \frac{1}{4N}S_{p|p} & \frac{1}{4N}S_{g|p} & \frac{2(N-1)h_p^2+1}{2N}S_{p|p} & \frac{2(N-1)h_g^2+1}{2N}S_{g|p} \\ \frac{1}{4N}S_{p|g} & \frac{1}{4N}S_{g|g} & \frac{2(N-1)h_p^2+1}{2N}S_{p|g} & \frac{2(N-1)h_g^2+1}{2N}S_{g|g} \end{bmatrix}. \tag{B.5}$$

B.3.2 Relatedness Calculations

To compute relatedness, we will need the following probabilities related to identity by descent:

- $f_e(n)$, the probability that two homologous alleles carried by the same offspring are IBD, given the environment is in state $e = p, g$ during generation n;

- $F_e(n)$, the probability that one allele, chosen uniformly from each of two individuals born on the same patch are IBD, given the environment is in state $e = p, g$ during generation n.

Exactly how we use $f_e(n)$ and $F_e(n)$ to calculate R_e and $\bar{R}_e$ depends on which model scenario we consider. For the sake of clarity, we treat the DM and MD models separately.

Dispersal before mating (DM)

For the DM model, we find

$$\left.\begin{aligned}
f_p(n+1) &= h_p^2 F_p(n) S_{p|p} + h_g^2 F_g(n) S_{g|p} \\
f_g(n+1) &= h_p^2 F_p(n) S_{p|g} + h_g^2 F_g(n) S_{g|g} \\
F_p(n+1) &= \left[\tfrac{1}{N}\left(\tfrac{1}{4} + \tfrac{h_p^2 F_p(n)}{2} + \tfrac{f_p(n)}{4}\right) + \tfrac{N-1}{N} h_p^2 F_p(n)\right] S_{p|p} \\
&\quad + \left[\tfrac{1}{N}\left(\tfrac{1}{4} + \tfrac{h_g^2 F_g(n)}{2} + \tfrac{f_g(n)}{4}\right) + \tfrac{N-1}{N} h_g^2 F_g(n)\right] S_{g|p} \\
F_g(n+1) &= \left[\tfrac{1}{N}\left(\tfrac{1}{4} + \tfrac{h_p^2 F_p(n)}{2} + \tfrac{f_p(n)}{4}\right) + \tfrac{N-1}{N} h_p^2 F_p(n)\right] S_{p|g} \\
&\quad + \left[\tfrac{1}{N}\left(\tfrac{1}{4} + \tfrac{h_g^2 F_g(n)}{2} + \tfrac{f_g(n)}{4}\right) + \tfrac{N-1}{N} h_g^2 F_g(n)\right] S_{g|g}
\end{aligned}\right\} \tag{B.6}$$

or, in matrix form

$$\begin{bmatrix} f_p(n+1) \\ f_g(n+1) \\ F_p(n+1) \\ F_g(n+1) \end{bmatrix} = \underbrace{\begin{bmatrix} 0 & 0 & h_p^2 S_{p|p} & h_g^2 S_{g|p} \\ 0 & 0 & h_p^2 S_{p|g} & h_g^2 S_{g|g} \\ \frac{1}{4N} S_{p|p} & \frac{1}{4N} S_{g|p} & \frac{2N-1}{2N} h_p^2 S_{p|p} & \frac{2N-1}{2N} h_g^2 S_{g|p} \\ \frac{1}{4N} S_{p|g} & \frac{1}{4N} S_{g|g} & \frac{2N-1}{2N} h_p^2 S_{p|g} & \frac{2N-1}{2N} h_g^2 S_{g|g} \end{bmatrix}}_{=Q} \begin{bmatrix} f_p(n) \\ f_g(n) \\ F_p(n) \\ F_g(n) \end{bmatrix} + \begin{bmatrix} 0 \\ 0 \\ \frac{1}{4N} \\ \frac{1}{4N} \end{bmatrix}. \tag{B.7}$$

Note that Q in equation (B.7) was identified above (equation B.2). As indicated in that subsection, the matrix $(I - Q)$ is invertible, and so the equilibrium solution to (B.6) is

$$\begin{bmatrix} f_p \\ f_g \\ F_p \\ F_g \end{bmatrix} = \underbrace{\begin{bmatrix} 1 & 0 & -h_p^2 S_{p|p} & -h_g^2 S_{g|p} \\ 0 & 1 & -h_p^2 S_{p|g} & -h_g^2 S_{g|g} \\ -\frac{1}{4N} S_{p|p} & -\frac{1}{4N} S_{g|p} & 1 - \frac{2N-1}{2N} h_p^2 S_{p|p} & -\frac{2N-1}{2N} h_g^2 S_{g|p} \\ -\frac{1}{4N} S_{p|g} & -\frac{1}{4N} S_{g|g} & -\frac{2N-1}{2N} h_p^2 S_{p|g} & 1 - \frac{2N-1}{2N} h_g^2 S_{g|g} \end{bmatrix}^{-1}}_{=\Theta=(I-Q)^{-1}} \begin{bmatrix} 0 \\ 0 \\ \frac{1}{4N} \\ \frac{1}{4N} \end{bmatrix}, \tag{B.8}$$

where Θ was also identified above (equation B.4).

Equation (B.8) can be understood as an expression of the likelihood that different pairs of alleles on the same patch are identical by descent. Tracing the ancestry of these alleles

backward in time, it is clear that their respective lines of descent must pass through distinct offspring on the patch, in the year that follows their coalescence. Thus, coalescence could occur in any year that precedes one in which alleles are found in distinct offspring on the same patch; in a neutral population this occurs with probability $1/(4N)$.

With the preceding comments in mind, consider a physically distinct pair of alleles, carried by the same offspring born into a poor environment. These alleles descended along lines that, themselves, spent $\Theta_{13} + \Theta_{14}$ years on the current patch, but in distinct individuals. During each of these years, we can assert that the lineages coalesced in the year previous with probability $1/(4N)$. Consequently,

$$f_p = \frac{\Theta_{13} + \Theta_{14}}{4N}$$

which agrees with equation (B.8). Similar interpretations are possible for f_g, F_p, and F_g, and these will be important for the perturbation analysis in a later section.

Turning our attention, now, to the calculation of relatedness, we consider the scenario in which offspring control their own dispersal phenotype. In this case, R_e is understood as the coefficient of consanguinity between and offspring and itself, given that the environment is in state e. Conditioning on the alleles being compared, we find

$$\text{Offspring Control:} \quad R_e = \frac{1}{2} \times 1 + \frac{1}{2} f_e = \frac{1 + f_e}{2}.$$

When offspring control dispersal, $\bar{R}_e$ is the coefficient of consanguinity between two offspring born on the same patch in environmental state e. It follows that

$$\text{Offspring Control:} \quad \bar{R}_e = F_e$$

by definition.

Second, consider the scenario in which parents control the dispersal phenotype exhibited by their offspring. In this case, R_e is understood as the coefficient of consanguinity between a parent and its offspring born in an environment in state e. This coefficient is calculated by

conditioning on whether or not the allele chosen from the offspring originated from the parent, and subsequently on the previous state of the environment. Conditioning in this way gives

$$\text{Parental Control:} \quad R_e = \frac{1}{2}\left(\frac{1 + f_p S_{p|e} + f_g S_{g|e}}{2}\right) + \frac{1}{2}\left(F_p h_p^2 S_{p|e} + F_g h_g^2 S_{g|e}\right) = \frac{1 + f_p S_{p|e} + f_g S_{g|e}}{4} + \frac{f_e}{2}$$

where the second equality follows from the fact that the system described by (B.6) is at equilibrium.

With parental control, $\bar{R}_e$ is the coefficient of consanguinity between an adult and the average offspring born on its patch. A conditioning argument similar to that used previously gives

$$\text{Parental Control:} \quad \bar{R}_e = \left[\frac{1}{N}\left(\frac{1}{4} + \frac{h_p^2 F_p}{2} + \frac{f_p}{4}\right) + \frac{N-1}{N} h_p^2 F_p(n)\right] S_{p|e} + \left[\frac{1}{N}\left(\frac{1}{4} + \frac{h_g^2 F_g}{2} + \frac{f_g}{4}\right) + \frac{N-1}{N} h_g^2 F_g(n)\right] S_{g|e} = F_e$$

where the final equality again follows from the fact that the system described in (B.6) is at equilibrium.

Dispersal after mating (MD)

Expressions for relatedness in the MD model are the same as those presented for the DM model, though the identity coefficients f_e and F_e change. Calculation of the identity coefficients for the MD model follow the procedure outlined above using the matrix Q given in equation (B.5).

B.4 Perturbation Methods

B.4.1 Dispersal Before Mating (DM)

As described in the main text, let $c = (c_p + c_g)/2$ and $\sigma = (c_p - c_g)/2 > 0$. Then, $c_p = c + \sigma$, and $c_g = c - \sigma$. Now assume that solutions to the model with environmental variation can be

expressed as

$$\begin{aligned} h_e &\approx h_0 + \eta_e \sigma + O(\sigma^2) \\ f_e &\approx f_0 + \phi_e \sigma + O(\sigma^2) \\ F_e &\approx F_0 + \Phi_e \sigma + O(\sigma^2) \end{aligned}$$

where leading terms come from the model without environmental variation [3]. In addition, let

$$Q = Q_0 + Q_0' \sigma + O(\sigma^2)$$

where

$$Q_0 = \begin{bmatrix} 0 & 0 & h_0^2 S_{p|p} & h_0^2 S_{g|p} \\ 0 & 0 & h_0^2 S_{p|g} & h_0^2 S_{g|g} \\ \frac{1}{4N} S_{p|p} & \frac{1}{4N} S_{g|p} & \frac{2N-1}{2N} h_0^2 S_{p|p} & \frac{2N-1}{2N} h_0^2 S_{g|p} \\ \frac{1}{4N} S_{p|g} & \frac{1}{4N} S_{g|g} & \frac{2N-1}{2N} h_0^2 S_{p|g} & \frac{2N-1}{2N} h_0^2 S_{g|g} \end{bmatrix}$$

and

$$Q_0' = 2h_0 \begin{bmatrix} 0 & 0 & S_{p|p} & S_{g|p} \\ 0 & 0 & S_{p|g} & S_{g|g} \\ 0 & 0 & \frac{2N-1}{2N} S_{p|p} & \frac{2N-1}{2N} S_{g|p} \\ 0 & 0 & \frac{2N-1}{2N} S_{p|g} & \frac{2N-1}{2N} S_{g|g} \end{bmatrix} \begin{bmatrix} 0 & & & \\ & 0 & & \\ & & \eta_p & \\ & & & \eta_g \end{bmatrix}.$$

Using (B.7), we note that

$$\begin{bmatrix} f_0 \\ f_0 \\ F_0 \\ F_0 \end{bmatrix} + \begin{bmatrix} \phi_p \\ \phi_g \\ \Phi_p \\ \Phi_g \end{bmatrix} \sigma = Q_0 \begin{bmatrix} f_0 \\ f_0 \\ F_0 \\ F_0 \end{bmatrix} + \begin{bmatrix} 0 \\ 0 \\ \frac{1}{4N} \\ \frac{1}{4N} \end{bmatrix} + Q_0 \begin{bmatrix} \phi_p \\ \phi_g \\ \Phi_p \\ \Phi_g \end{bmatrix} \sigma + Q_0' \begin{bmatrix} f_0 \\ f_0 \\ F_0 \\ F_0 \end{bmatrix} \sigma + O(\sigma^2).$$

By applying the definition of coefficients f_0 and F_0, respectively, and by ignoring higher-order terms in σ, the previous line rearranges to

$$\begin{bmatrix} \phi_p \\ \phi_g \\ \Phi_p \\ \Phi_g \end{bmatrix} = (I - Q_0)^{-1} Q_0' \begin{bmatrix} f_0 \\ f_0 \\ F_0 \\ F_0 \end{bmatrix}. \tag{B.9}$$

Using the fact that

$$Q_0' \begin{bmatrix} f_0 \\ f_0 \\ F_0 \\ F_0 \end{bmatrix} = 2h_0 F_0 \begin{bmatrix} S_{p|p} & S_{g|p} \\ S_{p|g} & S_{g|g} \\ \frac{2N-1}{2N} S_{p|p} & \frac{2N-1}{2N} S_{g|p} \\ \frac{2N-1}{2N} S_{p|g} & \frac{2N-1}{2N} S_{g|g} \end{bmatrix} \begin{bmatrix} \eta_p \\ \eta_g \end{bmatrix}$$

we can re-write equation (B.9) so to express the left-hand side, as

$$\begin{bmatrix} \phi_p \\ \phi_g \\ \Phi_p \\ \Phi_g \end{bmatrix} = 2h_0 F_0 \Theta_0 \begin{bmatrix} S_{p|p} & S_{g|p} \\ S_{p|g} & S_{g|g} \\ \frac{2N-1}{2N} S_{p|p} & \frac{2N-1}{2N} S_{g|p} \\ \frac{2N-1}{2N} S_{p|g} & \frac{2N-1}{2N} S_{g|g} \end{bmatrix} \begin{bmatrix} \eta_p \\ \eta_g \end{bmatrix} \tag{B.10}$$

where $\Theta_0 = (I - Q_0)^{-1}$ is the matrix of expectations described in Appendix B.3 with $\sigma = 0$.

Equation (B.10) suggests an interpretation based on coalescence ideas introduced in Appendix B.3. Consider a year in which the environment is in state e, and consider two physically distinct alleles carried by the same offspring born in that year. By virtue of their position, the alleles in question must have descended from ones carried by distinct individuals in the previous year. The environmental change means that the likelihood that these ancestors were native is altered at rate $2h_0(\eta_p S_{p|e} + \eta_g S_{g|e})$. Given that the ancestors were indeed native, uniform-random alleles selected from each ultimately descended from a common ancestor with approximate probability F_0. It follows that for every year that two distinct lines of descent pass through the

same individual, and the likelihood of their eventual coalescence is changed by

$$2h_0(\eta_p S_{p|e} + \eta_g S_{g|e})F_0 \tag{B.11}$$

approximately.

Now consider a year in which the environment is in state e, and consider two alleles carried by different offspring born on the same patch in that year. It is worth noting that, with probability $1/(4N) + f_0 \times 1/(4N)$ the lineages followed by these alleles coalesce in the previous generation, but this coalescence is not altered by increased environmental variability. Probabilities of coalescence are only changed in years during which lineages pass through distinct individuals. The probability that lines of descent followed by the chosen alleles do in fact pass through distinct individuals in the previous year is $1 - 1/(4N) - 1/(4N) = (2N-1)/(2N)$. Following the previous discussion, the likelihood of the eventual coalescence is altered by

$$\frac{2N-1}{2N} 2h_0(\eta_p S_{p|e} + \eta_g S_{g|e})F_0 \tag{B.12}$$

approximately.

If τ_{ij} denotes the ijth entry of Θ_0, then we use τ_{ij}s to weight changes in lines (B.11) and (B.12), respectively, and we obtain

$$\begin{aligned}
\phi_p &= (\tau_{11} + \tfrac{2N-1}{2N}\tau_{13})2h_0(\eta_p S_{p|p} + \eta_g S_{g|p})F_0 + (\tau_{12} + \tfrac{2N-1}{2N}\tau_{14})2h_0(\eta_p S_{p|g} + \eta_g S_{g|g})F_0 \\
\phi_g &= (\tau_{21} + \tfrac{2N-1}{2N}\tau_{23})2h_0(\eta_p S_{p|p} + \eta_g S_{g|p})F_0 + (\tau_{22} + \tfrac{2N-1}{2N}\tau_{24})2h_0(\eta_p S_{p|g} + \eta_g S_{g|g})F_0 \\
\Phi_p &= (\tau_{31} + \tfrac{2N-1}{2N}\tau_{33})2h_0(\eta_p S_{p|p} + \eta_g S_{g|p})F_0 + (\tau_{32} + \tfrac{2N-1}{2N}\tau_{34})2h_0(\eta_p S_{p|g} + \eta_g S_{g|g})F_0 \\
\Phi_g &= (\tau_{41} + \tfrac{2N-1}{2N}\tau_{43})2h_0(\eta_p S_{p|p} + \eta_g S_{g|p})F_0 + (\tau_{42} + \tfrac{2N-1}{2N}\tau_{44})2h_0(\eta_p S_{p|g} + \eta_g S_{g|g})F_0
\end{aligned} \tag{B.13}$$

which agrees with equation (B.10). For later use, suppose $S_{g|p} = S_{p|g} = 1/2$. In such a case, $\eta_p = -\eta_g$ would ensure that the expressions in (B.13) vanish; i.e. relatedness would remain at its time-averaged value. Despite those observations, the equations in (B.13) are easier to work

with if they are re-written as,

$$\begin{aligned}
\phi_p = \quad & \eta_p \left[S_{p|p}(\tau_{11} + \tfrac{2N-1}{2N}\tau_{13}) + S_{p|g}(\tau_{12} + \tfrac{2N-1}{2N}\tau_{14}) \right] 2h_0F_0 \\
& + \eta_g \left[S_{g|p}(\tau_{11} + \tfrac{2N-1}{2N}\tau_{13}) + S_{g|g}(\tau_{12} + \tfrac{2N-1}{2N}\tau_{14}) \right] 2h_0F_0, \\
\phi_g = \quad & \eta_p \left[S_{p|p}(\tau_{21} + \tfrac{2N-1}{2N}\tau_{23}) + \eta_p S_{p|g}(\tau_{22} + \tfrac{2N-1}{2N}\tau_{24}) \right] 2h_0F_0 \\
& + \eta_g \left[S_{g|p}(\tau_{21} + \tfrac{2N-1}{2N}\tau_{23}) + S_{g|g}(\tau_{22} + \tfrac{2N-1}{2N}\tau_{24}) \right] 2h_0F_0, \\
\Phi_p = \quad & \eta_p \left[S_{p|p}(\tau_{31} + \tfrac{2N-1}{2N}\tau_{33}) + S_{p|g}(\tau_{32} + \tfrac{2N-1}{2N}\tau_{34}) \right] 2h_0F_0 \\
& + \eta_g \left[S_{g|p}(\tau_{31} + \tfrac{2N-1}{2N}\tau_{33}) 2h_0F_0 + S_{g|g}(\tau_{32} + \tfrac{2N-1}{2N}\tau_{34}) \right] 2h_0F_0, \\
\Phi_g = \quad & \eta_p \left[S_{p|p}(\tau_{41} + \tfrac{2N-1}{2N}\tau_{43}) + S_{p|g}(\tau_{42} + \tfrac{2N-1}{2N}\tau_{44}) \right] 2h_0F_0 \\
& + \eta_g \left[S_{g|p}(\tau_{41} + \tfrac{2N-1}{2N}\tau_{43}) + S_{g|g}(\tau_{42} + \tfrac{2N-1}{2N}\tau_{44}) \right] 2h_0F_0.
\end{aligned} \tag{B.14}$$

These equations are the ones upon which we will rely.

Parental control

For the DM model with Parental Control, the equilibrium level of conditional dispersal satisfies

$$\begin{aligned}
-\left(\tfrac{1+3f_0}{4} + \tfrac{\phi_p S_{p|p} + \phi_g S_{g|p}}{4}\sigma + \tfrac{\phi_p}{2}\sigma \right)(c+\sigma) + (h_0 + \eta_p\sigma)(F_0 + \Phi_p\sigma) + O(\sigma^2) &= 0 \\
-\left(\tfrac{1+3f_0}{4} + \tfrac{\phi_p S_{p|g} + \phi_g S_{g|g}}{4}\sigma + \tfrac{\phi_g}{2}\sigma \right)(c-\sigma) + (h_0 + \eta_g\sigma)(F_0 + \Phi_g\sigma) + O(\sigma^2) &= 0
\end{aligned}$$

which rearranges to

$$\begin{aligned}
-\tfrac{1+3f_0}{4}c + h_0F_0 + \left(F_0\eta_p + h_0\Phi_p - \tfrac{\phi_p S_{p|p} + \phi_g S_{g|p}}{4}c - \tfrac{\phi_p}{2}c - \tfrac{1+3f_0}{4} \right)\sigma + O(\sigma^2) &= 0 \\
-\tfrac{1+3f_0}{4}c + h_0F_0 + \left(F_0\eta_g + h_0\Phi_g - \tfrac{\phi_p S_{p|g} + \phi_g S_{g|g}}{4}c - \tfrac{\phi_g}{2}c + \tfrac{1+3f_0}{4} \right)\sigma + O(\sigma^2) &= 0.
\end{aligned}$$

Given $F_0 = f_0/h_0^2 = 1/(4N - (4N-1)h_0^2)$ comes from $(I - Q_0)^{-1} \cdot [0, 0, 1/(4N), 1/(4N)]$ [see also 3], we can solve $-\frac{1+3f_0}{4}c + h_0F_0 = 0$ to find

$$h_0 = \frac{2Nc}{1+H}$$

where $H = \sqrt{1 + 4N(N-1)c^2}$ [3]. Substituting this expression for h_0 along with the expressions in (B.14) into

$$\begin{aligned} F_0\eta_p + h_0\Phi_p - \tfrac{\phi_p S_{p|p} + \phi_g S_{g|p}}{4} c - \tfrac{\phi_p}{2} c - \tfrac{1+3f_0}{4} &= 0 \\ F_0\eta_g + h_0\Phi_g - \tfrac{\phi_p S_{p|g} + \phi_g S_{g|g}}{4} c - \tfrac{\phi_g}{2} c + \tfrac{1+3f_0}{4} &= 0 \end{aligned}$$

results in a system of equations that can be solved for η_p and η_g, respectively. Using $S_{g|p} = S_{p|g} = s$, we find

$$\eta_p = -\frac{H-1}{2(N-1)c^2} \frac{2H + 8N^2c^2s - 4Nc^2s^2 - 3Nc^2 + 2}{2(4N(N-1)c^2s - H^2) + H(4Nc^2s(s-2) + 3Nc^2 - 2)} \tag{B.15}$$

and

$$\eta_g = \frac{H-1}{2(N-1)c^2} \frac{2H + 8N^2c^2s - 4Nc^2s^2 - 3Nc^2 + 2}{2(4N(N-1)c^2s - H^2) + H(4Nc^2s(s-2) + 3Nc^2 - 2)}, \tag{B.16}$$

and it is η_p that is presented as δh in the main text. Note that for $N = 1$, $h_e = c_e = c \pm \sigma$. It follows that for $N = 1$, the coefficient $\eta_p = +1$ and $\eta_g = -1$. Treating N as a continuous variable and taking the limit of (B.15) and (B.16), respectively, as $N \to 1$ yields the same result.

As a further check on the correctness of (B.15) and (B.16), we observe that if $s = 0$ we find that the expressions η_p and η_g give the correct first-order term from a Taylor expansion about $\sigma = 0$ of the temporally homogeneous result [3], when the cost of dispersal is $c \pm \sigma$. A second check is obtained when $s = 1/2$; then $\eta_p = (1 + 3f_0)/(4F_0) = h_0/c$ and $\eta_g = -(1 + 3f_0)/(4F_0) = -h_0/c$ as expected from the comments following equations (B.13).

For the DM model with Parental Control, the equilibrium level of unconditional dispersal can be found by considering $\Delta w_e/(1 - d_e)$. After substituting in known values of zeroth-order equilibrium solutions, we get

$$\begin{aligned} \tfrac{1}{2}\tfrac{1}{1-d_0} h_0 \left(F_0\eta_p + h_0\Phi_p - \tfrac{\phi_p S_{p|p} + \phi_g S_{g|p}}{4} c - \tfrac{\phi_p}{2} c - \tfrac{1+3f_0}{4} \right) \sigma + O(\sigma^2) &= 0 \\ \tfrac{1}{2}\tfrac{1}{1-d_0} h_0 \left(F_0\eta_g + h_0\Phi_g - \tfrac{\phi_p S_{p|g} + \phi_g S_{g|g}}{4} c - \tfrac{\phi_g}{2} c + \tfrac{1+3f_0}{4} \right) \sigma + O(\sigma^2) &= 0 \end{aligned}$$

where we have assumed $S_{p|g} = S_{g|p} = s$. By definition, $\eta_p = -\eta_g$ in the unconditional-dispersal

model, but the equations (B.15) and (B.16) show that $S_{p|g} = S_{g|p} = s$ guarantees that this restriction holds. Those equations, then, offer us the solution to the unconstrained dispersal problem as well. It follows that $h = h_0 + O(\sigma^2)$ in the model. In other words, the solution is simply the one presented by Taylor [3], using the time-averaged cost of dispersal.

Offspring control

For the DM model with Offspring Control, the equilibrium level of conditional dispersal rearranges to

$$\begin{aligned} -\tfrac{1+f_0}{2}c + F_0 h_0 + \left(\Phi_p h_0 + F_0\eta_p - \tfrac{\phi_p}{2}c - \tfrac{1+f_0}{2}\right)\sigma + O(\sigma^2) &= 0 \\ -\tfrac{1+f_0}{2}c + F_0 h_0 + \left(\Phi_g h_0 + F_0\eta_g - \tfrac{\phi_g}{2}c + \tfrac{1+f_0}{2}\right)\sigma + O(\sigma^2) &= 0 \end{aligned}$$

Given $F_0 = f_0/h_0^2 = 1/(4N - (4N-1)h_0^2)$, we can solve $-\frac{1+f_0}{2}c + F_0 h_0 = 0$ to find

$$h_0 = \frac{4Nc}{1+H}$$

where $H = \sqrt{1 + 8N(2N-1)c^2}$ now [3]. Using this information, and the expressions in (B.14), we again solve for η_p and η_g. In this case,

$$\begin{aligned} \eta_p &= -\frac{H-1}{2(2N-1)c^2}\,\frac{H + 16N^2c^2s - 8Nc^2s^2 - 2Nc^2 + 1}{4Nc^2s(4N-1-2s) + H(2Nc^2 - 1 - 4Nc^2s) - H^2} \\ \eta_g &= \frac{H-1}{2(2N-1)c^2}\,\frac{H + 16N^2c^2s - 8Nc^2s^2 - 2Nc^2 + 1}{4Nc^2s(4N-1-2s) + H(2Nc^2 - 1 - 4Nc^2s) - H^2} \end{aligned}$$

where $S_{p|g} = S_{g|p} = s$. These expressions pass the same checks as those described for their counterparts under Parental Control. They also agree with expressions, found in the main text, keeping in mind that $\eta_p = \delta h$.

B.4.2 Dispersal After Mating (MD)

The perturbation analysis for the MD model proceeds in a manner analogous to that described for the DM model. For the MD model, however, we have

$$Q_0 = \begin{bmatrix} 0 & 0 & S_{p|p} & S_{g|p} \\ 0 & 0 & S_{p|g} & S_{g|g} \\ \frac{1}{4N}S_{p|p} & \frac{1}{4N}S_{g|p} & \frac{2(N-1)h_0^2+1}{2N}S_{p|p} & \frac{2(N-1)h_0^2+1}{2N}S_{g|p} \\ \frac{1}{4N}S_{p|g} & \frac{1}{4N}S_{g|g} & \frac{2(N-1)h_0^2+1}{2N}S_{p|g} & \frac{2(N-1)h_0^2+1}{2N}S_{g|g} \end{bmatrix} \tag{B.17}$$

and

$$Q_0' = 2h_0\frac{N-1}{N}\begin{bmatrix} 0 & 0 & 0 & 0 \\ 0 & 0 & 0 & 0 \\ 0 & 0 & S_{p|p} & S_{g|p} \\ 0 & 0 & S_{p|g} & S_{g|g} \end{bmatrix}\begin{bmatrix} 0 & & & \\ & 0 & & \\ & & \eta_p & \\ & & & \eta_g \end{bmatrix}. \tag{B.18}$$

Parental control

Taylor [3] does not supply the solution to the zeroth order MD model with Parental Control. It is easy to show that

$$h_0 = \begin{cases} c & N = 1 \\ \frac{H-1}{(N-1)c} & N \geq 2 \end{cases} \tag{B.19}$$

where $H = \sqrt{1 + (N-1)(N+1)c^2}$. For the conditional dispersal model $h_e \approx h_0 + \eta_e\sigma$, where

$$\begin{aligned} \eta_p &= -\frac{H-1}{(N-1)c^2}\frac{(8Ns+4s^2-8N-1)-(8Ns-4s^2+16s-7)H}{2s(4N-4s^2+8s-3)-(1-2s)(4s^2-8s+7)H^2-H(8Ns+4s^2-8N-1)}, \\ \eta_g &= \frac{H-1}{(N-1)c^2}\frac{(8Ns+4s^2-8N-1)-(8Ns-4s^2+16s-7)H}{2s(4N-4s^2+8s-3)-(1-2s)(4s^2-8s+7)H^2-H(8Ns+4s^2-8N-1)}, \end{aligned} \tag{B.20}$$

and taking a limit as $N \to 1$ gives $\eta_p = 1$ and $\eta_g = -1$, as expected. In addition, expressions η_p and η_g pass the same checks described above.

As previously mentioned, η_p is presented as δh in the main text. Also, in keeping with the analysis of the DM model, the unconditional likelihood of remaining on one's natal site is h_0.

Offspring control

For the MD model with Offspring Control, the zeroth-order model coincides with the DM model with Parental Control [3]. When perturbed, however, the models differ in general. For MD with Offspring control, we find

$$\begin{aligned}\eta_p &= -\frac{H-1}{2(N-1)c^2}\frac{[8s(N+1)-(4s^2+3)](N-1)c^2+2(1-2s)(H-1)}{2[s-H^2(1-s)]-H(1-2s)[2((N-1)c^2s-1)-3(N-1)c^2]}\\ \eta_g &= \frac{H-1}{2(N-1)c^2}\frac{[8s(N+1)-(4s^2+3)](N-1)c^2+2(1-2s)(H-1)}{2[s-H^2(1-s)]-H(1-2s)[2((N-1)c^2s-1)-3(N-1)c^2]}\end{aligned} \tag{B.21}$$

where $H = \sqrt{1+4N(N-1)c^2}$. Taking a limit as $N \to 1$ we find that $\eta_p = 1$ and $\eta_g = -1$, and in this case the match with DM and Parental Control is restored. Expressions in (B.21) again pass the same checks as analogous expressions in other model scenarios.

B.5 Computational Methods

The numerical procedure we used to find equilibrium phenotype pairs takes as its input four different pairs of estimates, the identity of the individual who controls dispersal (parent or offspring), as well as numerical values for parameters N, $c_p = c + \sigma$, $c_g = c - \sigma$, and s. Each pair of estimates is updated independently by (i) calculating corresponding inclusive-fitness effects (equation 4.4), and then (ii) incrementing or decrementing each member of the pair by a small amount depending on the sign taken by the corresponding inclusive-fitness effect. This updating is repeated either until all four guesses are sufficiently close to one another, or until some maximum number of iterations is exceeded (in practice, we never found a case where the maximum number of iterations was exceeded). Note that the procedure can also find endpoints of natural selection that lie on the boundary of phenotype space, when they exist. The numerical procedure we used to find equilibrium phenotypes was similar to the one just described. However, in this case only two estimates are used, and are updated using equation (4.5). Python code for both numerical procedures are attached in Appendix C.3, and file names are described in Table B.1.

Table B.1: Summary of files containing Python code (a) for implementing numerical procedures, and (b) for carrying out individual-based simulation.

File	Description
(a) Numerical Procedures	
`DM_TwoTraits_num.py`	Finds equilibrium pair (d_p, d_g) for DM Model, both Parental and Offspring Control
`MD_TwoTraits_num.py`	Finds equilibrium (d_p, d_g) for MD Model, both Parental and Offspring Control
`DM_OneTrait_num.py`	Finds equilibrium d for DM Model, both Parental and Offspring Control
`MD_OneTrait_num.py`	Finds equilibrium d for MD Model, both Parental and Offspring Control
(b) Individual-Based Simulation	
`DM_ParCtrl_TwoTraits.py`	Simulates DM Parental Control with conditional dispersal
`DM_OffCtrl_TwoTraits.py`	Simulates DM Offspring Control with conditional dispersal
`MD_ParCtrl_TwoTraits.py`	Simulates MD Parental Control model with conditional dispersal
`MD_OffCtrl_TwoTraits.py`	Simulates MD Offspring Control model with conditional dispersal
`DM_ParCtrl_OneTrait.py`	Simulates DM Parental Control with unconditional dispersal
`DM_OffCtrl_OneTrait.py`	Simulates DM Offspring Control with unconditional dispersal
`MD_ParCtrl_OneTrait.py`	Simulates MD Parental Control model with unconditional dispersal
`MD_OffCtrl_OneTrait.py`	Simulates MD Offspring Control model with unconditional dispersal

The individual-based simulations we used are all based on multinomial sampling procedures, carried out in a population made up of M patches each of size N. Simulation procedures are most easily explained by using a raffle analogy. We treat each of the MN available breeding opportunities as raffle prizes that can be won through female function. There are MN raffle prizes to be won through male function as well. In our simulation, every adult in the population is issued the same number of raffle tickets. A fraction of an individual's tickets can be entered into raffles for non-local breeding opportunities next year. This fraction is often, but not always, related to that individual's dispersal phenotype, and the number of tickets it represents is always decreased by a fraction that reflects the cost of dispersing. The remaining fraction of tickets is entered into raffles for local breeding opportunities and is not affected by costs associated with dispersal. Raffles themselves are conducted in a hierarchical manner by first conducting a raffle among patches (tickets pooled) to identify the patch on which the winner lives, then conducting a raffle among members of the winning patch in order to identify the recipient of the prize. To simulate Offspring Control, one additional level in the hierarchy is considered, namely a raffle between parents. Each of the $2MN$ raffles is conducted with replacement of tickets, and so success in one raffle is independent of that in another. Each raffle is also conducted after the current state of the environment has been determined (see Appendix B.1). The winner of a prize copies its genotype or phenotype (depending on the scenario) into the next generation, but some small mutational error was included.

The algorithm itself begins by randomly assigning dispersal phenotypes (or genotypes depending on the model scenario) using a uniform random number generator. Raffling of MN prizes is repeated over a large number of generations. As we have suggested above, exact details depend on the model scenario considered, but all details are provided in the form of Python computer code (Table B.1b).

We found close agreement between predictions made by our numerical procedures, and the average predictions made by independent simulation replicates (Figures B.1 and B.2). Discrepancies between numerical results and average simulation results did appear as numerical

predictions approached extreme values of zero or one. We attributed this discrepancy to mutational bias included in our simulation: genotypes or phenotypes that fell outside the unit interval following mutation were forced to return to the closer endpoint. We also note that the time it took for individual-based simulation to find numerical predictions varied with mutation rate and varied between model scenarios (compare Figures B.1 and B.2).

B.6 Supplementary Figures

Here we provide some figures (Figures B.3 - B.8) as a supplement to figures in the main part.

Bibliography

[1] A. M. M. Rodrigues and A. Gardner. Evolution of helping and harming in heterogeneous populations. *Evolution*, 66:2065–2079, 2012. doi: 10.1111/j.1558.5646.2012.01594.x.

[2] S. M. Ross. *Introduction to probability models*. Academic Press, San Diego, CA, 7th edition, 2000.

[3] P. D. Taylor. An inclusive fitness model for dispersal of offspring. *Journal of Theoretical Biology*, 130:363–378, 1988. doi: 10.1016/S0022-5193(88)80035-3.

[4] P. D. Taylor and S. A. Frank. How to make a kin selection model. *Journal of Theoretical Biology*, 180:27–37, 1996. doi: 10.1006/jtbi.1996.0075.

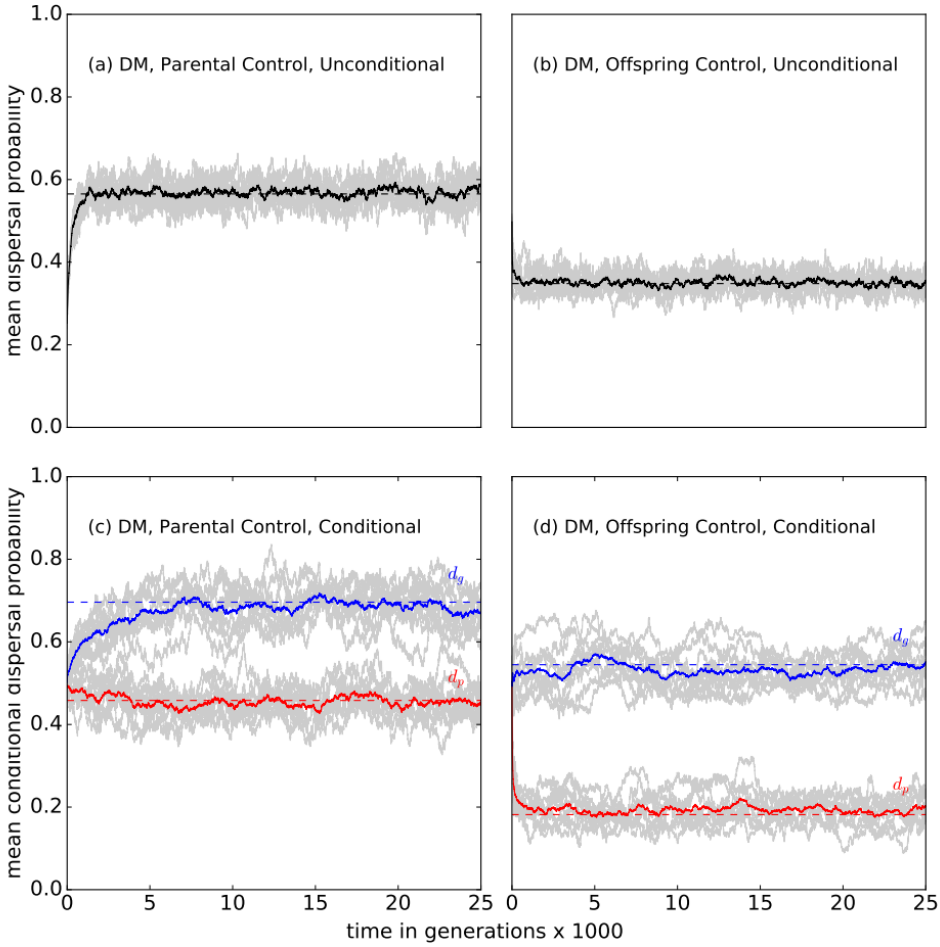

Figure B.1: A comparison of predictions made by iterative numerical determination of equilibrium or equilibrium pairs, and the outcome of individual-based simulation of the DM model life history. Panels (a) and (b) show dispersal rates that are not expressed conditional on the state of the environment (i.e. unconditional), while (c) and (d) show conditional dispersal rates. Panels (a) and (c) show results for the Parental Control model, while (b) and (d) show results for Offspring Control. Numerical predictions for correpsonding equilibrium or equilibrium pairs are presented as horizontal dashed lines. Results for ten replicate simulations are presented as grey lines, and mean-average d, d_p, and d_g values across all replicates are presented as solid black lines, solid red lines, and solid blue lines, respectively. All results assume $N = 2$, $c_p = 0.4$, $c_g = 0.2$, $s = 0.3$, and simulation results assumed the population was comprised of 250 patches. The figure shows that numerical predictions agree with the average prediction made by simulation.

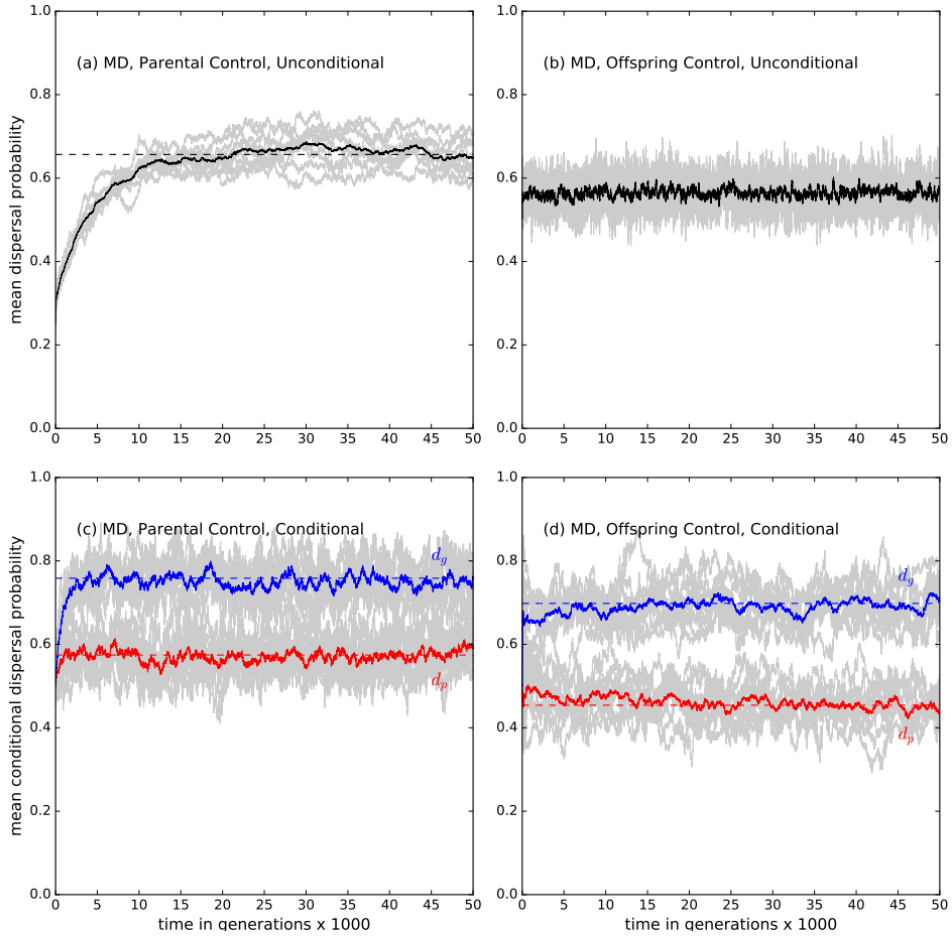

Figure B.2: A comparison of predictions made by iterative numerical determination of equilibrium or equilibrium pairs, and the outcome of individual-based simulation of the MD model life history. Panels (a) and (b) show dispersal rates that are not expressed conditional on the state of the environment (i.e. unconditional), while (c) and (d) show conditional dispersal rates. Panels (a) and (c) show results for the Parental Control model, while (b) and (d) show results for Offspring Control. Numerical predictions for correpsonding equilibrium or equilibrium pairs are presented as horizontal dashed lines. Results for ten replicate simulations are presented as grey lines, and mean-average d, d_p, and d_g values across all replicates are presented as solid black lines, solid red lines, and solid blue lines, respectively. All results assume $N = 2$, $c_p = 0.4$, $c_g = 0.2$, $s = 0.3$, and simulation results assumed the population was comprised of 250 patches. The figure shows that numerical predictions agree with the average prediction made by simulation.

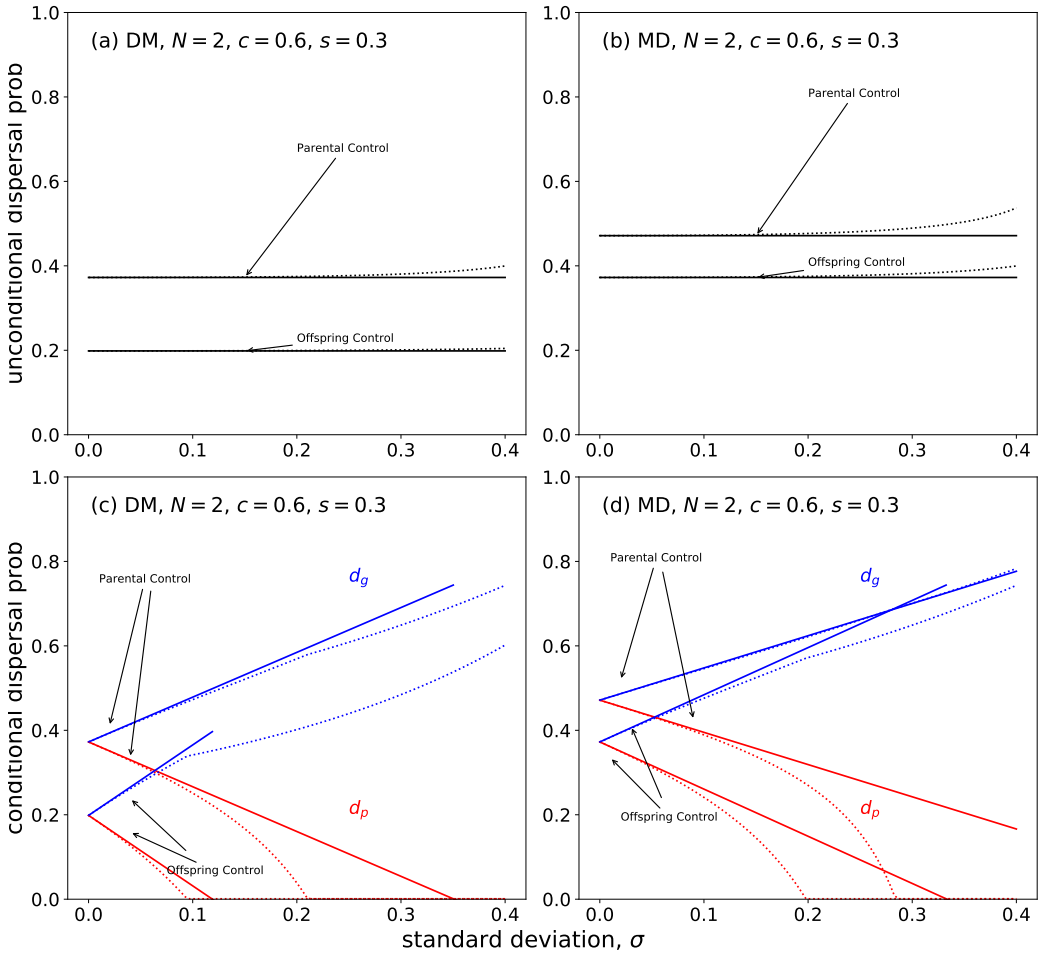

Figure B.3: A comparison of predictions made by iterative numerical determination of equilibrium or equilibrium pairs (dotted lines), and those made by approximations based on small degree of environmental variation (solid lines) (compare to Figure 4.2). Results are presented for the DM and MD models, respectively, with either Parental or Offspring control of dispersal. We assume (a, b) unconditional expression of dispersal, or (c,d) conditional expression of dispersal (red = poor environmental state, blue = good environmental state). As expected, agreement begins to break down as environmental variation, measured by σ, increases. However, numerical predictions and approximations are still close. Approximations are not valid whenever at least one of d_p or d_g takes a boundary value of zero or one.

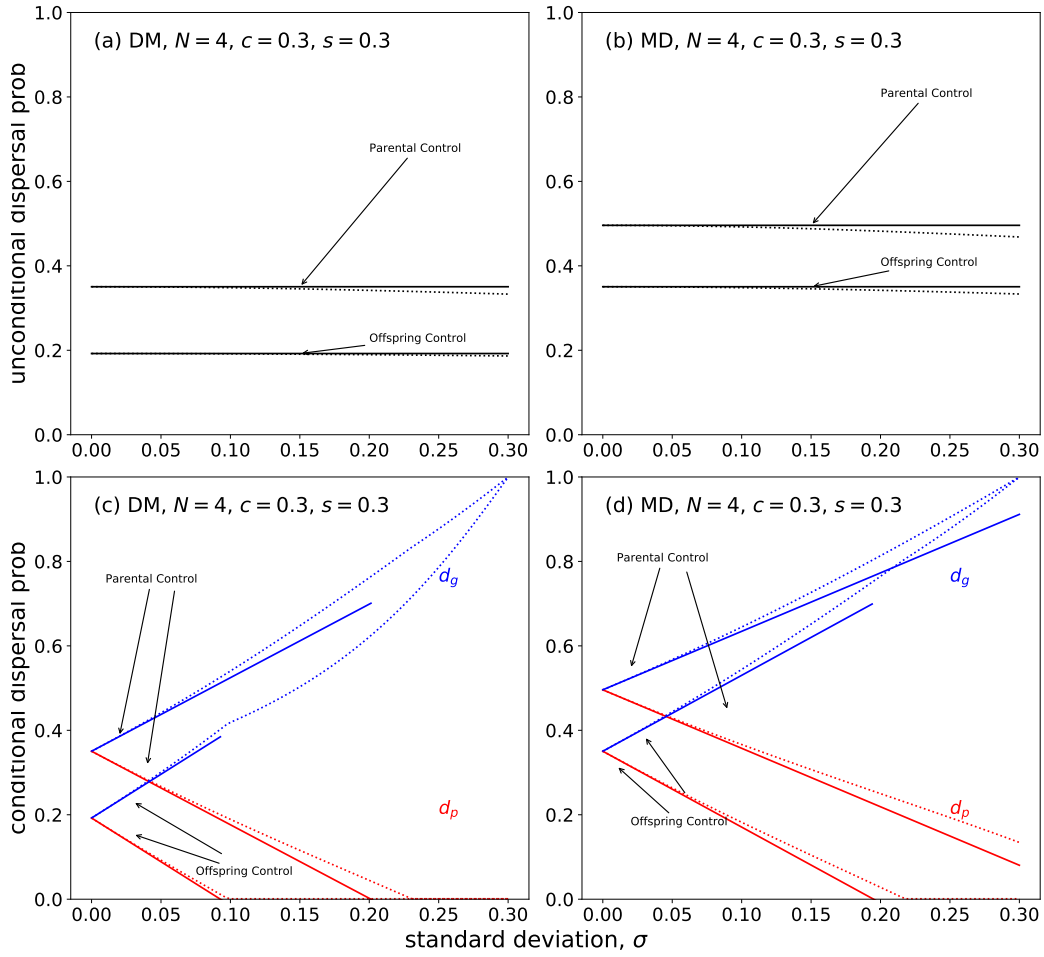

Figure B.4: A comparison of predictions made by iterative numerical determination of equilibrium or equilibrium pairs (dotted lines), and those made by approximations based on small degree of environmental variation (solid lines) (compare to Figure 4.2). Results are presented for the DM and MD models, respectively, with either Parental or Offspring control of dispersal. We assume (a, b) unconditional expression of dispersal, or (c,d) conditional expression of dispersal (red = poor environmental state, blue = good environmental state). As expected, agreement begins to break down as environmental variation, measured by σ, increases. However, numerical predictions and approximations are still close. Approximations are not valid whenever at least one of d_p or d_g takes a boundary value of zero or one.

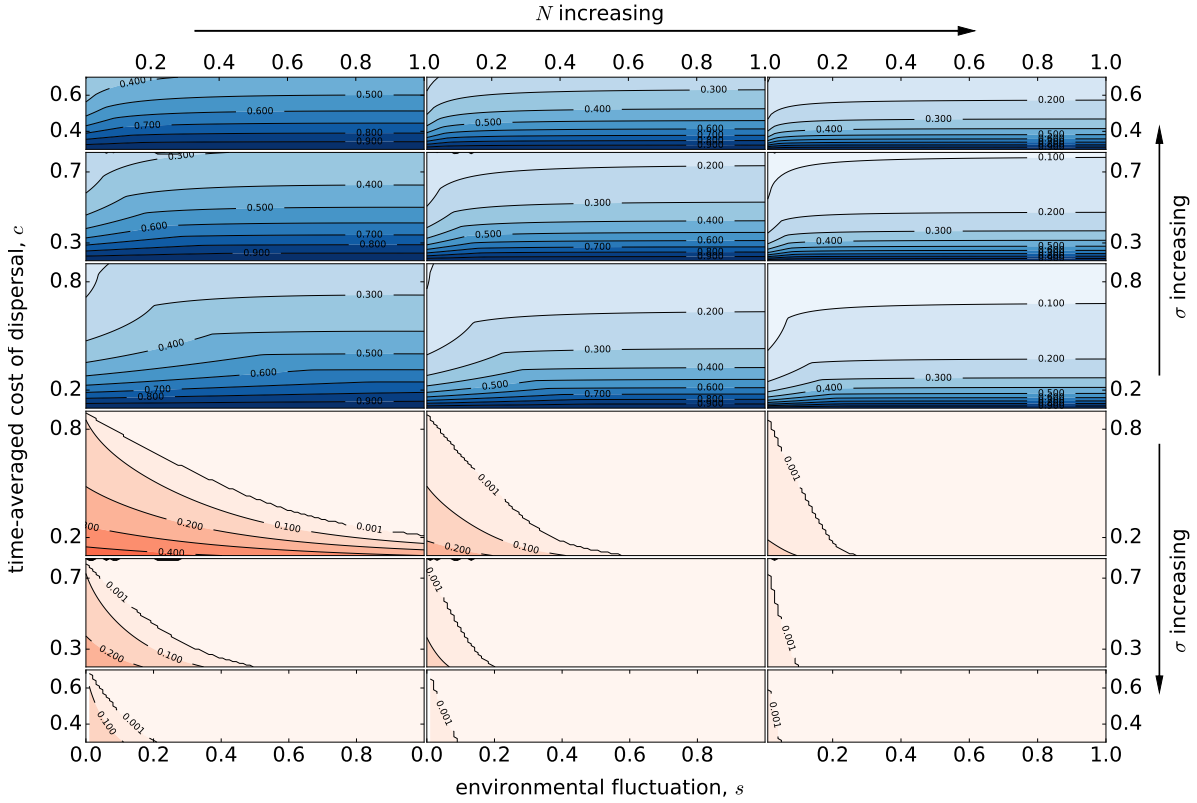

Figure B.5: The relationship between environmental fluctuation, time-averaged cost of dispersal, and the conditional probability of dispersing for the DM Model with Offspring Control of dispersal (compare to Figure 4.3). Contours showing numerical predictions for dispersal when environmental state is good are shown in blue (top three rows), while those for dispersal when environmental state is poor are shown in red (bottom three rows). Results for group size $N = 2, 4, 8$ and for standard deviation in cost $\sigma = 0.1, 0.2, 0.3$ are shown. All else being equal, increased environmental fluctuation is predicted to promote dispersal under good conditions, and philopatry when conditions are poor. Increased time-averaged cost is predicted to reduce conditional dispersal, as is increasing group size. The wavy nature of the contour of height 0.001 is an artefact of the numerical procedure.

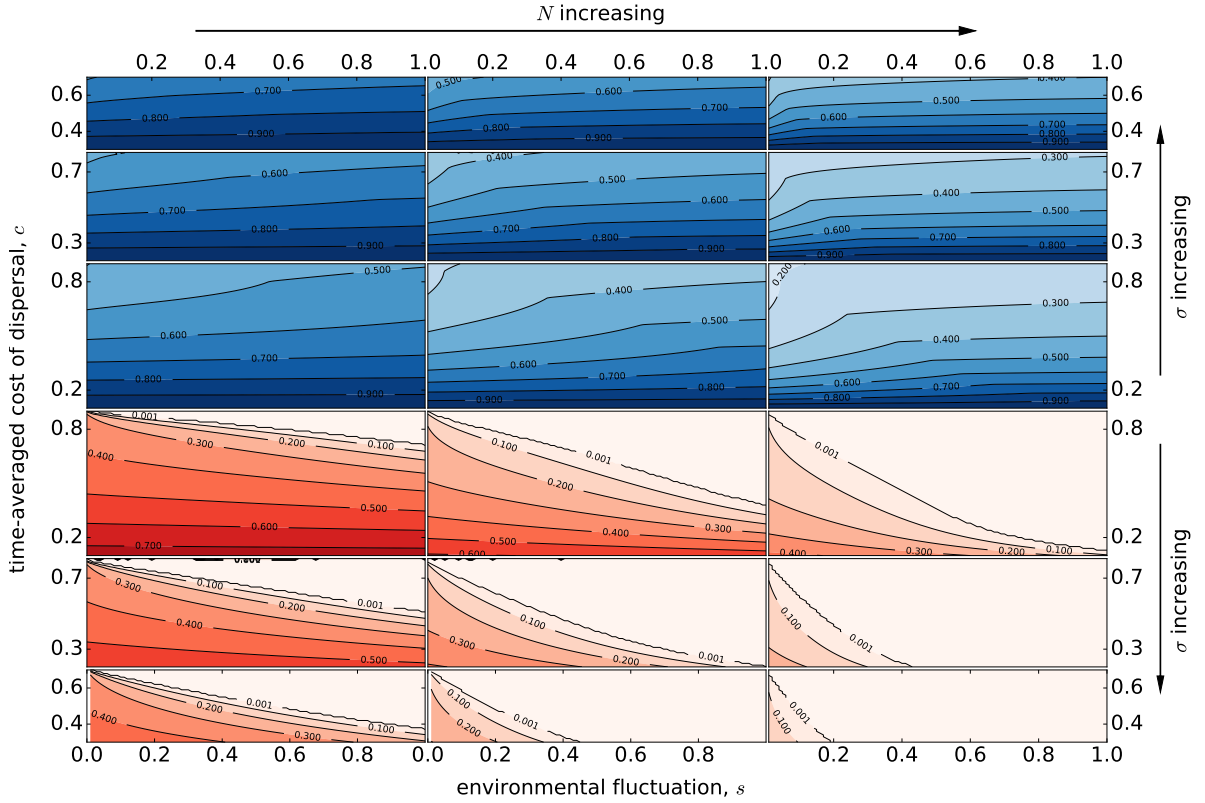

Figure B.6: The relationship between environmental fluctuation, time-averaged cost of dispersal, and the conditional probability of dispersing for the MD Model with Parental Control of dispersal (compare to Figure 4.3). Contours showing numerical predictions for dispersal when environmental state is good are shown in blue (top three rows), while those for dispersal when environmental state is poor are shown in red (bottom three rows). Results for group size $N = 2, 4, 8$ and for standard deviation in cost $\sigma = 0.1, 0.2, 0.3$ are shown. All else being equal, increased environmental fluctuation is predicted to promote dispersal under good conditions, and philopatry when conditions are poor. Increased time-averaged cost is predicted to reduce conditional dispersal, as is increasing group size. The wavy nature of the contour of height 0.001 is an artefact of the numerical procedure.

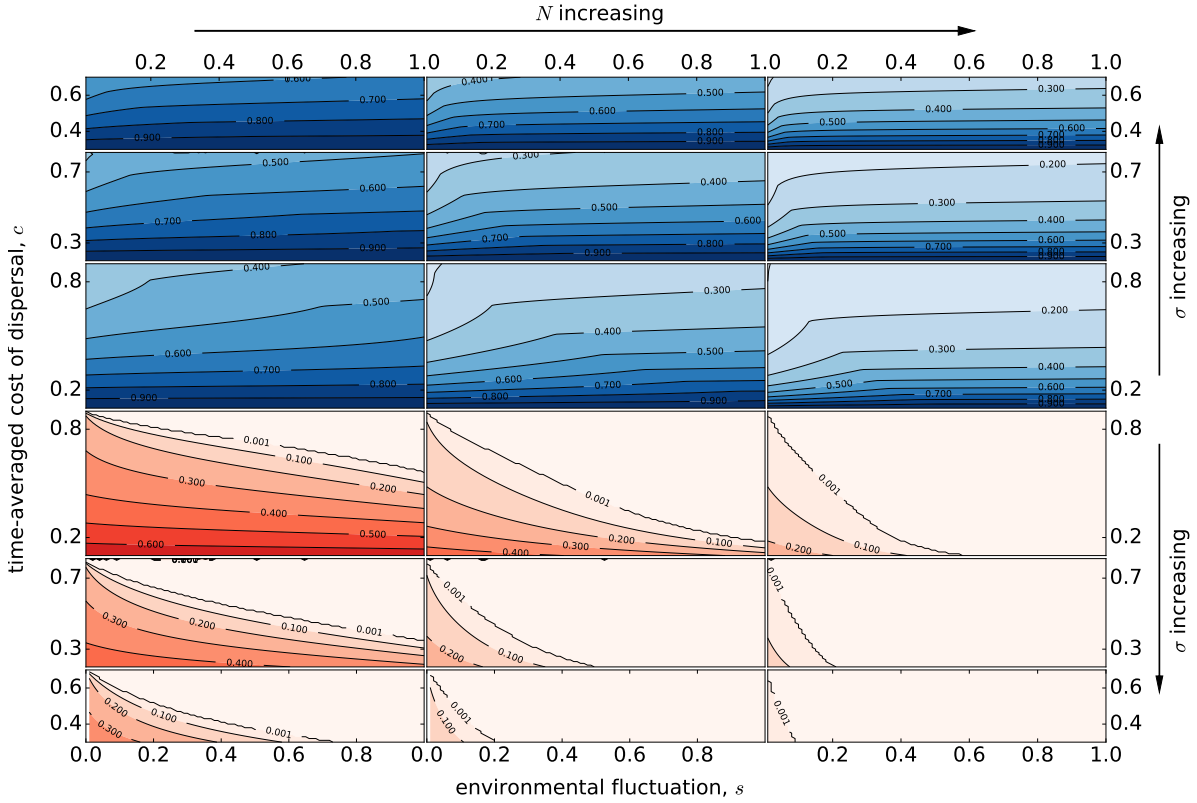

Figure B.7: The relationship between environmental fluctuation, time-averaged cost of dispersal, and the conditional probability of dispersing for the MD Model with Offspring Control of dispersal (compare to Figure 4.3). Contours showing numerical predictions for dispersal when environmental state is good are shown in blue (top three rows), while those for dispersal when environmental state is poor are shown in red (bottom three rows). Results for group size $N = 2, 4, 8$ and for standard deviation in cost $\sigma = 0.1, 0.2, 0.3$ are shown. All else being equal, increased environmental fluctuation is predicted to promote dispersal under good conditions, and philopatry when conditions are poor. Increased time-averaged cost is predicted to reduce conditional dispersal, as is increasing group size. The wavy nature of the contour of height 0.001 is an artefact of the numerical procedure.

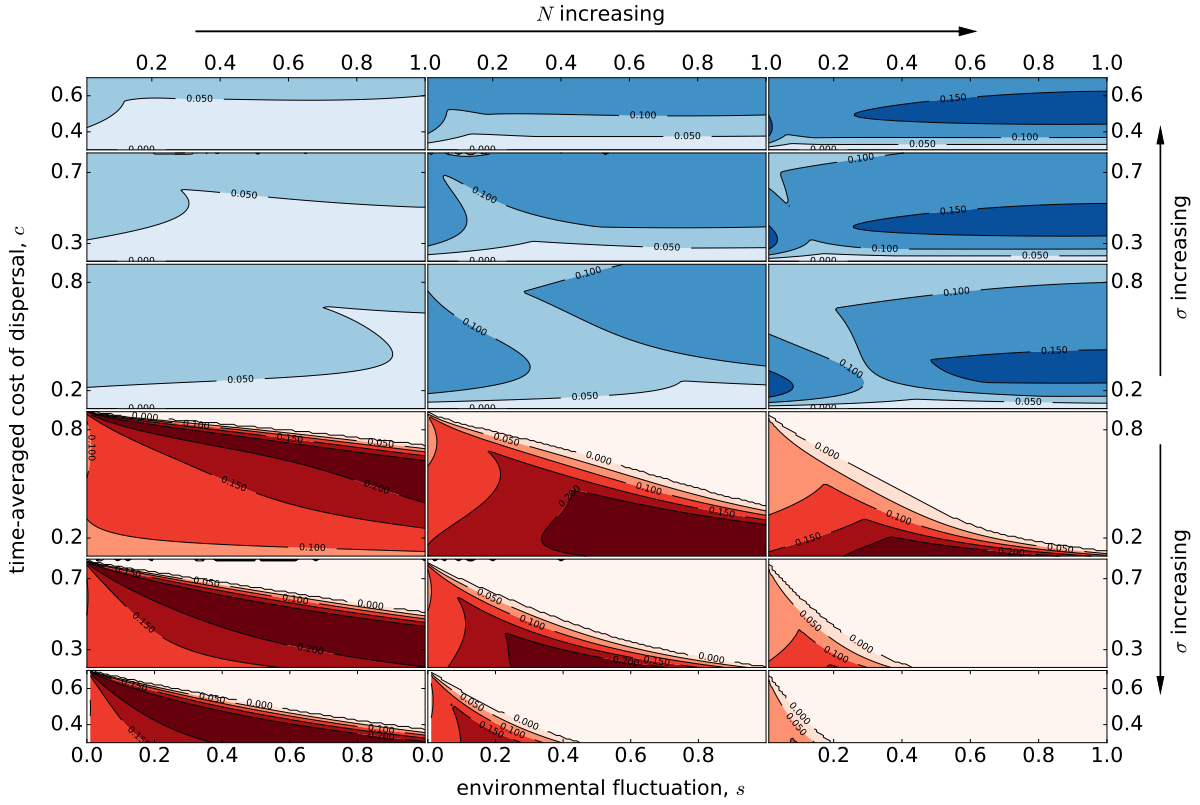

Figure B.8: The relationship between environmental fluctuation, time-averaged cost of dispersal, and the extent of parent-offspring conflict over conditional tendency to disperse for the MD Model (compare to Figure 4.4). Here, the extent of conflict is measured as d_e with Parental Control minus d_e with Offspring Control. Contours showing numerical predictions for dispersal when environmental state is good are shown in blue (top three rows), while those for dispersal when environmental state is poor are shown in red (bottom three rows). Results for group size $N = 2, 4, 8$ and for standard deviation in cost $\sigma = 0.1, 0.2, 0.3$ are shown. The wavy nature of the contour of height 0.000 is an artefact of the numerical procedure.

Appendix C

Code

C.1 Code for Chapter 2

Matlab and c++ are used to generate figures, and figure numbering is within Chapter 2.

C.1.1 myode_dm.m

myode_dm.m

```
% 2017-09-10 the system from "dispersal effect on metapopulation persistence
 ↪  with social structure"
function dydt = myode_dm(t,y,d,m)
dydt = zeros(3,1);
dydt(1) = -m*y(1)+(1+d)*(1-y(1)-y(2)-y(3))*y(3)+2*m*y(2)-(1+d)*y(1)*y(3);
dydt(2) = -y(2)+(3*m+d)*y(3)-2*m*y(2)+(1+d)*y(1)*y(3);
dydt(3) = y(2)-(3*m+d)*y(3);
```

C.1.2 fig2.m

fig2.m

```
clear, clc
d = .55;
mlength = 5000;
m = linspace(0.,0.3,mlength);
Disc = (d+1-2.*(d+3.*m).*m).^2-8.*m.^2.*(d+3.*m).*(d+3.*m+1);
Discp = Disc;


for i = 1:mlength
    if (Disc(i)<0)
        Discp(i) = NaN;
    end
end


zzp = NaN(1,mlength);
zzm = zzp;
```

```
zzp = (d+1-2.*(d+3.*m).*m+sqrt(Discp))./(2.*(d+3.*m+1).*(d+1));
zzm = (d+1-2.*(d+3.*m).*m-sqrt(Disc.*(Disc>0)))./(2.*(d+3.*m+1).*(d+1));
% Here is a benign bug. It's better to use "Discp", instead of
 ↪  "Disc.*(Disc>0)".
% However, this does not change the figure we need.
% ----- by Jingjing Xu

%whos
rg = [-1 2.5 -0.1 1];
plot(d,zzm,':k',Discp,zzp,'-k','LineWidth',3)

% plot(Discp,zzm,':k',Discp,zzp,'-k','LineWidth',3)
hold on
plot(rg(1:2),[0 0],'-k','LineWidth',3)
hold off
axis(rg)

xlabel D
ylabel 'density of state-3 habitats (z)'

x1 = 1.5;
y1 = 0.5;
txt1 = '\downarrow';
text(x1,y1,txt1)
txt1b = 'E_+';
text(x1,y1+0.06,txt1b)



x2 = 0.5;
y2 = 0.13;
txt2 = '\downarrow';
text(x2,y2,txt2)
txt2b = 'E_-';
text(x2,y2+0.06,txt2b)

x2 = -0.5;
y2 = 0.05;
txt2 = '\downarrow';
text(x2,y2,txt2)
txt2b = 'E_0';
text(x2,y2+0.06,txt2b)

xticks(-1:1:2)
yticks(0:0.2:1)
```

C.1.3 fig3.m

fig3.m

```
%% time is a decreasing function of D, which is INDEED what I am expecting.
 ↪  BUT, see file "fig3official.mlx" for an exception.
clear, clc, close all
dvec = 0:0.04:5;
m = .212;
for i = 1:length(dvec)
    d = dvec(i);
    Disc(i) = (d+1-2.*(d+3.*m).*m).^2-8.*m.^2.*(d+3.*m).*(d+3.*m+1);
end
whos
d_tmp=find(Disc<0);
d_max=dvec(d_tmp(1))
%
%Disc
plot(dvec,Disc)
xlabel 'dispersal rate (d)';
ylabel 'discriminant D';
%
tspan = [0 200];
y0 = [0.2 0.0 0.4];
global xx yy zz neighbour flag_0;
neighbour= 1e-6;
correct = NaN(length(dvec),1);
for i=1:length(dvec)
    d = dvec(i);
    if (Disc(i)>0)
        xx = 2*(d+3*m)*m/(1+d);
        zz = (d+1-2*(d+3*m)*m+sqrt(Disc(i)))/(2*(d+3*m+1)*(d+1));
        yy = (d+3*m)*zz;
    end
    %[xx,yy,zz]
    options =
     ↪  odeset('Events',@dmsysEventscorrect,'RelTol',1e-5,'AbsTol',1e-5,...
        'NonNegative',1);%,'OutputFcn',@odeplot,'Stats','on'
    y0 = [xx,yy,zz]*0.99;
    [t,y,te,ye,ie] = ode45(@(t,y) myode_dm(t,y,d,m), tspan, y0,options);
    %y(end,:)
    if (Disc(i)<0)
        correct(i)=NaN;
    else if (te>0)
            correct(i) = te;
        end
    end
end
whos correct

```

```
figure
plot(Disc, correct,'LineWidth',3)

ylabel 'time to recover from 10% perturbation of E_+';
xlabel 'discriminant D';



figure
plot(dvec, correct,'LineWidth',3)

ylabel 'time to recover from 10% perturbation of E_+';
xlabel 'd';


%%
% a single solution using ode45
clear
clc
close all
d=0.4;
m=0.218;
tspan=[0,25];
y0=[0.1,0.2,0.3];
[t,y] = ode45(@(t,y) myode_dm(t,y,d,m), tspan, y0);

% plot (x,y,z)
plot(t,y(:,1))
hold on
plot(t,y(:,2))
plot(t,y(:,3))
hold off
xlabel 't'
title(['plot (x,y,z)'])
% plot x+y+z
figure
plot(t,sum(y,2))
title(['plot x+y+z'])
xlabel 't'

%%
% a single solution using ode15s
clear
clc
close all
d=0.4;
m=0.218;
```

```
tspan=[0,25];
y0=[0.1,0.2,0.3];
[t,y] = ode15s(@(t,y) myode_dm(t,y,d,m), tspan, y0);

% plot (x,y,z)
plot(t,y(:,1))
hold on
plot(t,y(:,2))
plot(t,y(:,3))
hold off
xlabel 't'
title(['plot (x,y,z)'])
% plot x+y+z
figure
plot(t,sum(y,2))
title(['plot x+y+z'])
xlabel 't'

% not seeing an obvious difference using ode45 and ode15s
```

C.1.4 fig4a.m

fig4a.m

```
clear, clc
myfun = @(d,m) (d+1-2.*(d+3.*m).*m).^2-8.*m.^2.*(d+3.*m).*(d+3.*m+1);  % parameterized function

dend = 16;% end of d range
dmax = 200;% maximum of d index
d = NaN(dmax,1);
m = NaN(dmax,1);
for i = 1:dmax
d(i) = (i-1)*dend/dmax+1e-8;                % parameter
fun = @(m) myfun(d(i),m);    % function of m alone
m(i) = fzero(fun,0.2);
end

plot(m,d,'k','LineWidth',2)
hold on
plot([m(end) m(end)],[0,dend],':k','LineWidth',2)
hold off
axis([0 0.3 0 dend-1])
yticks(0:5:15)
xticks([0,0.1,m(end),m(1), 0.3])
xticklabels({0,0.1,'m_1','m_0', 0.3})

xlabel 'mortality rate (m)'
ylabel 'dispersal rate (d)'
```

```
25
26 text(0.10,dend*0.5,'D>0','FontSize',15)
27 text(0.24,dend*0.5,'D<0','FontSize',15)
28
29 ax = gca; % current axes
30 ax.FontSize = 12;
31 %ax.TickDir = 'out';
32 %ax.TickLength = [0.02 0.02];
33 %ax.YLim = [-2 2];
34
35 m(1)
36 m(end)
```

C.1.5 fig4b.m

fig4b.m

```
1  clear, clc
2
3  for i = -2:2
4  d = 10^(i);
5  mlength = 5000;
6  m = linspace(0.,0.3,mlength);
7  Disc = (d+1-2.*(d+3.*m).*m).^2-8.*m.^2.*(d+3.*m).*(d+3.*m+1);
8  mp = m;
9  for i = 1:mlength
10     if (Disc(i)<0)
11         mp(i) = NaN;
12     end
13 end
14 zzp = NaN(1,mlength);
15 zzm = zzp;
16 zzp = (d+1-2.*(d+3.*m).*m+sqrt(Disc.*(Disc>0)))./(2.*(d+3.*m+1).*(d+1));
17 zzm = (d+1-2.*(d+3.*m).*m-sqrt(Disc.*(Disc>0)))./(2.*(d+3.*m+1).*(d+1));
18 % Here, "Disc.*(Disc>0)" is used to plot the figure. This works for our
19 % model because we also plot a vertical line "0" for the extinction
20 % equilibrium. It can be seen as a begign bug, but the figure is still
21 % correct.
22 % ------ Jingjing Xu
23
24 %whos
25
26 rg = [0.01 0.3 1e-8 1];
27 semilogy(mp,zzm,':k',mp,zzp,'-k','LineWidth',2)
28 hold on
29 plot(rg(1:2),[0 0],'-k','LineWidth',2)
30 axis(rg)
31 xlabel D
32 ylabel 'density of state-3 habitats (z)'
```

```
yticks(10.^[-8:0])
%xticks(0:0.05:0.3)
end
hold off

txt1 = 'd = 0.01';
text(0.23,4*1e-1,txt1)
text(0.23,1.6*1e-1,'d = 0.1')

text(0.2083,0.6*1e-1,'d = 1')

text(0.2083,1.5e-2,'d = 10')

text(0.2082,1.5e-3,'d = 100')

ax = gca; % current axes
ax.FontSize = 12;
xticks([0,0.1,0.2082,0.2275, 0.3])
xticklabels({0,0.1,'m_1','m_0', 0.3})
hold on
plot([0.2082,0.2082],rg(3:4),':k')
hold off
```

C.1.6 fig5.m

fig5.m

```
% This file shows how to generate figure 5.
%------------------------------------------------------------------------



clear, clc
% choose a pair of (d,m) with m<m_0
m = 0.212;
d = 2;
% Discriminant should be positive
Disc = (d+1-2.*(d+3.*m).*m).^2-8.*m.^2.*(d+3.*m).*(d+3.*m+1)
% positive stable equilibrium E_+ = (px,py,pz)
px = 2*(d+3*m)*m/(1+d);
pz = (d+1-2*(d+3*m)*m+sqrt(Disc))/(2*(d+3*m+1)*(d+1));
py = (d+3*m)*pz;
E_p=[px, py, pz]
% positive unstable equilibrium E_- = (ux,uy,uz)
ux = 2*(d+3*m)*m/(1+d);
uz = (d+1-2*(d+3*m)*m-sqrt(Disc))/(2*(d+3*m+1)*(d+1));
uy = (d+3*m)*uz;
E_m=[ux, uy, uz]
% %% plot the two positive equilibria and the extinction equilibrium (0,0,0)
% figure
```

```
% axis([0 1 0 1 0 1])
% xlabel x
% ylabel y
% zlabel z
% box on
% hold on
% plot3(ux,uy,uz,'.k','markers',19)
% plot3(px,py,pz,'.r','markers',19)
% plot3(0,0,0,'.r','markers',19)
% view([-130,25])
% axis square
% hold off

% grid of points in the cube [0,1]^3
pts = 81;
x = linspace(0,1,pts);
y = x;
z = x;
[X,Y,Z] = meshgrid(x,y,z);

% matrices to show if a point converges to one of the two possible
 ↪  equilibria.
flag_e0 = NaN(pts,pts,pts);
flag_ep = flag_e0;

options = odeset('Events',@dmsysEventscorrect,'RelTol',1e-4,...
    'AbsTol',1e-4,'NonNegative',1);
tspan = [0,100];

tic
% inside the region {(x,y,z)| x>0,y>0,z>0,x+y+z<1}, scan through all possible
 ↪  points.
for iz = 1:pts
    for iy = 1:max(pts-iz-1,1)
        for ix = 1:max(pts-iz-iy,1)
            % y0 is the initial point in each simulation
            y0 = [X(ix,iy,iz),Y(ix,iy,iz),Z(ix,iy,iz)];
            if (sum(y0)<1.01) % make sure x+y+z<1.
                [t,y] = ode45(@(t,y) myode_dm(t,y,d,m), tspan, y0, options);
                % simulated equilibrium (psudo);
                sx = y(end,1);
                sy = y(end,2);
                sz = y(end,3);
                if (sx^2+sy^2+sz^2<1e-4) % y0 converges to (0,0,0)
                    flag_e0(ix,iy,iz) = 1;
                elseif ((sx-px)^2+(sy-py)^2+(sz-pz)^2<1e-4) % y0 converges to
                 ↪  E_+
```

```
                    flag_ep(ix,iy,iz) = 1;
                    break; % stop iterations once having one point converging
                     ↪  to E_+
                end
            end
        end
    end
end
toc

%%

bd_ep = NaN(pts,pts,pts);
for iz = 1:pts
    for iy = 1:max(pts-iz-1,1)
        for ix = 2:max(pts-iz-iy,1)
            if (flag_ep(ix-1,iy,iz)~=1)&&(flag_ep(ix,iy,iz)>0)
                %ix,iy,iz
                bd_ep(ix,iy,iz)=1;
                break;
            end
        end
    end
end

% move the boundary back to (0,0,0) by a fraction of the stepsize 1/(pts-1)
dev = 1;
Xpb = X.*bd_ep-1/(pts-1)*dev;
Ypb = Y.*bd_ep-1/(pts-1)*dev;
Zpb = Z.*bd_ep-1/(pts-1)*dev;



%% plotting
figure
axis([0 1 0 1 0 1])
xlabel x
ylabel y
zlabel z

hold on
axis square
box on
view([-130,25])

% plot the boundary of basins of attraction for E_0 and E_+
plot3(Xpb(:),Ypb(:),Zpb(:),'.b','markers',5)
```

```
% plot three equilibria
plot3(ux,uy,uz,'.b','markers',25)
plot3(px,py,pz,'.r','markers',25)
plot3(0,0,0,'.k','markers',25)

% shaded region is {(x,y,z)| x>0,y>0,z>0,x+y+z<1}
p=patch([1 0 0 ], [0 1 0 ], [0 0 0 ]);
p.FaceAlpha=0.2;
plot3([0 0],[1 0],[0 1],'-k')
plot3([1 0],[0 0],[0 1],'-k')
color=0.2;
p=fill3([0 0 1 ], [0 0 0 ], [1 0 0 ],[color,color,color]) ;
p.FaceAlpha=0.2;
hold off

% Note: the point E_- is not on the surface visually, which is because of the
 ↪  meshgrid is not fine enough.
% We choose the mesh size to be 80, so that we can give the reader a sense of
 ↪  the relative position of
% the boundary and the equilibria. A more accurate demonstration will take
 ↪  longer CPU time.
```

C.1.7 figure 6

Use c++ to obtain the figures.

ode0913.h

ode0913.h

```
struct myode_params
  {
    double d,m;
  };

int
func (double t, const double yvec[], double f[],
      void *params)
{
  (void)(t); /* avoid unused parameter warning */
  struct myode_params *p
    = (struct myode_params *) params;
  double m = p->m;
  double d = p->d;



  double x, y, z;
  x=yvec[0];
```

```
  y=yvec[1];
  z=yvec[2];


   f[0] = - x*m + (1.0+d) * (1.0-x-y-z)*z+2.0*m*y-(1.0+d)*x*z;
   f[1] = - y + (3.0*m+d) * z-2.0*m*y+(1.0+d)*x*z;
   f[2] = + y - (3.0*m+d) * z;
  return GSL_SUCCESS;
}

int
jac (double t, const double yvec[], double *dfdy,
     double dfdt[], void *params)
{
  (void)(t); /* avoid unused parameter warning */
  struct myode_params *p
    = (struct myode_params *) params;
  double m = p->m;
  double d = p->d;



  double x, y, z;
  x=yvec[0];
  y=yvec[1];
  z=yvec[2];


  gsl_matrix_view dfdy_mat
    = gsl_matrix_view_array (dfdy, 3, 3);
  gsl_matrix * ma = &dfdy_mat.matrix;
  gsl_matrix_set (ma, 0, 0, (-2.0*d-2.0)*z-m);
  gsl_matrix_set (ma, 0, 1, (-d-1.0)*z+2.0*m);
  gsl_matrix_set (ma, 0, 2, -(2.0*x+y+2.0*z-1.0)*(1.0+d));
  gsl_matrix_set (ma, 1, 0, (1.0+d)*z);
  gsl_matrix_set (ma, 1, 1, -1.0-2.0*m);
  gsl_matrix_set (ma, 1, 2, 3.0*m+d+(1.0+d)*x);
  gsl_matrix_set (ma, 2, 0, 0.0);
  gsl_matrix_set (ma, 2, 1, 1.0);
  gsl_matrix_set (ma, 2, 2, -3.0*m-d);
  dfdt[0] = 0.0;
  dfdt[1] = 0.0;
  dfdt[2] = 0.0;
  return GSL_SUCCESS;
}
```

fig6a.cpp

fig6a.cpp

```
// This file obtains the volume size for the basin of the non_trivial equilibrium // based on file "BV0912.cpp"
//   ||-----------------------||
//      g++ fig6a.cpp -lgsl
//   ||-----------------------||

// 2017-09-14

#include <stdio.h>
#include <gsl/gsl_matrix.h>
#include <gsl/gsl_math.h>
#include <gsl/gsl_eigen.h>
#include <gsl/gsl_rng.h>
#include <math.h>
#include <time.h>

#include <gsl/gsl_errno.h>
#include <gsl/gsl_odeiv2.h>

#include <iostream>  // std::cout, std::fixed
#include <iomanip>   // std::setprecision
using namespace std;


#include "ode0913.h"


//#include <cmath>  //abs// Global variable declaration:

/* int if_nontriv(double xin, double yin, double zin, void *params)
{

return yes;
}

*/

int main (void)
{
srand(time(NULL));
clock_t tStart = clock();

// pre-initializing a, b, c

double m, d;

```

```
46
47 // define gsl_rng_alloc
48 const gsl_rng_type * T;
49 gsl_rng * r;
50 gsl_rng_env_setup();
51 T = gsl_rng_default;
52 r = gsl_rng_alloc (T);
53
54 printf("#     d      m        Delta  BofA_E_+  BofA_E_0  total\n");
55
56 double eps, tol;
57 int sample;
58
59 double epsabs, epsrel;
60 for (int ieps = 1; ieps < 2; ieps++) {
61 for (int isam = 5; isam < 6; isam++) {
62
63
64 //double mvec[4]={0.117, 0.207, 0.212, 0.217};
65
66 double mend = 0.25;
67 int mgrid = 40;
68
69 for (int im = 0; im < mgrid+1; im++) {
70
71          m = im * mend/mgrid +1e-8; //im from 0 to 40;
72
73         printf("%.3f\n",m);
74
75         double dend = 20;
76         int dgrid = 40;
77         for (int id = 0; id < dgrid+1; id++) {
78
79         //d = id * 1 + 1e-8;
80          d = id * dend/dgrid +1e-8; //id from 0 to 40;
81
82
83
84         eps = pow(10,-(ieps+5))/1.0;//1e-6
85         tol = 1e-4;//1e-3
86
87         sample = 1.0*pow(10,isam-3);
88         //define eqn (xx, yy, zz);
89         double xx, yy, zz;
90         double Disc; //discriminant
91         Disc =
           ↪  pow((d+1.0-2.0*(d+3.0*m)*m),2)-8.0*m*m*(d+3.0*m)*(d+3.0*m+1.0);
```

```
92
93          if (Disc<0)
94          {       printf(" %6.2f  %.3f  %+.4e  %.6f  ",
95          d, m, Disc, 0.0);
96          printf("\n");}
97          else
98          {
99
100
101         //printf("D = %.5f\n",Disc);
102         // construct parameter
103         struct myode_params params = {d, m};
104         // calculate Equilibrium (xx, yy, zz)
105         xx = 2.0*(d+m*3.0)*m/(1.0+d);
106         zz =
             ↪  (d+1.0-2.0*(d+3.0*m)*m+pow(Disc,0.5))/(2.0*(d+3.0*m+1.0)*(d+1.0));
107         yy = (d+m*3.0)*zz;
108
109         //printf("%.5f %.5f %.5f \n",xx,yy,zz);
110         //end calculate Equ
111         int vol_total = 0;// total number in domain
112         int vol_E_p = 0;// number of initial conditions converging to (x, y,
             ↪  z);
113         int vol_E_0 = 0;// number of initial conditions converging to (0, 0,
             ↪  0);
114
115         // to obtain simulated number of vol_** hits:
116         for (int i = 0; i < 60000;i++) // sampling initial conditions
117
118
119                 { // initializing x_initial, y_initial, z_initial
120                 double xin = gsl_rng_uniform (r);
121                 double yin = gsl_rng_uniform (r);
122                 double zin = gsl_rng_uniform (r);
123 /*                 xin = 0.45;
124                 yin = 0.03;
125                 zin = 0.5;
126
127          */
128         //printf(" i_sample = %d, sum_xinyinzin = %.5f\n", i,xin+yin+zin);
129
130                 if ( xin+yin+zin < 1.0 ) // count number in domain
131                         {
132                         ++vol_total;// l
133
134                         gsl_odeiv2_system sys = {func, jac, 3, &params};
135                         double hstart = 1e-5;// !!!! CAN NOT BE ZERO!!!!
```

```
136                         epsabs = 1e-8;//1e-8;
137                         epsrel = 1e-5;//1e-5;
138 
139                         //printf("epsabs = %.2e\n",epsabs);
140 
141                         gsl_odeiv2_driver * driver =
                             ↪  gsl_odeiv2_driver_alloc_y_new (&sys,
                             ↪  gsl_odeiv2_step_rkf45, hstart, epsabs, epsrel);
142                         // gsl_odeiv2_driver * gsl_odeiv2_driver_alloc_y_new
                             ↪  (const gsl_odeiv2_system * sys, const
                             ↪  gsl_odeiv2_step_type * T, const double hstart,
                             ↪  const double epsabs, const double epsrel)
143                         /* These functions return a pointer to a newly
                             ↪  allocated instance of a driver object.
144                         The functions automatically allocate and initialise
    ↪  the evolve, control and stepper objects for ODE system sys using stepper
    ↪  type T. The initial step size is given in hstart.
145                         hstart, epsabs, epsrel=relative error*/
146                         int ii = 1;
147                         double t = 0.0, t1 = 100.0;
148                         // INITIALIZE ODE   !!!!!! get rid of reused "y"s
149                         double y[3] = { xin, yin, zin};
150 
151                         // initializing difference between two points before
                             ↪  and after one iteration
152                         double diff = 1.0;
153                         // defining previous point
154                         double ypre[3];
155 
156                         while(diff > eps) // while loop to find the
                             ↪  convergence point of (xin, yin, zin)
157                                 { // save the previous point
158                                 ypre[0] = y[0];
159                                 ypre[1] = y[1];
160                                 ypre[2] = y[2];
161                                 //printf (" %.5f %.5f %.5f\n", ypre[0],
                                     ↪  ypre[1], ypre[2]);
162 
163                                 //    d
164                                 double ti = ii * t1 / 100.0;
                                     ↪  //??????????????????????????
165                                 int status = gsl_odeiv2_driver_apply (driver,
                                     ↪  &t, ti, y);
166                                 if (status != GSL_SUCCESS)
167                                         {
168                                           printf ("error, return value=%d\n",
                                             ↪  status);
```

```
169                                         break;
170                                       }
171                                 diff = pow(pow(ypre[0] -
                                     ↪  y[0],2.0)+pow(ypre[1] - y[1],
                                     ↪  2.0)+pow(ypre[2] - y[2], 2.0), 1.0/2.0);
172                                 // print the results
173                                 /* if (ii%1==0)
174                                 {
175                                 ////printf ("     %.1f %.5f %.5f %.5f
    ↪  %.5e\n", t, y[0], y[1], y[2], diff);
176                                 } */
177                                 ii++;
178                                 }
179
180                           gsl_odeiv2_driver_free (driver);
181
182                           int yes = -1;
183
184                           if (pow((pow(y[0] , 2) + pow(y[1] , 2) +  pow(y[2] ,
                               ↪  2) ), 0.5) < tol)
185                                 {yes = 0;}// trivial flag
186                           else if(Disc>0)
187                                 {
188                                 //// printf ("--\nEQM %.5f %.5f %.5f\n",  xx,
                                     ↪  yy, zz);
189
190                                 if (pow((pow(y[0] -xx, 2) + pow(y[1] -yy, 2)
                                     ↪  +  pow(y[2] -zz, 2) ), 0.5) < tol)
191                                 yes = 1; // non_trivial count
192                                 }
193                           //cout<<"yes = "<<yes<<endl;
194 /*                           cout<<"tol =
    ↪  "<<tol<<endl;
195                           cout<<"eps = "<<eps<<endl;         */
196
197                           ////cout<<"###############  yes =
                               ↪  "<<yes<<endl;
198
199
200                           int yeah = yes;//if_nontriv(xin, yin, zin, &params);
201                           if (yeah == 1)
202                                 {vol_E_p++;}
203                           else if (yeah == 0)
204                                 {vol_E_0++;}
205                           }//end if
206                     }// end for i
207           // finished counting number of vol_** hits
```

```
208
209         //---//printf("# vols: vol_total = %.2d, vol_E_p = %.2d, vol_E_0 =
              %.2d \n",vol_total,vol_E_p,vol_E_0);
210
211
212         double prob_E_p = (double)vol_E_p/(double)vol_total;
213         double prob_E_0 = (double)vol_E_0/(double)vol_total;
214
215         printf(" %6.2f  %.3f  %+.4e  %.6f  %.6f  %.5f  ",
216         d, m, Disc, prob_E_p, prob_E_0, prob_E_p+prob_E_0);
217         printf("\n");
218
219         //printf("-----------------------------\n");
220         }
221         }
222
223 printf("#     d      m        Delta  BofA_E_+  BofA_E_0  total\n");
224
225 //printf("# eps = %.2e\n",eps);
226 printf("\n\n");
227 }
228 printf("# neighbour = %.2e\n",tol);
229 printf("# epsrel = %.2e\n",epsrel);
230 printf("# epsabs = %.2e\n",epsabs);
231 printf("# sample = %d\n",sample);
232 }
233 }
234
235
236 gsl_rng_free (r);
237 printf("Time taken: %.2fs\n", (double)(clock() - tStart)/CLOCKS_PER_SEC);
238
239 //(void) x;
240 //(void) z;
241 return 0;
242 }
```

fig6a_plot.p

fig6a_plot.p

```
1 #// 2017-09-14
2
3 # size 500,500
4 #set termial png enhanced color font 'Arial,25' dashed
5
6 set term postscript png enhanced color font 'Arial,25' dashed
7
8 set output "fig6a.png"
```

```
set ylabel "dispersal rate (d)"
set xlabel "mortality rate (m)"
set xrange [0:0.25]
set xtics 0.05

set yrange [0.0: 20]
set ytics 5

#set key out vert
set key off #out vert
#set key center right

#set label 1 at  10,0.08
#set label 1 "D>0"
#set label 2 at 0.2, 10
#set label 2 "D<0"



#set palette defined (1 0 0 1,  4 1 0 0)# red and blue
set palette rgbformula 33,13,10#30,31,32#3,11,6
# see http://gnuplot.sourceforge.net/docs_4.2/node216.html
# 33,13,10 ... rainbow (blue-green-yellow-red)
set cbrange [0.8:1]
set cblabel "Fraction of Volume of BofA for E_+"
set cbtics 0.2
#unset cbtics

plot 'fig6a_md40by40.dat' using 2:1:4 with image


#

unset xrange
unset yrange
unset tmargin
unset bmargin
unset rmargin
unset title
unset size
unset xtics
unset label
reset
```

fig6b.cpp

fig6b.cpp

```
// This file obtains the volume size for the basin of the non_trivial equilibrium // based on file "BV0912.cpp"
//   ||----------------------||
//      g++ fig6b.cpp -lgsl
//   ||----------------------||

// 2017-09-14

#include <stdio.h>
#include <gsl/gsl_matrix.h>
#include <gsl/gsl_math.h>
#include <gsl/gsl_eigen.h>
#include <gsl/gsl_rng.h>
#include <math.h>
#include <time.h>

#include <gsl/gsl_errno.h>
#include <gsl/gsl_odeiv2.h>

#include <iostream>  // std::cout, std::fixed
#include <iomanip>   // std::setprecision
using namespace std;


#include "ode0913.h"


//#include <cmath>  //abs// Global variable declaration:

/* int if_nontriv(double xin, double yin, double zin, void *params)
{

return yes;
}

*/

int main (void)
{
srand(time(NULL));
clock_t tStart = clock();

// pre-initializing a, b, c

double m, d;

```

```
46
47 // define gsl_rng_alloc
48 const gsl_rng_type * T;
49 gsl_rng * r;
50 gsl_rng_env_setup();
51 T = gsl_rng_default;
52 r = gsl_rng_alloc (T);
53
54 printf("#     d      m        Delta  BofA_E_+  BofA_E_0  total\n");
55
56 double eps, tol;
57 int sample;
58
59 double epsabs, epsrel;
60 for (int ieps = 1; ieps < 2; ieps++) {
61 for (int isam = 5; isam < 6; isam++) {
62
63
64 double mvec[4]={0.177, 0.207, 0.212, 0.217};
65
66 for (int im = 0; im < 4; im++) {
67
68         m = mvec[im];
69
70         printf("%.3f\n",m);
71
72         for (int id = 0; id < 26; id++) {
73
74         /*
75         m = 0.177;
76         d = 1.0;
77          */
78
79         d = id * 1 + 1e-8;
80
81
82
83
84         eps = pow(10,-(ieps+5))/1.0;//1e-6
85         tol = eps*10.0;//1e-3
86
87         sample = 1.0*pow(10,isam);
88         //define eqn (xx, yy, zz);
89         double xx, yy, zz;
90         double Disc; //discriminant
91         Disc =
            ↪  pow((d+1.0-2.0*(d+3.0*m)*m),2)-8.0*m*m*(d+3.0*m)*(d+3.0*m+1.0);
```

```
92          //printf("D = %.5f\n",Disc);
93          // construct parameter
94          struct myode_params params = {d, m};
95          // calculate Equilibrium (xx, yy, zz)
96          xx = 2.0*(d+m*3.0)*m/(1.0+d);
97          zz =
             ↪  (d+1.0-2.0*(d+3.0*m)*m+pow(Disc,0.5))/(2.0*(d+3.0*m+1.0)*(d+1.0));
98          yy = (d+m*3.0)*zz;
99
100         //printf("%.5f %.5f %.5f \n",xx,yy,zz);
101         //end calculate Equ
102         int vol_total = 0;// total number in domain
103         int vol_E_p = 0;// number of initial conditions converging to (x, y,
             ↪  z);
104         int vol_E_0 = 0;// number of initial conditions converging to (0, 0,
             ↪  0);
105
106         // to obtain simulated number of vol_** hits:
107         for (int i = 0; i < sample;i++) // sampling initial conditions
108
109
110                 { // initializing x_initial, y_initial, z_initial
111                 double xin = gsl_rng_uniform (r);
112                 double yin = gsl_rng_uniform (r);
113                 double zin = gsl_rng_uniform (r);
114
115 /*          xin = 0.33;
116         yin = 0.23;
117         zin = 0.13; */
118
119
120         //printf(" i_sample = %d, sum_xinyinzin = %.5f\n", i,xin+yin+zin);
121
122                 if ( xin+yin+zin < 1.0 ) // count number in domain
123                         {
124                         ++vol_total;// 1
125
126                         gsl_odeiv2_system sys = {func, jac, 3, &params};
127                         double hstart = 1e-5;// !!!! CAN NOT BE ZERO!!!!
128                         epsabs = 1e-8;//1e-8;
129                         epsrel = 1e-5;//1e-5;
130
131                         //printf("epsabs = %.2e\n",epsabs);
132
133                         gsl_odeiv2_driver * driver =
                          ↪  gsl_odeiv2_driver_alloc_y_new (&sys,
                          ↪  gsl_odeiv2_step_rkf45, hstart, epsabs, epsrel);
```

```
134                         // gsl_odeiv2_driver * gsl_odeiv2_driver_alloc_y_new
                             ↪  (const gsl_odeiv2_system * sys, const
                             ↪  gsl_odeiv2_step_type * T, const double hstart,
                             ↪  const double epsabs, const double epsrel)
135                         /* These functions return a pointer to a newly
                             ↪  allocated instance of a driver object.
136                         The functions automatically allocate and initialise
    ↪  the evolve, control and stepper objects for ODE system sys using stepper
    ↪  type T. The initial step size is given in hstart.
137                         hstart, epsabs, epsrel=relative error*/
138                         int ii = 1;
139                         double t = 0.0, t1 = 500.0;
140                         // INITIALIZE ODE   !!!!!! get rid of reused "y"s
141                         double y[3] = { xin, yin, zin};
142
143                         //printf("xin = %.2f, yin = %.2f zin = %.2f \n", xin,
                             ↪  yin, zin);//*/
144
145                         // initializing difference between two points before
                             ↪  and after one iteration
146                         double diff = 1.0;
147                         // defining previous point
148                         double ypre[3];
149
150                         while(diff > eps) // while loop to find the
                             ↪  convergence point of (xin, yin, zin)
151                                 { // save the previous point
152                                 ypre[0] = y[0];
153                                 ypre[1] = y[1];
154                                 ypre[2] = y[2];
155                                 //printf (" %.5f %.5f %.5f\n", ypre[0],
                                     ↪  ypre[1], ypre[2]);
156
157                                 //    d
158                                 double ti = ii * t1 / 100.0;
                                     ↪  //??????????????????????????
159                                 int status = gsl_odeiv2_driver_apply (driver,
                                     ↪  &t, ti, y);
160                                 if (status != GSL_SUCCESS)
161                                         {
162                                           printf ("error, return value=%d\n",
                                               ↪  status);
163                                           break;
164                                         }
165                                 diff = pow(pow(ypre[0] -
                                     ↪  y[0],2.0)+pow(ypre[1] - y[1],
                                     ↪  2.0)+pow(ypre[2] - y[2], 2.0), 1.0/2.0);
```

```
166                                 // print the results
167                                 /* if (ii%1==0)
168                                 {
169                                 ////printf ("     %.1f %.5f %.5f %.5f
    ↪  %.5e\n", t, y[0], y[1], y[2], diff);
170                                 } */
171                                 ii++;
172                                 }
173
174                         gsl_odeiv2_driver_free (driver);
175
176                         int yes = -1;
177
178                         if (pow((pow(y[0] , 2) + pow(y[1] , 2) +  pow(y[2] ,
                             ↪  2) ), 0.5) < tol)
179                                 {yes = 0;}// trivial flag
180                         else if(Disc>0)
181                                 {
182                                 //// printf ("--\nEQM %.5f %.5f %.5f\n",  xx,
                                     ↪  yy, zz);
183
184                                 if (pow((pow(y[0] -xx, 2) + pow(y[1] -yy, 2)
                                     ↪  +  pow(y[2] -zz, 2) ), 0.5) < tol)
185                                 yes = 1; // non_trivial count
186                                 }
187                         //cout<<"yes = "<<yes<<endl;
188 /*                          cout<<"tol =
    ↪  "<<tol<<endl;
189                         cout<<"eps = "<<eps<<endl;         */
190
191                         ////cout<<"###############  yes =
                             ↪  "<<yes<<endl;
192
193
194                         int yeah = yes;//if_nontriv(xin, yin, zin, &params);
195                         if (yeah == 1)
196                                 {vol_E_p++;}
197                         else if (yeah == 0)
198                                 {vol_E_0++;}
199                         }//end if
200                 }// end for i
201         // finished counting number of vol_** hits
202
203         //---//printf("# vols: vol_total = %.2d, vol_E_p = %.2d, vol_E_0 =
             ↪  %.2d \n",vol_total,vol_E_p,vol_E_0);
204
205
```

```
206         double prob_E_p = (double)vol_E_p/(double)vol_total;
207         double prob_E_0 = (double)vol_E_0/(double)vol_total;
208 
209         printf(" %6.2f  %.3f  %+.4e  %.6f  %.6f  %.5f  ",
210         d, m, Disc, prob_E_p, prob_E_0, prob_E_p+prob_E_0);
211         printf("\n");
212 
213         //printf("----------------------------\n");
214         }
215 
216 printf("#     d      m        Delta  BofA_E_+  BofA_E_0  total\n");
217 
218 //printf("# eps = %.2e\n",eps);
219 printf("\n\n");
220 }
221 printf("# neighbour = %.2e\n",tol);
222 printf("# epsrel = %.2e\n",epsrel);
223 printf("# epsabs = %.2e\n",epsabs);
224 printf("# sample = %d\n",sample);
225 }
226 }
227 
228 
229 gsl_rng_free (r);
230 printf("Time taken: %.2fs\n", (double)(clock() - tStart)/CLOCKS_PER_SEC);
231 
232 //(void) x;
233 //(void) z;
234 return 0;
235 }
```

fig6b_plot.p

fig6b_plot.p

```
1  #// 2017-09-14
2 
3  set term postscript eps enhanced color font 'Arial,25' dashed
4 
5  #set termoption dash
6 
7  set output "fig6b.eps"
8 
9  unset xrange
10 unset yrange
11 set xlabel "dispersal rate (d)"
12 set ylabel "Fraction of Volume of BofA for E_+"
13 set xrange [0:25]
14 #set title ''
```

```
set xtics 5

set yrange [-0.1: 1.1]
set ytics 0.2

#set key out vert
set key off #out vert
#set key center right
set label 1 at 8, 1.05
set label 1 "m = 0.117"
set label 2 at 6, 0.93
set label 2 "m = 0.207"
set label 3 at 2, 0.8
set label 3 "m = 0.212"
set label 4 at 0.5, 0.7
set label 4 "m = 0.217"
set label 5 at 0.0, -0.05
set label 5 "m = 0.250"           #tc lt 3


#          show label

set style line 1 lc rgb '#0060ad' lt 1 lw 3 #pt 7 ps 1.5   # --- blue
set style line 2 lc rgb '#dd181f' lt 1 lw 3 #pt 5 ps 1.5   # --- red
set style line 3 lt 2 lc rgb "yellow" lw 3
set style line 4 lt 2 lc rgb "red" lw 3
#set style line 3 lc rgb '#3b0b7a' lt 1 lw 2 pt 3 ps 1.5   # --- purple
plot 'fig6b.dat'  index 0 using 1:4 with line ls 1 t 'm = '.columnhead(1), \
     ''           index 1 using 1:4 with line ls 1 t 'm = '.columnhead(1), \
     ''           index 2 using 1:($4>0?$4:1/0) with line ls 2 t 'm =
      ↪  '.columnhead(1), \
     ''           index 2 using 1:($4>0?1/0:$4) with line ls 2 t 'm =
      ↪  '.columnhead(1), \
     ''           index 3 using 1:($4>0?$4:1/0) with line ls 2 t 'm =
      ↪  '.columnhead(1), \
     ''           index 3 using 1:($4>0?1/0:$4) with line ls 2 t 'm =
      ↪  '.columnhead(1), \
     ''           index 2 using 1:4 with line dt 2 lc rgb '#dd181f' lw 3, \
     ''           index 3 using 1:4 with line dt 2 lc rgb '#dd181f' lw 3, \
         ''           index 0 using 1:($4>2?1:0) with line dt 4 lc rgb
          ↪  "black" lw 3, \



##positive part #zero part #connecting with dashed line

```

```
############### fix color, dashed lines,  adjust text positions.
         # add zero line,



unset xrange
unset yrange

unset tmargin
unset bmargin
unset rmargin
unset title
unset size
unset xtics
unset label
reset
```

C.2 Code for Chapter 3

Matlab is used to generate figures, and figure numbering is within Chapter 3.

C.2.1 fig2

main function for figure 2

fig2.m

```
figure;
subplot(3,1,1)
hold on
tau =3.1;
sol = dde23(@ddex1de,[tau],@ddex1hist,[0, tfinal]);
plot(sol.x,sol.y)
plot([0,tfinal],[1 - 2.0/3.0, 1-2.0/3.0])
title('\tau = 3.1');
ylabel('solution p');
hold off

subplot(3,1,2)
hold on
tau =3.14;
sol = dde23(@ddex1de,[tau],@ddex1hist,[0, tfinal]);
plot(sol.x,sol.y)
plot([0,tfinal],[1 - 2.0/3.0, 1-2.0/3.0])
title('\tau = 3.14');
ylabel('solution p');
hold off

```

```
subplot(3,1,3)
hold on
tau =3.16;
sol = dde23(@ddex1de,[tau],@ddex1hist,[0, tfinal]);
plot(sol.x,sol.y)
plot([0,tfinal],[1 - 2.0/3.0, 1-2.0/3.0])
title('\tau = 3.15');
xlabel('time t');
ylabel('solution p');
hold off
```

DDE history function and DDE function should be saved in separate files with valid names and in the same folder of the main function.

ddex1de.m

ddex1de.m

```
function dydt = ddex1de(t,y,Z)
% Differential equations function
ylag = Z;
dydt = 1.5 * (1-ylag) * y - 1.0 * y;
end
```

ddex1hist.m

ddex1hist.m

```
function s = ddex1hist(t)
% Constant history function
numbDEs = 1;
s = 0.2*ones(numbDEs,1);
end
```

C.2.2 Changes made in dde23

The author made a few changes to the routine `odefinalize` called by `dde23` to constrain the dependent variables in $[0, 1]$. The following lines are inserted between line 58 and line 59 in the original routine `odefinalize`:

add_to_odefinalize.m

```
        sol.y(sol.y<0) = 0;
        sol.y(sol.y>1) = 1;
```

C.3 Code for Chapter 4

Here are the code listed in table B.1. Use python to generate figures.

C.3.1 Numerical Procedures

DM_TwoTraits_num.py

DM_TwoTraits_num.py

```
import numpy as np

p=0
g=1

# relatedness
def MatrixForRecursions(n,h,s):
  p=0
  g=1
  return np.array([\
        [0,0,s[p,p]*h[p]**2, s[g,p]*h[g]**2],\
        [0,0,s[p,g]*h[p]**2, s[g,g]*h[g]**2],\
        [s[p,p]/(4*n),s[g,p]/(4*n),\
        (2*n-1)*s[p,p]*h[p]**2/(2*n), (2*n-1)*s[g,p]*h[g]**2/(2*n)],\
        [s[p,g]/(4*n),s[g,g]/(4*n),\
        (2*n-1)*s[p,g]*h[p]**2/(2*n), (2*n-1)*s[g,g]*h[g]**2/(2*n)]\
        ])

def CC(Q,n):
  b = np.array([0,0,0.25/n,0.25/n])
  A = np.identity(4) - Q
  Ainv = np.linalg.inv(A)
  F = np.dot(Ainv,b)
  return F

# total RV
def TotalRV(T,d,c):
  p=0
  g=1
  pi=np.array([ T[p,g]/(T[g,p]+T[p,g]), T[g,p]/(T[g,p]+T[p,g]) ])
  v=np.array([ 1/(1-c[p]*d[p]), 1/(1-c[g]*d[g]) ])
  alpha = v*pi
  return alpha

# input details about the environment

ss=3
sprob = ss*0.1

T=np.array([ [1-sprob,sprob], [sprob,1-sprob] ])
S=np.empty((2,2),dtype=float)
S[p,p]=T[p,p]/(T[p,p]+T[p,g])
S[g,p]=T[p,g]/(T[p,p]+T[p,g])
S[p,g]=T[g,p]/(T[g,p]+T[g,g])
```

```
S[g,g]=T[g,g]/(T[g,p]+T[g,g])

def myloop(d,N,c,offCtrl):
  for iter in range(250):
    # calculate h
    h = (1-d)/(1-c*d)
    # solve CC recursions
    F=CC(MatrixForRecursions(N,h,S),N)
    # determine relatedness
    if offCtrl == True:
      R=np.array([0.5*(1+F[0]),0.5*(1+F[1])])
    else:
      R=np.array([ 0.5*F[0] + 0.25*(1+F[0]*S[0,0]+F[1]*S[1,0]),\
          0.5*F[1] + 0.25*(1+F[0]*S[0,1]+F[1]*S[1,1]) ])
    Rbar=np.array([F[2],F[3]])
    # determine IF changes
    dw = -R*c + Rbar*h
    # update d
    d += 0.1*dw
    d = np.clip(d,0.001, 0.999)
  return d

N=2
cc=3
cavg=cc*0.1
myOffCtrl = False#False
if myOffCtrl == True:
    outfile = open("DM_OffCtrl_N=%s_c=0pt%s_s=0pt%s.dat"%(N,cc,ss), "w")
else:
    outfile = open("DM_ParCtrl_N=%s_c=0pt%s_s=0pt%s.dat"%(N,cc,ss), "w")

upperBnd=np.min([1-cavg,cavg])
sigmas=np.linspace(0,upperBnd,100)

tol=1e-08
maxiter = 10
for sigma in sigmas:
  c = np.array([cavg + sigma, cavg - sigma])

  done = np.array([0.01,0.02])
  dtwo = np.array([0.99,0.98])
  dtre = np.array([0.01,0.99])
  dfor = np.array([0.98,0.02])

  mydist = [ np.linalg.norm(done-dtwo),\
    np.linalg.norm(done-dtre),\
    np.linalg.norm(done-dfor),\
```

```
    np.linalg.norm(dtwo-dtre),\
    np.linalg.norm(dtwo-dfor),\
    np.linalg.norm(dtre-dfor)]

  iter = 0
  while np.max(mydist) > tol and iter < maxiter:
    done = myloop(done,N,c,myOffCtrl)
    dtwo = myloop(dtwo,N,c,myOffCtrl)
    dtre = myloop(dtre,N,c,myOffCtrl)
    dfor = myloop(dfor,N,c,myOffCtrl)
    mydist = [ np.linalg.norm(done-dtwo),\
      np.linalg.norm(done-dtre),\
      np.linalg.norm(done-dfor),\
      np.linalg.norm(dtwo-dtre),\
      np.linalg.norm(dtwo-dfor),\
      np.linalg.norm(dtre-dfor)]
    iter += 1

  dp = np.mean([ done[0], dtwo[0], dtre[0], dfor[0] ])
  dg = np.mean([ done[1], dtwo[1], dtre[1], dfor[1] ])
  outstr = str(sigma) + "," + str(dp) + "," + str(dg) + "\n"
  outfile.write(outstr)

outfile.close()
```

MD_TwoTraits_num.py

MD_TwoTraits_num.py

```
import numpy as np

p=0
g=1

# relatedness
def MatrixForRecursions(n,h,s):
  p=0
  g=1
  return np.array([\
        [0,0,s[p,p], s[g,p]],\
        [0,0,s[p,g], s[g,g]],\
        [s[p,p]/(4*n),s[g,p]/(4*n),\
        (2*(n-1)*h[p]**2 + 1)*s[p,p]/(2*n), (2*(n-1)*h[g]**2 +
         ↪  1)*s[g,p]/(2*n)],\
        [s[p,g]/(4*n),s[g,g]/(4*n),\
        (2*(n-1)*h[p]**2 + 1)*s[p,g]/(2*n), (2*(n-1)*h[g]**2 +
         ↪  1)*s[g,g]/(2*n)]\
        ])

```

```
def CC(Q,n):
  b = np.array([0,0,0.25/n,0.25/n])
  A = np.identity(4) - Q
  Ainv = np.linalg.inv(A)
  F = np.dot(Ainv,b)
  return F

# total RV
def TotalRV(T,d,c):
  p=0
  g=1
  pi=np.array([ T[p,g]/(T[g,p]+T[p,g]), T[g,p]/(T[g,p]+T[p,g]) ])
  v=np.array([ 1/(1-c[p]*d[p]), 1/(1-c[g]*d[g]) ])
  alpha = v*pi
  return alpha

# input details about the environment

ss=3
sprob = ss*0.1
T=np.array([ [1-sprob,sprob], [sprob,1-sprob] ])
S=np.empty((2,2),dtype=float)
S[p,p]=T[p,p]/(T[p,p]+T[p,g])
S[g,p]=T[p,g]/(T[p,p]+T[p,g])
S[p,g]=T[g,p]/(T[g,p]+T[g,g])
S[g,g]=T[g,g]/(T[g,p]+T[g,g])

def myloop(d,N,c,offCtrl):
  for iter in range(250):
    # calculate h
    h = (1-d)/(1-c*d)
    # solve CC recursions
    F=CC(MatrixForRecursions(N,h,S),N)
    # determine relatedness
    if offCtrl == True:
      R=np.array([0.5*(1+F[0]),0.5*(1+F[1])])
    else:
      R=np.array([ 0.5*F[0] + 0.25*(1+F[0]*S[0,0]+F[1]*S[1,0]),\
          0.5*F[1] + 0.25*(1+F[0]*S[0,1]+F[1]*S[1,1]) ])
    Rbar=np.array([F[2],F[3]])
    # determine IF changes
    dw = -0.5*(R+Rbar)*c + Rbar*h
    # update d
    d += 0.1*dw
    d = np.clip(d,0.001, 0.999)
  return d

```

```
N=2
cc=3
cavg=cc*0.1
myOffCtrl = False#False
if myOffCtrl==True:
    outfile = open("MD_OffCtrl_N=%s_c=0pt%s_s=0pt%s.dat"%(N,cc,ss), "w")
else:
    outfile = open("MD_ParCtrl_N=%s_c=0pt%s_s=0pt%s.dat"%(N,cc,ss), "w")



upperBnd=np.min([1-cavg,cavg])
sigmas=np.linspace(0,upperBnd,100)

tol=1e-08
maxiter=10

for sigma in sigmas:
  c = np.array([cavg+sigma,cavg-sigma])

  done = np.array([0.01,0.02])
  dtwo = np.array([0.99,0.98])
  dtre = np.array([0.01,0.99])
  dfor = np.array([0.98,0.02])

  mydist = [ np.linalg.norm(done-dtwo),\
    np.linalg.norm(done-dtre),\
    np.linalg.norm(done-dfor),\
    np.linalg.norm(dtwo-dtre),\
    np.linalg.norm(dtwo-dfor),\
    np.linalg.norm(dtre-dfor)]

  iter = 0

  while np.max(mydist) > tol and iter < maxiter:
    done = myloop(done,N,c,myOffCtrl)
    dtwo = myloop(dtwo,N,c,myOffCtrl)
    dtre = myloop(dtre,N,c,myOffCtrl)
    dfor = myloop(dfor,N,c,myOffCtrl)
    mydist = [ np.linalg.norm(done-dtwo),\
      np.linalg.norm(done-dtre),\
      np.linalg.norm(done-dfor),\
      np.linalg.norm(dtwo-dtre),\
      np.linalg.norm(dtwo-dfor),\
      np.linalg.norm(dtre-dfor)]
    iter += 1

```

```
  dp = np.mean([ done[0], dtwo[0], dtre[0], dfor[0] ])
  dg = np.mean([ done[1], dtwo[1], dtre[1], dfor[1] ])

  outstr = str(sigma) + "," + str(dp) + "," + str(dg) + "\n"
  outfile.write(outstr)

outfile.close()
```

DM_OneTrait_num.py

DM_OneTrait_num.py

```
import numpy as np

p=0
g=1

# relatedness
def MatrixForRecursions(n,h,s):
  p=0
  g=1
  return np.array([\
        [0,0,s[p,p]*h[p]**2, s[g,p]*h[g]**2],\
        [0,0,s[p,g]*h[p]**2, s[g,g]*h[g]**2],\
        [s[p,p]/(4*n),s[g,p]/(4*n),\
        (2*n-1)*s[p,p]*h[p]**2/(2*n), (2*n-1)*s[g,p]*h[g]**2/(2*n)],\
        [s[p,g]/(4*n),s[g,g]/(4*n),\
        (2*n-1)*s[p,g]*h[p]**2/(2*n), (2*n-1)*s[g,g]*h[g]**2/(2*n)]\
        ])

def CC(Q,n):
  b = np.array([0,0,0.25/n,0.25/n])
  A = np.identity(4) - Q
  Ainv = np.linalg.inv(A)
  F = np.dot(Ainv,b)
  return F

# total RV
def TotalRV(T,d,c):
  p=0
  g=1
  pi=np.array([ T[p,g]/(T[g,p]+T[p,g]), T[g,p]/(T[g,p]+T[p,g]) ])
  v=np.array([ 1/(1-c[p]*d[p]), 1/(1-c[g]*d[g]) ])
  alpha = v*pi
  return alpha

# input details about the environment

ss=3
```

```
sprob = ss*0.1

T=np.array([ [1-sprob,sprob], [sprob,1-sprob] ])
S=np.empty((2,2),dtype=float)
S[p,p]=T[p,p]/(T[p,p]+T[p,g])
S[g,p]=T[p,g]/(T[p,p]+T[p,g])
S[p,g]=T[g,p]/(T[g,p]+T[g,g])
S[g,g]=T[g,g]/(T[g,p]+T[g,g])

def myloop(d,N,c,offCtrl):
  for iter in range(250):
    # calculate h
    h = (1-d)/(1-c*d)
    # solve CC recursions
    F=CC(MatrixForRecursions(N,h,S),N)
    # determine relatedness
    if offCtrl == True:
      R=np.array([0.5*(1+F[0]),0.5*(1+F[1])])
    else:
      R=np.array([ 0.5*F[0] + 0.25*(1+F[0]*S[0,0]+F[1]*S[1,0]),\
          0.5*F[1] + 0.25*(1+F[0]*S[0,1]+F[1]*S[1,1]) ])
    Rbar=np.array([F[2],F[3]])
    # determine IF changes
    wts = TotalRV(T,d,c)*np.ones((2,2), dtype=float)
    dw = -R*c + Rbar*h
    # update d
    d += 0.1 * np.dot(wts,dw)
    d = np.clip(d,0.001, 0.999)
  return d

N=2
cc=3
cavg=cc*0.1
myOffCtrl = False#False
if myOffCtrl == True:
    outfile = open("DM_OffCtrl_uncond_N=%s_c=0pt%s_s=0pt%s.dat"%(N,cc,ss),
     ↪  "w")
else:
    outfile = open("DM_ParCtrl_uncond_N=%s_c=0pt%s_s=0pt%s.dat"%(N,cc,ss),
     ↪  "w")


upperBnd=np.min([1-cavg,cavg])
sigmas=np.linspace(0,upperBnd,100)

tol=1e-08
maxiter=10
```

```
83
84  for sigma in sigmas:
85
86    c = np.array([cavg+sigma,cavg-sigma])
87
88    done = np.array([0.01,0.01])
89    dtwo = np.array([0.99,0.99])
90
91    mydist = np.linalg.norm(done-dtwo)
92    iter = 0
93
94    while np.max(mydist) > tol and iter < maxiter:
95      done = myloop(done,N,c,myOffCtrl)
96      dtwo = myloop(dtwo,N,c,myOffCtrl)
97      mydist = np.linalg.norm(done-dtwo)
98      iter += 1
99
100   d = np.mean([ done[0], dtwo[0], done[1], dtwo[1] ])
101   outstr = str(sigma) + "," + str(d) + "\n"
102   outfile.write(outstr)
103
104 outfile.close()
```

MD_OneTrait_num.py

MD_OneTrait_num.py

```
1  import numpy as np
2
3  p=0
4  g=1
5
6  # relatedness
7  def MatrixForRecursions(n,h,s):
8    p=0
9    g=1
10   return np.array([\
11         [0,0,s[p,p], s[g,p]],\
12         [0,0,s[p,g], s[g,g]],\
13         [s[p,p]/(4*n),s[g,p]/(4*n),\
14         (2*(n-1)*h[p]**2 + 1)*s[p,p]/(2*n), (2*(n-1)*h[g]**2 +
           ↪  1)*s[g,p]/(2*n)],\
15         [s[p,g]/(4*n),s[g,g]/(4*n),\
16         (2*(n-1)*h[p]**2 + 1)*s[p,g]/(2*n), (2*(n-1)*h[g]**2 +
           ↪  1)*s[g,g]/(2*n)]\
17         ])
18
19 def CC(Q,n):
20   b = np.array([0,0,0.25/n,0.25/n])
```

```
  A = np.identity(4) - Q
  Ainv = np.linalg.inv(A)
  F = np.dot(Ainv,b)
  return F

# total RV
def TotalRV(T,d,c):
  p=0
  g=1
  pi=np.array([ T[p,g]/(T[g,p]+T[p,g]), T[g,p]/(T[g,p]+T[p,g]) ])
  v=np.array([ 1/(1-c[p]*d[p]), 1/(1-c[g]*d[g]) ])
  alpha = v*pi
  return alpha

# input details about the environment

ss=3
sprob = ss*0.1

T=np.array([ [1-sprob,sprob], [sprob,1-sprob] ])
S=np.empty((2,2),dtype=float)
S[p,p]=T[p,p]/(T[p,p]+T[p,g])
S[g,p]=T[p,g]/(T[p,p]+T[p,g])
S[p,g]=T[g,p]/(T[g,p]+T[g,g])
S[g,g]=T[g,g]/(T[g,p]+T[g,g])

def myloop(d,N,c,offCtrl):
  for iter in range(250):
    # calculate h
    h = (1-d)/(1-c*d)
    # solve CC recursions
    F=CC(MatrixForRecursions(N,h,S),N)
    # determine relatedness
    if offCtrl == True:
      R=np.array([0.5*(1+F[0]),0.5*(1+F[1])])
    else:
      R=np.array([ 0.5*F[0] + 0.25*(1+F[0]*S[0,0]+F[1]*S[1,0]),\
          0.5*F[1] + 0.25*(1+F[0]*S[0,1]+F[1]*S[1,1]) ])
    Rbar=np.array([F[2],F[3]])
    # determine IF changes
    wts = TotalRV(T,d,c)*np.ones((2,2), dtype=float)
    dw = -0.5*(R+Rbar)*c + Rbar*h
    # update d
    d += 0.1 * np.dot(wts,dw)
    d = np.clip(d,0.001, 0.999)
  return d

```

```
N=2
cc=3
cavg=cc*0.1
myOffCtrl = False#False

if myOffCtrl==True:
    outfile = open("MD_OffCtrl_uncond_N=%s_c=0pt%s_s=0pt%s.dat"%(N,cc,ss),
     ↪  "w")
else:
    outfile = open("MD_ParCtrl_uncond_N=%s_c=0pt%s_s=0pt%s.dat"%(N,cc,ss),
     ↪  "w")




upperBnd = np.min([1-cavg,cavg])
sigmas=np.linspace(0, upperBnd, 100)

tol=1e-08
maxiter=10

for sigma in sigmas:

  c = np.array([cavg+sigma,cavg-sigma])

  done = np.array([0.01,0.01])
  dtwo = np.array([0.99,0.99])

  mydist = np.linalg.norm(done-dtwo)
  iter = 0

  while np.max(mydist) > tol and iter < maxiter:
    done = myloop(done,N,c,myOffCtrl)
    dtwo = myloop(dtwo,N,c,myOffCtrl)
    mydist = np.linalg.norm(done-dtwo)
    iter += 1

  d = np.mean([ done[0], dtwo[0], done[1], dtwo[1] ])
  outstr = str(sigma) + "," + str(d) + "\n"
  outfile.write(outstr)

outfile.close()
```

C.3.2 Individual-Based Simulation

DM_ParCtrl_TwoTraits.py

DM_ParCtrl_TwoTraits.py

```
import numpy as np
import matplotlib.pyplot as plt

m=250
n=2
cp=0.4
cg=0.2
s = 0.3

def enviroChange(state, s):
  x = np.random.binomial(1,s)
  if x == 0:
    return state
  else:
    return abs(state-1)

DataFile = open("DM_ParCtrl_Fig_7.dat","w")

for trial in range(3):
  dold=np.random.uniform(0,1,(2,m,n))
  dnew=np.random.uniform(0,1,(2,m,n))

  tfinal=3
  d=np.empty((2,tfinal),dtype=float)

  state = np.random.binomial(0.5,1)
  altstate = abs(state-1)

  for t in range(tfinal):
    # number tickets that emigrate from patch i
    emigrantTix = np.sum( dold[state], axis=1 )

    # number of tickets that remain on patch i
    nativeTix = n - emigrantTix

    # number of tickets that are in dispersal pool
    dpoolTix = np.sum( emigrantTix )

    # number of tickets that arrive on any patch
    if state == 0:
      c = cp
    else:
      c = cg

```

```
    immigrantTix = (1-c)*dpoolTix/m

    for i in range(m):
      for j in range(n):
        dtmp=[0.0,0.0]
        for parent in range(2):
          pLocal = nativeTix[i]/(nativeTix[i] + immigrantTix)
          x = np.random.binomial( 1, pLocal )
          if x==1:
            iwin = i
            p = (1-dold[state,iwin])/nativeTix[iwin]
            y = np.random.multinomial( 1, p )
            jwin = np.argmax(y)
          else:
            q = emigrantTix/dpoolTix
            z = np.random.multinomial( 1, q )
            iwin = np.argmax(z)
            p = dold[state,iwin]/emigrantTix[iwin]
            y = np.random.multinomial( 1, p )
            jwin = np.argmax(y)
          dtmp[state] += 0.5*(dold[state,iwin,jwin] +
           ↪  np.random.normal(0,0.05,1))
          dtmp[altstate] += 0.5*dold[altstate,iwin,jwin]
        dnew[state,i,j] = dtmp[state]
        dnew[altstate,i,j] = dtmp[altstate]
    dnew = np.clip(dnew, 0.001, 0.999)
    (dold,dnew) = (dnew,dold)
    state=enviroChange(state, s)
    altstate=abs(state-1)

    d[0,t] = np.mean( np.mean( dold[0] ) )
    d[1,t] = np.mean( np.mean( dold[1] ) )

  mystr = ""
  for kk in range(2):
    for elem in d[kk]:
      if kk==0:
        mystr += str( elem ) + ","
      else:
        mystr += str( 0 ) + ","
    mystr += "\n"

  DataFile.write(mystr)

DataFile.close()

#plt.figure( figsize=(6,5) )
```

```
#plt.plot(np.arange(tfinal), d[0], '-r')
#plt.plot(np.arange(tfinal), d[1], '-b')
#plt.plot([0,tfinal],[0.367]*2, '--r')
#plt.plot([0,tfinal],[0.707]*2, '--b')
#plt.ylim([0,1])
#mylabels=[]
#for i in range(6):
#  mylabels.append(str(5*i))
#plt.xticks( 5000*np.arange(6), mylabels)
#plt.xlabel("time in generations x 1000", fontsize=12)
#plt.ylabel("mean conditional dispersal prob", fontsize=12)
#plt.show()
```

DM_OffCtrl_TwoTraits.py

DM_OffCtrl_TwoTraits.py

```
import numpy as np
import matplotlib.pyplot as plt

m=250
n=2
cp=0.4
cg=0.2
s=0.3

def enviroChange(state, s):
  x = np.random.binomial(1,s)
  if x == 0:
    return state
  else:
    return abs(state-1)

DataFile = open("DM_OffCtrl_Fig_7.dat", "a")

tfinal=25000
for trial in range(10):
  gold=np.random.uniform(0,1,(2,2,m,n))
  gnew=np.random.uniform(0,1,(2,2,m,n))
  d=np.empty((2,tfinal),dtype=float)

  state=np.random.binomial(1,0.5)
  altstate=abs(state-1)

  for t in range(tfinal):
    # modification
    dold = np.mean(gold[state],axis=0)
    dalt = np.mean(gold[altstate],axis=0)
    d[state,t] = np.mean( np.mean( dold ) )
```

```
    d[altstate,t] = np.mean( np.mean( dalt ) )

    # number tickets that emigrate from patch i
    emigrantTix = np.sum( dold, axis=1 )

    # number of tickets that remain on patch i
    nativeTix = n - emigrantTix

    # number of tickets that are in dispersal pool
    dpoolTix = np.sum( emigrantTix )

    # number of tickets that arrive on any patch
    if state == 0:
      c = cp
    else:
      c = cg

    immigrantTix = (1-c)*dpoolTix/m

    for i in range(m):
      for j in range(n):
        for parent in range(2):
          pLocal = nativeTix[i]/(nativeTix[i] + immigrantTix)
          x = np.random.binomial( 1, pLocal )
          if x==1:
            iwin = i
            p = (1-dold[iwin])/nativeTix[iwin]
            y = np.random.multinomial( 1, p )
            jwin = np.argmax(y)
            # modification (within-pair competition)
            pxtra = (1-gold[state,1,iwin,jwin]) / (1-gold[state,0,iwin,jwin]
             ↪  + 1-gold[state,1,iwin,jwin])
            kwin = np.random.binomial(1,pxtra)
          else:
            q = emigrantTix/dpoolTix
            z = np.random.multinomial( 1, q )
            iwin = np.argmax(z)
            p = dold[iwin]/emigrantTix[iwin]
            y = np.random.multinomial( 1, p )
            jwin = np.argmax(y)
            # modification (within-pair competition)
            pxtra = gold[state,1,iwin,jwin]/(gold[state,0,iwin,jwin] +
             ↪  gold[state,1,iwin,jwin])
            kwin = np.random.binomial(1,pxtra)
          #modification
          gnew[state,parent,i,j] = gold[state,kwin,iwin,jwin] +
           ↪  np.random.normal(0,0.0025,1)
```

```
            gnew[altstate,parent,i,j] = gold[altstate,kwin,iwin,jwin]
    gnew = np.clip(gnew, 0.0001, 0.9999)
    (gold,gnew) = (gnew,gold)
    state = enviroChange(state,s)
    altstate=abs(state-1)

  mystr =""
  for kk in range(2):
    for elem in d[kk]:
      mystr += str(elem) + ","
    mystr += "\n"

  DataFile.write(mystr)

DataFile.close()
#plt.figure( figsize=(6,5) )
#plt.plot(np.arange(tfinal), d[0], '-b')
#plt.plot(np.arange(tfinal), d[1], '-r')
#plt.plot([0,tfinal],[0.58]*2, '--b')
#plt.plot([0,tfinal],[0.065]*2, '--b')
#plt.ylim([0,1])
#plt.xlabel("time in generations", fontsize=12)
#plt.ylabel("global mean dispersal prob", fontsize=12)
#plt.show()
```

MD_ParCtrl_TwoTraits.py

MD_ParCtrl_TwoTraits.py

```
import numpy as np
import matplotlib.pyplot as plt

m=250
n=2
cp=0.4
cg=0.2
s = 0.3

def enviroChange(state, s):
  x = np.random.binomial(1,s)
  if x == 0:
    return state
  else:
    return abs(state-1)

DataFile = open("MD_ParCtrl_FigA.dat","a")

for trial in range(3):
  dold=np.random.uniform(0,1,(2,m,n))
```

```
dnew=np.random.uniform(0,1,(2,m,n))

tfinal=50000
d=np.empty((2,tfinal),dtype=float)

state = np.random.binomial(0.5,1)
altstate = abs(state-1)

for t in range(tfinal):
  # number tickets that emigrate from patch i
  emigrantTix = np.sum( dold[state], axis=1 )

  # number of tickets that remain on patch i
  nativeTix = n - emigrantTix

  # number of tickets that are in dispersal pool
  dpoolTix = np.sum( emigrantTix )

  # number of tickets that arrive on any patch
  if state == 0:
    c = cp
  else:
    c = cg

  immigrantTix = (1-c)*dpoolTix/m

  for i in range(m):
    for j in range(n):
      dtmp=[0.0,0.0]
      for parent in range(2):
        if parent == 0:
          # mom
          pLocal = nativeTix[i]/(nativeTix[i] + immigrantTix)
          x = np.random.binomial( 1, pLocal )
          if x==1:
            iwin = i
            p = (1-dold[state,iwin])/nativeTix[iwin]
            y = np.random.multinomial( 1, p )
            jwin = np.argmax(y)
          else:
            q = emigrantTix/dpoolTix
            z = np.random.multinomial( 1, q )
            iwin = np.argmax(z)
            p = dold[state,iwin]/emigrantTix[iwin]
            y = np.random.multinomial( 1, p )
            jwin = np.argmax(y)
        else:
```

```
            # dad (NB iwin is established)
            p = [1./n]*n
            y = np.random.multinomial( 1, p )
            jwin = np.argmax(y)
          dtmp[state] += 0.5*(dold[state,iwin,jwin] +
           ↪  np.random.normal(0,0.05,1))
          dtmp[altstate] += 0.5*dold[altstate,iwin,jwin]
        dnew[state,i,j] = dtmp[state]
        dnew[altstate,i,j] = dtmp[altstate]
    dnew = np.clip(dnew, 0.001, 0.999)
    (dold,dnew) = (dnew,dold)
    state=enviroChange(state, s)
    altstate=abs(state-1)

    d[0,t] = np.mean( np.mean( dold[0] ) )
    d[1,t] = np.mean( np.mean( dold[1] ) )

  mystr = ""
  for kk in range(2):
    for elem in d[kk]:
      mystr += str( elem ) + ","
    mystr += "\n"

  DataFile.write(mystr)

DataFile.close()

#plt.figure( figsize=(6,5) )
#plt.plot(np.arange(tfinal), d[0], '-r')
#plt.plot(np.arange(tfinal), d[1], '-b')
#plt.plot([0,tfinal],[0.367]*2, '--r')
#plt.plot([0,tfinal],[0.707]*2, '--b')
#plt.ylim([0,1])
#mylabels=[]
#for i in range(6):
#  mylabels.append(str(5*i))
#plt.xticks( 5000*np.arange(6), mylabels)
#plt.xlabel("time in generations x 1000", fontsize=12)
#plt.ylabel("mean conditional dispersal prob", fontsize=12)
#plt.show()
```

MD_OffCtrl_TwoTraits.py

MD_OffCtrl_TwoTraits.py

```
import numpy as np
import matplotlib.pyplot as plt

m=250
```

```
n=2
cp=0.4
cg=0.2
s=0.3

def enviroChange(state, s):
  x = np.random.binomial(1,s)
  if x == 0:
    return state
  else:
    return abs(state-1)

DataFile = open("MD_OffCtrl_Fig.dat", "a")

tfinal=50000
for trial in range(10):
  gold=np.random.uniform(0,1,(2,2,m,n))
  gnew=np.random.uniform(0,1,(2,2,m,n))
  d=np.empty((2,tfinal),dtype=float)

  state=np.random.binomial(1,0.5)
  altstate=abs(state-1)

  for t in range(tfinal):
    # modification
    dold = np.mean(gold[state],axis=0)
    dalt = np.mean(gold[altstate],axis=0)
    d[state,t] = np.mean( np.mean( dold ) )
    d[altstate,t] = np.mean( np.mean( dalt ) )

    # number tickets that emigrate from patch i
    emigrantTix = np.sum( dold, axis=1 )

    # number of tickets that remain on patch i
    nativeTix = n - emigrantTix

    # number of tickets that are in dispersal pool
    dpoolTix = np.sum( emigrantTix )

    # number of tickets that arrive on any patch
    if state == 0:
      c = cp
    else:
      c = cg

    immigrantTix = (1-c)*dpoolTix/m

```

```
    for i in range(m):
      for j in range(n):
        for parent in range(2):
          if parent ==0:
          # mom
            pLocal = nativeTix[i]/(nativeTix[i] + immigrantTix)
            x = np.random.binomial( 1, pLocal )
            if x==1:
              iwin = i
              p = (1-dold[iwin])/nativeTix[iwin]
              y = np.random.multinomial( 1, p )
              jwin = np.argmax(y)
              # modification (within-pair competition)
              pxtra = (1-gold[state,1,iwin,jwin]) /
               ↪  (1-gold[state,0,iwin,jwin] + 1-gold[state,1,iwin,jwin])
              kwin = np.random.binomial(1,pxtra)
            else:
              q = emigrantTix/dpoolTix
              z = np.random.multinomial( 1, q )
              iwin = np.argmax(z)
              p = dold[iwin]/emigrantTix[iwin]
              y = np.random.multinomial( 1, p )
              jwin = np.argmax(y)
              # modification (within-pair competition)
              pxtra = gold[state,1,iwin,jwin]/(gold[state,0,iwin,jwin] +
               ↪  gold[state,1,iwin,jwin])
              kwin = np.random.binomial(1,pxtra)
          else:
            # dad (NB iwin is established)
            p = [1./n]*n
            y = np.random.multinomial( 1, p )
            jwin = np.argmax(y)
            # within-pair competition
            kwin = np.random.binomial(1,0.5)
          #modification
          gnew[state,parent,i,j] = gold[state,kwin,iwin,jwin] +
           ↪  np.random.normal(0,0.0025,1)
          gnew[altstate,parent,i,j] = gold[altstate,kwin,iwin,jwin]
    gnew = np.clip(gnew, 0.0001, 0.9999)
    (gold,gnew) = (gnew,gold)
    state = enviroChange(state,s)
    altstate=abs(state-1)

  mystr =""
  for kk in range(2):
    for elem in d[kk]:
      mystr += str(elem) + ","
```

```
    mystr += "\n"

  DataFile.write(mystr)

DataFile.close()
#plt.figure( figsize=(6,5) )
#plt.plot(np.arange(tfinal), d[0], '-b')
#plt.plot(np.arange(tfinal), d[1], '-r')
#plt.plot([0,tfinal],[0.58]*2, '--b')
#plt.plot([0,tfinal],[0.065]*2, '--b')
#plt.ylim([0,1])
#plt.xlabel("time in generations", fontsize=12)
#plt.ylabel("global mean dispersal prob", fontsize=12)
#plt.show()
```

DM_ParCtrl_OneTrait.py

DM_ParCtrl_OneTrait.py

```
import numpy as np
import matplotlib.pyplot as plt

m=250
n=2
c=0.4

def taylor88(n,c):
  const = np.sqrt( 1 + 4*n*(n-1)*c**2 )
  return (const + 1 - 2*n*c)/(const + 1 - 2*n*c**2)

dold=0.5*np.random.uniform(0,1,(m,n))
dnew=np.random.uniform(0,1,(m,n))

tfinal=10000
d=np.empty(tfinal,dtype=float)

for t in range(tfinal):
  # number tickets that emigrate from patch i
  emigrantTix = np.sum( dold, axis=1 )

  # number of tickets that remain on patch i
  nativeTix = n - emigrantTix

  # number of tickets that are in dispersal pool
  dpoolTix = np.sum( emigrantTix )

  # number of tickets that arrive on any patch
  immigrantTix = (1-c)*dpoolTix/m

```

```
  for i in range(m):
    for j in range(n):
      dtmp=0.0
      for parent in range(2):
        pLocal = nativeTix[i]/(nativeTix[i] + immigrantTix)
        x = np.random.binomial( 1, pLocal )
        if x==1:
          iwin = i
          p = (1-dold[iwin])/nativeTix[iwin]
          y = np.random.multinomial( 1, p )
          jwin = np.argmax(y)
        else:
          q = emigrantTix/dpoolTix
          z = np.random.multinomial( 1, q )
          iwin = np.argmax(z)
          p = dold[iwin]/emigrantTix[iwin]
          y = np.random.multinomial( 1, p )
          jwin = np.argmax(y)
        dtmp += 0.5*(dold[iwin,jwin] + np.random.normal(0,0.05,1))
      dnew[i,j] = dtmp
  dnew = np.clip(dnew, 0.001, 0.999)
  (dold,dnew) = (dnew,dold)

  d[t] = np.mean( np.mean( dold ) )

theory = 'Taylor 1988: ' + str(taylor88(n,c))
simuln = 'Simulation: ' + str( np.mean(d[-3*tfinal/4:]) )

plt.figure( figsize=(6,5) )
plt.plot(np.arange(tfinal), d, '-r')
plt.plot([0,tfinal],[taylor88(n,c)]*2, '--b')
plt.text( 100, 0.2, theory )
plt.text( 100, 0.1, simuln )
plt.ylim([0,1])
plt.xlabel("time in generations", fontsize=12)
plt.ylabel("global mean dispersal rate", fontsize=12)
plt.show()
```

DM_OffCtrl_OneTrait.py

DM_OffCtrl_OneTrait.py

```
import numpy as np
import matplotlib.pyplot as plt

m=250
n=2
c=0.4

```

```
def taylor88(n,c):
  const = np.sqrt( 1 + 8*n*(2*n-1)*c**2 )
  return (const + 1 - 4*n*c)/(const + 1 - 4*n*c**2)

gold=np.random.uniform(0,1,(2,m,n))
gnew=np.random.uniform(0,1,(2,m,n))

tfinal=10000
d=np.empty(tfinal,dtype=float)

for t in range(tfinal):
  # modification
  dold = np.mean(gold,axis=0)
  d[t] = np.mean( np.mean( dold ) )

  # number tickets that emigrate from patch i
  emigrantTix = np.sum( dold, axis=1 )

  # number of tickets that remain on patch i
  nativeTix = n - emigrantTix

  # number of tickets that are in dispersal pool
  dpoolTix = np.sum( emigrantTix )

  # number of tickets that arrive on any patch
  immigrantTix = (1-c)*dpoolTix/m

  for i in range(m):
    for j in range(n):
      for parent in range(2):
        pLocal = nativeTix[i]/(nativeTix[i] + immigrantTix)
        x = np.random.binomial( 1, pLocal )
        if x==1:
          iwin = i
          p = (1-dold[iwin])/nativeTix[iwin]
          y = np.random.multinomial( 1, p )
          jwin = np.argmax(y)
          # modification (within-pair competition)
          pxtra = (1-gold[1,iwin,jwin]) / (1-gold[0,iwin,jwin] +
           ↪  1-gold[1,iwin,jwin])
          kwin = np.random.binomial(1,pxtra)
        else:
          q = emigrantTix/dpoolTix
          z = np.random.multinomial( 1, q )
          iwin = np.argmax(z)
          p = dold[iwin]/emigrantTix[iwin]
          y = np.random.multinomial( 1, p )
```

```
            jwin = np.argmax(y)
            # modification (within-pair competition)
            pxtra = gold[1,iwin,jwin]/(gold[0,iwin,jwin] + gold[1,iwin,jwin])
            kwin = np.random.binomial(1,pxtra)
          #modification
          gnew[parent,i,j] = gold[kwin,iwin,jwin] + np.random.normal(0,0.025,1)
    gnew = np.clip(gnew, 0.001, 0.999)
    (gold,gnew) = (gnew,gold)

theory = 'Taylor 1988: ' + str(taylor88(n,c))
simuln = 'Simulation: ' + str( np.mean(d[-3*tfinal/4:]) )

plt.figure( figsize=(6,5) )
plt.plot(np.arange(tfinal), d, '-r')
plt.plot([0,tfinal],[taylor88(n,c)]*2, '--b')
plt.text( 100, 0.2, theory )
plt.text( 100, 0.1, simuln )
plt.ylim([0,1])
plt.xlabel("time in generations", fontsize=12)
plt.ylabel("global mean dispersal rate", fontsize=12)
plt.show()
```

MD_ParCtrl_OneTrait.py

MD_ParCtrl_OneTrait.py

```
import numpy as np
import matplotlib.pyplot as plt

m=250
n=2
c=0.4

def taylor88(n,c):
  const = np.sqrt( 1 + 4*n*(n-1)*c**2 )
  return (const + 1 - 2*n*c)/(const + 1 - 2*n*c**2)

dold=0.5*np.random.uniform(0,1,(m,n))
dnew=np.random.uniform(0,1,(m,n))

tfinal=10000
d=np.empty(tfinal,dtype=float)

for t in range(tfinal):
  # number tickets that emigrate from patch i
  emigrantTix = np.sum( dold, axis=1 )

  # number of tickets that remain on patch i
  nativeTix = n - emigrantTix
```

```
24
25    # number of tickets that are in dispersal pool
26    dpoolTix = np.sum( emigrantTix )
27
28    # number of tickets that arrive on any patch
29    immigrantTix = (1-c)*dpoolTix/m
30
31    for i in range(m):
32      for j in range(n):
33        dtmp=0.0
34        for parent in range(2):
35          if parent == 0:
36            # mom
37            pLocal = nativeTix[i]/(nativeTix[i] + immigrantTix)
38            x = np.random.binomial( 1, pLocal )
39            if x==1:
40              iwin = i
41              p = (1-dold[iwin])/nativeTix[iwin]
42              y = np.random.multinomial( 1, p )
43              jwin = np.argmax(y)
44            else:
45              q = emigrantTix/dpoolTix
46              z = np.random.multinomial( 1, q )
47              iwin = np.argmax(z)
48              p = dold[iwin]/emigrantTix[iwin]
49              y = np.random.multinomial( 1, p )
50              jwin = np.argmax(y)
51          else:
52            # dad (NB iwin is established)
53            p = [1./n]*n
54            y = np.random.multinomial( 1, p )
55            jwin = np.argmax(y)
56          dtmp += 0.5*(dold[iwin,jwin] + np.random.normal(0,0.05,1))
57        dnew[i,j] = dtmp
58    dnew = np.clip(dnew, 0.001, 0.999)
59    (dold,dnew) = (dnew,dold)
60
61    d[t] = np.mean( np.mean( dold ) )
62
63  theory = 'Taylor 1988: ' + str(taylor88(n,c))
64  simuln = 'Simulation: ' + str( np.mean(d[-3*tfinal/4:]) )
65
66  plt.figure( figsize=(6,5) )
67  plt.plot(np.arange(tfinal), d, '-r')
68  plt.plot([0,tfinal],[taylor88(n,c)]*2, '--b')
69  plt.text( 100, 0.2, theory )
70  plt.text( 100, 0.1, simuln )
```

```
plt.ylim([0,1])
plt.xlabel("time in generations", fontsize=12)
plt.ylabel("global mean dispersal rate", fontsize=12)
plt.show()
```

MD_OffCtrl_OneTrait.py

MD_OffCtrl_OneTrait.py

```
import numpy as np
import matplotlib.pyplot as plt

m=250
n=2
c=0.4

def taylor88(n,c):
  const = np.sqrt( 1 + 4*n*(n-1)*c**2 )
  return (const + 1 - 2*n*c)/(const + 1 - 2*n*c**2)

gold=np.random.uniform(0,1,(2,m,n))
gnew=np.random.uniform(0,1,(2,m,n))

tfinal=10000
d=np.empty(tfinal,dtype=float)

for t in range(tfinal):
  # modification
  dold = np.mean(gold,axis=0)
  d[t] = np.mean( np.mean( dold ) )

  # number tickets that emigrate from patch i
  emigrantTix = np.sum( dold, axis=1 )

  # number of tickets that remain on patch i
  nativeTix = n - emigrantTix

  # number of tickets that are in dispersal pool
  dpoolTix = np.sum( emigrantTix )

  # number of tickets that arrive on any patch
  immigrantTix = (1-c)*dpoolTix/m

  for i in range(m):
    for j in range(n):
      for parent in range(2):
        if parent == 0:
          # mom
          pLocal = nativeTix[i]/(nativeTix[i] + immigrantTix)
```

```
          x = np.random.binomial( 1, pLocal )
          if x==1:
            iwin = i
            p = (1-dold[iwin])/nativeTix[iwin]
            y = np.random.multinomial( 1, p )
            jwin = np.argmax(y)
            # modification (within-pair competition)
            pxtra = (1-gold[1,iwin,jwin]) / (1-gold[0,iwin,jwin] +
             ↪  1-gold[1,iwin,jwin])
            kwin = np.random.binomial(1,pxtra)
          else:
            q = emigrantTix/dpoolTix
            z = np.random.multinomial( 1, q )
            iwin = np.argmax(z)
            p = dold[iwin]/emigrantTix[iwin]
            y = np.random.multinomial( 1, p )
            jwin = np.argmax(y)
            # modification (within-pair competition)
            pxtra = gold[1,iwin,jwin]/(gold[0,iwin,jwin] + gold[1,iwin,jwin])
            kwin = np.random.binomial(1,pxtra)
        else:
          # dad (NB iwin is established and x is established)
          p = [1./n]*n
          y = np.random.multinomial( 1, p )
          jwin = np.argmax(y)
          # within-pair competition
          if x==1:
            kwin = np.random.binomial(1,0.5)
          else:
            kwin = np.random.binomial(1,0.5)
        #modification
        gnew[parent,i,j] = gold[kwin,iwin,jwin] + np.random.normal(0,0.025,1)
  gnew = np.clip(gnew, 0.001, 0.999)
  (gold,gnew) = (gnew,gold)

theory = 'Taylor 1988: ' + str(taylor88(n,c))
simuln = 'Simulation: ' + str( np.mean(d[-3*tfinal/4:]) )

plt.figure( figsize=(6,5) )
plt.plot(np.arange(tfinal), d, '-r')
plt.plot([0,tfinal],[taylor88(n,c)]*2, '--b')
plt.text( 100, 0.2, theory )
plt.text( 100, 0.1, simuln )
plt.ylim([0,1])
plt.xlabel("time in generations", fontsize=12)
plt.ylabel("global mean dispersal rate", fontsize=12)
plt.show()
```

Jingjing Xu | Curriculum Vitae

PhD Candidate – University of Western Ontario

Specializations: Mathematical Biology, Population Dynamics, Evolution of Cooperation, Kin Selection, Metapopulation, Ordinary Differential Equations

Education

Doctor of Philosophy in Applied Mathematics **09/2013–present**
University of Western Ontario (Western), London, Canada
- Thesis: Ecology and Evolution of Dispersal in Metapopulations

Master of Science in Applied Mathematics **09/2010–07/2013**
Beijing Normal University (BNU), Beijing, China
- Thesis: Hierarchy Dominance may Induce Full Cooperation–Evolution of Cooperation in a Population with Hierarchy

Bachelor of Science in Applied Mathematics **09/2005–07/2009**
Beijing Normal University, Beijing, China
- Thesis: Dynamic Analysis of Models of *Citellus dauricus* Population in Jilin Province

Relevant Publications

[1] **Jingjing Xu** and Geoff Wild. "Dispersal altering local states has a limited effect on persistence of a metapopulation". In: *Journal of biological dynamics* 12.1 (2018), pp. 455–470.

[2] **Jingjing Xu** and Geoff Wild. "Evolution of Dispersal with Temporal, Global-Scale Fluctuations". In: *The American Naturalist* (under review) (2018).

Relevant Presentations and Posters

- *Talk: ' "Paradox of Enrichment" in Metapopulations with Delays' (coauthored with Geoff Wild), The Sixth G. J. Butler International Conference on Differential Equations and Population Biology, July 23-27, 2018, University of Alberta, Edmonton, Canada.*

- *Poster: 'The two sides of delayed dispersal on persistence of metapopulations' (coauthored with Geoff Wild), 2017 Canadian Mathematical Society (CMS) 01–04/ Meeting, Dec 8-11, 2017, Waterloo, Canada.*

- *Talk: 'Effect of dispersal on the persistence of metapopulation with social structure' (coauthored with Geoff Wild), 2017 CAIMS Annual Meeting, July 17-21, 2017, Dalhousie University, Halifax, Canada.*

- *Poster: 'The Two Sides of Delayed Dispersal in Metapopulation Dynamics' (coauthored with Geoff Wild), Living on the Precipice: Interdisciplinary Conference on Resilience in Complex Natural and Human Systems, May 16-17, 2017, Waterloo, Canada.*

Supervisory Experience

Undergraduate Supervisor **05/2017–08/2017**
University of Western Ontario, London, ON, Canada
- Train an undergraduate assistant for the summer term, adjust communication based on the mathematical level of the assistant, discuss problems concerning both analytic and biological significance, and supervise the progress of the work.

Research Experience

Research Assistant **09/2013–08/2018**
University of Western Ontario, London, ON, Canada
- Supervised by Geoff Wild.

Research Assistant in the Group of Theoretical Ecology **09/2011–08/2013**
Institute of Zoology (IOZ), Chinese Academy of Science, Beijing, China
- Supervised by Zhonglai Li (BNU) and Dr. Yi Tao (IOZ).

Teaching Experience

Teaching Assistant for Applied Mathematics for Engineers **09–12/2016, 01–04/2017**
Department of Applied Mathematics, Western, London, Canada

Teaching Assistant for Calculus **09–12/2013, 01–04/2014/16**
Department of Applied Mathematics, Western, London, Canada

Teaching Assistant for Calculus with Analysis for Statistics **09–12/2015**
Department of Applied Mathematics, Western, London, Canada

Teaching Assistant for Applied Mathematical Methods **09–12/2014**
Department of Applied Mathematics, Western, London, Canada

Teaching Assistant for Advanced Mathematics **09/2010–07/2013**
Department of Mathematics, BNU, Beijing, China

Volunteer Experience

Volunteer, the Applied Mathematics Social Committee **09/2013–Present**
Department of Applied Mathematics, Western, London, Canada

Volunteer for ICMA-V **10/2015**
Western, London, Canada

Departmental Councilor **11/2015–10/2016**
Society of Graduate Students (SOGS), Western, London, Canada

Honours and Awards

Western Graduate Research Scholarship **09/2013-08/2017**
Department of Applied Mathematics, Western, London, Canada

Roger Migneron Memorial Travel Awards **06/2017**
Department of Applied Mathematics, Western, London, Canada